Università degli Studi di Padova

Department of Mathematics "Tullio Levi-Civita"

PhD Course in *Mathematical Sciences* Curriculum: *Computational Mathematics*

XXXVIII Series

Stochastic approaches to open quantum systems and the modeling of non-standard environments

Thesis written with the financial contribution of the European Union - Next Generation EU - National Recovery and Resilience Plan (NRRP), M4C2 – Investment 1.4. Strengthening of research and creation structures of "national R&D champions" on some Key Enabling Technologies. "CN1 National Centre for HPC, big data and Quantum Computing" Program – CUP C93C22002800006.

Coordinator

Prof. Giovanni Colombo

Supervisor

Prof. Giulio G. Giusteri

Co-Supervisor

Prof.ssa Barbara Fresch

PhD candidate

Pietro De Checchi

Abstract

Quantum systems are inevitably influenced by the environments in which they are embedded. From molecular and nanoscale systems interacting with complex surroundings, to engineered platforms for quantum technologies subject to control imperfections and external noise, the interplay between coherent dynamics and environmental effects is unavoidable. Accurately modeling such interactions is therefore essential not only for understanding fundamental processes such as charge and energy transfer, but also for the reliable operation of quantum devices, where decoherence directly impacts performance. When environmental fluctuations deviate from idealized white-noise assumptions, capturing their effects becomes both conceptually and computationally challenging.

In this thesis, we contribute to the investigation of the dynamics of open quantum systems interacting with structured and time-correlated environments, with a particular emphasis on stochastic formulations and their connection to reduced dynamics. After reviewing the main approaches to quantum master equations and their microscopic derivation, we develop and compare stochastic unraveling strategies, with a particular focus on stochastic Hamiltonian methods and numerical simulation strategies. We extend these approaches to correlated noise and process models, leading to non-Markovian master equations that require trajectory-based numerical treatments. Within this setting, we analyze the dynamical consequences of time-correlated environments, highlighting regimes exhibiting multi-timescale relaxation, long-lived coherences, and nontrivial stationary behavior. To obtain a practical closed description and physical intuition, we introduce a Redfield-inspired perturbative closure for these correlation terms, providing an effective master equation for the mean dynamics and leading to the definition of an alternative version of the Redfield tensor. To further characterize such dynamics, we introduce a trajectory-based densification measure and associated descriptors, which extract information from stochastic ensembles that is not accessible at the level of the reduced density matrix alone. Finally, we connect stochastic Hamiltonian formulations to the simulation of open quantum dynamics on digital quantum computers, analyzing a quantum trajectory-based algorithm and establishing its convergence properties and clarifying the role of quantum measurement statistics in its performance.

Mathematics knows no races or geographic boundaries; for mathematics, the cultural world is one country.
– D. Hilbert

The more progress physical sciences make, the more they tend to enter the domain of mathematics, which is a kind of center to which they all converge. We may even judge the degree of perfection to which a science has arrived by the facility with which it may be submitted to calculation.
– A. Quetelet, 1828

We have to remember that what we observe is not nature in itself but nature exposed to our method of questioning
– W. K. Heisemberg, 1955

La realtà rovina i modelli (Reality spoils models)
– P. Pravatto, 2020

Acknowledgements

In italiano...

Sono una persona che si prende sempre il tempo e la cura di leggere i ringraziamenti alla fine di ogni libro che legge. Trovo che, quando non sono ovviamente ed evidentemente finti e costruiti, siano la parte più genuina di tutto un lavoro. Eppure, allo stesso tempo, ci sono così tante persone a cui devo così tanto che questi ringraziamenti saranno inevitabilmente un tentativo fallimentare. E, siccome saranno sempre troppo corti, troppo pochi, e troppe le persone che rischio di non menzionare nel momento in cui scrivo, a ridosso della scadenza per la consegna, cercherò di tenerli corti a priori.

Ci sono state due spinte decisive che mi hanno portato a iniziare questo percorso, e portato avanti fino ed oltre questa tesi: Barbara, che mi ha convinto a riprovare un percorso di dottorato - per di più in matematica! - dopo un primo tentativo che ha portato le sue difficoltà ed in cui mi è stata di grande conforto e aiuto pratico oltre i soli legami istituzionali. Dalla tesi magistrale in poi, mi hai portato ad apprezzare la ricerca, quelle discussioni che dovrebbero durare una mezz'ora al massimo e finiscono a coprire interi pomeriggi. Se i nostri meeting sono lunghi oltre misura, la colpa forse è di nessuno, il merito di entrambi. Giulio, che mi ha guidato e formato in questo nuovo campo, lasciandomi però una libertà rara nel pormi domande e decidere come tentare e trovare risposte e linee di ricerca. Nelle sfide di pensiero ed indipendenza, mi sono sempre sentito stimato, rispettato e sentito *pari*.

Tutti i file che oggi compongono questa tesi, ogni capitolo, ogni sezione, sono stati creati contenendo solo questa frase *"I definitely have to write something meaningful in this thesis, or at least something that makes sense."* Se, e sta a voi deciderlo, sono riuscito in questo mio intento, il merito è di tutte quelle persone che mi circondano e mi supportano, che l'hanno fatto nel corso di questi anni e continuano a farlo - anche se non c'è più la scusa di condividere lo stesso ufficio, la stessa città, o vivere nello stesso paese.

Ringrazio la mia famiglia, la più allargata possibile. Il primo punto di fuoco. Fuoco della discussione, nel bene e nel male, quando ci si costringe a dibattere per ogni piccola cosa e inezia, fuoco della passione nel cercare tanto le risposte quanto nuove domande. Fuoco in senso ottico, ogni commento ed opinione servono a mettere meglio a fuoco me

stesso ed il mio rapporto con ciò che mi circonda. Grazie per avermi supportato in quelli che sono stati momenti difficili e nella fatica di tutti i giorni, e di essere sempre pronti a festeggiare tutti i momenti belli.

Un grazie a tutti i colleghi e le colleghe, e tutta la vostra disponibilità e gentilezza spontanea. Innumerevoli volte ho battuto sulla spalla di un collega per un consiglio, quasi altrettante volte ci siamo persi davanti a una lavagna non più vuota, di quasi tutte queste ho dovuto ricordarvi che stavate facendo altro e non volevo rubarvi intere ore, e più volte ancora sono uscito conoscendo un po' di più e arricchito. Tra tutte le battute per cui io sono *il chimico*, mi avete costantemente ricordato che ormai sono anche un matematico e che appartengo anche a questo vostro, nostro, mondo. In questa transizione da chimico a matematico, grazie a tutti i colleghi del DiSC e del gruppo di teorica, che mi hanno fatto sentire come se non me ne fossi mai andato e mi hanno accolto sempre, tanto da finire in quasi tutte le foto di gruppo.

Tutte le persone conosciute tra conferenze e visiting - per quanto per poco tempo, abbiamo condiviso tanto, e che bellezza è sentirsi veramente parte attiva di questa grande famiglia scientifica che creiamo e che si ramifica su tutto il mondo. Salutando l'IFISC di Palma, ci siamo chiesti "è possibile che sembri parte del gruppo da sempre?" e la risposta, per questo motivo, è che tutti ne abbiamo fatto, e ne faremo, parte da sempre.

Ci sono delle intersezioni forti tra colleghi e amici, e Federico oltre a questo è stato un compagno essenziale in tutto questo percorso, che difficilmente sarebbe stato portato a termine in modo così fruttuoso e con così tanto piacere. Grazie per tutta la disponibilità, i confronti e il lavoro.

Siamo già oltre alla pagina, e non proverò nemmeno a fare l'affronto di dimenticarmi qualche nome. Grazie a tutti voi amici. Se sono sano di mente è merito vostro, *se* vi è stato difficile farmi parlare d'altro o interrompere le mille parentesi continuo ad aprire, come gli incisi in un discorso scritto, che potrebbero continuare ed annidarsi all'infinito, come... grazie per lo sforzo, grazie per le risate, la vostra presenza ed il vostro calore. Sia che ci conosciamo da una vita intera o sia stata raccontata e vissuta in poche lune o poche sere.

Grazie.

...and in English

I am a person who always takes the time and the care to read the acknowledgments at the end of every book I read. I find that, when not obvious otherwise, it is the most genuine piece of the production. Yet, at the same time, there are so many people to whom I owe so much that these acknowledgments will inevitably be a doomed attempt. And since they will always be too short, too limited, and too many people risk being left out as I write, so close to the submission deadline, I will try to keep them brief from the outset.

There have been two decisive figures that led me to begin this journey, and carried me through it and beyond this thesis. Barbara, who convinced me to attempt a PhD again — and in mathematics, no less! — after a first experience with its own difficulties, and during which she was a source of great support and practical help well beyond institutional

ties. From my master's thesis onward, you led me to *truly* appreciate research: those discussions that are meant to last no more than half an hour and instead end up filling entire afternoons. If our meetings tend to stretch far beyond what was planned, perhaps it is no one's fault — and both our merit. Giulio, who guided and trained me in this new field, while granting me a rare degree of freedom in formulating questions and in deciding how to approach and pursue answers and research directions. In facing challenges of thought and independence, I have always felt valued, respected, and treated as an equal.

Every file that now makes up this thesis - for each chapter, section, and part - started containing only the same one line, *"I definitely have to write something meaningful in this thesis, or at least something that makes sense."* If -and it is up to you to decide- I achieved this goal, the credit goes especially to all the people surrounding and supporting me, who have done so over these years and continue to do so - even if there is no longer the excuse of sharing in the same office, city, or living in the same country.

First of all, immense gratitude to my family, in the broadest possible sense. The first focal point - and here the bilingual symmetry breaks down, as in Italian I used *fuoco*, a word that simultaneously means fire and focus, the latter the root of the former. A fire of discussion, for better or worse, where one is compelled to debate every small detail and triviality; a fire of passion, in the search for both answers and new questions. A focus in the optical sense: every comment and opinion helps bring into sharper focus both myself and my relationship with what surrounds me. Thank you for supporting me through difficult moments and through the effort of everyday life, and for always being ready to celebrate all the good ones.

My thanks to all colleagues, for your constant availability and spontaneous kindness. Countless times I have tapped on a colleague's shoulder for advice, and almost as many times we have found ourselves lost in front of a no-longer-empty blackboard. In most of these cases, I eventually had to remind you that you had other things of your own to do, and that I did not want to steal entire hours of your time. Even more often than these countless times, I walked away knowing a little more, enriched. Within the jokes of being *the chemist*, you never stopped reminding me that I am now a mathematician too and that I belong. In this transition from chemist to mathematician, thanks to all colleagues at DiSC and in the theoretical chemistry group, who made me feel as if I had never really left, and always welcomed me back, so much so that I ended up in almost every group picture.

To all the people I met through conferences and visiting periods: even if only for a short time, we shared a great deal. There is something beautiful in truly feeling part of this large scientific family that we collectively build, branching out across the world. When saying goodbye at IFISC in Palma, we wondered: *"how is it possible that you seem to have always been part of the group?"* — and the answer, for this very reason, is that we have all always been, and will always be, part of it.

There are strong intersections between colleagues and friends, and Federico, beyond this, has been an essential companion throughout this entire journey, one that would hardly have been as fruitful and enjoyable without him. Thank you for your constant availability, for the discussions, and for the work we shared.

We are already beyond a page, and I will not even attempt the offense of leaving someone out by naming names. Thank you to all of you, my friends.

If I am still sane, it is thanks to you. *If* it has been difficult to make me talk about something else, or to interrupt the endless parentheses I keep opening, like digressions in a written sentence, which could continue and nest indefinitely, you know, like when.... thank you for the effort. Thank you for the laughter, for your presence, and for your warmth. Whether we have known each other for a lifetime, or whether that time has been told and lived in a short while, or a few evenings.

Thank you all.

Contents

Chapter I

Introduction

One century has passed since what is unanimously considered the beginning of quantum mechanics [1–3], from the groundbreaking work of W. Heisenberg [4], the famous E. Schrödinger proposal of the equation rightfully known as Schrödinger Equation [5, 6] - which will play a central role throughout the whole body of this dissertation - and other seminal contributions. The first years and the pioneering generation at the beginning of the *quantum era* established a formal quantum-mechanical description of physical reality, paving the way to the subsequent *quantum revolutions*.

Quantum mechanics provided a deeper understanding of the behavior of particles, nanoscaled systems, and molecules, proving to be a powerful theory capable of both explaining and predicting natural phenomena. Building upon the knowledge developed within this new branch of physics enabled major technological breakthroughs, often referred to as the *first quantum revolution*, which are now an integral part of everyone's daily life. Lasers, magnetic resonance imaging, light-emitting diodes, and even GPS-based navigation are among the many technologies whose operation relies on quantum-mechanical principles.

From quantum mechanics as a theoretical framework to the effective realization of quantum technologies, we are witnessing the convergence of an exceptionally broad range of fields, not just physics, but also mathematics, chemistry, and various branches of engineering, in collaborations that are growing increasingly widespread and active. The advances in practical engineering of specific quantum systems, together with the development of increasingly refined protocols of control enabling the direct manipulation of quantum states and their evolution, combined with information science approaches, have brought us into the midst of the fervent *second quantum revolution* [2, 7, 8], some already envisioning the future revolutions that may follow [9].

Among the numerous advances that emerged from the dawn of the 21st century - such as quantum sensors and quantum cryptography - quantum computing stands out as the most prominent and extensively explored, attracting substantial investment from research institutions and national initiatives worldwide. Quantum computers (QC) are regarded as promising platforms capable of outperforming classical solutions for specific classes of problems, theoretically proven to be capable of solving NP-hard problems, and recently supported by experimental proof-of-concept demonstrations [10–14]. At the same time, advances in theoretical understanding and the development of new classical algorithms have led to valuable insights regarding regimes of "classical advantage" [15–17], highlighting the nuanced boundaries between quantum and classical computational capabilities.

Despite these rapid advances, the theoretical models underlying quantum technologies often rely on idealized systems — particularly the qubit, which represents an ideal two-level quantum system. In practice, however, physical implementations inevitably deviate from this idealization. This realization motivates two central directions explored in this work: first, the need to address the pervasive influence of noise and decoherence; and second, we can exploit the intrinsic properties of both idealized quantum registers and realistic ones to design algorithms to simulate quantum system dynamics and problems that can be mapped to such architectures.

In moving from ideal, unperturbed quantum systems toward more realistic descriptions, one must necessarily consider the presence of external influences and interactions. Quantum systems are never fully isolated. Molecules and nano-structures, both natural and artificial, are embedded in some medium, such as solid-state matrices or fluids. Even almost-isolated systems in high vacuum, such as the neutral atoms and trapped ions used in quantum computing architectures, interact with the control apparatus and external fields. The surroundings and all the secondary degrees of freedom are part of the so-called environment of the system.

The unavoidable interactions with the environment can strongly influence the behavior of a system by changing its energy landscape and dynamics, modifying the expected ideal behavior of quantum systems, inducing decoherence and dissipation [18, 19], as they cannot be considered closed systems any longer. One first important example is in quantum computing, where quantum coherence is exploited for computational purposes and dissipation is almost always detrimental. Controlling environmental noise can allow achieving error mitigation and correction in the most common digital architectures [20–22]. On the other hand, opportunely tuned system-environment interactions can be exploited for less-known dissipative quantum computation strategies [23–28]. In other cases, the interplay between coherent contributions and environment-induced dephasing can enhance the efficiency of certain processes, such as quantum energy transport in chromophore aggregates of some photosynthetic organisms [29, 30], with application in photosynthetic mimicking [31].

In this context, theoretical models serve as essential tools for understanding natural phenomena and proposing engineered systems-environment interactions for useful applications. An effective treatment of open quantum systems (OQS) then requires shifting from

the unitary evolution of a wavefunction to a density matrix description, whose evolution does not follow a universal equation of motion but instead depends on the approximations and modeling strategies that one employs.

The present dissertation is devoted to the study of quantum systems subject to stochastic and environmental influences, and to the development of models and simulation strategies that bridge the gap between theoretical idealizations and experimentally accessible regimes. By combining analytical approaches from open quantum systems theory with numerical and quantum-simulation methodologies, this work aims to provide insight into how randomness, decoherence, and control interact in realistic quantum dynamics.

The remainder of this introduction outlines background preliminaries and conceptual foundations relevant to the discussion of open quantum systems and quantum computing. Revising the fundamental postulates of quantum mechanics, we introduce the derivation of open quantum systems from scratch, starting from the dynamics of isolated systems, their composition rules, and introducing the density matrix formalism. Defining the properties and interpretation of these objects naturally leads to the definition of mixed states and reduced states, which describe the physics of a portion of the whole composite system — the effective open system of interest in our work.

I.1 Isolated and closed quantum systems

We briefly recall and introduce isolated and closed quantum systems, as necessary preliminaries and as foundational building blocks of ideal quantum computing architectures. We start with the first few postulates of quantum mechanics in the wavefunction formalism [32, 33], while the others will be introduced in the following section and eventually translated to the more general density matrix formalism [34], showing how open quantum systems theory naturally arises.

The first postulate of quantum mechanics, or state space postulate, asserts that *"to every quantum system is associated a Hilbert space"*,

$$\mathcal{H} = \mathbb{C}^d \,, \tag{I.1}$$

equipped with an inner product

$$\langle v|w\rangle = \sum_{j=1}^{d} v_j^* w_j = c_{vw} \in \mathbb{C} \,, \tag{I.2}$$

where we make use of the *bra-ket* notation, so that the *ket* $|v\rangle$ denotes a vector v in a complex vector space and the *bra* $\langle v| = (|v\rangle)^\dagger$ denotes the adjoint, i.e., the transposed Hermitian conjugate, of the vector v.

Physically acceptable quantum states are described by statevectors, or wave functions,

which are linear combinations of states of the basis set composing the Hilbert space,[1]

$$|\Psi(t)\rangle = \sum_{j=1}^{d} c_j(t)|\phi_j\rangle\,, \quad |\psi\rangle \in \mathcal{H}_d = \mathbb{C}^d, \quad \{|\phi_j\rangle \perp^1 \mathcal{H}_d\}_{j=1}^{d} \tag{I.3}$$

such that their L_2-norm is unitary,

$$\langle\psi_t|\psi_t\rangle = \||\psi_t\rangle\|_{L_2}^2 = \sum_{j=1}^{d} |c_j(t)|^2 = 1 \tag{I.4}$$

Under this constraint, the coefficient $c_j(t) \in \mathbb{C}$ are interpreted as *probability amplitudes*: the probabilistic nature of quantum mechanics depends on the meaning of the square norm of the amplitudes of the state vectors.

Before discussing the time evolution of quantum systems, we briefly recall the definition of measuring a quantum state, further clarifying the *probabilistic* nature of quantum mechanics. The fourth postulate of quantum mechanics states that *"when a quantum system is measured, its state instantaneously collapses, transforming from a superposition of possible states to a single definite eigenstate corresponding to the measured value, with a probability determined by the absolute square of its probability amplitude coefficient"*. Take the expression of the wavefunction in eq. (I.3), and a set of measurements given by the projection to each basis state subspace $\{\Pi_j = |\phi_j\rangle\langle\phi_j|\}_{j=1}^{d}$, the outcome of measurement of the system in state $|\phi_k\rangle$ is

$$|\psi\rangle \mapsto \frac{\Pi_j}{\sqrt{p_k}}|\psi\rangle \equiv |\phi_k\rangle \tag{I.5}$$

with probability

$$p_k = \mathbb{P}(\text{meas. } |\phi_k\rangle) = \langle\psi|\Pi_k\Pi_k|\psi\rangle = |\langle\phi_k|\psi\rangle|^2 = |c_k|^2\,. \tag{I.6}$$

For a generic measure, these two equations constitute the so-called Born rule. Then, we can summarize the physical meaning and interpretation of the vectors we deal with in the wavefunction formalism as follows. The components of the wavefunction ψ describe probability amplitudes, and their modulus squared $|\psi|^2$ is a discrete probability distribution on the basis vector used to represent ψ. Furthermore, rather than states, we might want to investigate physical quantities associated with the quantum system, one simple example being the polarization of a system. The second part of the fourth postulates states that *"to every physical measurable quantity is associated an observable, i.e. an Hermitian operator A"*. Thanks to the Hermiticity of A, physical observables admit a spectral decomposition $A = \sum_a \lambda_a|a\rangle\langle a|$. The eigenvalues of the operator are $\lambda_a \in \mathbb{R}$, and the set of their eigenvectors is an orthonormal basis set, each associated with a projector $\Pi_a = |a\rangle\langle a|$, the set of projectors constituting a set of measurements. By eqs. (I.5) and (I.6), we obtain the state obtained after a measurement λ_a of the observable and its associated probability p_a.

[1] where, as an arbitrary but convenient choice, the basis set is chosen to be an orthonormal ($\perp^1$) basis of the Hilbert space.

What we can actually measure is the expectation value of an observable, defined as

$$\langle A\rangle = \sum_a \lambda_a p_a \tag{I.7a}$$

$$= \sum_a \lambda_a \langle\psi|\Pi_a|\psi\rangle \tag{I.7b}$$

$$= \langle\psi| \left(\textstyle\sum_a \lambda_a \Pi_a\right) |\psi\rangle \tag{I.7c}$$

$$= \langle\psi|A|\psi\rangle\,. \tag{I.7d}$$

This consideration returns the probabilistic meaning of the interpretation of quantum mechanics: the averaging of identical measures on a set of identical replicas of the system returns the value measured instrumentally.

I.1.1 Unitary dynamics

The time evolution of a closed quantum system, i.e., a system that evolves under the action of unitary operators, is given by the time-dependent Schrödinger equation [6], which reads

$$\frac{\mathrm{d}}{\mathrm{d}t}|\psi(t)\rangle = -\frac{i}{\hbar}H|\psi(t)\rangle\,, \tag{I.8}$$

where H is the Hermitian operator known as the Hamiltonian. For simplicity, we set $\hbar = 1$ in the following, and throughout the thesis when not specified otherwise. The solution of this differential equation returns the third postulate of quantum mechanics, namely that *"there exists a unitary operator $U(t)$ such that the time evolution of a state is given by*

$$|\psi(t)\rangle = U(t)|\psi(0)\rangle\,, \tag{I.9}$$

or, equivalently, that the statevector satisfies the Schrödinger equation". Indeed, in the simpler case when the Hamiltonian is time-independent, the solution of this differential equation reads

$$|\Psi(t)\rangle = e^{-iHt}|\Psi(0)\rangle\,, \tag{I.10}$$

where the unitary operator takes the form $U(t) = e^{-iHt}$, with initial condition $U(0) = \mathbb{1}$, and is commonly referred to as the *propagator*. The propagation operator has the special property of being *unitary*, meaning that its inverse exists and it corresponds to its adjoint operator ($U^{-1}(t) = U^\dagger(t)$), so that $U^\dagger(t)U(t) = \mathbb{1}$ holds. Because of this relation, the evolution of a system according to the SE is *time-reversible*, hence it can always be inverted to recover a valid past state. In this kind of systems, there is no exchange of energy and matter (hence, of information), and they are properly referred to as *isolated*. In closed systems, we allow interaction with external fields, e.g., a classical electromagnetic field; thus, their dynamics are described by a time-dependent Hamiltonian $H(t)$. The integration of eq. (I.8) leads then to the following solution for the propagator,

$$U(t) = \mathcal{T}_+ e^{-i\int_0^t H(\tau)\,\mathrm{d}\tau}\,, \tag{I.11}$$

where $\mathcal{T}_+$ represents the time-ordering operator. The implication of such a description will be discussed in later Chapters, and, for the time being, we will discuss only time-independent Hamiltonians governing our systems.

One important remark is the following. These kinds of evolutions are the ones governing ideal qubits dynamics, as in ideal conditions, all qubits of a QC form a closed quantum system that interacts only with the control apparatus (the time-dependent component of the Hamiltonian), and evolve according to their own Hamiltonians when controls are turned off (the time-independent component of the Hamiltonian). This means that quantum gates are all unitary propagators, which encode unitary dynamics.

I.1.2 Composition of quantum systems

The wavefunction $|\psi\rangle$ lives in a d-dimensional space, and could then describe a system of any dimensionality. In many applications, it can be beneficial to view the space as a composition of different systems. A clear example is a quantum register, a collection of interacting qubit systems, further discussed in section I.3.

By the second postulate of quantum mechanics, *"given two quantum systems with respective spaces $\mathcal{H}_A$ and $\mathcal{H}_B$, the composite system is associated to the Hilbert space given by $\mathcal{H} = \mathcal{H}_A \otimes \mathcal{H}_B$, where $\otimes$ denotes the tensor product"*. For two generic state vectors $|\psi\rangle \in \mathcal{H}_A$ and $|\varphi\rangle \in \mathcal{H}_B$, respectively of dimensions $\dim(\mathcal{H}_A) = n$ and $\dim(\mathcal{H}_B) = m$, the state of the composite system $|\Psi\rangle$ is the following, defining the the tensor product as

$$\mathcal{H} \ni |\psi\rangle \otimes |\varphi\rangle = \begin{pmatrix} \psi_1 \\ \vdots \\ \psi_n \end{pmatrix} \otimes \begin{pmatrix} \varphi_1 \\ \vdots \\ \varphi_m \end{pmatrix} \cong \begin{pmatrix} \psi_1\varphi_1 \\ \vdots \\ \psi_1\varphi_m \\ \vdots \\ \psi_n\varphi_m \end{pmatrix} . \tag{I.12}$$

Take two operators A and B acting respectively on each subspace; these can act independently of each other, so we write $A \otimes \mathbb{1}_B$ and $\mathbb{1}_A \otimes B$, or they act as a bilinear coupling so that $V = A \otimes B$. One sees that each operator acts on its subspace, so

$$(A \otimes \mathbb{1}_B)|\psi\rangle \otimes |\varphi\rangle = A|\psi\rangle \otimes |\varphi\rangle \tag{I.13a}$$

$$(\mathbb{1}_A \otimes B)|\psi\rangle \otimes |\varphi\rangle = |\psi\rangle \otimes |\varphi\rangle \tag{I.13b}$$

$$(A \otimes B)|\psi\rangle \otimes |\varphi\rangle = A|\psi\rangle \otimes B|\varphi\rangle \, . \tag{I.13c}$$

I.2 From isolated to open quantum systems

The notions and settings introduced hitherto provide a sufficient basis for dealing with isolated and closed quantum systems: we know what the wavefunction of the system describes, how to measure it to obtain physically relevant information, and how to describe its evolution in time; finally, we know how to compose closed systems into one. The last point is fundamental for allowing interactions among systems and is mandatory in this

formalism in order to describe any system interacting with another. We can foresee the avalanche effect of such a notion, as no quantum system is truly isolated and is bound to interact with adjacent systems, which in turn interact with their surroundings. In other words, *it is bound to be disturbed by the environment in which it is naturally embedded and with which it inevitably interacts* - a statement we introduced in the very beginning, and clarified in the following.

I.2.1 Density matrix

Because of the probabilistic nature of quantum mechanics, as stated above, the observables of any quantum system can be obtained only by a statistical average of repeated measurements on copies of the system, which is the same as measuring an ensemble of independent systems described by the same statevector. Importantly, the individual systems composing the ensemble can assume different states, and this is equivalent to saying that the state of a system is not always perfectly known.

It is then convenient to introduce the density matrix formalism when dealing with ensembles of quantum systems, and we will rephrase the postulates of quantum mechanics in this formalism.

We start from a state of the system that is not known a priori. So, let us take a Ψ, not known, but we know its probability p_k to be in the state $|\psi_k\rangle$, and the probability of being any of the states normalized to 1, $\sum_k p_k = 1$, meaning that we are describing all possible states of the system. Then we can write the density matrix of the ensemble as the sum of the projectors to each state subspace, weighted by their probability,

$$\rho = \sum_k p_k |\psi_k\rangle\langle\psi_k| \,. \tag{I.14}$$

If the state of the system is known, the density matrix is defined as the outer product of the wavefunction of the system with itself, and that describes a *pure* state, $\rho = |\psi\rangle\langle\psi|$. Note that this is equivalent to setting one probability $p_k = 1$ in the definition above. Otherwise, the state is said to be a *mixed state* of the system, as it describes a combination of possible states.

We can recast the postulates of quantum mechanics for this more general object, and this helps clarify its properties and the strength of its use compared to the wavefunction.

Then, the first postulate of quantum mechanics is modified so that the state of the system is described by linear operators ρ that are *positive semidefinite self-adjoint* linear operators acting on $\mathcal{H}$ with *unit trace*:

$$\rho = \sum_k p_k |\psi_k\rangle\langle\psi_k| \,, \quad |\psi_k\rangle \in \mathcal{H} \,, \quad \mathrm{Tr}[\rho] = 1 \,, \quad p_k \in [0,1] \,, \quad \rho \in \mathcal{L}(\mathcal{H}) \,, \tag{I.15}$$

where $\mathrm{Tr}[\cdot]$ is the trace operator, summing over all diagonal elements of a matrix, and $\mathcal{L}(\mathcal{H}) = \mathcal{H} \otimes \mathcal{H}^*$ is the space of linear operators acting on the $\mathcal{H}$ space.

We comment on the meanings and interpretations of this object. First, we remark that

the set

$$p = \left\{ p_k \,:\, p_k \in [0,1], \sum_{k=1}^{d} p_k = 1 \right\} \tag{I.16}$$

is a probability distribution of a pure states ensemble. This is composed of the diagonal term of the density matrix, and its elements are referred to as *populations* of the system. Conversely, the off-diagonal elements, when in a non-diagonal basis, are named *coherences*, representing superposition of states. Note then that the density matrix is, at the same time, (i) a state of the system by definition, (ii) a (or a sum of) projection operator(s), and (iii) a probability density.

The trace operator ($\mathrm{Tr} : \mathcal{L}(\mathcal{H}) \to \mathbb{C}$) acts then as an average. For the sole density matrix, this is the sum of the probabilities, therefore normalized. Given an observable $A = \sum_a \lambda_a |a\rangle\langle a|$, a Hermitian operator, now λ_a the outcomes of a measure, we can now directly compute the expectation value of A for the system ρ, as

$$\langle A \rangle_\rho = \sum_a \lambda_a p_a = \mathrm{Tr}[A\rho] \,. \tag{I.17}$$

This returns the recasting of the fourth postulate of quantum mechanics.

In this representation, the dynamics of the system are given by the Liouville-Von Neumann equation, which reads:

$$\frac{\mathrm{d}}{\mathrm{d}t}\rho(t) = -i[H, \rho(t)] \tag{I.18}$$

where $[A, B]$ is the commutator $AB - BA$. Easily derived from the SE solution and the definition of the density matrix ρ, it has the formal solution:

$$\rho(t) = U(t)\rho(0)U^\dagger(t) = \mathcal{U}_t[\rho(0)] \tag{I.19}$$

where $\mathcal{U}_t[\cdot]$ is the dynamical map of the evolution. Again, the evolution of the system is unitary.

I.2.2 Combining system and environment

What we have discussed so far are the closed dynamics of a single system. Let us first recast the composition postulate of quantum mechanics in the density matrix formalism and elaborate on its effect on the objects at hand. We will then pose the fundamental question leading to the open quantum systems theory, which we will begin supporting with some useful mathematical tools.

Let us now consider a more complex setting, a total system composed of two parts, with respective spaces $\mathcal{H}_A$ and $\mathcal{H}_B$. Given two orthonormal basis sets for the two subsystems, namely $\{|a\rangle \perp^1 \mathcal{H}_A\}_1^N$ and $\{|\mu\rangle \perp^1 \mathcal{H}_B\}_1^M$, from the second postulate of quantum mechanics, it follows that the total Hilbert space associated with the composite system is

$$\mathcal{H} = \mathcal{H}_A \otimes \mathcal{H}_B = \mathrm{span}\{|a\rangle_A \otimes |\mu\rangle_B\} \,. \tag{I.20}$$

We can define any pure states ensemble of the composite system as

$$\left\{ |\psi_k\rangle \in \mathcal{H}\,,\, p_k \;:\; |\psi_k\rangle = \sum_{i,\mu} c_{k;a,\mu} |a\rangle_A \otimes |\mu\rangle_B \,,\, \sum_k p_k = 1 \right\}, \tag{I.21}$$

where the coefficients $c_{k;a,\mu}$ are the products of the coefficients of each basis $|a\rangle$ and $|\mu\rangle$ in each pure wavefunctuion $|\psi_k\rangle$. The associated generic density matrix can then be written

$$\rho = \sum_k p_k |\psi_k\rangle\langle\psi_k| = \sum_{ab\mu\nu} \lambda_{ab\mu\nu} |a\rangle\langle b|_A \otimes |\mu\rangle\langle\nu|_B \,, \tag{I.22}$$

where

$$\lambda_{ab\mu\nu} = \sum_k p_k c_{k;a\mu} c^*_{k;b\nu} \,. \tag{I.23}$$

On the one hand, the wavefunction describes coherent states, which are captured by the coherence terms of a pure-state density matrix. On the other hand, for composite systems, with the coefficients $\lambda_{ab\mu\nu}$, we can describe classical correlation (and its absence) and entanglement, a specific characteristic of correlation of quantum systems.

With the example of the bipartite system presented above, we say that it is *uncorrelated* if the global density matrix can be written a single tensor product of the subsystems density matrices, i.e.,

$$\rho = \rho_A \otimes \rho_B \,, \tag{I.24}$$

equivalent to say that the system in eq. (I.22) is a specific state k, with $p_k = 1$ and that its coefficient factorize as $\lambda_{ab\mu\nu} = \lambda^A_{ab}\lambda^B_{\mu\nu} = c_{k;a\mu}c^*_{k;b\nu}$ for the one specific k. In all other cases, the two systems are correlated.

Classical correlation can be seen when the system, which we can define as a *separable* system, can be decomposed as a convex combination of factorized contributions,

$$\rho = \sum_k p_k \rho^{(k)}_A \otimes \rho^{(k)}_B = \sum_k \sum_{ab\mu\nu} c_{k;a\mu} c^*_{k;b\nu} |a\rangle\langle b|_A \otimes |\mu\rangle\langle\nu|_B \tag{I.25}$$

where the coefficients are themselves a linear combination of factorized contributions. Correlation exists, but it is of a classical nature, depending on the ignorance of which k system we are dealing with.

Finally, two subsystems are said to be *entangled* if they cannot be expressed in either eqs. (I.24) and (I.25) form, i.e., if the system is not separable. An interesting way to write such systems, which gives an intuitive picture that will come in handy later, is to write the system as

$$\rho = \sum_k p_k \rho^{(k)}_A \otimes \rho^{(k)}_B + \varrho^{\text{corr}} \,, \tag{I.26}$$

a sum of a separable state plus an operator accounting for the pure quantum correlation between the system, which, to preserve the physical validity of the state, must be a traceless operator.

Example I.1 | Bipartite system correlation and entanglement

Take two identical two-level systems, with space $\mathcal{H}_A$ and $\mathcal{H}_B$ each with basis set $\{|0\rangle_a, |1\rangle_a\}_{a=A,B}$. Let's construct three simple examples of uncorrelated, classically correlated, and entangled composite systems.

Uncorrelated system (product state). Let the two subsystems be independent and, for the sake of simplicity, we define the states to be $|\psi_A\rangle = |0\rangle_A$ and $|\psi_B\rangle = |1\rangle_B$. The composite system wavefunction is

$$|\Psi\rangle = |\psi_A\rangle \otimes |\psi_B\rangle = |0\rangle_A \otimes |1\rangle_B \,,$$

that we can write for simplicity as $|01\rangle$, referencing in order (from left to right) to the systems A and B, and the density matrix is then

$$\rho^{\text{uncorr}} = |0\rangle\langle 0|_A \otimes |1\rangle\langle 1|_B \,,$$

clearly a product state of the two density matrices. In matrix form, expandend in the basis $\{|00\rangle, |01\rangle, |10\rangle, |11\rangle\}$, reads

$$\rho^{\text{uncorr}} = \begin{pmatrix} 0 & 0 & 0 & 0 \\ 0 & 1 & 0 & 0 \\ 0 & 0 & 0 & 0 \\ 0 & 0 & 0 & 0 \end{pmatrix} .$$

Classically correlated system (separable state). Consider now an ensemble of two possible global wavefunctions $|\Psi_1\rangle$ and $|\Psi_2\rangle$, each with equal probability $p = \frac{1}{2}$, namely the set

$$\left\{ |\Psi_1\rangle = |00\rangle \,,\ |\Psi_2\rangle = |11\rangle;\ p_1 = p_2 = \frac{1}{2} \right\} .$$

The density matrix now reads

$$\rho^{c-\text{corr}} = \frac{1}{2}|00\rangle\langle 00| + \frac{1}{2}|11\rangle\langle 11| \,,$$

which can be written as the convex combination of factorized states

$$\rho^{c-\text{corr}} = \frac{1}{2}\Big(|0\rangle\langle 0|_A \otimes |0\rangle\langle 0|_B + |1\rangle\langle 1|_A \otimes |1\rangle\langle 1|_B \Big) \,,$$

and that in matrix form reads

$$\rho^{c-\text{corr}} = \frac{1}{2}\begin{pmatrix} 1 & 0 & 0 & 0 \\ 0 & 0 & 0 & 0 \\ 0 & 0 & 0 & 0 \\ 0 & 0 & 0 & 1 \end{pmatrix} .$$

Then, the systems are correlated, as when the system A is in its state $|0\rangle$, that is also true for the system B. But this correlation depends only on the initial (and classical) ignorance of not knowing which system of the ensemble we are dealing with.

Quantum and classically correlated system (entangled state). Finally, consider the composite system to live in a superposition, defined by one of the so-called Bell states, namely

$$|\Psi\rangle = \frac{1}{\sqrt{2}}\Big(|00\rangle + |11\rangle\Big) .$$

The associated density matrix takes the form

$$\rho = \frac{1}{2}\Big(|00\rangle\langle 00| + |00\rangle\langle 11| + |11\rangle\langle 00| + |11\rangle\langle 11|\Big) ,$$

which we cannot decompose into a convex combination of products, and they rather take the peculiar form

$$\lambda_{ab\mu\nu} = \begin{cases} \frac{1}{2} & (a,b,\mu,\nu) \in \{(0,0,0,0),\, (1,0,1,0),\, (0,1,0,1),\, (1,1,1,1)\} \\ 0 & \text{otherwise} \end{cases} ,$$

that, expanding the density matrix, leads to

$$\rho = \frac{1}{2}\begin{pmatrix} 1 & 0 & 0 & 1 \\ 0 & 0 & 0 & 0 \\ 0 & 0 & 0 & 0 \\ 1 & 0 & 0 & 1 \end{pmatrix} .$$

One feature of quantum correlation can be clearly appreciated in this form, as the coherence term of the composite system are not null, and we can recognize the form $\rho = \sum_k p_k \rho_A^{(k)} \otimes \rho_B^{(k)} + \varrho^{\text{corr}}$, the sum expressing the classically correlated state in the example above and the correlation operator to be $\varrho^{\text{corr}} = \frac{1}{2}(|00\rangle\langle 11| + |11\rangle\langle 00|)$.

Now, we are able to compose systems, describe their dynamics, and measure their observables. Still, we are working with closed dynamics, and with the composite system

as a whole. This begs the question: what if we are only interested in a small portion of the composite system?

Let us consider the typical case when studying molecular processes, a realistic situation. One is interested in the specific behavior of one of the subsystems, which is generally much smaller compared to the other one. An interesting case study is the transfer of energy quanta in coupled molecular aggregates [35, 36]. During the excitation process, for instance, due to the interaction with an electromagnetic field (a light source such as a laser in lab experiments, or sunlight for natural photosynthetic complexes), delocalized states are formed, known as excitons [37, 38]. Then, the excited states on the basis of the sites of the aggregates, or on the basis of the new delocalized states, are the subsystems of interest. This component is the effective *open*, or *reduced*, *system*, and we will refer to it for simplicity as the system $\mathcal{S}$. All the remaining degrees of freedom of the aggregates, such as molecular vibrations, and of all the surroundings, such as the solvent degrees of freedom and external fields, are part of the subsystem that we refer to as the *environment*, or *bath*, $\mathcal{B}$. We refer to the whole composite system of *open system* $\mathcal{S}$ and *environment* $\mathcal{B}$ as the *universe system*. A commonly used schematic representation for the clarification of this composition is in Figure I.1.

Since we are interested in the properties of the open system and not of the whole universe, we need to recover that information, reducing the description to the smaller component. To do so, we introduce the *partial trace* operator, which is a linear operator that maps from the total Liouville space $\mathcal{L}(\mathcal{H})$ of the composite system to the subspace $\mathcal{L}(\mathcal{H}_\mathcal{S})$ of the reduced system of interest, i.e., $\mathrm{Tr}_\mathcal{B} : \mathcal{L}(\mathcal{H}) \mapsto \mathcal{L}(\mathcal{H}_\mathcal{S})$. Given a generic separable operator acting on the total statevector, $A = A_\mathcal{S} \otimes A_\mathcal{B}$, we define its partial trace over the bath degrees of freedom as

$$\mathrm{Tr}_\mathcal{B}[A] = \mathrm{Tr}_\mathcal{B}[A_\mathcal{S} \otimes A_\mathcal{B}] \tag{I.27a}$$

$$= \sum_{\mu \in \mathcal{H}_\mathcal{B}} \langle \mu | [A_\mathcal{S} \otimes A_\mathcal{B}] | \mu \rangle \tag{I.27b}$$

$$= A_\mathcal{S} \sum_{\mu \in \mathcal{H}_\mathcal{B}} \langle \mu | A_\mathcal{B} | \mu \rangle \tag{I.27c}$$

$$= A_\mathcal{S} \, \mathrm{Tr}[A_\mathcal{B}] = \tilde{A}_\mathcal{S} \, , \tag{I.27d}$$

where $|\mu\rangle$ are an orthonorml basis for the environment Hilbert space, $\{|\mu\rangle \perp^1 \mathcal{H}_\mathcal{B}\}$. We remark on a few fundamental aspects before showing its use for density matrices. The sum in eq. (I.27b), whose elements are partial matrix elements, defines a working route for computing a partial trace independent of the form of the global operator, practical in theory but possibly not feasible, as we will show shortly. The step in eq. (I.27c) explains the name of the operator, as its effect is the trace over only one of the subspaces, eventually weighting the matrix elements of the operator acting on the intended subspace, eq. (I.27d).

When the operator we act on is the universe density matrix, we exploit notions and properties of density matrices. Take again, for simplicity, an uncorrelated density matrix $\rho = \rho_\mathcal{S} \otimes \rho_\mathcal{B}$. On the one hand, we recognize that the trace on the environment

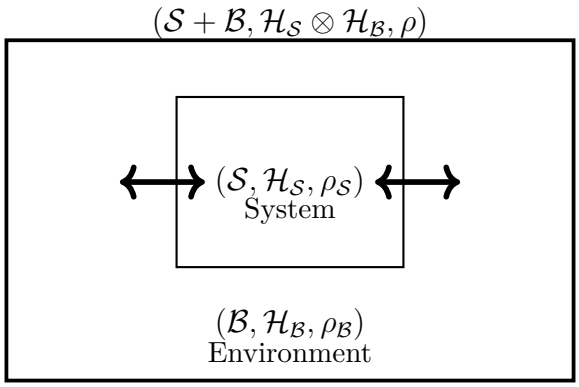

Figure I.1: A common schematic representation of an open quantum system, composed of a system of interest $\mathcal{S}$ (the *open system* itself), surrounded by an environment system $\mathcal{B}$, interacting, composing the universe system $\mathcal{S}+\mathcal{B}$.

subspace equals one, by definition. Moreover, in the probabilistic interpretation of these objects, while the trace operator acts as an average, the partial trace returns the marginal distributions

$$\mathrm{Tr}_\mathcal{B}[\rho_\mathcal{S}\otimes\rho_\mathcal{B}] = \rho_\mathcal{S}\,\mathrm{Tr}[\rho_\mathcal{B}] = \rho_\mathcal{S} \tag{I.28a}$$

$$\mathrm{Tr}_\mathcal{S}[\rho_\mathcal{S}\otimes\rho_\mathcal{B}] = \rho_\mathcal{B}\,\mathrm{Tr}[\rho_\mathcal{S}] = \rho_\mathcal{B}\,. \tag{I.28b}$$

This is always true, regardless of the degree of correlation between the two subsystems. We can apply the definition to the density matrix of the last system in Example I.1, and by simple computation, one obtains that $\rho_A = \mathbb{1}_A/2$, and the same for the secondary identical system, $\rho_B = \mathbb{1}_B/2$.[2]

Using the definition of the generic density matrix for a bipartite system, in eq. (I.22), we can write the partial trace operation as

$$\mathrm{Tr}_\mathcal{B}[\rho] = \sum_{\omega\in\mathcal{H}_\mathcal{B}} \langle\omega| \left(\sum_{ab\mu\nu} \lambda_{ab\mu\nu}|a\rangle\langle b|_\mathcal{S}\otimes|\mu\rangle\langle\nu|_\mathcal{B}\right)|\omega\rangle \tag{I.29}$$

$$= \sum_{ab\mu\nu}\left[\lambda_{ab\mu\nu}|a\rangle\langle b|_\mathcal{S}\otimes\left(\sum_{\omega\in\mathcal{H}_\mathcal{B}}\langle\omega|\mu\rangle_\mathcal{B}\langle\nu|\omega\rangle\right)\right] \tag{I.30}$$

where, assuming $|\omega\rangle$, $|\mu\rangle$, and $|\nu\rangle$ to be orthonormal, the sum over the environment subspace becomes $\sum_\omega\langle\omega|\mu\rangle\langle\nu|\omega\rangle = \sum_\omega \delta_{\omega\mu}\delta_{\nu\omega}$, and leads to

$$\mathrm{Tr}_\mathcal{B}[\rho] = \sum_{ab}\bar{\lambda}_{ab}|a\rangle\langle b| = \rho_\mathcal{S}\,, \tag{I.31}$$

where $\bar{\lambda}_{ab} = \sum_\omega \lambda_{ab\omega\omega}$.

While normally the dimension of the Hilbert space of the system $\mathcal{S}$ is quite small, more

[2]Note that, computing the partial traces of the density matrix of the example, the decomposition into classically correlated component plus quantum correlation is different. We can write now an uncorrelated state $\rho_A\otimes\rho_B = (\mathbb{1}_A\otimes\mathbb{1}_B)/4 = \mathbb{1}_{A+B}/4$, and by the definition we can recover the correlation matrix $\varrho^{\mathrm{corr}} = \rho - \rho_A\otimes\rho_B$, that now contains all the correlation terms.

generally, it has a finite dimension $\dim(\mathcal{H}_\mathcal{S}) = d$, the environment should, in principle, be taken large enough to include all the interactions necessary to describe the universe system. On the one hand, this allows us to regard the universe as a closed system, thereby describing its dynamics with the Liouville-von Neumann equation, eq. (I.18). Then, applying the partial trace on the time-evolved $\rho(t)$, we recover the system density matrix at each time. This procedure corresponds to the upper red branch of the commutative diagram in Figure I.2, and to the following equation

$$\rho_\mathcal{S}(t) = \mathrm{Tr}_\mathcal{B}[\rho(t)] = \mathrm{Tr}_\mathcal{B}[\mathcal{U}_t[\rho(0)]]\,. \tag{I.32}$$

On the other hand, several problems with this approach are evident. As we mentioned, this route may not be feasible on most occasions. Including all environmental degrees of freedom means including all system-environment couplings, as well as within all environmental particles and, cascading, to all other interactions. Usually, then, the dimension of the environment tends to infinity! It is clear that a numerical solution to this problem is unfeasible, let alone its dynamical evolution, due to the dimension of the environment subspace. That would mean, first, knowing the orthonormal basis set of the entire environment, and secondly, being able to compute an infinite sum.

Hence, until this moment, what we have written would be the exact description of the dynamics of a system. In this regard, we must make assumptions about the system we are investigating and, eventually, make approximations.

I.2.3 Describing the reduced dynamics

In realistic situations, we therefore cannot simulate the whole universe system; different methodologies and theoretical frameworks to describe the dynamics of the sole system of interest have been proposed over the last several decades by communities of physicists, theoretical and physical chemists, mathematicians, and information scientists. Despite their differences, all the methods rely on the density matrix formalism, and we present their common features in the following.

The unavoidable interactions with the environment influence the expected ideal behavior of quantum systems, inducing decoherence and dissipation phenomena [18, 19]. Therefore, while the dynamics of the universe are described by a unitary map, the mapping of the reduced system is described by a non-unitary mapping, generally a contractive map,

$$\rho_\mathcal{S}(t) = \mathcal{E}_t[\rho_\mathcal{S}(0)]\,. \tag{I.33}$$

This is the mapping in the central branch of the commutative diagram in Figure I.2. Further, we know that the system, if considered isolated, would evolve according to its own coherent dynamics, dictated by the system Hamiltonian $H_\mathcal{S}$ in a Liouville-von Neumann equation. At the price of losing some generality, both on the form of the dissipator and the conditions of the initial state, in this case mandatorily a factorized state, it is convenient to look at this map in its differential form as a *quantum master equation* (QME), which

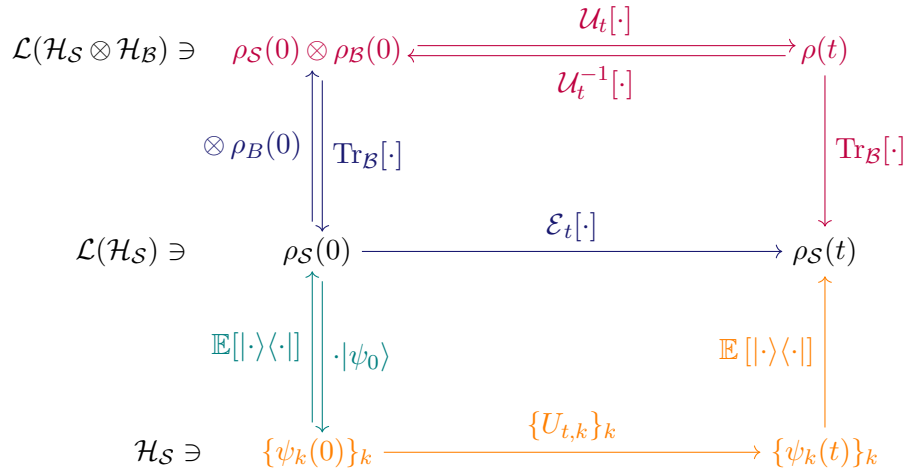

Figure I.2: A conceptual map as a commutative diagram, illustrating different strategies to describe the subsystem state $\rho_\mathcal{S}(t)$ evolution in time, the dynamical maps, the operation to move from one description to another, and the spaces these objects live in.

reads

$$\frac{\mathrm{d}}{\mathrm{d}t}\rho_S(t) = -i[H_S, \rho_S(t)] + \mathcal{D}[\rho_S(t)] \tag{I.34}$$

where the description of the dynamic of the system as if isolated from the environment is captured by the first term on the r.h.s., and the second term is a superoperator called the *dissipator*. This term models the effect of the relaxations and dephasing of the open system due to its interaction with the environment [18, 19, 39], addressing exchange of energy and information from the system to the environment (and, for more complex systems, also *vice versa*). Because of this operator, the information initially contained in the open system can be lost, either partially or totally, and the dynamics of the system is no longer reversible, the resulting map is non-unitary as stated above. A simple example of the effects of a dissipator on a two-level system dynamics is depicted in Figure I.3. The dissipator *contracts* the space of accessible states of the reduced system, and in the example figure, one can appreciate this effect to the dynamics of the reduced density matrix populations, the accessible values decreasing from the whole $[0, 1]$ to a single point $\rho_{ii} = \frac{1}{2}$.

We said, at the price of losing generality. Indeed, the dissipator does not need to be an operator acting neither linearly nor time-locally on the reduced density matrix, and eq. (I.34) defines a specific class of dynamics. In the following Chapters of this work, we start from different and more general assumptions, clarifying this concept, and eventually expanding the diagram of Figure I.2.

To treat effectively the dynamics of the open system, meaning practically obtain the dynamical map $\mathcal{E}_t$ or the underlying QME, two complementary perspectives are commonly adopted. In the first one, the density matrix describing the system of interest results from the partial trace over the environmental degrees of freedom and evolves deterministically under a quantum master equation. This approach requires starting from a microscopically explicit model of the environment and its interactions with the system, followed by either numerically-intensive reduction schemes, such as the hierarchical equations of motion (HEOM) or the time-evolving density matrix using the orthogonal polynomials

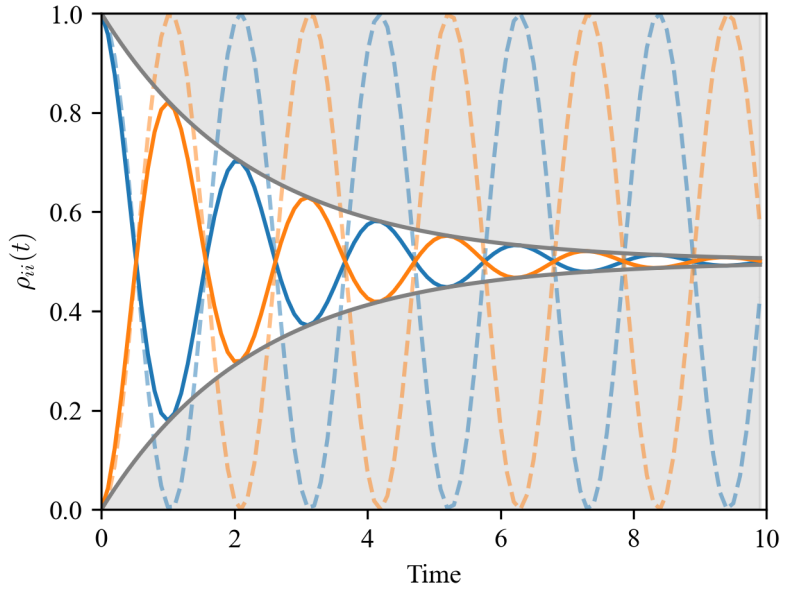

Figure I.3: Example of the effect of dissipation of the dynamics and the contraction (grey enveloping line) of the space for a two-level quantum system with coupled states. For comparison, the dynamics of the closed system are in transparent dashed lines.

algorithm (TEDOPA) [40–45], or clear-cut approximations on the interaction strength and timescale separation, as in the seminal derivation of the reduced dynamics proposed by Redfield [46, 47]. The most approximate version of the Redfield formulation leads to Lindblad-form master equations [48–50], an algebraically derived form that would admit only purely phenomenological application, if not derived from a Redfield approach. These are approaches that model around the upper branch of the commutative diagram in Figure I.2.

In the second approach, the density matrix dynamics of the system is understood as the statistical averaging over an ensemble of stochastic pure-state trajectories. This is commonly referred to as unraveling of the dynamics, reflected in the lower (orange) branch in Figure I.2, a graphical example in Figure I.4. There exist many different formulations of this approach. In stochastic Hamiltonians (SH), environmental influence is represented by time-dependent random fluctuations of system parameters, which are inserted directly into the Hamiltonian. This framework offers a physically intuitive and computationally versatile route to include environmental effects in the dynamics, and has proven particularly powerful in the interpretation of spectroscopic observables where noise-induced dephasing and spectral diffusion play a central role and are reflected in the spectral lineshape [51–55] and, more recently, to the development of sophisticated techniques to control and drive the quantum state for information processing in the context of noisy intermediate-scale quantum (NISQ) devices [56–63]. Another common framework is that of the stochastic Schrödinger Equation (SSE) [64, 65]. The stochastic Schrödinger equation is a more general formalism in which the pure state of an open quantum system evolves according to a stochastic differential equation driven by noise terms, the interaction of the system of interest with the environment is modeled as a stochastic time-dependent fluctuation of op-

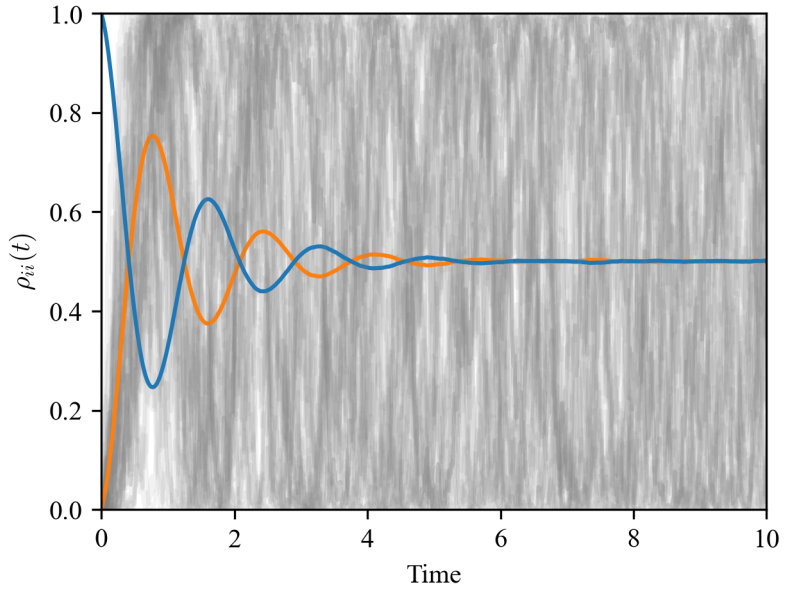

Figure I.4: Example of the unraveling of an open system dynamics of a two-level system in terms of stochastic trajectories. The average dynamics of the population of the density matrix are in solid blue and orange lines, and a swarm of 50 trajectories is in gray transparency lines.

erators acting on the system space [66–71]. These noise terms are interpreted as specific environment models and in connection with specific measurement protocols, "quantum jumps" or continuous measurement back-action [18, 65, 72]. The SH and SSE approaches introduced are of a phenomenological nature. This is conceptually different from the exact treatment of open quantum dynamics starting from a microscopically defined environment, another interesting route for stochastic approaches to open quantum dynamics, which we will not deal with in this dissertation. In this case, the elimination of the environment's degrees of freedom leads to specific stochastic forms like those originating from the Feynman-Vernon (path-integral) formalism [73, 74], non-Markovian quantum state diffusion (NMQSD) [75–77], the hierarchy of pure states (HOPS) [78], the HEOM approach[40–42], the generalized Langevin equations (GLE) [79–81] and others [82–84].

Averaging over realizations recovers the mixed-state dynamics of an open system, converging, in the large-number limit, to a quantum master equation. The numerical effort of these methods scales with $\mathcal{O}(d^2)$ rather than $\mathcal{O}(d^4)$ with the associated density matrix, being d the dimension of the system's Hilbert space. Considering the necessity of running a large number N of independent trajectories, the total scaling is $\mathcal{O}(d^2N)$, which can always be parallelized to speed up the computation. Because of this, renewed interest in this method has recently emerged in diverse fields, and trajectory approaches are often used to simulate large systems, where computing the density-matrix evolution is often prohibitive, as is, for instance, the case in molecular modeling [85, 86].

I.3 Basics of quantum computing

The first clear proposal of using quantum systems to simulate other quantum systems was advanced by Feynman in 1981, in his famous talk [87], the famous quote *"Nature isn't classical, dammit, and if you want to make a simulation of Nature, you'd better make it quantum mechanical"*. Just a couple of years later, D. Deutsch formalized universal quantum computing, introducing the Deutsch-Church-Turing principle [88, 89], by extension of the Church-Turing principle [90, 91]. A couple of years before, russian mathematician Y. Manin [92] emphasized the exponential scaling of simulating many-body physics, highlighting the different dimensions of the spaces of quantum systems compared to those of classical ones. The problem of the dimension of the variable space is at the core of the idea of quantum computation. The dimensions of quantum many-body systems scale exponentially [92, 93], as we need to account for all the superpositions of linear combinations that can describe the system - i.e., all the coherent and entangled states - while classical systems, such as classical computers, scale linearly with their dimensions. Take a simple n-particle system, each described by k levels; the space required to store its wavefunction is k^n. To then evolve and operate on this object, we would need to write a $k^n \times k^n$ matrix, and then exponentiate it to propagate the system!

Therefore, the core idea is to use *controllable* quantum systems to simulate the dynamics of other systems under investigation. The common protocol is to accurately map the target quantum system to another, both the state and its Hamiltonian, and therefore to initialize it to a specific state and control the evolution of the system. Then, the system is measured, and the quantities of interest are traced back to the reference system. Two main routes, paradigms, of quantum computing can be followed to achieve this task: analog and digital quantum computing. For those interested, we refer to an accessible and gentle, even if dated, overview in ref. [94]. Analogue quantum simulators (AQS) are highly controllable quantum systems that exploit mathematical similarities between the problem to solve and the AQS to mimic its evolution [94–98]. Mathematical similarities beckon physical similarity, and AQS are dedicated devices for the solution of their restricted class of problems, a drawback for a possible general usage, and therefore it will not be discussed in this work.

A digital quantum computer (DQC, QC for the sake of brevity) is a system composed of a set of, ideally identical and independent, two-level quantum systems, named *qubits*, which can be initialized, coherently manipulated and measured, the devices needed to perform such operations and an interface with a classical computer to control remotely the operations and to collect the data (the backbone of this protocol is depicted in Figure I.5).A key strength of the DQC approach to quantum computing is its universality, meaning that choosing the correct mapping and algorithm, any quantum system can be simulated [99].

In analogy with classical computing, the basis of the qubits is defined $\{|0\rangle, |1\rangle\}$, where

$$|0\rangle = \begin{pmatrix} 1 \\ 0 \end{pmatrix}, \qquad |1\rangle = \begin{pmatrix} 0 \\ 1 \end{pmatrix}. \tag{I.35}$$

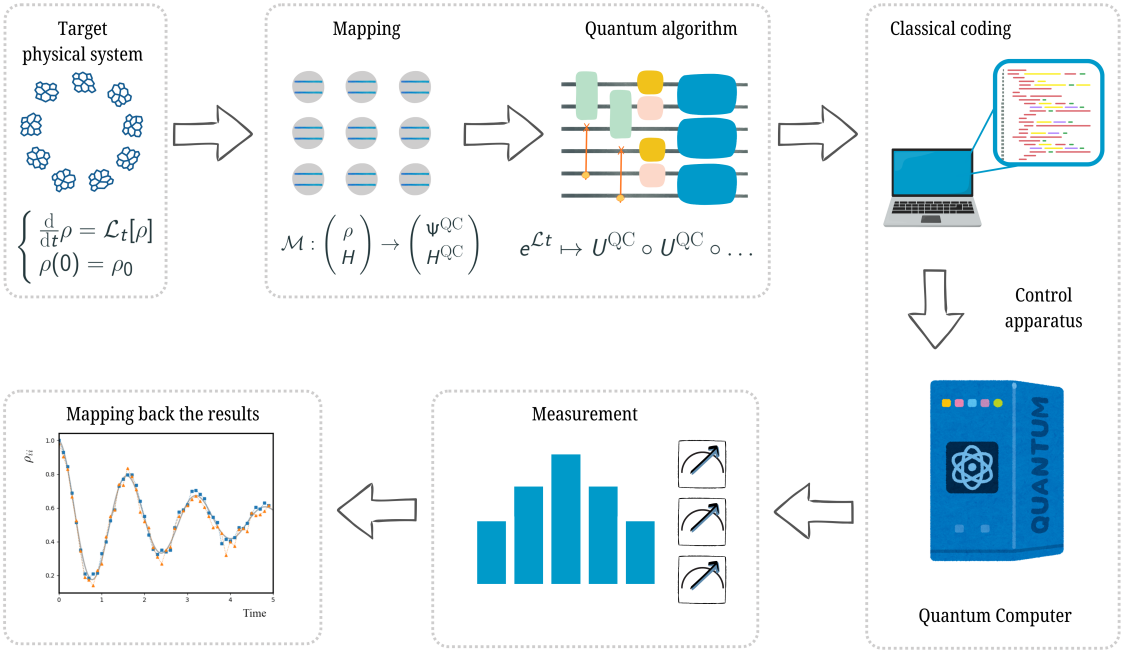

Figure I.5: A graphical scheme of the quantum simulation of a target system with a digital quantum computer. From the study of a physical system, we derive a theoretical model to describe its properties and dynamics. Then, the problem is mapped to the quantum computing architecture, and a quantum algorithm is designed to reproduce the propagation of the system in terms of unitary propagators (gates) and projective measurements. The algorithm is translated to "high-level" code on a classical computer, a researcher's personal laptop, and the instructions are sent to a control apparatus that translates them into physical operations (e.g., voltage, electromagnetic pulse, and so on) performed on the quantum processor (the secondary physical system). The state of the composition of qubits is sampled through measurements and sent back to the user as a classical register, which has to be elaborated and mapped back to the target system to obtain the results of the computation.

While a classical two-level system can encode only a binary integer (a *bit* of information), either 0 or 1, a qubit is a two-level quantum system, whose Hilbert space is $\mathcal{H} = \mathbb{C}^2$, and whose state is described by eq. (I.3), namely

$$|q\rangle = \alpha|0\rangle + \beta|1\rangle, \tag{I.36}$$

and it encodes a continuum of 2 complex numbers such that $|\alpha|^2 + |\beta|^2 = 1$. A useful tool to visualize the state of a qubit, and stress the difference with a classical bit, is the Bloch sphere [100–103]. This is a geometrical representation of any two-level system state as a three-dimensional real vector, which enables us to visualize it in the usual Cartesian space. Starting from the wavefunction defined in eq. (I.36), we can write the coefficients in such a way that they can be interpreted as a spherical coordinate system, namely

$$|q\rangle = e^{i\gamma}\left(\cos\frac{\theta}{2}|0\rangle + e^{i\varphi}\sin\frac{\theta}{2}|1\rangle\right) \tag{I.37}$$

where $\gamma, \theta, \varphi \in \mathbb{R}$. We can ignore the phase factor in front as it bears no observable

effects, and recognize θ and φ to define a point on a unit three-dimensional sphere, called the Bloch sphere. The qubit state can then be visualized as a vector of unit norm on the sphere, see Figure I.6. At the pole of the sphere, we have the original basis states, which we refer to as the *computational basis*, but we remark the other particular orthogonal basis states marked on the sphere in the figure. Identifying the vertical axis as the z axis, on the basis on the x axis is formed of states $\{|+\rangle, |-\rangle\}$ delocalized on the original basis, namely

$$|+\rangle = \frac{1}{\sqrt{2}}\begin{pmatrix}1\\1\end{pmatrix} = \frac{|0\rangle + |1\rangle}{\sqrt{2}}, \qquad |-\rangle = \frac{1}{\sqrt{2}}\begin{pmatrix}1\\-1\end{pmatrix} = \frac{|0\rangle - |1\rangle}{\sqrt{2}}, \tag{I.38}$$

and on the y axis, its complex version $\{|+i\rangle, |-i\rangle\}$

$$|+i\rangle = \frac{1}{\sqrt{2}}\begin{pmatrix}1\\i\end{pmatrix} = \frac{|0\rangle + i|1\rangle}{\sqrt{2}}, \qquad |-i\rangle = \frac{1}{\sqrt{2}}\begin{pmatrix}1\\-i\end{pmatrix} = \frac{|0\rangle - i|1\rangle}{\sqrt{2}}. \tag{I.39}$$

The choice of the axis is not accidental. Moving to the density matrix formalism enables us to clarify this choice, introduce fundamental operators in quantum computing, and expand the description to include mixed states. First, we can write the pure qubit state equivalently as the density matrix

$$\rho = \begin{pmatrix} a & b \\ b^* & 1-a \end{pmatrix} \tag{I.40}$$

thanks to Hermicity and constant unitary trace properties, and recognizing $a = |\alpha|^2$ and, for the pure state, $b = \alpha^*\beta$. This can be parametrized and decomposed in a form

$$\rho = \frac{1}{2}\left(\mathbb{1} + \sum_{j=x,y,z} \sigma_j v_j\right) = \frac{1}{2}\begin{pmatrix} 1+v_z & v_x - iv_y \\ v_x + iv_y & 1-v_z \end{pmatrix} \tag{I.41}$$

where σ_j are Pauli matrices, and we can recognize the Cartesian coordinates of the vector describing the qubit state, defining $\vec{v} = (v_x, v_y, v_z) \in \mathbb{R}^3$ the Bloch vector. The norm of this reflects the purity of the state, so that when the system is pure $\|v\| = 1$ and the vector points to the surface of the sphere. When the state is mixed, then $\|v\| < 1$, and the loss of purity leads to the vector pointing inside the volume of the sphere.

Pauli matrices are a set of Hermitian, traceless, involutory matrices, in the following,

$$\sigma_x = \begin{pmatrix} 0 & 1 \\ 1 & 0 \end{pmatrix}, \quad \sigma_y = \begin{pmatrix} 0 & -i \\ i & 0 \end{pmatrix}, \quad \sigma_z = \begin{pmatrix} 1 & 0 \\ 0 & -1 \end{pmatrix}, \tag{I.42}$$

with commutation relationship $[\sigma_j, \sigma_k] = 2i\epsilon_{jkl}\sigma_l$, where ϵ_{jkl} is the Ricci-Curbastro symbol (also referred to as the Levi-Civita symbol). Throughout the manuscript, we will indicate them as shown above, as they are commonly indicated in quantum physics, and for clarity, we recall that in quantum information science they are often indicated together with the identity as $\{I, X, Y, Z\}$ while in mathematics as $\{\sigma_0, \sigma_1, \sigma_2, \sigma_3\}$.

Pauli matrices are of clear importance as, together with the unity matrix and up to

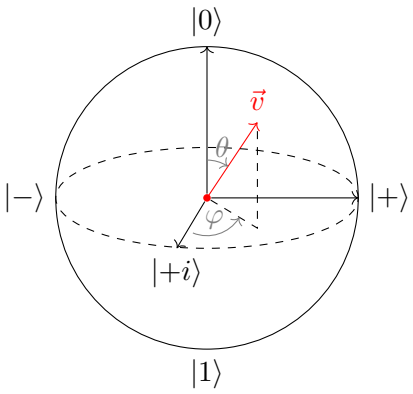

Figure I.6: Bloch sphere representation for a qubit state. A generic pure state is represented on the sphere by the vector $\vec{v}$.

multiplication with a constant $1/\sqrt{2}$ factor, they form an orthogonal basis of the qubit Liouville space $\mathcal{L}(\mathcal{H})$, where the eigenvectors of each matrix are the orthogonal basis sets $\{|+\rangle, |-\rangle\}$, $\{|+i\rangle, |-i\rangle\}$ and $\{|0\rangle, |1\rangle\}$, and since they are a complete set of Hermitian matrices, they span the space of observables of the qubit.

Importantly, we can also notice that when multiplied by the imaginary factor i they form a set of generators of unitary rotations on the Bloch sphere.[3] We can therefore write unitary rotation operators as

$$R_X(\theta) = e^{-i\theta\sigma_x/2} = \begin{pmatrix} \cos\frac{\theta}{2} & -i\sin\frac{\theta}{2} \\ -i\sin\frac{\theta}{2} & \cos\frac{\theta}{2} \end{pmatrix} \tag{I.43a}$$

$$R_Y(\theta) = e^{-i\theta\sigma_y/2} = \begin{pmatrix} \cos\frac{\theta}{2} & -\sin\frac{\theta}{2} \\ \sin\frac{\theta}{2} & \cos\frac{\theta}{2} \end{pmatrix} \tag{I.43b}$$

$$R_Z(\theta) = e^{-i\theta\sigma_z/2} = \begin{pmatrix} e^{-i\frac{\theta}{2}} & 0 \\ 0 & e^{-i\frac{\theta}{2}} \end{pmatrix} \tag{I.43c}$$

These will serve as one of the foundations to describe the evolution of the qubit system and the way to implement Hamiltonian dynamics.

Using the qubit as the building block, we can define the quantum computing unit, the *quantum register*, as the composition of multiple qubits, exploiting the second postulate of quantum mechanics introduced in eq. (I.12). Then, the wavefunction of the quantum register is

$$|\Psi^{\mathrm{QR}}\rangle = \bigotimes_{j=0}^{n-1} |q_j\rangle \tag{I.44a}$$

$$= |q_{n-1}\rangle \otimes |q_{n-2}\rangle \otimes \cdots \otimes |q_1\rangle \otimes |q_0\rangle \tag{I.44b}$$

$$= \sum_{l_i} c_{l_{n-1}\ldots l_0} |l_{n-1} l_{n-2} \ldots l_1 l_0\rangle, \quad l = 0, 1 \tag{I.44c}$$

[3] Pauli matrices are generators of a representation of the Lie algebra $\mathfrak{su}(2)$, isomorphic to $\mathfrak{so}(3)$, and are a representation of the Clifford algebra $\mathrm{Cl}(\mathbb{R}^3)$. After multiplication by the imaginary factor and exponentiation, they represent the basis of SU(2) and the rotations of SO(3).

where we show commonly used equivalent representations of the quantum register. The overall Hilbert space of the quantum computer is then $\mathcal{H} = (\mathbb{C}^2)^{\otimes n}$ for a register of n qubits, and the dimension of the computational base is 2^n, all the possible combination of $|l_{n-1} \dots l_0\rangle$, each weighted by its complex coefficient $c_{l_{n-1}\dots l_0}$, eventually storing a total of their 2^n amplitudes.

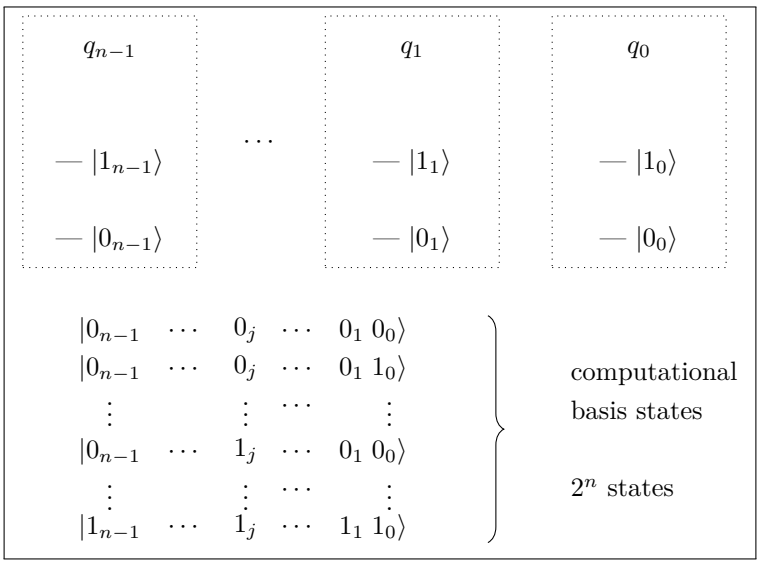

Now that we have defined the quantum system we are acting on, we need to be able to manipulate its state and to retrieve the results of our computation. The "instructions" to the DQC are *quantum gates*, in analogy to the logical gates in classical computing. These gates are linear unitary operators acting on the quantum register, and they are one of the two building blocks to transpose a *quantum algorithm* to a *quantum circuit*, the ordered sequence of gates applied to each qubit of the register. In theory, we can write our circuit with n-qubit gates, for example a unitary acting on the whole register or a simultaneous rotation of multiple qubits, yet in practice only one- and two-qubits gates are implemented: those that can be physically executed, and particularly those that form a set of *universal gates*. The circuit itself is therefore *transpiled*, i.e., rewritten in terms of executable gates and adapted to the topology of the specific quantum device.

The last element required to complete a quantum computation is a measurement. Measurements are projective operators, and they can be inserted in the quantum circuit as an element of the algorithm, and they are the only non-unitary operation allowed in a QC. Most importantly, they are the conclusion of any quantum circuit: the state of the whole quantum register is measured, and it represents the solution of the algorithm.

To conclude, we remark and expand the discussion on several key points. In quantum computing, we exploit intrinsic features that are not shared by classical information: randomness, uncertainty, and entanglement. In what follows, we will set aside the second peculiar feature and focus on the first and the last. The former underlies the ideas we will exploit and introduce, and can be either seen as a resource or as a problem to overcome. In many applications - such as quantum random number generation [104, 105], quantum cryptography [106, 107], and quantum key distribution [108, 109] - the randomness of the

projective outcome is a key feature exploited fruitfully.

In contrast, for other applications involving the characterization of some quantity encoded in the register - such as the study of quantum systems and their dynamics - the randomness of the measurement outcome, which collapses the register, is detrimental. Due to the probabilistic nature of quantum mechanics, we need to perform multiple measurements and repetitions of the circuit to recover statistical information about the density matrix; eventually, if one wants to know the state completely (a procedure known as quantum state tomography), this leads to the problem of requiring an exponential scaling number of measurements $\mathcal{O}(4^n)$ to sample correctly all the states of the register [110, 111].

Entanglement, on the other hand, is the key strength allowing for quantum computations. Indeed, if we were to use only separable states, only $2n$ complex numbers can be stored, therefore scaling as a classical computer. It is only through highly entangled states, spanning the full computational basis of the register, that we can access the Hilbert-space structure enabling the exponential scaling needed for QC speed-up.

However, soon after the earliest proposals for quantum computing, P. Benioff concerned himself about the issue of decoherence and dissipation in quantum systems, phenomena that destroy coherences and entanglement, thereby undermining the functioning of quantum processors [112, 113]. This problem has been discussed and emphasized later, most notably by R. Landauer [114–116] and others [117, 118], and remains an open problem [119, 120] despite substantial progress [12, 58, 121–124].

Today's QCs are known as noisy intermediate-scale quantum (NISQ) devices [56–58], as they are limited to a maximum of a few hundred qubits,[4] with incomplete connectivity, preventing arbitrary pairs of qubits from being directly entangled, and they have a non-negligible interaction with their environment, causing dissipation and limiting the coherence time of the quantum processor. Nevertheless, NISQ devices have already shown some notable results and promises of further real-life applications [12, 56, 125–129]. A wide variety of experimentally controllable systems have been proposed for realizing qubits and quantum registers [94, 130], from the most used superconducting circuits [131, 132], to arrays of trapped ions [133–135], atoms in optical lattices and atoms in arrays of cavities [136–138], photons [139–142], and many others [94, 143–145].

These constraints pose significant challenges for both physicists and engineers, who aim to develop architectures and control strategies capable of mitigating noise and enabling scalable quantum computation.

For theorists, this motivates the development of models and methodologies that address noise at a fundamental level as a fundamental component of the dynamics, improving the theoretical understanding and the effective description of open quantum system dynamics, and their controlled manipulation, either by exploiting its structure or by systematically counteracting its effects.

[4]The latest IBM quantum processor, Nighthawk, is composed of 120 qubits, while the previous version, Heron, of 156 qubits but with less connectivity. Note that larger processors exist, such as IBM Condor (1121 qubits), Atom Computing AC1000 (1125 qubits), but connectivity and control limitations render their practical performance comparable to, or below, that of smaller architectures.

I.4 Structure of the thesis

The thesis structure can be organized along two complementary lines: as the ordinary sequence of Chapters and a conceptual map linking non-adjacent Chapters through shared ideas and applications.

Chapters I and II provide the general introduction and preliminaries. After the general introduction given in this Chapter, Chapter II is dedicated to the description of the reduced dynamics of open quantum systems, presenting an overview of the main forms of quantum master equations, and the routes to obtain them. This chapter further establishes the language and notation, highlighting the signatures of each form and the approximations underlying them. The subsequent Chapters III and IV main focus is on the use of stochastic approaches to the dynamics of open quantum systems.

In Chapter III (adapted from our publication [146]), we discuss the family of stochastic Hamiltonian methods, showing how different approaches and frameworks can be recast as stochastic Hamiltonians, and how each formulation naturally maps to distinct numerical workflows, amenable to efficient classical trajectory integration or to quantum-algorithmic implementations, providing a useful toolkit for the simulation of open-system.

Chapter IV (based on our paper [147]), extends on the unraveling of correlated quantum master equations, employing a generalization of stochastic Schrödinger equations and introducing memory effects via a non-standard noise drive. This generalization leads to open-form master equations, in particular to a correlated QME, whose solutions require numerical integration over ensembles of trajectories and their averages. Using a two-level system as an example, we show how a cross-correlation term arising in the correlated master equation affects the coherence relaxation time. We observe the emergence of multiple dissipation time scales and the formation of a robust coherent steady state, depending on the noise correlation time, intensity, and the system's symmetry properties. While Chapter IV naturally follows Chapter III, the interpretation of the nontrivial features of the dynamics is addressed by reconnecting to the microscopic derivation of master equations introduced in Chapter II. We propose and analyze a microscopic-inspired model for the correlation contributions appearing in the SSE formulation. The resulting link between the Redfield-like derivation and the colored SSE allows us to provide a microscopic interpretation of the dynamics obtained from direct numerical simulations of the latter.

Chapter V hinges on the stochastic approach to the open quantum dynamics to recover additional information about their characteristic properties. Along with a comparison of known metrics and descriptors, we show how we access information encoded in each realization, and building on a correct metric of the quantum state space, we propose quantitative descriptors inferred from the stochastic unraveling.

Finally, in Chapter VI we exploit the formalism discussed in Chapter III to discuss the implementation of open quantum dynamics in digital quantum computers, showing how stochastic Hamiltonian dynamics naturally map onto quantum simulators. We formally analyze the convergence of a quantum algorithm in terms of computational effort, demonstrating how the intrinsic probabilistic nature of quantum measurements is not detrimental for this class of algorithms.

Beyond the immediate Chapter sequence, we can connect the arguments of this thesis conceptually beyond the immediate chapter sequence, see Figure I.7. Chapters II and III establish the basis of the theory of open quantum systems underlying the subsequent discussions. Chapters III and VI follow the line of thought of *quantum computers for* open quantum systems, using quantum computers to simulate open-system dynamics within a trajectory-based framework that explicitly avoids Hilbert space dilation and naturally allows for structured environments driving. On the other hand, Chapters IV and V focus on non-standard environments and their effect to the dynamics, showing how the study and characterization of such environments can lead to strategies improving coherence robustness *for quantum computing* implementations.

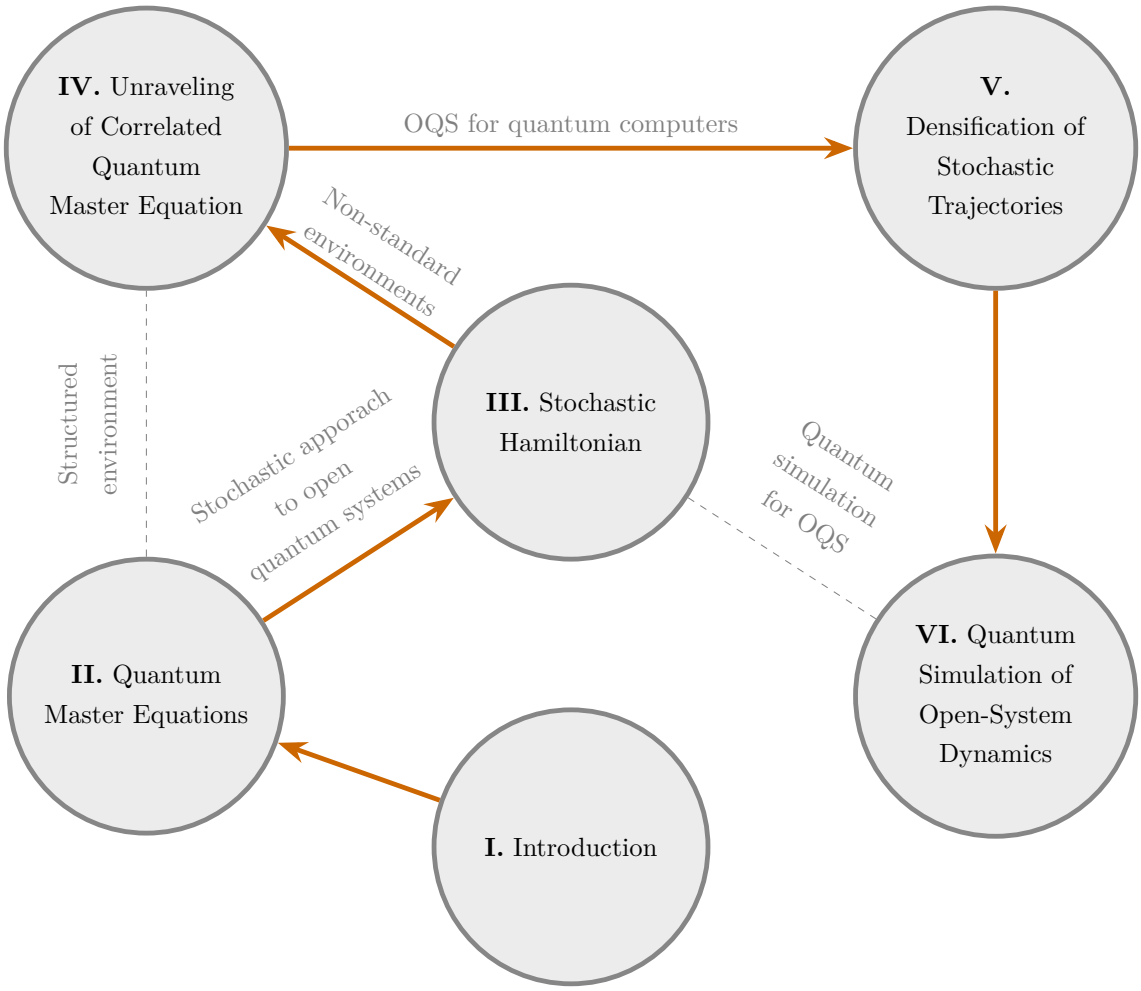

Figure I.7: Graphical structure of the thesis and thematic connections between Chapters.

I.5 Publications

Part of the research presented in this thesis has appeared in peer-reviewed publications, while additional results are currently in preparation or are intended to form the basis of future papers. This section provides a concise overview of these works, their current status, and the author's specific contributions.

The material contained in Chapter III and in the first Section of Chapter VI have been published in *"On the Noisy Road to Open Quantum Dynamics: The Place of Stochastic Hamiltonians"*, **Annalen der Physik 538**, *e00482 (2026)* [146]. The results discussed in Chapter IV are reported in the manuscript *"Quantum trajectories and reduced dynamics in time-correlated environments"*, available as a preprint on the ArXiv [147], submitted to the **Journal of Chemical Physics** and currently under review. Overall, these works arise directly from the doctoral research and collectively represent its main scientific outcomes. Where published material is included in the thesis, it has been adapted and expanded to ensure coherence of presentation, and clearly referenced.

Beyond these published and submitted works, further developments presented in this thesis are the basis for ongoing and future research outputs. In particular, the final part of Chapter IV is being developed and extended into a manuscript currently in preparation. Chapter 5 presents a broader framework whose results are expected to lead to at least one dedicated publication, currently under investigation with Prof. B. Fresch and Dr. F. Campaioli. Additionally, selected aspects of Chapter 6 are being considered for inclusion in future articles, potentially in combination with further developments.

Regarding individual contributions, the author was responsible for developing the theoretical framework, implementing the numerical methods, and analyzing and interpreting the results across all works described above. The co-authors contributed through conceptual guidance, discussion of the results, and revision of the manuscripts.

In addition, the research carried out in this thesis led to the development of computational tools and algorithms for SSE implementation, QME limits and closure models, and the analysis of the results. These implementations are publicly available at [148], to support reproducibility and further applications.

References

[1] V. Venkatasubramanian, "Celebrating the Birth Centenary of Quantum Mechanics: A Historical Perspective", Industrial & Engineering Chemistry Research **64**, 9443–9456 (2025) 10.1021/ACS.IECR.5C00942

[2] D. Bruß, "Editorial: Celebrating the First Century of Quantum Physics and Preparing for the Next One", Physical Review Letters **134**, 150001 (2025) 10.1103/PhysRevLett.134.150001

[3] "Quantum mechanics 100 years on: an unfinished revolution", Nature **637**, 251–252 (2025) 10.1038/D41586-025-00014-5

[4] W. Heisenberg, "Über quantentheoretische Umdeutung kinematischer und mechanischer Beziehungen.", Zeitschrift für Physik **33**, 879–893 (1925) 10.1007/BF01328377

[5] E. Schrödinger, "Quantisierung als Eigenwertproblem", Annalen der Physik **384**, 361–376 (1926) 10.1002/ANDP.19263840404

[6] E. Schrödinger, "An Undulatory Theory of the Mechanics of Atoms and Molecules", Physical Review **28**, 1049 (1926) 10.1103/PhysRev.28.1049

[7] I. H. Deutsch, "Harnessing the Power of the Second Quantum Revolution", PRX Quantum **1**, 020101 (2020) 10.1103/PRXQuantum.1.020101

[8] S. Satanassi and O. Levrini, "Second quantum revolution: The progressive design of an approach to value its cultural and conceptual scope", Physical Review Physics Education Research **21**, 010112 (2025) 10.1103/PhysRevPhysEducRes.21.010112

[9] A. Celi, A. Sanpera, V. Ahufinger, and M. Lewenstein, "Quantum optics and frontiers of physics: the third quantum revolution", Physica Scripta **92**, 013003 (2016) 10.1088/1402-4896/92/1/013003

[10] K. Korzekwa and M. Lostaglio, "Quantum Advantage in Simulating Stochastic Processes", Physical Review X **11**, 021019 (2021) 10.1103/PhysRevX.11.021019/

[11] F. Arute, K. Arya, R. Babbush, D. Bacon, J. C. Bardin, R. Barends, R. Biswas, S. Boixo, F. G. Brandao, D. A. Buell, B. Burkett, Y. Chen, Z. Chen, B. Chiaro, R. Collins, W. Courtney, A. Dunsworth, E. Farhi, B. Foxen, A. Fowler, C. Gidney, M. Giustina, R. Graff, K. Guerin, S. Habegger, M. P. Harrigan, M. J. Hartmann, A. Ho, M. Hoffmann, T. Huang, T. S. Humble, S. V. Isakov, E. Jeffrey, Z. Jiang, D. Kafri, K. Kechedzhi, J. Kelly, P. V. Klimov, S. Knysh, A. Korotkov, F. Kostritsa, D. Landhuis, M. Lindmark, E. Lucero, D. Lyakh, S. Mandrà, J. R. McClean, M. McEwen, A. Megrant, X. Mi, K. Michielsen, M. Mohseni, J. Mutus, O. Naaman, M. Neeley, C. Neill, M. Y. Niu, E. Ostby, A. Petukhov, J. C. Platt, C. Quintana, E. G. Rieffel, P. Roushan, N. C. Rubin, D. Sank, K. J. Satzinger, V. Smelyanskiy, K. J. Sung, M. D. Trevithick, A. Vainsencher, B. Villalonga, T. White, Z. J. Yao, P. Yeh, A. Zalcman, H. Neven, and J. M. Martinis, "Quantum supremacy using a programmable superconducting processor", Nature **574**, 505–510 (2019) 10.1038/S41586-019-1666-5

[12] Y. Kim, A. Eddins, S. Anand, K. X. Wei, E. van den Berg, S. Rosenblatt, H. Nayfeh, Y. Wu, M. Zaletel, K. Temme, and A. Kandala, "Evidence for the utility of quantum computing before fault tolerance", Nature **618**, 500–505 (2023) 10.1038/S41586-023-06096-3

[13]Y. Wu, W. S. Bao, S. Cao, F. Chen, M. C. Chen, X. Chen, T. H. Chung, H. Deng, Y. Du, D. Fan, M. Gong, C. Guo, C. Guo, S. Guo, L. Han, L. Hong, H. L. Huang, Y. H. Huo, L. Li, N. Li, S. Li, Y. Li, F. Liang, C. Lin, J. Lin, H. Qian, D. Qiao, H. Rong, H. Su, L. Sun, L. Wang, S. Wang, D. Wu, Y. Xu, K. Yan, W. Yang, Y. Yang, Y. Ye, J. Yin, C. Ying, J. Yu, C. Zha, C. Zhang, H. Zhang, K. Zhang, Y. Zhang, H. Zhao, Y. Zhao, L. Zhou, Q. Zhu, C. Y. Lu, C. Z. Peng, X. Zhu, and J. W. Pan, "Strong Quantum Computational Advantage Using a Superconducting Quantum Processor", Physical Review Letters **127**, 180501 (2021) 10.1103/PhysRevLett.127.180501

[14]L. S. Madsen, F. Laudenbach, M. F. Askarani, F. Rortais, T. Vincent, J. F. Bulmer, F. M. Miatto, L. Neuhaus, L. G. Helt, M. J. Collins, A. E. Lita, T. Gerrits, S. W. Nam, V. D. Vaidya, M. Menotti, I. Dhand, Z. Vernon, N. Quesada, and J. Lavoie, "Quantum computational advantage with a programmable photonic processor", Nature **606**, 75–81 (2022) 10.1038/S41586-022-04725-X

[15]Y. Liu, Y. Chen, C. Guo, J. Song, X. Shi, L. Gan, W. Wu, W. Wu, H. Fu, X. Liu, D. Chen, Z. Zhao, G. Yang, and J. Gao, "Verifying Quantum Advantage Experiments with Multiple Amplitude Tensor Network Contraction", Physical Review Letters **132**, 030601 (2024) 10.1103/PhysRevLett.132.030601

[16]J. Tindall, M. Fishman, E. M. Stoudenmire, and D. Sels, "Efficient Tensor Network Simulation of IBM's Eagle Kicked Ising Experiment", PRX Quantum **5**, 010308 (2024) 10.1103/PRXQuantum.5.010308

[17]R. LaRose, "A brief history of quantum vs classical computational advantage", (2024)

[18]H.-P. Breuer and F. Petruccione, *The Theory of Open Quantum Systems*, 1st ed. (Oxford University Press, Oxford, Jan. 2002), 10.1093/acprof:oso/9780199213900.001.0001

[19]B. Vacchini, *Open Quantum Systems: Foundations and Theory* (Springer Cham, Dec. 2024), 10.1007/978-3-031-58218-9

[20]A. U. Rahman, N. Zidan, S. M. Zangi, and H. Ali, "Quantum memory assisted entropic uncertainty and entanglement dynamics: Two qubits coupled with local fields and Ornstein Uhlenbeck noise", 10.48550/arXiv.2111.11312 (2021) 10.48550/arXiv.2111.11312

[21]E. P. Butler, G. E. Fux, C. Ortega-Taberner, B. W. Lovett, J. Keeling, and P. R. Eastham, "Optimizing Performance of Quantum Operations with Non-Markovian Decoherence: The Tortoise or the Hare", Physical Review Letters **132**, 060401 (2024) 10.1103/PhysRevLett.132.060401

[22]M. Cattaneo, M. A. Rossi, G. García-Pérez, R. Zambrini, and S. Maniscalco, "Quantum Simulation of Dissipative Collective Effects on Noisy Quantum Computers", PRX Quantum **4**, 010324 (2023) 10.1103/PRXQuantum.4.010324

[23]F. Verstraete, M. M. Wolf, and J. Ignacio Cirac, "Quantum computation and quantum-state engineering driven by dissipation", Nature Physics 2009 5:9 **5**, 633–636 (2009) 10.1038/nphys1342

[24]D. Braun, "Creation of Entanglement by Interaction with a Common Heat Bath", Physical Review Letters **89**, 277901 (2002) 10.1103/PhysRevLett.89.277901

[25]F. Pastawski, L. Clemente, and J. I. Cirac, "Quantum memories based on engineered dissipation", Physical Review A **83**, 012304 (2011) 10.1103/PhysRevA.83.012304

[26]K. Fujii and K. Nakajima, "Harnessing Disordered-Ensemble Quantum Dynamics for Machine Learning", Physical Review Applied **8**, 024030 (2017) 10.1103/PhysRevApplied.8.024030

[27]J. Chen and H. I. Nurdin, "Learning nonlinear input–output maps with dissipative quantum systems", Quantum Information Processing **18**, 1–36 (2019) 10.1007/S11128-019-2311-9

[28]A. Sannia, R. Martínez-Peña, M. C. Soriano, G. L. Giorgi, and R. Zambrini, "Dissipation as a resource for Quantum Reservoir Computing", Quantum **8**, 1291 (2024) 10.22331/q-2024-03-20-1291

[29]M. B. Plenio and S. F. Huelga, "Dephasing-assisted transport: quantum networks and biomolecules", New Journal of Physics **10**, 113019 (2008) 10.1088/1367-2630/10/11/113019

[30]P. Rebentrost, M. Mohseni, I. Kassal, S. Lloyd, and A. Aspuru-Guzik, "Environment-assisted quantum transport", New Journal of Physics **11**, 033003 (2009) 10.1088/1367-2630/11/3/033003

[31]C. Uchiyama, W. J. Munro, and K. Nemoto, "Environmental engineering for quantum energy transport", npj Quantum Information 2018 4:1 **4**, 1–7 (2018) 10.1038/s41534-018-0079-x

[32]J. M. Jauch, E. P. Wigner, and M. M. Yanase, *Part I: Particles and Fields. Part II: Foundations of Quantum Mechanics*, edited by A. S. Wightman, 1st ed. (Springer Berlin Heidelberg, Berlin, Heidelberg, 1997), pp. 475–482, 10.1007/978-3-662-09203-3

[33]J. M. Jauch, E. P. Wigner, and M. M. Yanase, "Some Comments Concerning Measurements in Quantum Mechanics", in *Part i: particles and fields. part ii: foundations of quantum mechanics* (Springer Berlin Heidelberg, Berlin, Heidelberg, 1997), pp. 475–482

[34]D. A. Lidar, *Lecture Notes on the Theory of Open Quantum Systems*, Los Angeles, Feb. 2019

[35]H. van Amerongen, R. van Grondelle, and L. Valkunas, *Photosynthetic Excitons* (WORLD SCIENTIFIC, June 2000), 10.1142/3609

[36]V. May and O. Kühn, *Charge and Energy Transfer Dynamics in Molecular Systems*, Third (Wiley-VCH, 2011)

[37]A. S. Davydov, *Theory of Molecular Excitons* (Springer US, 1971), 10.1007/978-1-4899-5169-4

[38]G. D. Scholes and G. Rumbles, *Excitons in nanoscale systems*, Sept. 2006, 10.1038/nmat1710

[39]J. A. Gyamfi, "Fundamentals of quantum mechanics in Liouville space", European Journal of Physics **41**, 063002 (2020) 10.1088/1361-6404/AB9FDD

[40]Y. Tanimura and R. Kubo, "Time Evolution of a Quantum System in Contact with a Nearly Gaussian-Markovian Noise Bath", Journal of the Physical Society of Japan **58**, 101–114 (1989)

[41]Y. Tanimura, "Nonperturbative expansion method for a quantum system coupled to a harmonic-oscillator bath", Physical Review A **41**, 6676 (1990) 10.1103/PhysRevA.41.6676

[42]Y. Tanimura, "Numerically "exact" approach to open quantum dynamics: The hierarchical equations of motion (HEOM)", Journal of Chemical Physics **153**, 10.1063/5.0011599 (2020) 10.1063/5.0011599

[43]A. H. Werner, D. Jaschke, P. Silvi, M. Kliesch, T. Calarco, J. Eisert, and S. Montangero, "Positive Tensor Network Approach for Simulating Open Quantum Many-Body Systems", Physical Review Letters **116**, 237201 (2016) 10.1103/PHYSREVLETT.116.237201

[44]T. Lacroix, B. L. Dé, A. Riva, A. J. Dunnett, and A. W. Chin, "MPSDynamics.jl: Tensor network simulations for finite-temperature (non-Markovian) open quantum system dynamics", Journal of Chemical Physics **161**, 84116 (2024) 10.1063/5.0223107/3310130

[45]M. Cygorek, M. Cosacchi, A. Vagov, V. M. Axt, B. W. Lovett, J. Keeling, and E. M. Gauger, "Simulation of open quantum systems by automated compression of arbitrary environments", Nature Physics 2022 18:6 **18**, 662–668 (2022) 10.1038/s41567-022-01544-9

[46]A. G. Redfield, "On the Theory of Relaxation Processes", IBM Journal of Research and Development **1**, 19–31 (1957) 10.1147/rd.11.0019

[47]A. G. Redfield, "The Theory of Relaxation Processes", Advances in Magnetic and Optical Resonance **1**, 1–32 (1965) 10.1016/B978-1-4832-3114-3.50007-6

[48]G. Lindblad, "Mathematical Physics On the Generators of Quantum Dynamical Semigroups", Communications in Mathematical Physics **48**, 119–130 (1976)

[49]V. Gorini, A. Kossakowski, and E. C. Sudarshan, "Completely positive dynamical semigroups of N-level systems", Journal of Mathematical Physics **17**, 821 (1976) 10.1063/1.522979

[50]D. Manzano, "A short introduction to the Lindblad master equation", AIP Advances **10**, 025106 (2020) 10.1063/1.5115323

[51]P. W. Anderson, "A Mathematical Model for the Narrowing of Spectral Lines by Exchange or Motion", Journal of the Physical Society of Japan **9**, 316–339 (1954) 10.1143/JPSJ.9.316

[52]R. Kubo and K. Tomita, "A General Theory of Magnetic Resonance Absorption", Journal of the Physical Society of Japan **9**, 888–919 (1954) 10.1143/JPSJ.9.888

[53]R. Kubo, "Stochastic Liouville Equations", Journal of Mathematical Physics **4**, 174–183 (1963) 10.1063/1.1703941

[54]H. Haken and G. Strobl, "An exactly solvable model for coherent and incoherent exciton motion", Zeitschrift für Physik **262**, 135–148 (1973) 10.1007/BF01399723

[55]F. Šanda and S. Mukamel, "Stochastic Liouville Equations for Coherent Multidimensional Spectroscopy of Excitons", Journal of Physical Chemistry B **112**, 14212–14220 (2008) 10.1021/JP801457C

[56]J. Preskill, "Quantum Computing in the NISQ era and beyond", Quantum **2**, 79 (2018) 10.22331/q-2018-08-06-79

[57]S. Brandhofer, S. Devitt, T. Wellens, and I. Polian, "Special session: Noisy intermediate-scale quantum (NISQ) Computers - How they work, how they fail, how to test them?", Proceedings of the IEEE VLSI Test Symposium **2021-April**, 10.1109/VTS50974.2021.9441047 (2021) 10.1109/VTS50974.2021.9441047

[58]K. Bharti, A. Cervera-Lierta, T. H. Kyaw, T. Haug, S. Alperin-Lea, A. Anand, M. Degroote, H. Heimonen, J. S. Kottmann, T. Menke, W. K. Mok, S. Sim, L. C. Kwek, and A. Aspuru-Guzik, "Noisy intermediate-scale quantum algorithms", Reviews of Modern Physics **94**, 015004 (2022) 10.1103/RevModPhys.94.015004

[59]R. J. De Keijzer, L. Y. Visser, O. Tse, and S. J. Kokkelmans, "Qubit fidelity distribution under stochastic Schrödinger equations driven by classical noise", Physical Review Research **7**, 023063 (2025) 10.1103/PHYSREVRESEARCH.7.023063

[60]A. Baratz, L. M. Cangemi, A. Hamo, S. Refaely-Abramson, and A. Levy, "Data-Driven Reconstruction and Characterization of Stochastic Dynamics via Dynamical Mode Decomposition", (2025)

[61]S. Cialdi, M. A. Rossi, C. Benedetti, B. Vacchini, D. Tamascelli, S. Olivares, and M. G. Paris, "All-optical quantum simulator of qubit noisy channels", Applied Physics Letters **110**, 81107 (2017) 10.1063/1.4977023

[62]S. Cialdi, C. Benedetti, D. Tamascelli, S. Olivares, M. G. Paris, and B. Vacchini, "Experimental investigation of the effect of classical noise on quantum non-Markovian dynamics", Physical Review A **100**, 052104 (2019) 10.1103/PhysRevA.100.052104

[63]Q. Huang and M. Merkli, "Qubit dynamics with classical noise", Physics Open **5**, 100043 (2020) 10.1016/J.PHYSO.2020.100043

[64]R. Biele and R. Dagosta, "A stochastic approach to open quantum systems", Journal of Physics: Condensed Matter **24**, 273201 (2012) 10.1088/0953-8984/24/27/273201

[65]A. Barchielli and M. Gregoratti, *Quantum Trajectories and Measurements in Continuous Time: The Diffusive Case, Lect. Notes Phys. 782* (Springer, Berlin Heidelberg, 2009), 10.1007/978-3-642-01298-3

[66]N. Gisin, "Quantum Measurements and Stochastic Processes", Physical Review Letters **52**, 1657 (1984) 10.1103/PhysRevLett.52.1657

[67]A. Barchielli and V. P. Belavkin, "Measurements continuous in time and a posteriori states in quantum mechanics", Journal of Physics A: Mathematical and General **24**, 1495 (1991) 10.1088/0305-4470/24/7/022

[68]L. Diósi, "Continuous quantum measurement and itô formalism", Physics Letters A **129**, 419–423 (1988) 10.1016/0375-9601(88)90309-X

[69]L. Diósi, "Localized solution of a simple nonlinear quantum Langevin equation", Physics Letters A **132**, 233–236 (1988) 10.1016/0375-9601(88)90555-5

[70]N. Gisin and I. C. Percival, "The quantum-state diffusion model applied to open systems", Journal of Physics A: Mathematical and General **25**, 5677 (1992) 10.1088/0305-4470/25/21/023

[71]H. J. Carmichael, *An Open Systems Approach to Quantum Optics, Lect. Notes in Phys. Monogr. 18*, edited by W. Beiglböck (Springer Berlin, Heidelberg, 1993), https://doi.org/10.1007/978-3-540-47620-7

[72]K. Jacobs and D. A. Steck, "A Straightforward Introduction to Continuous Quantum Measurement", Contemporary Physics **47**, 279–303 (2006) 10.1080/00107510601101934

[73]R. P. Feynman and F. L. Vernon, "The theory of a general quantum system interacting with a linear dissipative system", Annals of Physics **24**, 118–173 (1963) 10.1016/0003-4916(63)90068-X

[74]H. Grabert, P. Schramm, and G. L. Ingold, "Quantum Brownian motion: The functional integral approach", Physics Reports **168**, 115–207 (1988) 10.1016/0370-1573(88)90023-3

[75]L. Diósi and W. T. Strunz, "The non-Markovian stochastic Schrödinger equation for open systems", Physics Letters A **235**, 569–573 (1997) 10.1016/S0375-9601(97)00717-2

[76]L. Diósi, N. Gisin, and W. T. Strunz, "Non-Markovian quantum state diffusion", Physical Review A **58**, 1699 (1998) 10.1103/PhysRevA.58.1699

[77]J. T. Stockburger and H. Grabert, "Non-Markovian quantum state diffusion", Chemical Physics **268**, 249–256 (2001) 10.1016/S0301-0104(01)00307-X

[78]D. Suess, A. Eisfeld, and W. T. Strunz, "Hierarchy of stochastic pure states for open quantum system dynamics", Physical Review Letters **113**, 150403 (2014) 10.1103/PHYSREVLETT.113.150403

[79]L. Stella, C. D. Lorenz, and L. Kantorovich, "Generalized Langevin equation: An efficient approach to nonequilibrium molecular dynamics of open systems", Physical Review B **89**, 134303 (2014) 10.1103/PhysRevB.89.134303

[80]H. Ness, L. Stella, C. D. Lorenz, and L. Kantorovich, "Applications of the generalized Langevin equation: Towards a realistic description of the baths", Physical Review B **91**, 014301 (2015) 10.1103/PhysRevB.91.014301

[81]D. Matos, M. A. Lane, I. J. Ford, and L. Kantorovich, "Efficient choice of colored noise in the stochastic dynamics of open quantum systems", Physical Review E **102**, 062134 (2020) 10.1103/PhysRevE.102.062134

[82]J. T. Stockburger and H. Grabert, "Exact c-number representation of non-Markovian quantum dissipation", Physical Review Letters **88**, 1704071–1704074 (2002) 10.1103/PhysRevLett.88.170407

[83]G. M. McCaul, C. D. Lorenz, and L. Kantorovich, "Partition-free approach to open quantum systems in harmonic environments: An exact stochastic Liouville equation", Physical Review B **95**, 125124 (2017) 10.1103/PhysRevB.95.125124

[84]L. Magazzù and M. Grifoni, "Feynman-Vernon influence functional approach to quantum transport in interacting nanojunctions: An analytical hierarchical study", Physical Review B **105**, 125417 (2022) 10.1103/PHYSREVB.105.125417

[85]E. Coccia, F. Troiani, and S. Corni, "Probing quantum coherence in ultrafast molecular processes: An ab initio approach to open quantum systems", The Journal of Chemical Physics **148**, 10.1063/1.5022976 (2018) 10.1063/1.5022976

[86]G. Dall'Osto, M. Vanzan, S. Corni, M. Marsili, and E. Coccia, "Stochastic Schrödinger equation for hot-carrier dynamics in plasmonic systems", The Journal of Chemical Physics **161**, 10.1063/5.0221179 (2024) 10.1063/5.0221179

[87]R. P. Feynman, "Simulating Physics with Computers", International Journal of Theoretical Physics **21** (1982)

[88]D. Deutsch, "Quantum theory, the Church–Turing principle and the universal quantum computer", Proceedings of The Royal Society of London, Series A: Mathematical and Physical Sciences **400**, 97–117 (1985) 10.1098/RSPA.1985.0070

[89]E. Bernstein and U. Vazirani, "Quantum Complexity Theory", SIAM Journal on Computing **26**, 1411–1473 (2006) 10.1137/S0097539796300921

[90]A. Church, "An Unsolvable Problem of Elementary Number Theory", American Journal of Mathematics **58**, 345 (1936) 10.2307/2371045

[91]A. M. Turing, "On Computable Numbers, with an Application to the Entscheidungsproblem", Proceedings of the London Mathematical Society **s2-42**, 230–265 (1936) 10.1112/PLMS/S2-42.1.230

[92]Y. I. Manin, *Vychislimoe i nevychislimoe [Computable and Uncomputable]* (Sovetskoye Radio, 1980)

[93]D. J. Thouless, *The Quantum Mechanics of Many-Body Systems*, Vol. 11 (Academic Press, London, 1961)

[94]I. Buluta and F. Nori, "Quantum simulators", Science **326**, 108–111 (2009) 10.1126/SCIENCE.1177838

[95]M. Zak, "Quantum Analog Computing", Chaos, Solitons & Fractals **10**, 1583–1620 (1999) 10.1016/S0960-0779(98)00215-X

[96]T. Kadowaki and H. Nishimori, "Quantum annealing in the transverse Ising model", Physical Review E **58**, 5355 (1998) 10.1103/PhysRevE.58.5355

[97]E. Farhi, J. Goldstone, S. Gutmann, and M. Sipser, "Quantum Computation by Adiabatic Evolution", (2000)

[98]H. Park, N. Heldman, P. Rebentrost, L. Abbondanza, A. Iagatti, A. Alessi, B. Patrizi, M. Salvalaggio, L. Bussotti, M. Mohseni, F. Caruso, H. C. Johnsen, R. Fusco, P. Foggi, P. F. Scudo, S. Lloyd, and A. M. Belcher, "Enhanced energy transport in genetically engineered excitonic networks", Nature Materials 2015 15:2 **15**, 211–216 (2015) 10.1038/nmat4448

[99]S. Lloyd, "Universal Quantum Simulators", Science **273**, 1073–1078 (1996) 10.1126/SCIENCE.273.5278.1073

[100]R. P. Feynman, F. L. Vernon, and R. W. Hellwarth, "Geometrical Representation of the Schrödinger Equation for Solving Maser Problems", Journal of Applied Physics **28**, 49–52 (1957) 10.1063/1.1722572

[101]F. T. Arecchi, E. Courtens, R. Gilmore, and H. Thomas, "Atomic Coherent States in Quantum Optics", Physical Review A **6**, 2211 (1972) 10.1103/PhysRevA.6.2211

[102]L. M. Narducci, C. A. Coulter, and C. M. Bowden, "Exact diffusion equation for a model for superradiant emission", Physical Review A **9**, 829 (1974) 10.1103/PhysRevA.9.829

[103]I. Bengtsson and K. Życzkowski, *Geometry of Quantum States: An Introduction to Quantum Entanglement*, 2nd ed. (Cambridge University Press, 2017)

[104]M. Herrero-Collantes and J. C. Garcia-Escartin, "Quantum random number generators", Reviews of Modern Physics **89**, 015004 (2017) 10.1103/RevModPhys.89.015004

[105]S. Pironio, A. Acín, S. Massar, A. B. De La Giroday, D. N. Matsukevich, P. Maunz, S. Olmschenk, D. Hayes, L. Luo, T. A. Manning, and C. Monroe, "Random numbers certified by Bell's theorem", Nature 2010 464:7291 **464**, 1021–1024 (2010) 10.1038/nature09008

[106]A. K. Ekert, "Quantum cryptography based on Bell's theorem", Physical Review Letters **67**, 661 (1991) 10.1103/PhysRevLett.67.661

[107]C. H. Bennett and G. Brassard, "An Update on Quantum Cryptography", Lecture Notes in Computer Science (including subseries Lecture Notes in Artificial Intelligence and Lecture Notes in Bioinformatics) **196 LNCS**, 475–480 (1985) 10.1007/3-540-39568-7{_}39

[108]C. H. Bennett and G. Brassard, "Quantum cryptography: Public key distribution and coin tossing", Theoretical Computer Science **560**, 7–11 (2014) 10.1016/J.TCS.2014.05.025

[109]H. W. Li, Z. Q. Yin, S. Wang, Y. J. Qian, W. Chen, G. C. Guo, and Z. F. Han, "Randomness determines practical security of BB84 quantum key distribution", Scientific Reports 2015 5:1 **5**, 16200– (2015) 10.1038/srep16200

[110]M. Paris and J. Řeháček, eds., *Quantum State Estimation*, Vol. 649, Lecture Notes in Physics (Springer Berlin Heidelberg, Berlin, Heidelberg, 2004), 10.1007/B98673

[111]M. Cramer, M. B. Plenio, S. T. Flammia, R. Somma, D. Gross, S. D. Bartlett, O. Landon-Cardinal, D. Poulin, and Y. K. Liu, "Efficient quantum state tomography", Nature Communications 2010 1:1 **1**, 149– (2010) 10.1038/ncomms1147

[112]J. Preskill, "Quantum Computing 40 Years Later", in *Feynman lectures on computation: anniversary edition*, edited by T. Hey, 2nd (CRC Press, Boca Raton, Jan. 2023), pp. 193–243, 10.1201/9781003358817-7

[113]P. Benioff, "The computer as a physical system: A microscopic quantum mechanical Hamiltonian model of computers as represented by Turing machines", Journal of Statistical Physics **22**, 563–591 (1980) 10.1007/BF01011339

[114]R. Landauer, "Information is Physical", Physics Today **44**, 23 (1991) 10.1063/1.881299

[115]R. Landauer, "Is quantum mechanics useful?", Philosophical Transactions of the Royal Society of London. Series A: Physical and Engineering Sciences **353**, 367–376 (1995) 10.1098/RSTA.1995.0106

[116]R. Landauer, "The physical nature of information", Physics Letters A **217**, 188–193 (1996) 10.1016/0375-9601(96)00453-7

[117]W. G. Unruh, "Maintaining coherence in quantum computers", Physical Review A **51**, 992 (1995) 10.1103/PhysRevA.51.992

[118]S. Haroche and J. M. Raimond, "Quantum computing: dream or nightmare?", Physics Today **49**, 50–51 (1996) 10.1063/1.881512

[119]M. Schlosshauer, "Decoherence and Quantum Computing", in *Decoherence and the quantum-to-classical transition* (Springer, Berlin, Heidelberg, July 2008), pp. 293–328, 10.1007/978-3-540-35775-9_7

[120]G. Massimo Palma, K. A. Suominen, and A. K. Ekert, "Quantum computers and dissipation", Proceedings of the Royal Society of London. Series A: Mathematical, Physical and Engineering Sciences **452**, 567–584 (1996) 10.1098/RSPA.1996.0029

[121]P. W. Shor, "Scheme for reducing decoherence in quantum computer memory", Physical Review A **52**, R2493 (1995) 10.1103/PhysRevA.52.R2493

[122]A. M. Steane, "Error Correcting Codes in Quantum Theory", Physical Review Letters **77**, 793 (1996) 10.1103/PhysRevLett.77.793

[123]T. E. O'Brien, G. Anselmetti, F. Gkritsis, V. E. Elfving, S. Polla, W. J. Huggins, O. Oumarou, K. Kechedzhi, D. Abanin, R. Acharya, I. Aleiner, R. Allen, T. I. Andersen, K. Anderson, M. Ansmann, F. Arute, K. Arya, A. Asfaw, J. Atalaya, J. C. Bardin, A. Bengtsson, G. Bortoli, A. Bourassa, J. Bovaird, L. Brill, M. Broughton, B. Buckley, D. A. Buell, T. Burger, B. Burkett, N. Bushnell, J. Campero, Z. Chen, B. Chiaro, D. Chik, J. Cogan, R. Collins, P. Conner, W. Courtney, A. L. Crook, B. Curtin, D. M. Debroy, S. Demura, I. Drozdov, A. Dunsworth, C. Erickson, L. Faoro, E. Farhi, R. Fatemi, V. S. Ferreira, L. Flores Burgos, E. Forati, A. G. Fowler, B. Foxen, W. Giang, C. Gidney, D. Gilboa, M. Giustina, R. Gosula, A. Grajales Dau, J. A. Gross, S. Habegger, M. C. Hamilton, M. Hansen, M. P. Harrigan, S. D. Harrington, P. Heu, M. R. Hoffmann, S. Hong, T. Huang, A. Huff, L. B. Ioffe, S. V. Isakov, J. Iveland, E. Jeffrey, Z. Jiang, C. Jones, P. Juhas, D. Kafri, T. Khattar, M. Khezri, M. Kieferová, S. Kim, P. V. Klimov, A. R. Klots, A. N. Korotkov, F. Kostritsa, J. M. Kreikebaum, D. Landhuis, P. Laptev, K. M. Lau, L. Laws, J. Lee, K. Lee, B. J. Lester, A. T. Lill, W. Liu, W. P. Livingston, A. Locharla, F. D. Malone, S. Mandrà, O. Martin, S. Martin, J. R. McClean, T. McCourt, M. McEwen, X. Mi, A. Mieszala, K. C. Miao, M. Mohseni, S. Montazeri, A. Morvan, R. Movassagh, W. Mruczkiewicz, O. Naaman, M. Neeley, C. Neill, A. Nersisyan, M. Newman, J. H. Ng, A. Nguyen, M. Nguyen, M. Y. Niu, S. Omonije, A. Opremcak, A. Petukhov, R. Potter, L. P. Pryadko, C. Quintana, C. Rocque, P. Roushan, N. Saei, D. Sank, K. Sankaragomathi, K. J. Satzinger, H. F. Schurkus, C. Schuster, M. J. Shearn, A. Shorter, N. Shutty, V. Shvarts, J. Skruzny, W. C. Smith, R. D. Somma, G. Sterling, D. Strain, M. Szalay, D. Thor, A. Torres, G. Vidal, B. Villalonga, C. Vollgraff Heidweiller, T. White, B. W. Woo, C. Xing, Z. J. Yao, P. Yeh, J. Yoo, G. Young, A. Zalcman, Y. Zhang, N. Zhu, N. Zobrist, D. Bacon, S. Boixo, Y. Chen, J. Hilton, J. Kelly, E. Lucero, A. Megrant, H. Neven, V. Smelyanskiy, C. Gogolin, R. Babbush, and N. C. Rubin, "Purification-based quantum error mitigation of pair-correlated electron simulations", Nature Physics **19**, 1787–1792 (2023) 10.1038/S41567-023-02240-Y

[124]F. Hu, S. A. Khan, N. T. Bronn, G. Angelatos, G. E. Rowlands, G. J. Ribeill, and H. E. Türeci, "Overcoming the coherence time barrier in quantum machine learning on temporal data", Nature Communications 2024 15:1 **15**, 7491– (2024) 10.1038/s41467-024-51162-7

[125]S. Boixo, S. V. Isakov, V. N. Smelyanskiy, R. Babbush, N. Ding, Z. Jiang, M. J. Bremner, J. M. Martinis, and H. Neven, "Characterizing quantum supremacy in near-term devices", Nature Physics 2018 14:6 **14**, 595–600 (2018) 10.1038/s41567-018-0124-x

[126]D. Main, P. Drmota, D. P. Nadlinger, E. M. Ainley, A. Agrawal, B. C. Nichol, R. Srinivas, G. Araneda, and D. M. Lucas, "Distributed quantum computing across an optical network link", Nature **638**, 383 (2025) 10.1038/S41586-024-08404-X

[127]M. Liu, R. Shaydulin, P. Niroula, M. DeCross, S. H. Hung, W. Y. Kon, E. Cervero-Martín, K. Chakraborty, O. Amer, S. Aaronson, A. Acharya, Y. Alexeev, K. J. Berg, S. Chakrabarti, F. J. Curchod, J. M. Dreiling, N. Erickson, C. Foltz, M. Foss-Feig, D. Hayes, T. S. Humble, N. Kumar, J. Larson, D. Lykov, M. Mills, S. A. Moses, B. Neyenhuis, S. Eloul, P. Siegfried, J. Walker, C. Lim, and M. Pistoia, "Certified randomness using a trapped-ion quantum processor", Nature **640**, 343 (2025) 10.1038/S41586-025-08737-1

[128]H. S. Zhong, H. Wang, Y. H. Deng, M. C. Chen, L. C. Peng, Y. H. Luo, J. Qin, D. Wu, X. Ding, Y. Hu, P. Hu, X. Y. Yang, W. J. Zhang, H. Li, Y. Li, X. Jiang, L. Gan, G. Yang, L. You, Z. Wang, L. Li, N. L. Liu, C. Y. Lu, and J. W. Pan, "Quantum computational advantage using photons", Science **370**, 1460–1463 (2020) 10.1126/Science.abe8770

[129]Y. Alexeev, D. Bacon, K. R. Brown, R. Calderbank, L. D. Carr, F. T. Chong, B. Demarco, D. Englund, E. Farhi, B. Fefferman, A. V. Gorshkov, A. Houck, J. Kim, S. Kimmel, M. Lange, S. Lloyd, M. D. Lukin, D. Maslov, P. Maunz, C. Monroe, J. Preskill, M. Roetteler, M. J. Savage, and J. Thompson, "Quantum Computer Systems for Scientific Discovery", PRX Quantum **2**, 017001 (2021) 10.1103/PRXQuantum.2.017001

[130]R. Van Meter and C. Horsman, "A blueprint for building a quantum computer", Communications of the ACM **56**, 84–93 (2013) 10.1145/2494568

[131]R. Barends, J. Kelly, A. Megrant, A. Veitia, D. Sank, E. Jeffrey, T. C. White, J. Mutus, A. G. Fowler, B. Campbell, Y. Chen, Z. Chen, B. Chiaro, A. Dunsworth, C. Neill, P. O'Malley, P. Roushan, A. Vainsencher, J. Wenner, A. N. Korotkov, A. N. Cleland, and J. M. Martinis, "Superconducting quantum circuits at the surface code threshold for fault tolerance", Nature 2014 508:7497 **508**, 500–503 (2014) 10.1038/nature13171

[132]H. L. Huang, D. Wu, D. Fan, and X. Zhu, "Superconducting quantum computing: a review", Science China Information Sciences 2020 63:8 **63**, 180501– (2020) 10.1007/S11432-020-2881-9

[133]C. J. Ballance, T. P. Harty, N. M. Linke, M. A. Sepiol, and D. M. Lucas, "High-Fidelity Quantum Logic Gates Using Trapped-Ion Hyperfine Qubits", Physical Review Letters **117**, 060504 (2016) 10.1103/PhysRevLett.117.060504

[134]P. Murali, D. M. Debroy, K. R. Brown, and M. Martonosi, "Architecting Noisy Intermediate-Scale Trapped Ion Quantum Computers", Proceedings - International Symposium on Computer Architecture **2020-May**, 529–542 (2020) 10.1109/ISCA45697.2020.00051

[135]D. Schwerdt, L. Peleg, Y. Shapira, N. Priel, Y. Florshaim, A. Gross, A. Zalic, G. Afek, N. Akerman, A. Stern, A. B. Kish, and R. Ozeri, "Scalable Architecture for Trapped-Ion Quantum Computing Using rf Traps and Dynamic Optical Potentials", Physical Review X **14**, 041017 (2024) 10.1103/PhysRevX.14.041017

[136]T. M. Graham, Y. Song, J. Scott, C. Poole, L. Phuttitarn, K. Jooya, P. Eichler, X. Jiang, A. Marra, B. Grinkemeyer, M. Kwon, M. Ebert, J. Cherek, M. T. Lichtman, M. Gillette, J. Gilbert, D. Bowman, T. Ballance, C. Campbell, E. D. Dahl, O. Crawford, N. S. Blunt, B. Rogers, T. Noel, and M. Saffman, "Multi-qubit entanglement and algorithms on a neutral-atom quantum computer", Nature 2022 604:7906 **604**, 457–462 (2022) 10.1038/s41586-022-04603-6

[137]G. Bornet, G. Emperauger, C. Chen, F. Machado, S. Chern, L. Leclerc, B. Gély, Y. T. Chew, D. Barredo, T. Lahaye, N. Y. Yao, and A. Browaeys, "Enhancing a Many-Body Dipolar Rydberg Tweezer Array with Arbitrary Local Controls", Physical Review Letters **132**, 263601 (2024) 10.1103/PhysRevLett.132.263601

[138]D. Bluvstein, S. J. Evered, A. A. Geim, S. H. Li, H. Zhou, T. Manovitz, S. Ebadi, M. Cain, M. Kalinowski, D. Hangleiter, J. P. Bonilla Ataides, N. Maskara, I. Cong, X. Gao, P. Sales Rodriguez, T. Karolyshyn, G. Semeghini, M. J. Gullans, M. Greiner, V. Vuletić, and M. D. Lukin, "Logical quantum processor based on reconfigurable atom arrays", Nature 2023 626:7997 **626**, 58–65 (2023) 10.1038/s41586-023-06927-3

[139]S. Slussarenko and G. J. Pryde, "Photonic quantum information processing: A concise review", Applied Physics Reviews **6**, 41303 (2019) 10.1063/1.5115814/997349

[140]J. Romero and G. Milburn, "Photonic Quantum Computing", Oxford Research Encyclopedia of Physics, 10.1093/acrefore/9780190871994.013.84 (2025) 10.1093/acrefore/9780190871994.013.84

[141]T. Giordani, F. Hoch, G. Carvacho, N. Spagnolo, and F. Sciarrino, "Integrated photonics in quantum technologies", La Rivista del Nuovo Cimento 2023 46:2 **46**, 71–103 (2023) 10.1007/S40766-023-00040-X

[142]H. Aghaee Rad, T. Ainsworth, R. N. Alexander, B. Altieri, M. F. Askarani, R. Baby, L. Banchi, B. Q. Baragiola, J. E. Bourassa, R. S. Chadwick, I. Charania, H. Chen, M. J. Collins, P. Contu, N. D'Arcy, G. Dauphinais, R. De Prins, D. Deschenes, I. Di Luch, S. Duque, P. Edke, S. E. Fayer, S. Ferracin, H. Ferretti, J. Gefaell, S. Glancy, C. González-Arciniegas, T. Grainge, Z. Han, J. Hastrup, L. G. Helt, T. Hillmann, J. Hundal, S. Izumi, T. Jaeken, M. Jonas, S. Kocsis, I. Krasnokutska, M. V. Larsen, P. Laskowski, F. Laudenbach, J. Lavoie, M. Li, E. Lomonte, C. E. Lopetegui, B. Luey, A. P. Lund, C. Ma, L. S. Madsen, D. H. Mahler, L. Mantilla Calderón, M. Menotti, F. M. Miatto, B. Morrison, P. J. Nadkarni, T. Nakamura, L. Neuhaus, Z. Niu, R. Noro, K. Papirov, A. Pesah, D. S. Phillips, W. N. Plick, T. Rogalsky, F. Rortais, J. Sabines-Chesterking, S. Safavi-Bayat, E. Sazhaev, M. Seymour, K. Rezaei Shad, M. Silverman, S. A. Srinivasan, M. Stephan, Q. Y. Tang, J. F. Tasker, Y. S. Teo, R. B. Then, J. E. Tremblay, I. Tzitrin, V. D. Vaidya, M. Vasmer, Z. Vernon, L. F. Villalobos, B. W. Walshe, R. Weil, X. Xin, X. Yan, Y. Yao, M. Zamani Abnili, and Y. Zhang, "Scaling and networking a modular photonic quantum computer", Nature 2025 638:8052 **638**, 912–919 (2025) 10.1038/s41586-024-08406-9

[143]E. Sebastian and R. C. Poonia, "Compendium of Qubit Technologies in Quantum Computing", Lecture Notes in Networks and Systems **686 LNNS**, 91–100 (2023) 10.1007/978-981-99-2100-3_8

[144]F. Toppan, "Braided Majorana qubits as a minimal ingredient for Topological Quantum Computation?", Proceedings of Proceedings of the Corfu Summer Institute 2024 "School and Workshops on Elementary Particle Physics and Gravity" — PoS(CORFU2024) **490**, 347 (2025) 10.22323/1.490.0347

[145]A. Tsintzis, R. S. Souto, K. Flensberg, J. Danon, and M. Leijnse, "Majorana Qubits and Non-Abelian Physics in Quantum Dot–Based Minimal Kitaev Chains", PRX Quantum **5**, 010323 (2024) 10.1103/PRXQuantum.5.010323

[146]P. De Checchi, F. Gallina, B. Fresch, and G. G. Giusteri, "On the Noisy Road to Open Quantum Dynamics: The Place of Stochastic Hamiltonians", Annalen der Physik **538**, e00482 (2026) 10.1002/ANDP.202500482

[147]P. De Checchi, F. Gallina, B. Fresch, and G. G. Giusteri, "Quantum trajectories and reduced dynamics in time-correlated environments", (2025), submitted.

[148]P. De Checchi, "NoMaCoN", GitHub repository, github.com/pietrodechecchi/NoMaCoN (2026)

Chapter II

Quantum Master Equations

The purpose of this Chapter is to establish the language that will be use thereafter, introducing the main forms of quantum master equations and providing an overview of common non-unitary mappings of the reduced density matrix of an open quantum system. Rather than presenting new results, the emphasis is placed on highlighting the approximations introduced in and underlying these descriptions, their characteristic signatures, and the limitations they entail, discussing well-known "variants". As anticipated in Chapter I.Introduction, quantum master equations (QME) may take different forms, and provide a general, approximate description of the reduced system dynamics. Two main routes leading to tractable QME forms will be discussed, corresponding to distinct theoretical perspectives: the Lindblad form and the Redfield microscopic approach. These approaches rely on different modeling assumptions for the environment and on different conceptual frameworks, yet both yield master equations that are linear and time-local in the system density matrix. Examining the domain of validity and the structural assumptions of these reduced models is instructive, as it highlights directions toward more general descriptions, which will be discussed using stochastic formulation extensions beyond the strictly Markovian regime, developed and exploited in the subsequent Chapters.

II.1 Completely positive trace preserving maps

Consider the total system, in the Hilbert space $\mathcal{H} = \mathcal{H}_{\mathcal{S}} \otimes \mathcal{H}_{\mathcal{B}}$, with unitary evolution described by the unitary propagator $U(t)$, the dynamics of the universe system is

$$\rho(t) = U(t)\rho(0)U^{\dagger}(t), \tag{II.1}$$

and tracing out the environment, as in eq. (I.32), the dynamics of the open system is

$$\rho_{\mathcal{S}}(t) = \mathrm{Tr}_{\mathcal{B}}\{U(t)\rho(0)U^{\dagger}(t)\} = \sum_{\mu\in\mathcal{H}_{\mathcal{B}}} \langle\mu|U(t)\rho(0)U^{\dagger}(t)|\mu\rangle \tag{II.2}$$

where $\{|\mu\rangle \perp^1 \mathcal{H}_{\mathcal{B}}\}$ is an orthonormal basis for the bath Hilbert space. This expression requires full knowledge of the universe, and we need to simplify the description, introducing assumptions and approximations.

We start assuming that the initial state of the universe is a product state, the system and the environment completely decoupled, $\rho = \rho_{\mathcal{S}}(0) \otimes \rho_{\mathcal{B}}(0)$. Whilst it is not an approximation by itself, we are either narrowing the range of physical systems we are describing, or we need to consider it as an actual approximation of a larger set of systems. Now, by definition, the environment density matrix admits a spectral decomposition in an orthonormal basis with non-negative eigenvalues,

$$\rho_{\mathcal{B}}(0) = \sum_{\nu\in\mathcal{H}_{\mathcal{B}}} \lambda_{\nu}|\nu\rangle\langle\nu| \tag{II.3}$$

and substituting the factorized state with the decomposed environment, we obtain

$$\rho_{\mathcal{S}}(t) = \sum_{\mu\in\mathcal{H}_{\mathcal{B}}} \langle\mu| \left[U(t)\rho_{\mathcal{S}}(0) \otimes \sum_{\nu\in\mathcal{H}_{\mathcal{B}}} \lambda_{\nu}|\nu\rangle\langle\nu|U^{\dagger}(t)\right] |\mu\rangle \tag{II.4a}$$

$$= \sum_{\mu,\nu\in\mathcal{H}_{\mathcal{B}}} \sqrt{\lambda_{\nu}}\langle\mu|U(t)|\nu\rangle\rho_{\mathcal{S}}(0)\langle\nu|U^{\dagger}(t)|\mu\rangle\sqrt{\lambda_{\nu}} \tag{II.4b}$$

$$= \sum_{\mu,\nu\in\mathcal{H}_{\mathcal{B}}} K_{\mu\nu}(t)\rho_{\mathcal{S}}(0)K^{\dagger}_{\mu\nu}(t) \tag{II.4c}$$

where we can identify environment-averaged operators driving the dynamics of the system, the Kraus operators,

$$K_{\mu\nu}(t) = \sqrt{\lambda_{\nu}}\langle\mu|U(t)|\nu\rangle, \tag{II.5}$$

and eq. (II.4c) is called the Kraus operator sum representation (OSR) [149].

Hence, with just one assumption about the initial state of the universe system, we have derived a simple form for the system's evolution. Therefore, the OSR representation is a map $\mathcal{E}(\cdot)$ of the system's evolution, possibly exact.

$$\begin{aligned} \mathcal{E} : \mathcal{L}(\mathcal{H}_{\mathcal{S}}) &\to \mathcal{L}(\mathcal{H}_{\mathcal{S}}) \\ \rho_{\mathcal{S}}(0) &\mapsto \rho_{\mathcal{S}}(t) = \sum_{\alpha} K_{\alpha}(t)\rho_{\mathcal{S}}(0)K^{\dagger}_{\alpha}(t) \end{aligned} \tag{II.6}$$

This formulation holds important properties, and for an in-depth discussion and the formal proofs of the following statements, we refer to ref. [34] and the references therein. By linearity and the cyclic property of the trace operator[1] these maps are linear and

[1] $\mathrm{Tr}(ABC) = \mathrm{Tr}(CAB) = \mathrm{Tr}(BCA)$

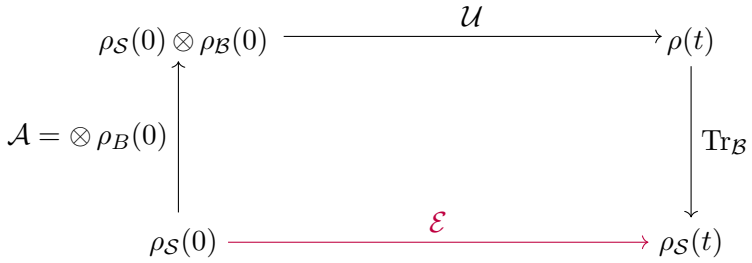

Figure II.1: Commutative diagram of the Kraus OSR as a composition of three maps, a recasting of the uppen branches of that presented in Figure I.2.

preserve the trace of the state

$$\mathrm{Tr}[\mathcal{E}(\rho_{\mathcal{S}})] = \mathrm{Tr}\left[\sum_{\alpha} K_\alpha(t)\rho_{\mathcal{S}}K_\alpha^\dagger(t)\right] = \mathrm{Tr}\left[\sum_{\alpha} K_\alpha^\dagger(t)K_\alpha(t)\rho_{\mathcal{S}}\right] = \mathrm{Tr}\left[\rho_{\mathcal{S}}\right] \tag{II.7}$$

where the closure property $\sum_\alpha K_\alpha^\dagger(t)K_\alpha(t) = \mathbb{1}$ of the Kraus operators comes from their definition. The map is also positive, mapping positive operators to positive operators. This property is fundamental, because it means that we are describing *valid* quantum states. Furthermore, this map is *completely positive*. This means that, composing the system with another auxiliary system $\{\mathcal{K}, \mathcal{H}_\mathcal{K}, \rho_\mathcal{K}\}$ of any $\dim(\mathcal{H}_\mathcal{K}) = k$ and in an arbitrary state $\rho' \in \mathcal{H}_\mathcal{S} \otimes \mathcal{H}_\mathcal{K}$, and acting with the map $\mathcal{E} \otimes \mathbb{1}_\mathcal{K}$ on the composite state, the resulting state is still a positive state, so $(\mathcal{E} \otimes \mathbb{1}_\mathcal{K})(\rho') > 0$.

These properties result to be sufficient and necessary conditions for a map to have a Kraus OSR, leading to the following theorem.

Theorem 1 (Choi-Kraus theorem)**.** *A linear map $\mathcal{E} : \mathcal{L}(\mathcal{H}) \to \mathcal{L}(\mathcal{H})$ is completely positive and trace-preserving (CPT) if and only if it has a Kraus operator sum representation:*

$$\mathcal{E}[\cdot] = \sum_\alpha K_\alpha(t)[\cdot]K_\alpha(t)^\dagger$$

with the operator $K_\alpha(t) \in \mathcal{L}(\mathcal{H})$ such that $\sum_\alpha K_\alpha^\dagger(t)K_\alpha(t) = \mathbb{1}$.

The proof of the theorem can be found in [149–151], and in a more synthetic way in [18, 34, 50, 152]. In particular, Choi's theorem gives sufficient conditions for a map to be completely positive [151], and Kraus's theorem adds the condition for trace preservation and formalizes the operator sum representation [149]. Maps that admit a Kraus OSR are usually referred to as quantum maps, or *quantum channels*.

We can see that a Kraus OSR is a composition of three maps,

$$\mathcal{E} = \mathrm{Tr}_\mathcal{B} \circ \mathcal{U} \circ \mathcal{A}, \tag{II.8}$$

where the first map $\mathcal{A}$ is an "assignment" map which associates to the system its environment, the composed system is then propagated with its unitary mapping and then the system state at time t is recovered *via* the partial trace, see Figure II.1. In this sense, this map can still be an exact description of the evolution of the system, from an initial time t_0

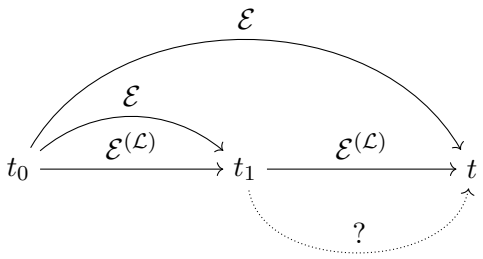

Figure II.2: A graphical note on temporal continuity, divisibility condition of Markovian contractive maps, and the differences in these properties of differently mapped evolutions.

when we either know or assume that the system is fully decoupled from its environment, i.e, the system satisfies the factorization condition, to a final time t. The important remark is that this still implies the assumption of knowing the propagator for the universe and an orthonormal decomposition for the environment, for an exact propagation.

These are quantities that we do not know, and even if we did, we can not start in an intermediate time $t_0 < t_1 < t$, as we would not be in a factorized condition anymore, see Figure II.2. Further assumptions and approximations are then needed to have a structured and solvable description of the dynamics.

II.2 Gorini-Kossakowski-Sudarshan-Lindblad Form

One of the most common approaches to open quantum dynamics is the use of the Gorini-Kossakowski-Sudarshan-Lindblad form of master equations, independently proposed by G. Lindblad [48] and V. Gorini, A. Kossakowski, and E.C. Sudarshan [49] fifty years ago, and is one of the most influential results in the theory of open quantum systems. Its advantage is that it allows for the description of CPT maps that undergo a Markovian dynamics, and therefore are valid at all times of the propagation, indicated in Figure II.2 with the approximate mapping $\mathcal{E}^{(\mathcal{L})}$. Markov processes, in probability theory, are processes whose future values depend only on the current state of the system. This means that we expect the following composition law to hold,

$$\mathcal{E}^{(\mathcal{L})}_{t_2,t_0} = \mathcal{E}^{(\mathcal{L})}_{t_2,t_1}\mathcal{E}^{(\mathcal{L})}_{t_1,t_0} \tag{II.9}$$

i.e., the map $\mathcal{E}^{(\mathcal{L})}$ is a *contraction semigroup*, and the composition above is known as *divisibility condition*. The key element of a semigroup is its generator, which we can identify by the solution of the first-order ODE for the dynamics of the system

$$\dot{\rho}_{\mathcal{S}}(t) = \mathcal{L}[\rho_{\mathcal{S}}(t)] \quad \rightarrow \quad \rho_{\mathcal{S}}(t) = e^{\mathcal{L}t}\rho_{\mathcal{S}}(0) = \mathcal{E}^{(\mathcal{L})}_{t,0}[\rho_{\mathcal{S}}(0)]\,. \tag{II.10}$$

The generator of the semigroup, and therefore the master equation and mapping, can be obtained through different routes [18, 34, 152–154]. Except for the derivation from a series of subsequent approximations that is presented in section II.3 as a particular case of the Redfield approach, these start from the Choi-Kraus theorem, Theorem 1, and introduce the Markovian approximation. For example, one can expand the density matrix around

$t = 0$ for the infinitesimal time $\mathrm{d}t$ and obtain the derivative of the density matrix at the initial time. Then, to obtain the generator, we need to assume that the expression derived is valid at all times t, exactly a Markovian approximation of the system, meaning that the memory of the system is reset at each timestep $\mathrm{d}t$, i.e., it is memoryless. This implies that, since the condition at the initial time is the factorization of the system-environment density matrix, the universe system remains factorized at all times, and the system and the bath are never coupled, either quantum mechanically or classically.

The form of the master equation obtained is generally referred to as the Lindblad form (or GKSL), for simplicity, and reads in the following theorem.

Theorem 2 (Lindblad '76; Gorini, Kossakowski, Sudarshan '76)**.** *The generator of any quantum operation satisfying the semigroup property must have the form*

$$\frac{\mathrm{d}\rho_{\mathcal{S}}(t)}{\mathrm{d}t} = -i[H_{\mathcal{S}}, \rho_{\mathcal{S}}(t)] + \sum_k \gamma_k \Big[L_k \rho_{\mathcal{S}}(t) L_k^\dagger - \frac{1}{2} \Big\{ L_k L_k^\dagger, \rho_{\mathcal{S}}(t) \Big\} \Big] \tag{II.11}$$

where $\gamma_k > 0$ are relaxation rates, L_k are Lindblad operators and $\{\cdot\,,\cdot\}$ is the anticommutator.

Since this form is derived from the Kraus OSR as a starting point, which by Theorem 1 defines the requirement for a map to be CPT, and by this theorem we define the only form admitting a generator, it follows that *the QME in the form of eq.* (II.11) *are all and only admitting the CPT properties of the map*, if not by invoking non-Markovianity and various techniques leading to complex and usually not solvable forms.

II.2.1 Signatures and limits of Lindblad QME

The Lindblad QME is an algebraically derived form, and its application to physical systems is therefore phenomenological. This poses the first limitation of the Lindblad forms. The structure of the generator is fixed by construction and requirements, without the connection to a physical system. As a consequence, the Lindblad operators must be chosen *a priori*, according to the phenomena one aims to describe, and the coefficients are introduced as effective parameters, typically inferred from experimental evidence or physical intuition.

Then, we need to acknowledge the Markovian approximation. Since Lindblad forms are CPT, we do not have evident signals of the unphysicality of a dynamics, and we need to be careful using them to describe systems that can be approximated by this form. Heuristically, the Markovian approximation is valid under two main conditions. First, the environment correlation time needs to be much shorter than the system *relaxation* time. Then, the evolution maps can be endowed with the divisibility property, as the correlation time of the environment is simplified to a δ-correlation, meaning that it affects only single time moments. Secondly, the environment state is assumed to be stationary in time, meaning that it does not change significantly during the dynamics and can be considered at equilibrium. The equilibrium condition ensures that we do not need to consider the time evolution of the environment, which would otherwise alter the map as time progresses.

Moreover, this implies that the interaction between the system and the environment is weak, and that the environment space is much larger than the system itself, according to the reason why a theory of open systems is required. These two constraints will be clearly discussed and their nature explained in the two main approaches used in this work, in section II.3 and in Chapter III. Lindblad forms allow for the description of completely positive and trace preserving dynamics; therefore, by CPT property, they ensure that we are mapping between valid states. Nevertheless, signatures of unphysicality due to the approximated nature of this approach persist. One problem is the stationary state, the dynamics leading to an equilibrium state independent of the system-bath coupling strength, accuracy issues effectively leading to a wrong steady state [155–159].

Another problem, intrinsic and easy to detect, is an unphysical non-zero velocity a the inversion of populations. In particular, as the mapping is contractive, we refer to the presence of a non-zero derivative at t_0. Then, with the initial hypothesis of the system being factorized and therefore null correlations, it is unphysical to have a non-null velocity, as if the environment is already dissipating the system dynamics. One can debate that this behavior accounts for the fact that the factorization approximation is, most of the time, indeed, an approximation. Yet, the Lindblad master equation fails to describe the short-time dynamics correctly.

Example II.1 | Pauli two-level decay model

Consider the spontaneous emission of a two-level system, which basis is $\{|g\rangle, |e\rangle\}$, from the excited state $|e\rangle$ to the ground state $|g\rangle$. The Hamiltonian of the system is

$$H = \varepsilon_g |g\rangle\langle g| + \varepsilon_e |e\rangle\langle e| \,. \tag{II.12}$$

To describe a decay from the excited state, the Lindblad operator is $\sigma_- = |g\rangle\langle e|$, its adjoint $\sigma_-^\dagger = \sigma_+ = |e\rangle\langle g|$, and the corresponding Lindblad equation, known as a Pauli master equation,

$$\frac{\mathrm{d}}{\mathrm{d}t}\rho_t = -i\left[H, \rho_t\right] + \gamma\left(\sigma_-\rho_t\sigma_+ - \frac{1}{2}\left\{\sigma_+\sigma_-, \rho_t\right\}\right). \tag{II.13}$$

The equations of motion of the populations read

$$\dot{\rho}_t^{(gg)} = \gamma\rho_t^{(ee)} = \gamma\left(1 - \rho_t^{(gg)}\right), \tag{II.14}$$

showing that the derivative of the density matrix at $t = 0$ is not zero, as the normalization and trace preservation $|\rho_t^{(gg)} + \rho_t^{(ee)}|^2 = 1$. Indeed, the solution

$$\rho_t^{(gg)} = 1 - \rho_0^{(ee)} e^{-\gamma t}, \tag{II.15}$$

meaning an exponential decay of the excited state population with rate γ.

II.3 Redfield master equation

The Bloch-Redfield master equation, Redfield master equation for brevity, is another milestone in the theory of open quantum system dynamics, one of the most used and useful, independently developed by A. G. Redfield [46] and F. Bloch [160] in 1957. Many different forms of equations are referred to as *Redfield* equation, stemming from different moment in its derivation steps,[2] one of the most common forms is the following,

$$\frac{\mathrm{d}}{\mathrm{d}t}\rho_{\mathcal{S}}(t) = -i[H_{\mathcal{S}}, \rho_{\mathcal{S}}(t)] - \sum_{k,l}\sum_{\omega,\omega'} \Gamma_{kl}(\omega') \left(\left[S_k^\dagger(\omega), S_l(\omega')\rho_{\mathcal{S}}(t) \right] e^{i(\omega-\omega')t} + \text{h.c.} \right), \quad \text{(II.16)}$$

where h.c. indicates the hermitian conjugate of the term inside the parentheses. We can note that this is a Markovian QME, a linear and time-local mapping of the density matrix, but we also immediately see that it is not in Lindblad form, and therefore is not a CP mapping either. Then, why is it so common and important?

The Redfield master equation is a Markovian master equation that, unlike the Lindblad form, is derived starting from the full definition of the system-environment Hamiltonian, applying assumptions and approximations along the way. This allows for precise physical assumptions, specifying conditions of validity and choosing which and how to apply them, until a distinct form is obtained; this is extremely useful for providing information on the dynamics and rationalization of occurring phenomena.

In particular, the Redfield equation stems from a second-order truncation on the system-environment interaction, considered as a *perturbation* of the system dynamics, the factorization assumption, and the Born and Markov approximations. Eventually, further approximations can be applied and will be introduced in the following, most notably the secular approximation that allows for the recovery of a Lindblad form.

II.3.1 A bottom-up microscopic derivation

On the Hilbert space of the composite universe system $\mathcal{H} = \mathcal{H}_{\mathcal{S}} \otimes \mathcal{H}_{\mathcal{B}}$, starting point is the microscopic definition of the global Hamiltonian in terms of the system, bath, and interaction Hamiltonians as

$$H = H_{\mathcal{S}} \otimes \mathbb{1}_{\mathcal{B}} + \mathbb{1}_{\mathcal{S}} \otimes H_{\mathcal{B}} + H_I, \quad \text{(II.17)}$$

where $H_{\mathcal{S}}, H_{\mathcal{B}}$ describe the two isolated subsystems and the interaction Hamiltonian $H_I \in \mathcal{H}$ is defined as

$$H_I = \sum_k S_k \otimes B_k. \quad \text{(II.18)}$$

where $S_k \in \mathcal{L}(\mathcal{H}_{\mathcal{S}}), B_k \in \mathcal{L}(\mathcal{H}_{\mathcal{B}})$ are interaction operators acting in the respective Hilbert spaces. From now on, we explicit $\hbar$ to clarify and distinguish terms and their relative weights, and we recall that its use is required for the numerical simulation of real ex-

[2] To cite some examples, Petruccione [18], Lidar [34], Vacchini [19] consider for example the integral form of the partial trace, Rivás [152], Gaspard and Nagaoka [161], the more explicit formulation - or for simplicity, mathematicians and theoretical physicists tend to relate to the first more implicit formulation, applied physicists and physical chemists to the more explicit one.

periments. The associated Liouville-Von Neumann equation of the universe system then reads

$$\frac{\mathrm{d}}{\mathrm{d}t}\rho(t) = -\frac{i}{\hbar}\left[H_{\mathcal{S}} \otimes \mathbb{1} + \mathbb{1} \otimes H_{\mathcal{B}} + H_I, \rho(t)\right] \tag{II.19}$$

and we transform to the so-called *interaction picture*, or Dirac picture,

$$\tilde{\rho}(t) = e^{\frac{i}{\hbar}(H_S+H_B)t}\rho(t)e^{-\frac{i}{\hbar}(H_S+H_B)t} \tag{II.20}$$

hence to a co-moving frame to the the free-evolution of the universe non-interacting system. The interaction Hamiltonian is transformed similarly, becoming a time-dependent Hamiltonian. The formal solution obtained by integration is

$$\tilde{\rho}(t) = \tilde{\rho}(0) - \frac{i}{\hbar}\int_0^t [\tilde{H}_I(t'), \tilde{\rho}(t')]\,\mathrm{d}t', \tag{II.21}$$

and substituting in the original Liouville-Von Neumann equation, we obtain the following open integrodifferential equation for the universe evolution

$$\frac{\mathrm{d}}{\mathrm{d}t}\tilde{\rho}(t) = -\frac{i}{\hbar}[\tilde{H}_I(t), \tilde{\rho}(0)] - \frac{1}{\hbar^2}\int_0^t \left[\tilde{H}_I(t), \left[\tilde{H}_I(t'), \tilde{\rho}(t')\right]\right]\mathrm{d}t'. \tag{II.22}$$

To obtain the system evolution, we trace out the bath degrees of freedom,

$$\frac{\mathrm{d}}{\mathrm{d}t}\tilde{\rho}_{\mathcal{S}}(t) = -\frac{i}{\hbar}\,\mathrm{Tr}_{\mathcal{B}}\left\{\left[\tilde{H}_I(t), \tilde{\rho}(0)\right]\right\} - \frac{1}{\hbar^2}\int_0^t \mathrm{Tr}_{\mathcal{B}}\left\{\left[\tilde{H}_I(t), \left[\tilde{H}_I(t'), \tilde{\rho}(t')\right]\right]\right\}\mathrm{d}t', \tag{II.23}$$

a recasting of the original equation that describes the exact evolution of the system. Now, we need to introduce approximations to obtain a solvable form, i.e., a closed form with respect to the system density matrix, and eventually obtain the Redfield form of the QME.

(R1) The first assumption, common to almost all approaches to OQS and already introduced above, is to consider the factorization of the initial density matrix in a product state

$$\rho(0) = \rho_{\mathcal{S}}(0) \otimes \rho_{\mathcal{B}}(0) = \rho_{\mathcal{S}}(0) \otimes \rho_{\mathcal{B}}^{\mathrm{eq}} \tag{II.24}$$

and we continue to assume the environment is at thermal equilibrium, defined $\rho_{\mathcal{B}}^{\mathrm{eq}} = \exp\left(-H_{\mathcal{B}}\beta\right)Z^{-1}$, where $\beta = (k_B T)^{-1}$ is the inverse of the temperature and $Z = \mathrm{Tr}(\exp\left(-H_{\mathcal{B}}\beta\right))$ is the partition function.

For the free evolution of the bath, this is a stationary condition, as $[H_{\mathcal{B}}, \rho_{\mathcal{B}}^{\mathrm{eq}}] = 0$. Substituting the factorized state eq. (II.24) and the interaction Hamiltonian definition eq. (II.18)

in the first term on the r.h.s. in eq. (II.23),

$$\mathrm{Tr}_{\mathcal{B}}\left\{\left[\tilde{H}_I(t),\tilde{\rho}(0)\right]\right\} = \sum_k \mathrm{Tr}_{\mathcal{B}}\left\{\left[\tilde{S}_k(t)\otimes\tilde{B}_k(t),\tilde{\rho}_{\mathcal{S}}(0)\otimes\tilde{\rho}_{\mathcal{B}}^{\mathrm{eq}}\right]\right\} \tag{II.25a}$$

$$= \sum_k \left[\tilde{S}_k(t),\tilde{\rho}_{\mathcal{S}}(0)\right]\mathrm{Tr}_{\mathcal{B}}\left\{\tilde{B}_k(t)\tilde{\rho}_{\mathcal{B}}^{\mathrm{eq}}\right\} \tag{II.25b}$$

$$= \sum_k \left[\tilde{S}_k(t),\tilde{\rho}_{\mathcal{S}}(0)\right]\langle B_k\rangle_{\mathrm{eq}} \tag{II.25c}$$

one gets a mean-field effect of the environment on the interaction energy, and one can account for it by redefining the system and interaction Hamiltonians, or more generally, one gets $\langle B_k\rangle_{\mathrm{eq}} = 0$. Then, the dynamics can be rewritten considering only the second term in the r.h.s. of eq. (II.23), the first term vanishing.

(R2) For couplings between system and environment small enough, we can consider a weak coupling and a perturbative interaction, the environment negligibly modified by its interaction with the system. We can apply the Born approximation, an application of perturbation theory, expanding the total density matrix at time t as the series $\rho(t) = \rho_{\mathcal{S}}(t)\otimes\rho_{\mathcal{B}}^{eq} + \mathcal{O}(\lambda)$, and neglecting the higher order terms.

This is a central approximation of the Redfield approach to open quantum systems. It explicitly states the choices that were left implicit in the Lindblad approach, section II.2.1, the system weakly coupled to a thermalized and much larger environment.

Substituting the approximated universe state and the interaction Hamiltonian in the nested commutator in eq. (II.23), we get

$$\frac{\mathrm{d}}{\mathrm{d}t}\tilde{\rho}_{\mathcal{S}}(t) = -\frac{1}{\hbar^2}\sum_{kl}\int_0^t \left(\mathrm{Tr}\left\{\tilde{B}_k(t)\tilde{B}_l(t')\rho_{\mathcal{B}}^{eq}\right\}\left[\tilde{S}_k(t),\tilde{S}_l(t')\tilde{\rho}_{\mathcal{S}}(t')\right] + \mathrm{h.c.}\right)\mathrm{d}t', \tag{II.26}$$

where, without loss of generality, we assume the operators B_k Hermitian. The trace of the combinations of bath operators acting at different times on the environment at its equilibrium is its stationary two-time correlation function

$$\mathrm{Tr}\left\{\tilde{B}_k(t)\tilde{B}_l(t')\rho_{\mathcal{B}}^{eq}\right\} = \left\langle\tilde{B}_k(t)\tilde{B}_l(t')\right\rangle_{\mathrm{eq}} = C_{kl}(t,t'). \tag{II.27}$$

Here, we can evaluate different environment models and their interaction Hamiltonian, either from physical assumptions or starting from microscopic approximated models of the surrounding environment. Well-known example of the first case is the choice of a δ-correlated environment, very fast correlation times w.r.t. the system evolution, we fall back to the Markovian assumption, which will eventually lead to the Lindblad equation. On the other hand, one can derive the correlation function from models, such as the well-known Caldeira-Leggett modeling of a set of independent quantum oscillators [162], or from overdamped Brownian oscillators, and many others.

By its construction, the stationary correlation function depends on the time difference between the time variables $\tau = t - t'$, and by the choice of Hermitian bath operators

the additional symmetry $C^*_{kl}(\tau) = C_{lk}(-\tau)$, the complex conjugate since quantum environments are in general complex valued. The resulting equation is an integrodifferential *non-Markovian master equation*,

$$\frac{\mathrm{d}}{\mathrm{d}t}\tilde{\rho}_{\mathcal{S}}(t) = -\frac{1}{\hbar^2}\sum_{kl}\int_0^t \Big(C_{kl}(t-t')\left[\tilde{S}_k(t), \tilde{S}_l(t')\tilde{\rho}_{\mathcal{S}}(t')\right] + \text{h.c.}\Big)\,\mathrm{d}t', \tag{II.28}$$

as it depends on the $\rho_{\mathcal{S}}$ at all previous times $t' \leq t$, and the correlatation function too. Then, two further approximations are required to obtain a form in the Makovian framework. Let us change the integration variable in eq. (II.28) to $t - t' = \tau$, allowing us to express the evolution of $\tilde{\rho}_{\mathcal{S}}(t)$ in terms of $\tilde{\rho}_{\mathcal{S}}(t-\tau)$, where τ measures the memory backward in time from the current instant t,

$$\frac{\mathrm{d}}{\mathrm{d}t}\tilde{\rho}_{\mathcal{S}}(t) = -\frac{1}{\hbar^2}\sum_{kl}\int_0^t \Big(C_{kl}(\tau)\left[\tilde{S}_k(t), \tilde{S}_l(t-\tau)\tilde{\rho}_{\mathcal{S}}(t-\tau)\right] + \text{h.c.}\Big)\,\mathrm{d}\tau. \tag{II.29}$$

(R3) The first Markov approximation is to assume that $\rho_S(t)$ varies more slowly than the decay of the correlation of the bath, allowing us to change

$$\tilde{\rho}_{\mathcal{S}}(t')\,\mathrm{d}t' \to \tilde{\rho}_{\mathcal{S}}(t)\,\mathrm{d}t'$$

in eq. (II.28), equivalent to approximate $\tilde{\rho}_{\mathcal{S}}(t-\tau) \approx \tilde{\rho}_{\mathcal{S}}(t)$.

The equation we obtain is now a time-local master equation known as the *Redfield equation with time-dependent coefficients*, the integration affecting now only correlation function and time-dependent operators $S_\alpha(t')$, hence time-local w.r.t. the system density matrix.

(R4) The second Markov approximation to remove the time dependency of the coefficients in the nested commutator. To do so, we follow the same reasoning as above, and consider that, as $\tilde{\rho}_S$ decays slowly with respect to the correlation function of the bath, the kernel decays fast enough to extend the integration upper bound to infinity.

We have finally obtained an equation that is time-local and closed for the system dynamics, the Redfield QME in the rotated frame

$$\frac{\mathrm{d}}{\mathrm{d}t}\tilde{\rho}_{\mathcal{S}}(t) = -\frac{1}{\hbar^2}\sum_{kl}\int_0^{+\infty} \Big(C_{kl}(\tau)\left[\tilde{S}_k(t), \tilde{S}_l(t-\tau)\tilde{\rho}_{\mathcal{S}}(t)\right] + \text{h.c.}\Big)\,\mathrm{d}\tau. \tag{II.30}$$

Expanding the operators $\tilde{S}_\alpha$ on the eigenbasis of the system Hamiltonian $H_{\mathcal{S}}$ and moving back to the Schrödinger picture we can evaluate the action of $e^{\pm\frac{i}{\hbar}H_{\mathcal{S}}t}$ on the eigenstates,

$$\tilde{S}_k(t) = \sum_{a,b\,\text{eigen}H_{\mathcal{S}}} \langle a|\tilde{S}_k(t)|b\rangle |a\rangle\langle b| \tag{II.31a}$$

$$= \sum_{a,b\,\text{eigen}H_{\mathcal{S}}} \langle a|e^{\frac{i}{\hbar}H_{\mathcal{S}}t}S_k e^{-\frac{i}{\hbar}H_{\mathcal{S}}t}|b\rangle |a\rangle\langle b| \tag{II.31b}$$

$$= \sum_{\omega=\omega_a-\omega_b} e^{i\omega t}S_k(\omega), \tag{II.31c}$$

where $e^{H_S}|a\rangle = e^{E_a}|a\rangle$, $E_a/\hbar = \omega_a$, and $\omega = \omega_a - \omega_b$ are the transition frequencies (or energy gaps) of the system. Finally, we obtain the original formulation of the Redfield presented in eq. (II.16),

$$\frac{\mathrm{d}}{\mathrm{d}t}\rho_{\mathcal{S}}(t) = -\frac{i}{\hbar}[H_{\mathcal{S}}, \rho_{\mathcal{S}}(t)] - \frac{1}{\hbar^2}\sum_{k,l}\sum_{\omega,\omega'}\Gamma_{kl}(\omega)\left(\left[S_k^\dagger(\omega'), S_l(\omega)\rho_{\mathcal{S}}(t)\right]e^{i(\omega-\omega')t} + \text{h.c.}\right), \tag{II.32}$$

where the coefficients $\Gamma_{kl}(\omega)$ are now clearly defined, particularly as the half-sided Fourier transform of the bath correlation function, evaluated at the system frequency ω,

$$\Gamma_{kl}(\omega) = \int_0^{+\infty} C_{kl}(\tau)e^{i\omega\tau}\,\mathrm{d}\tau, \tag{II.33}$$

and form the elements of the *Redfield relaxation tensor*.

II.3.2 Spectral and dispersion functions and spectral density

From eqs. (II.32) and (II.33) we can appreciate that, within Redfield theory, the relaxations occur on the basis of the system eigenstates, and the environment influence on the dynamics is defined by its correlation function through its one-sided Fourier transform. For practical reasons of computation and to introduce further consideration and approximations, it is convenient to define the environment effect through its full Fourier transform, its spectral function,

$$J_{kl}(\omega) = \int_{-\infty}^{+\infty} C_{kl}(\tau)e^{i\omega\tau}\,\mathrm{d}\tau = \Gamma_{kl}(\omega) + \Gamma_{lk}^*(\omega), \tag{II.34}$$

where, by symmetry of $C_{kl}(\tau)$, we have $J_{kl}(\omega)$ Hermitian. As for the correlation function, the spectral function satisfies the Kubo-Martin-Schwinger (KMS) condition [18], which reads

$$J_{lk}(-\omega) = e^{-\omega\beta}J_{kl}(\omega), \tag{II.35}$$

where β is again the inverse of the temperature. Then, the spectral function at a finite temperature is not symmetric w.r.t the system frequencies ω, and we can split it into two components, a symmetric and an antisymmetric part,

$$J_{kl}(\omega) = J_{kl}^{\text{sym}}(\omega) + J_{kl}^{\text{anti-sym}}(\omega), \tag{II.36}$$

where

$$J_{kl}^{\text{sym}}(\omega) = \frac{1+e^{-\omega\beta}}{2}J_{kl}(\omega), \qquad J_{kl}^{\text{anti-sym}}(\omega) = \frac{1-e^{-\omega\beta}}{2}J_{kl}(\omega) \tag{II.37}$$

The antisymmetric component is the correct *spectral density* of the environment. There are two important considerations to note, and will be further remarked in the following Chapter IV. For high-temperature baths, we can approximate the temperature as tending to infinity, and as the exponential tends to 1, the antisymmetric component vanishes.

Therefore, in the infinite temperature limit, the spectral density and spectral function coincide. Then note that if the correlation is classical, i.e., when a real stochastic process is used to approximate the environment, the correlation function is real-valued and even, and by linearity of the Fourier transform, so is the spectral function.

We can further split the components of the Redfield tensor into a Hermitian and an anti-Hermitian part,

$$\Gamma_{kl}(\omega) = \frac{1}{2}J_{kl}(\omega) + \frac{1}{2}i\Lambda_{kl}(\omega), \tag{II.38}$$

where the spectral function is the Hermitian part and $i\Lambda_{kl}(\omega)$ is the anti-Hermitian component. The matrix $\Lambda(\omega)$ is then a Hermitian matrix, the *dispersion function* of the environment, connected through the Kramers-Kronig relation

$$\Lambda(\omega) = \mathcal{P}\int \frac{J(\omega')}{\omega - \omega'}\,\mathrm{d}\omega', \tag{II.39}$$

where $\mathcal{P}$ indicates the Cauchy principal value of the integral [163], and to the Redfield tensor by

$$\Lambda_{kl}(\omega) = \int_0^{+\infty} \left[C_{kl}(\tau)e^{i\omega\tau} - C^*_{lk}(\tau)e^{-i\omega\tau}\right]\mathrm{d}\tau = \frac{\Gamma_{kl}(\omega) - \Gamma^*_{lk}(\omega)}{2i}. \tag{II.40}$$

II.3.3 Secular Redfield equation

Further assumptions can be considered, and approximations can be applied, leading to different recastings of this form. The most notable example is the recovery of a Lindblad form from this microscopic approach by applying the secular approximation [18, 34, 50, 164, 165], commonly known also as the rotating wave approximation (RWA).

This approximation consists of neglecting the fast oscillating terms in eq. (II.32), motivated by a choice of coarse-graining [166–169], which is somehow implicit in the Markov approximations (R3) and (R4), and further refined. As the system evolves slowly compared to the environment, the oscillations due to the terms $e^{i(\omega-\omega')}$ for $\omega \neq \omega'$ are considered fast and cancel out during the integration. Then, the timescale that we can use to observe the dynamics must be larger than the inverse of the minimal system energy separation, which, together with the considerations for the Markov approximations, leads to the condition

$$\tau_r \gg \tau \gg \tau_{c_{kl}} \wedge \max_{a,b} \hbar|E_b - E_a|^{-1}. \tag{II.41}$$

where τ_r is the characteristic timescale of the system relaxation, τ is the dynamics timescale and $\tau_{c_{kl}}$ is the characteristic correlation timescale of the environemt.

Then, the Redfield tensor is split into the dispersion and spectral components; the first one renormalizes the system Hamiltonian, accounting for the interaction with the environment, and the second one reduces to the matrix of relaxation rates of the quantum channels. Finally, the Lindblad form is recovered, ensuring CPT properties.

This is the strongest approximation that we can apply to the Redfield equation. However, conversely to the direct use of a Lindblad form, the operators in the dissipator and

the relaxation rates are derived from a microscopic model, retaining the characteristic quantities of a microscopic derivation [170–172]. Furthermore, one can avoid applying a *full* secular approximation and rather perform *partial* secular approximations. One approach is clustering sets of frequencies, and then the secular approximation is applied at the cluster level, in a frequency coarse-graining [173]. Another is to remove only the faster oscillating terms, but keep others [167, 168, 174, 175].

Whilst the secular approximation ensures positivity of the map by yielding a Lindblad form, we conclude by noting that the non-positivity of the Redfield equation can be a useful indicator [176], signaling conditions that are incompatible with the assumptions and approximations underlying the derivation. Rather than attempting to recover positivity a posteriori, given that Lindblad and Redfield forms rely on the same range of validity, see section II.2.1, such behavior should be taken as an indication that other approaches are required.

II.3.4 Redfield tensor without imaginary component

Another approximation that can be applied, softer than the secular, consists in neglecting the imaginary component of the Redfield relaxation tensor Γ. This approach has been proposed in the context of light-harvesting molecular complexes, most notably the Fenna-Matthews-Olson complex [177], and has been further studied in different scenarios [171, 178]. Within this approximation, the dispersive contribution to the Redfield tensor in eq. (II.38) is neglected by setting $\Lambda_{kl}(\omega) = 0$. These terms constitute the anti-Hermitian part of Γ and give rise to an effective correction Hamiltonian, known as the Lamb shift Hamiltonian H_{LS}, which acts as a renormalization of the system's energy levels. Specifically, non-degenerate levels are shifted, while degenerate levels may be split. Therefore, neglecting this contribution amounts to disregarding environment-induced energy shifts.

This reasoning applies to the secularized form of the Redfield equation, where the Lamb shift term is clearly identified, but additional care is required when dealing with alternative forms, as we discuss in further detail in section IV.6.5.

References

[18]H.-P. Breuer and F. Petruccione, *The Theory of Open Quantum Systems*, 1st ed. (Oxford University Press, Oxford, Jan. 2002), 10.1093/acprof:oso/9780199213900.001.0001

[19]B. Vacchini, *Open Quantum Systems: Foundations and Theory* (Springer Cham, Dec. 2024), 10.1007/978-3-031-58218-9

[34]D. A. Lidar, *Lecture Notes on the Theory of Open Quantum Systems*, Los Angeles, Feb. 2019

[46]A. G. Redfield, "On the Theory of Relaxation Processes", IBM Journal of Research and Development **1**, 19–31 (1957) 10.1147/rd.11.0019

[48]G. Lindblad, "Mathematical Physics On the Generators of Quantum Dynamical Semigroups", Communications in Mathematical Physics **48**, 119–130 (1976)

[49]V. Gorini, A. Kossakowski, and E. C. Sudarshan, "Completely positive dynamical semigroups of N-level systems", Journal of Mathematical Physics **17**, 821 (1976) 10.1063/1.522979

[50]D. Manzano, "A short introduction to the Lindblad master equation", AIP Advances **10**, 025106 (2020) 10.1063/1.5115323

[149]K. Kraus, *States, Effects, and Operations: Fundamental Notions of Quantum Theory*, edited by K. Kraus, A. Böhm, J. D. Dollard, and W. H. Wootters (Springer Berlin, Heidelberg, Aug. 1983), p. 40, https://doi.org/10.1007/3-540-12732-1

[150]M. D. Choi, "Positive Linear Maps on C*-Algebras", Can. J. Math **XXIV**, 520–529 (1972) 10.4153/CJM-1972-044-5

[151]M. D. Choi, "Completely positive linear maps on complex matrices", Linear Algebra and its Applications **10**, 285–290 (1975) 10.1016/0024-3795(75)90075-0

[152]Á. Rivas and S. F. Huelga, *Open Quantum Systems. An Introduction*, 1st ed. (Springer Berlin, Heidelberg, Apr. 2011), 10.1007/978-3-642-23354-8

[153]D. Chruściński and S. Pascazio, "A Brief History of the GKLS Equation", Open Systems & Information Dynamics **24**, 10.1142/S1230161217400017 (2017) 10.1142/S1230161217400017

[154]M. Merkli, "Dynamics of Open Quantum Systems II, Markovian Approximation", Quantum **6**, 616 (2022) 10.22331/q-2022-01-03-616

[155]T. Becker, A. Schnell, and J. Thingna, "Canonically consistent quantum master equation", Physical Review Letters **129**, 200403 (2022) 10.1103/PhysRevLett.129.200403

[156]J. Thingna, J. S. Wang, and P. Hänggi, "Generalized Gibbs state with modified Redfield solution: Exact agreement up to second order", Journal of Chemical Physics **136**, 194110 (2012) 10.1063/1.4718706/190418

[157]A. S. Trushechkin, M. Merkli, J. D. Cresser, and J. Anders, "Open quantum system dynamics and the mean force Gibbs state", AVS Quantum Science **4**, 12301 (2022) 10.1116/5.0073853/2835284

[158]D. Tupkary, A. Dhar, M. Kulkarni, and A. Purkayastha, "Fundamental limitations in Lindblad descriptions of systems weakly coupled to baths", Physical Review A **105**, 032208 (2022) 10.1103/PhysRevA.105.032208

[159]T. Ikeuchi and T. Mori, "Error bounds on the universal Lindblad equation in the thermodynamic limit", Physical Review B **112**, 10.1103/bn2y-tw49 (2025) 10.1103/bn2y-tw49

[160]F. Bloch, "Generalized Theory of Relaxation", Physical Review **105**, 1206 (1957) 10.1103/PhysRev.105.1206

[161]P. Gaspard and M. Nagaoka, "Slippage of initial conditions for the Redfield master equation", The Journal of Chemical Physics **111**, 5668–5675 (1999) 10.1063/1.479867

[162]A. O. Caldeira and A. J. Leggett, "Path integral approach to quantum Brownian motion", Physica A: Statistical Mechanics and its Applications **121**, 587–616 (1983) 10.1016/0378-4371(83)90013-4

[163]A. C. Pipkin, "Evaluation of Principal Value Integrals", in *A course on integral equations. texts in applied mathematics*, Vol. 9 (Springer, New York, NY, 1991), pp. 173–202, 10.1007/978-1-4612-4446-2_9

[164]E. B. Davies, "Markovian master equations", Communications in Mathematical Physics **39**, 91–110 (1974) 10.1007/BF01608389

[165]R. S. Whitney, "Staying positive: going beyond Lindblad with perturbative master equations", Journal of Physics A: Mathematical and Theoretical **41**, 175304 (2008) 10.1088/1751-8113/41/17/175304

[166]G. Schaller and T. Brandes, "Preservation of positivity by dynamical coarse graining", Physical Review A - Atomic, Molecular, and Optical Physics **78**, 022106 (2008) 10.1103/PHYSREVA.78.022106

[167]M. Cattaneo, G. L. Giorgi, S. Maniscalco, and R. Zambrini, "Local versus global master equation with common and separate baths: superiority of the global approach in partial secular approximation", New Journal of Physics **21**, 113045 (2019) 10.1088/1367-2630/AB54AC

[168]D. Farina and V. Giovannetti, "Open-quantum-system dynamics: Recovering positivity of the Redfield equation via the partial secular approximation", Physical Review A **100**, 012107 (2019) 10.1103/PhysRevA.100.012107

[169]L. Bello, W. Fan, A. Gandotra, and H. E. Türeci, "Systematic time-coarse-graining for driven quantum systems", Physical Review Applied **23**, 054042 (2025) 10.1103/PhysRevApplied.23.054042

[170]G. McCauley, B. Cruikshank, D. I. Bondar, and K. Jacobs, "Accurate Lindblad-form master equation for weakly damped quantum systems across all regimes", npj Quantum Information **6**, 1–14 (2020) 10.1038/s41534-020-00299-6

[171]D. F. De La Pradilla, E. Moreno, and J. Feist, "Recovering an accurate Lindblad equation from the Bloch-Redfield equation for general open quantum systems", Physical Review A **109**, 062225 (2024) 10.1103/PhysRevA.109.062225

[172]F. Nathan and M. S. Rudner, "Universal Lindblad equation for open quantum systems", Physical Review B **102**, 115109 (2020) 10.1103/PhysRevB.102.115109

[173]D. Davidović, "Completely Positive, Simple, and Possibly Highly Accurate Approximation of the Redfield Equation", Quantum **4**, 326 (2020) 10.22331/q-2020-09-21-326

[174]B. Bellomo, G. L. Giorgi, G. M. Palma, and R. Zambrini, "Quantum synchronization as a local signature of super- and subradiance", Physical Review A **95**, 043807 (2017) 10.1103/PHYSREVA.95.043807/

[175]F. Galve, A. Mandarino, M. G. Paris, C. Benedetti, and R. Zambrini, "Microscopic description for the emergence of collective dissipation in extended quantum systems", Scientific Reports 2017 7:1 **7**, 42050– (2017) 10.1038/srep42050

[176]R. Hartmann and W. T. Strunz, "Accuracy assessment of perturbative master equations: Embracing nonpositivity", Physical Review A **101**, 012103 (2020) 10.1103/PHYSREVA.101.012103

[177] A. Ishizaki and G. R. Fleming, "On the adequacy of the Redfield equation and related approaches to the study of quantum dynamics in electronic energy transfer", Journal of Chemical Physics **130**, 234110 (2009) 10.1063/1.3155214/924762

[178] F. Gallina, "Models And Quantum Algorithms For Open Systems Dynamics: The Case Study Of Exciton Transport In Molecular Networks", PhD thesis (University of Padova, 2022)

Chapter III

Stochastic Derivation of Open Dynamics

An alternative family of approaches to the description of open quantum system dynamics is the use of stochastic methods to understand, efficiently compute, and derive quantum master equations. As introduced in section I.2.3, there are two main routes one can follow: an effective description of the system, of phenomenological nature, or a microscopic treatment that starts from the definition of a quantum environment and its subsequent elimination. Two formalisms are central to effective description approaches, namely the stochastic Hamiltonian (SH) and a more general formulation, the stochastic Schrödinger equation (SSE). The first one offers the possibility of a description of random fluctuation in the parameters of the system Hamiltonian, either modeling the effects of the physical surroundings of the system and its hidden degrees of freedom, or its interaction with external apparatuses. Recently, a wide range of sophisticated techniques have been developed to control and drive the quantum state for information processing, and when the control field is described within a semiclassical framework, the inclusion of fluctuations in the driving protocol directly maps onto a stochastic Hamiltonian description. This perspective is especially relevant in the context of NISQ devices [56–58], where unavoidable imperfections and control noise manifest as stochastic perturbations of the system Hamiltonian, thereby shaping both dynamics and computational fidelity [59–62]. The second formalism, the stochastic Schrödinger equation, is more general, and allows more than the insertion of random fluctuation in the Hamiltonian, allowing for a wider range of descriptions.

In this Chapter, we aim to provide a clear analysis of these methods by uncovering and elaborating on their common roots in the basic concepts of stochastic calculus. Our main interest is in dynamics governed by stochastic Hamiltonians (SH), which we show

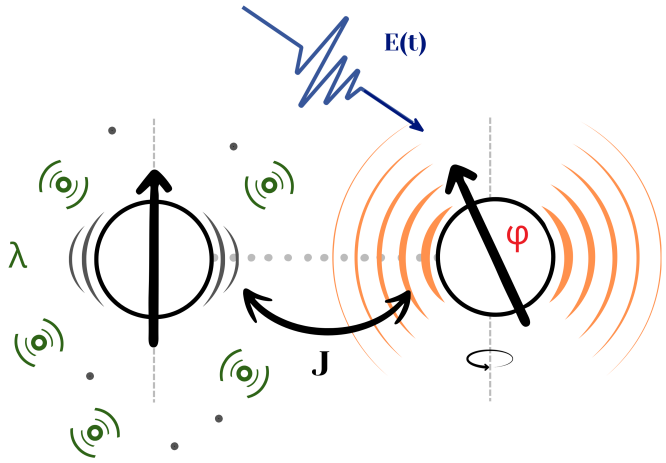

Figure III.1: A schematic example of various of the possible contributions to the stochasticity of an open system, proposed as a two-spin system, or two molecules interacting through their dipoles. In green and labeled λ, particles of the surrounding (a solvent, a fluid, a solid matrix), oscillating and changing at each time the potential embedding of the spin. This affects the second spin through the coupling J. In orange, we consider the different oscillations of the particle, not included in the system's full quantum description. In the red φ, we point at the different orientations that the spins (dipoles) can have with respect to each other at each time, the difference precession frequencies, and so on. In blue, if interacting with an external field, for example an electromagnetic field $E(t)$, that carries its own randomness and instrumental error.

can be identified as a constrained instance of the stochastic Schrödinger equation (SSE) for pure states and of the stochastic Liouville equation (SLE) for generally mixed states.

We present a unified perspective that bridges methodological developments using stochastic Hamiltonians across chemical physics and quantum information science. We trace how different choices in the formalism determine implementation pathways: numerical quadrature of stochastic trajectories versus random-unitary maps, the latter being well-suited for integration into quantum algorithms. Therefore, we do not intend to provide a comprehensive review of all the stochastic approaches to open quantum systems; rather, to assemble selected tools and results known from specific applications and draw explicit connections among them within a single stochastic-calculus framework, providing a self-contained synthesis that clarifies foundations, equivalences, and computational consequences, yielding a practical toolkit for simulating open-system dynamics with stochastic Hamiltonians. To this end, we will make use of the two main interpretations of stochastic calculus, named after Itō and Stratonovich, presented in section III.2, and point out explicitly the difference between a stochastic process and a noise. We further show how each formulation naturally maps to distinct numerical workflows, amenable to efficient classical trajectory integration or to quantum-algorithmic implementations.

This Chapter is based on the results originally developed by the author in Ref. [146]. The material is here primarily contextualized within the scope of the thesis, while several aspects are further expanded in Chapters IV and VI.

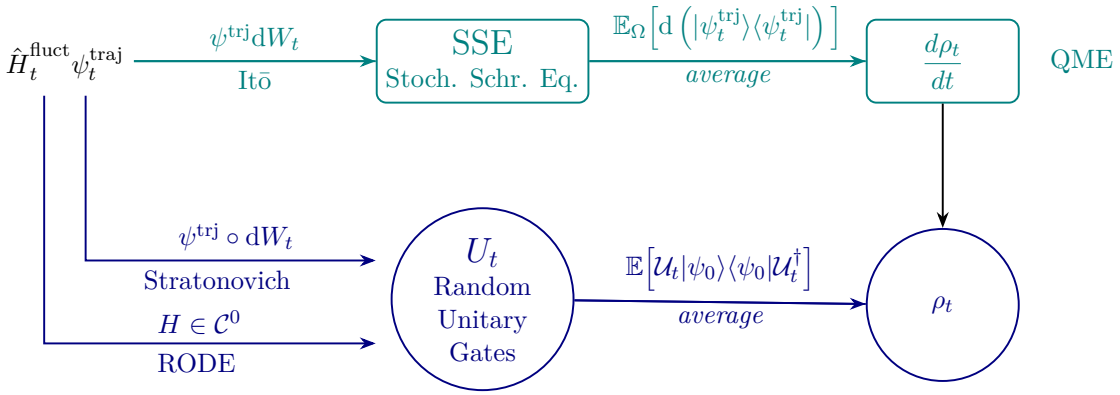

Figure III.2: A schematic map of the two mathematical frameworks and relative workflows for the stochastic Hamiltonian applied to a wavefunction dynamics, based on the Itō (upper green branch) and Stratonovich (lower blue branch) interpretations. The Stratonovich pathway connects stochastic Hamiltonians to direct simulations of the density matrix dynamics through random unitary gates, while the Itō pathway provides the correct formulation for analytically obtaining quantum master equations (QME). The random ordinary differential equation (RODE) case appears as a special limit when dealing with continuous stochastic processes as Hamiltonian fluctuations.

III.1 Modeling of the stochastic Hamiltonian

Let us start from the dynamics induced by a stochastic Hamiltonian [53, 54, 179], as it provides a particularly direct and versatile route to model environmental effects without the need for a complete microscopic model of the underlying system-environment dynamics. In this framework, the effective Hamiltonian H_t^{eff} is composed of the bare system Hamiltonian H plus a randomly fluctuating term H_t^{fluct}, so that we can write

$$H_t^{\text{eff}} = H + H_t^{\text{fluct}} = H + Z_t R \tag{III.1}$$

where R is a Hermitian operator in the system space that defines the interaction with the environment, and $(Z_t)_{t\geq 0}$ is either a continuous stochastic process or a discontinuous noise that models the effect of the environment on the system. Since the specific form of the system Hamiltonian H is not relevant to our discussion, we will consider it as a generic time-independent Hermitian operator, but our conclusions can be easily generalized to the time-dependent case.

In the following, we show how this description arises from the classicization of the bath under some assumptions, and then we employ different mathematical frameworks to obtain specific descriptions.

III.1.1 Classicization of the environment

Many elegant rationalizations have been proposed that justify the approximation of an environment with some stochastic model [180–185]. The first works using these approaches were related to the stochastic behavior of the reduced density matrix [52, 54, 186, 187], and then formulated for wavefunction dynamics [66, 67, 70, 71].

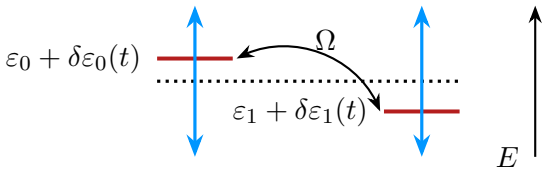

Figure III.3: Example of the effect of a stochastic fluctuation at a time t on the Hamiltonian energy levels in site basis for the single-exciton manifold of a system of two degenerate sites, i.e. $\varepsilon_0 = \varepsilon_1$, indicated by the central dotted line. The vertical blue lines indicate the variance of the stochastic energy fluctuation, the red lines the instantaneous energy of each level at a time t, namely $\varepsilon_i + \delta\varepsilon_i(t)$. The two levels are coupled by a term of constant Ω, shown as a black line.

We start from a system-environment interaction Hamiltonian of the type

$$H_{\text{int}} = cS\hat{B} + c^* S^\dagger \hat{B}^\dagger \tag{III.2}$$

where S acts on the system and $\hat{B}$ is the operator acting on the environment. Choosing $\hat{B}$ Hermitian, we can write

$$H_{\text{int}} = \left(cS + c^* S^\dagger\right) \hat{B}. \tag{III.3}$$

To confine the description within the Hilbert space of the system only, the environment operator $\hat{B}$ must be replaced with a function B_t. This is the first step of numerous embedding schemes, where the environment is reflected in a possibly time-dependent potential. Notice that when such a potential has a stochastic character, the expected change of the purity of the system state, typical of open quantum systems, can be recovered by averaging over different trajectories [180, 188].

In some cases, the stochastic field can be considered as a surrogate environment, originating from the coupling Hamiltonian and the state of the original microscopic environment [181–183]. A prominent example used in triplet exciton dynamics is the replacement of a wide-bandwidth bosonic bath in the high-temperature limit with Gaussian white noise, which acts as a genuine surrogate field [54]. More commonly, the use of stochastic fluctuations in the Hamiltonian is postulated to represent the dominant environmental influence, with no reference to a microscopically defined environment.

The fluctuating interaction Hamiltonian, now acting on the system subspace only, becomes

$$H_t^{\text{fluct}} = Z_t S + Z_t^* S^\dagger \tag{III.4}$$

where

$$Z_t = cB_t. \tag{III.5}$$

For real interaction coefficients c, we obtain real processes Z_t, allowing us to identify the operator

$$R = S + S^\dagger, \tag{III.6}$$

and retrieve eq. (III.1).

The dynamics of the reduced system, which originates from the evolution of the system

plus environment under the Hamiltonian $H' = H + H_{\text{int}}$, unravels in terms of trajectories evolving according to the effective Hamiltonian in eq. (III.1). We can write the Schrödinger equation for a system with the stochastic Hamiltonian as

$$\frac{\mathrm{d}}{\mathrm{d}t}\psi_t^{\text{trj}} = -i\,(H + Z_t R)\,\psi_t^{\text{trj}}, \tag{III.7}$$

where the superscript acknowledges the random nature of the single evolution, a trajectory. Depending on the formal structure of Z_t and the target implementation, different formalisms should be used to ensure that eq. (III.7) is well defined, as we show below.

The reduced density matrix of the open system is obtained as the averaged density matrix over all the possible trajectories, that is

$$\rho_t = \mathbb{E}\left[\rho_t^{\text{trj}}\right] = \mathbb{E}\left[|\psi_t^{\text{trj}}\rangle\langle\psi_t^{\text{trj}}|\right], \tag{III.8}$$

where ρ_t^{trj} is the density matrix of the system along a trajectory and $\mathbb{E}[\cdot]$ indicates the expected value of the argument, obtained as the ensemble average. In any practical case, the average over the ensemble of all possible trajectories is approximated by a finite averaging

$$\mathbb{E}[\rho_t^{\text{trj}}] = \lim_{m\to\infty}\frac{1}{m}\sum_{n=1}^{m}\rho_t^{(n)} \;\simeq \frac{1}{N}\sum_{n=1}^{N}\rho_t^{(n)}\,. \tag{III.9}$$

Note that the averaged density matrix, eq. (III.8), does not describe a pure state, but rather the mixed state of an ensemble where dissipative effects stem from the fluctuations induced by the stochastic component. Importantly, the average maps are completely positive and trace-preserving (CPT) [189] by construction, as the mean dynamics derives from the average of pure quantum states.

To exemplify the formalisms introduced above and the further development in the following sections, we will consider examples of quantum two-level systems. In what follows, we recall the stochastic Hamiltonian formulation of coherence decay between two excited states, originally proposed in the context of triplet exciton dynamics by Haken and Strobl [54].

Example III.1 | Haken-Strobl

Let the system basis be composed of two sites $\{|0\rangle, |1\rangle\}$, with energy ε_0 and ε_1, respectively, and let them interact by a coupling Ω that coherently switches between the sites. The total Hamiltonian, H in eq. (III.1), is then

$$H = \varepsilon_0|0\rangle\langle 0| + \varepsilon_1|1\rangle\langle 1| + \Omega\Big(|0\rangle\langle 1| + |1\rangle\langle 0|\Big)\,. \tag{III.10}$$

A stochastic fluctuation, modeled as white noise (see Appendix III.A), is applied to the site energies to replicate the effect of a rapid Markovian environ-

ment, Figure III.3. We can therefore write the fluctuation Hamiltonian as

$$\hat{H}_t^{\text{fluct}} = \delta\varepsilon_0(t)|0\rangle\langle 0| + \delta\varepsilon_1(t)|1\rangle\langle 1|\,. \tag{III.11}$$

From a comparison with eq. (III.1), we can identify two noise variables $Z_0(t) = \delta\varepsilon_0(t)$ and $Z_1(t) = \delta\varepsilon_1(t)$, and the two associated operators $R_0 = |0\rangle\langle 0|$ and $R_1 = |1\rangle\langle 1|$. This setting reflects a Haken-Strobl model [54], the prototypical description of site dephasing in a quantum system. The trajectory dynamics are computed according to eq. (III.7), the formal explanation for this choice will become clear in section III.3, and the mean dynamics is obtained as the average over trajectories, see eq. (III.9). It is well known (see section III.4 for the details) that the average dynamics of this model is exactly the solution of a Lindblad equation, reported in Appendix III.B. In Figure III.4, a swarm of trajectories is depicted, showing the random character of each realization, and the effect of the different sizes of the sample space is highlighted in the two panels by comparison with the exact solution of the associated Lindblad master equation. Note that, differently from the average behavior, each trajectory maintains the coherent (oscillating) character typical of pure states. The system parameters used for the example are reported in Appendix III.B.

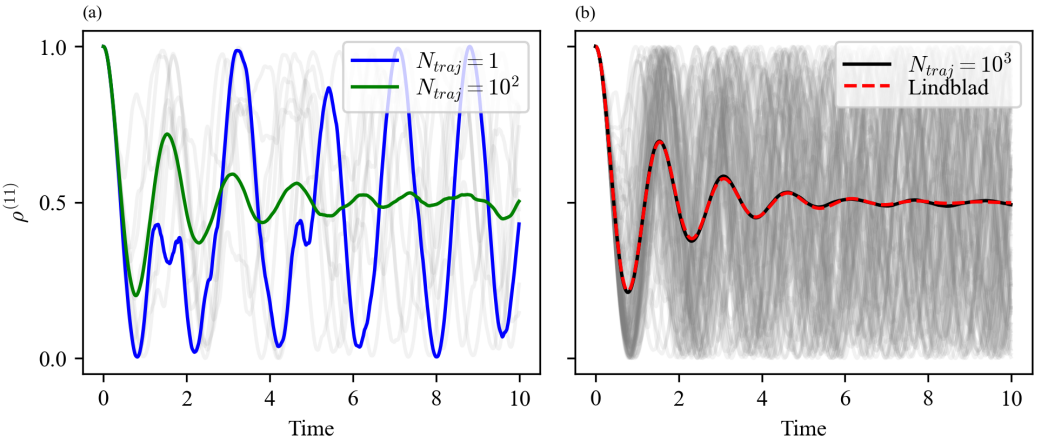

Figure III.4: Stochastic trajectories and average dynamics of the population $\rho_t^{(11)} = \langle 1|\rho_t|1\rangle$ for the Haken–Strobl model presented in the text, computed with the stochastic Hamiltonian approach. (a) Individual realizations of a small ensemble of 10^2 trajectories (grey lines in transparency), one single trajectory highlighted (blue line), and their average (green line). In panel (b), the average over 10^3 trajectories (black line) is compared with the exact solution of the corresponding Lindblad master equation (red dashed line), showing agreement between the stochastic and the master equation descriptions.

III.2 Stochastic calculus tools

Introducing stochastic potentials to model random contributions to a system's dynamics naturally calls for the use of stochastic calculus tools. Within this section, we provide a brief review of essential concepts. We recall the differences between the approaches by Itō [190] and Stratonovich [191] to stochastic calculus as they will be central to appreciate the application-oriented analysis of the following sections.

We introduce the definitions of stochastic differential and stochastic integral, needed to formalize the definitions of stochastic process and noise, in the two main frameworks that we need in the following. For a comprehensive and accessible introduction to the topic, we refer the reader to Ref. [192].

We define a stochastic differential equation (SDE) as the formal expression

$$\mathrm{d}Z_t = f(t, Z_t)\,\mathrm{d}t + g(t, Z_t)\,\mathrm{d}W_t \tag{III.12}$$

where $\mathrm{d}Z_t$ is the stochastic differential of the process Z_t, $f(t, Z_t)$ and $g(t, Z_t)$ are either functionals of the process or simple functions of time, W_t is a Brownian motion (Wiener process), and $\mathrm{d}W_t$ its differential with scaling $\mathrm{d}W_t \sim \sqrt{\mathrm{d}t}$, see Appendix III.A for more details. Indeed, this type of notation is needed because the time derivative of the Wiener process is not a well-defined function; hence, the same is true for the time derivative of the generic process Z_t.

Eq. III.12 is a shorthand notation for the integral equation

$$Z_t = Z_0 + \int_0^t f(s, Z_s)\,\mathrm{d}s + \int_0^t g(s, Z_s)\,\mathrm{d}W_s, \tag{III.13}$$

implying that we need to find a way to define an integral of the form

$$\int_0^T g(t, Z_t)\,\mathrm{d}W_t, \tag{III.14}$$

that cannot be understood as an ordinary integral.

Expressing the integral as its Riemann-sum approximation on a partition of m elements of the time interval $[0, T]$, we write

$$\int_0^T g(t, Z_t)\,\mathrm{d}W_t \approx \sum_{k=0}^{m-1} g(\tau_k, Z_{\tau_k})\,(W(t_{k+1}) - W(t_k)) \tag{III.15}$$

where τ_k is a point that lies within the subinterval $[t_k, t_{k+1}]$, i.e.

$$\tau_k = \lambda t_{k+1} + (1-\lambda)t_k \quad \lambda \in [0, 1]. \tag{III.16}$$

The choice of the parameter λ defines different integral interpretations, introducing different frameworks [192, 193].

Itō's integration is identified by $\lambda = 0$, which corresponds to setting $\tau_k = t_k$, the left-hand point of each subinterval. This choice means that we do not need previous knowledge of the function at future values, in agreement with the idea that the stochastic potential

provides unpredictable random perturbations to the system. In this interpretation of the stochastic differentials, the product rule for the differentials is not the ordinary one, but Itō's product rule: for two differentials of the form $\mathrm{d}Z_i = F_i\,\mathrm{d}t + G_i\,\mathrm{d}W_t$, the differential of the product is

$$\mathrm{d}(Z_1 Z_2) = Z_2\,\mathrm{d}Z_1 + Z_1\,\mathrm{d}Z_2 + G_1 G_2\,\mathrm{d}t, \tag{III.17}$$

where, compared to ordinary calculus, we find the additional term $G_1 G_2\,\mathrm{d}t$ due to the scaling $(\mathrm{d}W)^2 \sim \mathrm{d}t$.

Alternatively, among the infinite other possible choices, setting $\lambda = \frac{1}{2}$ leads to the Stratonovich integral definition. In this definition, the integral is time-symmetric, with both the function and the Wiener differential "sticking out toward the future" and the functional $g(Z_t, t)$ being now *anticipating*, or *non-adapted*. This means that the information at any time t depends on some future-time values, but it agrees with the notion of a mid-point rule. Thus, in the differential Stratonovich notation, commonly identified by a circle before the stochastic differential $\circ\,\mathrm{d}W$, we can write

$$\circ\,\mathrm{d}(Z_1 Z_2) = Z_1 \circ \mathrm{d}Z_2 + Z_2 \circ \mathrm{d}Z_1 \tag{III.18}$$

where the usefulness of restoring the basic rules of differential calculus justifies the tricky anticipatory nature of this interpretation. A fundamental point now is the definition of the $\circ$ symbol we used to indicate the Stratonovich differential as an actual multiplication, known as the *symmetric Q-multiplication* [193] which, for two time-dependent random variables Y_t and Z_t, is

$$Y_t \circ \mathrm{d}Z_t := Y_t\,\mathrm{d}Z_t + \frac{1}{2}\,\mathrm{d}Z_t\,\mathrm{d}Y_t \tag{III.19}$$

with the differential on the r.h.s. now expressed in the Itō interpretation. Then, by combinations, and possibly iteration, of eqs. (III.18) and (III.19) we can transform a Stratonovich SDE into an Itō SDE.

Hereforth, we define a stochastic *process* as the integrated form of any Itō stochastic differential equation,

$$Z_t = \int \mathrm{d}Z_t\,, \tag{III.20}$$

that is the solution of eq. (III.13). The term *noise* corresponds instead to the *formal* time derivative of the stochastic process in a distributional sense,

$$\dot{Z}_t = \mathrm{d}Z_t/\,\mathrm{d}t. \tag{III.21}$$

Therefore, in the SDE formulation, we define *noise-inducing* the stochastic differential $\mathrm{d}Z_t$ itself. This definition can be understood by formally dividing eq. (III.12) by the time differential $\mathrm{d}t$ and obtaining a Langevin-like form, where the presence of a noisy drive is evident in the equation of motion for the process.

III.3 Unitary propagation under stochastic Hamiltonians

Looking for the solution of eq. (III.7), under ordinary calculus rules, we expect to be able to write a formal propagator of the form

$$U_{t,t_0} = \mathcal{T}_+ \exp\left\{-i \int_{t_0}^{t} H_s^{\text{eff}} \, \mathrm{d}s\right\} \tag{III.22}$$

where $\mathcal{T}_+$ is the time-ordering operator, leading to solutions of the wavefunction evolution in the form

$$\psi_t = U_{t,t_0}\psi_0 \tag{III.23}$$

with initial value ψ_0, meaning that we should be able to propagate each trajectory through this unitary. As anticipated in section III.1, we want to write eq. (III.7) in a formally correct way. We start writing the random potential as a noise, for simplicity the common white noise ξ_t of intensity γ, by setting

$$Z_t = \xi_t = \gamma \frac{\mathrm{d}W_t}{\mathrm{d}t}, \tag{III.24}$$

where $\mathrm{d}W_t$ is a proper stochastic differential and the formal time derivative is a distribution, the white noise distribution. Substituting this definition into eq. (III.7) and multiplying both sides by $\mathrm{d}t$, we obtain a mathematically correct formulation of the equation:

$$\mathrm{d}\psi_t = -iH\psi_t \, \mathrm{d}t - i\gamma R\psi_t \circ \mathrm{d}W_t. \tag{III.25}$$

The choice of the Stratonovich interpretation of the differential is fundamental, as it allows us to write the analytical solution to eq. (III.25), since in this formalism the rules of ordinary calculus are indeed valid. As for the solution of the Schrödinger equation, we obtain

$$\psi_t = \mathcal{T}_+ \exp\left\{-i \int_{t_0}^{t} H \, \mathrm{d}t - i\gamma \int_{t_0}^{t} R \circ \mathrm{d}W_t\right\} \psi_{t_0} \,, \tag{III.26}$$

where we recognize in the time-ordered exponential the propagator of the dynamics, meaning that each trajectory can be propagated through this unitary. These solutions, proposed using white noise for the sake of clarity, can be easily generalized for colored noise, paying attention to the correct integration of the deterministic and stochastic parts. We point out, in the following section III.4, that this is not always the case in the Itō formalism, and further constraints must be introduced.

Care must be used in the description of the dynamics of the mean density matrix of the open system, whose equation cannot be obtained by adhering to this formalism. Indeed, while eq. (III.8) holds true, if we take the product differential $\mathrm{d}(\psi_t\psi_t^\dagger)$ and we average,

$$\mathbb{E}\left[\mathrm{d}(\psi_t\psi_t^\dagger)\right] = -i\left[H, \psi_t\psi_t^\dagger\right] \mathrm{d}t - i\gamma \, \mathbb{E}\left(\left[R, \psi_t\psi_t^\dagger\right] \circ \mathrm{d}W_t\right) \tag{III.27}$$

we do not directly obtain the expected form of the master equation, a Lindblad form in the case of white noise stochastic driving. We refer to section III.4 for the computation of the QME, for which one needs to work with Itō calculus.

III.3.1 Advantages of the Stratonovich interpretation

In this framework, we obtain the expression of the propagator as a unitary operator, ensuring norm preservation trajectory-wise. We can obtain the numerical solution for the evolution in the time interval $[0, T]$, discretizing time into S small time steps $\tau = T/S$

$$U_t = \prod_{s=1}^{S} U_{s\tau,(s-1)\tau} \tag{III.28}$$

and approximating at each time step the time-ordered unitary propagator with a first-order Magnus expansion [194, 195]:

$$U_{s\tau,(s-1)\tau} \approx \exp\left\{ -i \int_{(s-1)\tau}^{s\tau} H \,\mathrm{d}r - i\gamma \int_{(s-1)\tau}^{s\tau} R \circ \mathrm{d}W_r \right\}. \tag{III.29}$$

This allows for the numerical integration of every trajectory solution, keeping the unitary character of the propagators. We highlight that the choice of a small time step is important for convergence to the exact time-ordering solution. Higher-order Magnus expansions can also be employed to achieve better convergence.

This numerical scheme may not be efficient for implementation on classical computers, as it requires computing matrix exponentials at every time step. Nonetheless, ensuring the norm-preservation trajectory-wise allows, on one hand, for a clear geometrical interpretation that we can exploit to visualize the state dynamics and gain information from, see Chapter V. Furthermore, it directly allows for the construction of quantum algorithms in digital quantum computer architectures, as we will discuss in Chapter VI.

III.4 Stochastic Schrödinger Equations: recovery of Quantum Master Equations

In this section, we present two different routes to obtain the equation that regulates the average dynamics. First, we show that the definition of stochastic Schrödinger equations (SSE) is based on Itō's calculus. We start with a general way to formulate the SSE, pointing out along the way the more general descriptions that this method allows for. We then rewrite the Stratonovich SDE in its equivalent Itō's form, the way we need to go to recover the Lindblad master equation, therefore showing the equivalence of the two methods if we impose constraints on the SSE. We refer then to section IV.2 for the derivation of more complicated open-form and correlated master equations starting from this stochastic framework.

A simple and general way to formulate the SSE is with a linear stochastic differential equation

$$\mathrm{d}\psi_t = A\psi_t \,\mathrm{d}t + B\psi_t \,\mathrm{d}Z_t \tag{III.30}$$

where the operator A contains the deterministic (Hamiltonian) evolution of the system and B is the operator setting the structure of the stochastic fluctuations encoded by the Itō's differential $\mathrm{d}Z_t$ of a stochastic process Z_t. This allows for a great variety of models

depending on the choice of the process and of the operators [59, 62, 147, 196, 197].

Linear SSEs do not, in principle, ensure the preservation of the norm of the state vector during a trajectory. In this framework, normalization can be obtained by ensuring the martingale property on the norm of the wavefunction, meaning that the norm of the wavefunction at any time is constant as an average over the ensemble. This gives the condition

$$\mathbb{E}\left[||\psi_t||^2\right] = \mathbb{E}\left[||\psi_{t_0}||^2\right] = 1 \implies \mathbb{E}\left[\mathrm{d}(\psi_t^\dagger \psi_t)\right] = 0. \tag{III.31}$$

Recalling Itō's product rule, eq. (III.17), and writing in braket notation, the condition above translates to

$$\begin{aligned}\mathbb{E}\Big[&\langle\psi_t|(A^\dagger + A)|\psi_t\rangle\,\mathrm{d}t + \langle\psi_t|(B^\dagger + B)|\psi_t\rangle\,\mathrm{d}Z_t \\ &+\langle\psi_t|B^\dagger B|\psi_t\rangle(\mathrm{d}Z_t)^2 + \mathcal{O}(\mathrm{d}t^2) + \mathcal{O}(\mathrm{d}t\,\mathrm{d}Z_t)\Big] = 0,\end{aligned} \tag{III.32}$$

where the second-order term w.r.t. $\mathrm{d}Z_t$ depends on the specific process $(Z_t)_{\geq 0}$ and terms of order $\mathcal{O}(\mathrm{d}t^{3/2})$ and higher are neglected. We note explicitly that these definitions do not make any assumptions on the stochastic process. Therefore, Equation (III.32) imposes constraints on the forms of operators A and B depending on the SDE of the noise $\mathrm{d}X_t$.

We briefly comment on an alternative approach to the normalization, leading to a different description of the system under continuous measurement. The wavefunction can be normalized as an *a posteriori* state, by the action of the measure, introducing $\tilde{\psi} = \psi/\|\psi\|$ for each trajectory realization. This leads to the study of *nonlinear* SDE, thoroughly discussed in Ref. [65], an approach that will not be considered further in this work.

III.4.1 Unraveling of Lindblad forms

We now focus the discussion on white-noise-driven systems for the sake of clarity and for a later comparison with the Stratonovich SDE. We let the generic noise of the SSE in eq. (III.30) be a white noise by setting

$$\mathrm{d}\psi_t = A\psi_t\,\mathrm{d}t + \gamma B\psi_t\,\mathrm{d}W_t. \tag{III.33}$$

When applying the normalization condition, first we have to expand the derivative of the inner product,

$$\mathrm{d}(\psi_t^\dagger\psi_t) = \mathrm{d}(\psi_t^\dagger)\psi_t + \psi_t^\dagger\,\mathrm{d}(\psi_t) + \mathrm{d}(\psi_t^\dagger)\,\mathrm{d}(\psi_t)\,, \tag{III.34}$$

that, thanks to Itō product rule in eq. (III.17), and eq. (III.32), reads

$$\begin{aligned}\mathrm{d}(\psi_t^\dagger\psi_t) = &\psi_t^\dagger A^\dagger\psi_t\,\mathrm{d}t + \gamma\psi_t^\dagger B^\dagger\psi_t\,\mathrm{d}W_t + \psi_t^\dagger A\psi_t\,\mathrm{d}t + \gamma\psi_t^\dagger B\psi_t\,\mathrm{d}W_t \\ &+\gamma^2\psi_t^\dagger B^\dagger B\psi_t\,\mathrm{d}t\,.\end{aligned} \tag{III.35}$$

In the usual braket notation, the argument of the average can be written $\mathrm{d}(\langle\psi_t|\psi_t\rangle)$, and the condition can be written equivalently as

$$\begin{aligned}\mathrm{d}(\langle\psi_t|\psi_t\rangle) = &\langle\psi_t|A^\dagger|\psi_t\rangle\,\mathrm{d}t + \gamma\langle\psi_t|B^\dagger|\psi_t\rangle\,\mathrm{d}W_t \\ &+ \langle\psi_t|A|\psi_t\rangle\,\mathrm{d}t + \gamma\langle\psi_t|B|\psi_t\rangle\,\mathrm{d}W_t \\ &+ \gamma^2\langle\psi_t|B^\dagger B|\psi_t\rangle\,\mathrm{d}t\,,\end{aligned} \tag{III.36}$$

from which it is easier to see the following recasting of the expression for the differential, and then the normalization condition as

$$\mathbb{E}\left[\mathrm{d}(\langle\psi_t|\psi_t\rangle)\right] = \mathbb{E}\left[\langle\psi_t|A^\dagger + A + \gamma^2 B^\dagger B|\psi_t\rangle\,\mathrm{d}t\right] + \gamma\mathbb{E}\left[\langle\psi_t|B^\dagger + B|\psi_t\rangle\,\mathrm{d}W_t\right]. \tag{III.37}$$

Thanks to the properties of white noise, the second term vanishes, averaging to zero, see Appendix III.A and Ref. [192]. To ensure the normalization at all times t, we must impose the term in $\mathrm{d}t$ to be zero, and it follows that the total operator acting within the braket must be null,

$$A^\dagger + A + \gamma^2 B^\dagger B = 0. \tag{III.38}$$

Since the operator A must contain the Hamiltonian of the system, so that the deterministic Schrödinger equation can be recovered in the absence of noise, we define it as

$$A = -\frac{i}{\hbar}H + C, \tag{III.39}$$

where the operator C is the correction term needed for the normalization. We reintroduce in this section the explicit use of $\hbar$ for the numerically oriented nature of this method, where different powers of $\hbar$ not set to unity would lead to incorrect results. Substituting the definition of A above, the Hamiltonian terms cancel out, and since it is always true that $B^\dagger B = (B^\dagger B)^\dagger$, the renormalization operator reads

$$C = -\frac{1}{2}\gamma^2 B^\dagger B\,, \tag{III.40}$$

leading to

$$A = -\frac{i}{\hbar}H - \frac{1}{2}\gamma^2 B^\dagger B, \tag{III.41}$$

where we stress again that $(B^\dagger B)$ is always Hermitian, even when B is not. To keep the units consistent, we set $B = L/\sqrt{\hbar}$.

The normalized SSE, for a system driven by white noise, is then

$$\mathrm{d}\psi_t = \left(-\frac{i}{\hbar}H - \frac{1}{2\hbar}\gamma^2 L^\dagger L\right)\psi_t\,\mathrm{d}t + \frac{\gamma}{\sqrt{\hbar}}L\psi_t\,\mathrm{d}W_t, \tag{III.42}$$

the form that allows us to numerically compute the stochastic dynamics of the system state. Using Itō's product rule, eq. (III.17), for the differential $\mathrm{d}(\psi\psi^\dagger) = \mathrm{d}(\rho^{\mathrm{trj}})$, we can write the corresponding equation for the evolution of the trajectory density matrix,

sometimes referred to as the quantum stochastic master equation (QSME), as

$$\begin{aligned} \mathrm{d}(\rho_t^{\mathrm{trj}}) = &-\frac{i}{\hbar}[H,\rho_t^{\mathrm{trj}}]\,\mathrm{d}t - \frac{\gamma^2}{2\hbar}\left\{L^\dagger L,\rho_t^{\mathrm{trj}}\right\}\mathrm{d}t \\ &+ \frac{\gamma}{\sqrt{\hbar}}(L\rho_t^{\mathrm{trj}} + \rho_t^{\mathrm{trj}}L^\dagger)\,\mathrm{d}W_t + \frac{\gamma^2}{\hbar}L\rho_t^{\mathrm{trj}}L^\dagger\,\mathrm{d}t \end{aligned} \tag{III.43}$$

where $[\cdot,\cdot]$ is the commutator and $\{\cdot,\cdot\}$ the anti-commutator. Finally, taking averages as in eq. (III.8), we obtain the associated QME in the form

$$\frac{\mathrm{d}}{\mathrm{d}t}\rho_t = -\frac{i}{\hbar}\left[H,\rho_t\right] + \frac{\Gamma}{\hbar}\left(L^\dagger\rho_t L - \frac{1}{2}\left\{L^\dagger L,\rho_t\right\}\right), \tag{III.44}$$

which is a generic Lindblad form with a single relaxation channel characterized by a constant dissipation rate $\Gamma = \gamma^2$. This is easily generalized to multiple dissipation channels (L_k,γ_k) using additive noise sources in eq. (III.30) [65, 198].

Since there are no constraints on the operator L, rightfully renamed L as a Lindblad (or jump) operator, this SSE describes a wide class of open system dynamics, wider than the stochastic Hamiltonian, as we clarify in the following section. In particular, when L does not commute with the Hamiltonian, the dissipative dynamics include transitions between the eigenstates of the Hamiltonian. Furthermore, when L is not Hermitian, upwards and downwards transitions in energy can occur with different rates, leading to non-uniform stationary states.

Example III.2 | Spontaneous emission

As an example of dissipative dynamics that can be described with a simple SSE but not with a stochastic Hamiltonian, we consider the spontaneous emission of a two-level system, as proposed in Example II.1, from the excited state $|e\rangle$ to the ground state $|g\rangle$. The Hamiltonian of the system is $H = \varepsilon_g|g\rangle\langle g| + \varepsilon_e|e\rangle\langle e|$. The operator for the stochastic component of the evolution is not Hermitian and takes the form $B = \sigma_- = |g\rangle\langle e|$. This is the jump operator that, in the corresponding Lindblad dissipator, describes the transition from the excited to the ground state. The associated normalized SSE that we can propagate numerically is

$$\mathrm{d}\psi_t = \left(-iH - \frac{1}{2}\gamma^2\sigma_+\sigma_-\right)\psi_t\,\mathrm{d}t + \gamma\sigma_-\psi_t\,\mathrm{d}W_t\,, \tag{III.45}$$

where $\sigma_+ = \sigma_-^\dagger$, and the corresponding Lindblad equation for the average dynamics reads

$$\frac{\mathrm{d}}{\mathrm{d}t}\rho_t = -i\left[H,\rho_t\right] + \Gamma\left(\sigma_-\rho_t\sigma_+ - \frac{1}{2}\left\{\sigma_+\sigma_-,\rho_t\right\}\right). \tag{III.46}$$

In terms of ground state population one obtains

$$\frac{\mathrm{d}}{\mathrm{d}t}\rho_t^{(gg)} = \Gamma\rho_t^{(ee)}\,, \tag{III.47}$$

with the solution

$$\rho_t^{(gg)} = 1 - \rho_0^{(ee)}e^{-\Gamma t}\,, \tag{III.48}$$

meaning an exponential decay of the excited state population with rate Γ, as it can be observed in Figure III.5. Note that, as the normalization is ensured *on average* in the stochastic formulation, in this case we can clearly observe that the single trajectories are not individually normalized.

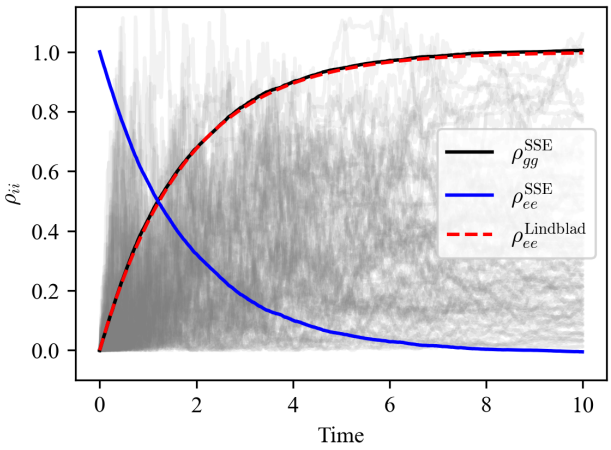

Figure III.5: Spontaneous emission dynamics of a two-level system simulated via stochastic Schrödinger equation (SSE) trajectories. The population of the excited state $\rho_t^{(ee)}$ (blue line) and the ground state $\rho_t^{(gg)}$ (black line) are obtained as averages over an ensemble of 10^3 stochastic realizations, shown for $\rho_t^{(gg)}$ (grey transparency lines). The averages show agreement with the exact solution of the Lindblad master equation (red dashed line).

III.4.2 The stochastic Hamiltonian as a stochastic Schrödinger equation subclass

Since every Lindblad form can be obtained from an SSE using white noise by an appropriate choice of the operator B, it is natural to wonder whether the stochastic Hamiltonian can be regarded as a specific case, a subclass, of this stochastic approach. Comparing the stochastic Hamiltonian formulation of eq. (III.7) with the general form of eq. (III.30), one may relate the two noise coupling operators as $B = iR$, where we set again $\hbar = 1$ for the sake of clarity of visualization. Notice that the stochastic Hamiltonian needs the additional constraint $R^\dagger = R$, to preserve the hermiticity of the effective Hamiltonian. However, this form prevents us from simply deriving the exponential solution as done previously in section III.3. Indeed, the incorrect exponentiation would lead to real negative contributions, causing the loss of wavefunction norm at each time step. This is due to

the interpretation of the stochastic differential, which does not allow for ordinary calculus rules. Therefore, to be able to obtain the correct unitary map eq. (III.22), we need to change the interpretation of the stochastic differential from the Itō form ($\mathrm{d}W_t$) to the Stratonovich one ($\circ\,\mathrm{d}W_t$).

Here, we show how to move from Stratonovich to Itō for the stochastic Hamiltonian class, hence recovering the Lindblad master equation, and showing the equivalence of the two methods.

Starting from the stochastic Hamiltonian definition in the Stratonovich formalism in eq. (III.25), using the definition of the Q-multiplication in eq. (III.19), we can write for the stochastic component in the wavefunction differential

$$-i\gamma R\psi_t \circ \mathrm{d}W_t = -i\gamma R\psi_t\,\mathrm{d}W_t - \frac{i\gamma}{2}R\,\mathrm{d}\psi_t\,\mathrm{d}W_t, \tag{III.49}$$

where we insert back the definition eq. (III.25) of the differential $\mathrm{d}\psi_t$ to obtain

$$-i\gamma R\psi_t \circ \mathrm{d}W_t = -i\gamma R\psi_t\,\mathrm{d}W_t - \frac{i\gamma}{2}R(-iH\psi_t\,\mathrm{d}t - i\gamma R\psi_t \circ \mathrm{d}W_t)\,\mathrm{d}W_t\,. \tag{III.50}$$

To avoid the inconsistency of dealing with mixed Itō and Stratonovich differential terms, we need to apply again eq. (III.49) to the Stratonovich term in the parentheses above obtaining, for the r.h.s. of eq. (III.50),

$$\begin{aligned} -i\gamma R\psi_t\,\mathrm{d}W_t - \frac{i\gamma}{2}R\Big\{ &- iH\psi_t\,\mathrm{d}t - i\gamma R\,\times \\ &\times\left[\psi_t\,\mathrm{d}W_t + \frac{1}{2}\left(-iH\psi\,\mathrm{d}t - i\gamma R\psi\circ\mathrm{d}W_t\right)\right]\Big\}\,\mathrm{d}W_t, \end{aligned} \tag{III.51}$$

where the terms of order $\mathcal{O}(\mathrm{d}t^{3/2})$ and higher [1] can be neglected. Then, the only terms that survive are the ones in $\mathrm{d}W_t$ and $(\mathrm{d}W_t)^2$:

$$-i\gamma R\psi_t \circ \mathrm{d}W_t = -i\gamma R\psi_t\,\mathrm{d}W_t - \frac{\gamma^2}{2}R^2\psi_t\,\mathrm{d}t. \tag{III.52}$$

Notice that the last term, proportional to γ^2, corresponds indeed to the normalization term required in the SSE approach using the Itō formalism. In the Stratonovich formalism for a stochastic Hamiltonian, the normalization is implied *a priori*, and does not need to be enforced, as it comes with the formalism, and the normalization term arises when rewriting into the Itō formalism.

The one additional constraint to be imposed for the normalized SSE in Itō formalism, eq. (III.42), to be equivalent to the Stratonovich stochastic Hamiltonian dynamics, eq. (III.25), is that the operator R must be Hermitian, eq. (III.6), together with the identification $B = iR$ anticipated at the beginning of this section. With this constraint, substituting eq. (III.52) into eq. (III.25), we obtain the norm-preserving SSE, eq. (III.42),

[1] $\mathcal{O}(\mathrm{d}t\,\mathrm{d}W) = \mathcal{O}(\mathrm{d}t^{3/2})$, $\mathcal{O}(\mathrm{d}t\,\mathrm{d}t) = \mathcal{O}(\mathrm{d}t^2)$, and since $\mathcal{O}(\mathrm{d}t\,\mathrm{d}W\circ\mathrm{d}W) > \mathcal{O}(\mathrm{d}t^3)$, any terms arising from a further expansion are evidently of order higher than $\mathcal{O}(\mathrm{d}t^{3/2})$.

and then by usual Itō's calculus we obtain again QMEs in Lindblad form. Notice that the additional condition on B, which is required to be anti-Hermitian in this case, defines a specific subclass of Lindblad dynamics, those unraveled by stochastic unitaries. Notable examples are pure decoherence dynamics and population transfer in the high temperature limit [183].

We conclude that, within this specific subclass of the SSE, one can use one mathematical formalism or the other to their convenience. Using Stratonovich for deriving a stochastic evolution in the form of a closed standard Hamiltonian dynamics and admitting fluctuations in the Hamiltonian, leads to a structure more immediate to understand, and that allows for direct quantum computing implementation. The construction from Itō formalism, leading to the SSE, is otherwise used for the analytical derivation of quantum master equations, and allows an efficient numerical implementation as further explained in the following. As long as the constraints presented for the equivalence of the two formulations hold, the transformation between them is well-defined, and one can use the description most suited to their needs.

III.4.3 Advantages of the Itō framework

The first clear advantage of the SSE approach and the Itō interpretation is that it allows the formal derivation of the associated QMEs. This is true independently of the form of the operators. Indeed, we can obtain a variety of dynamics much wider than the sole stochastic Hamiltonian class. Restricting ourselves to this smaller class, we still have flexibility with the choice of the noise-inducing differential $\mathrm{d}Z_t$, and we can generalize to non-linear SSE, and to various measurement interpretations [65].

As of today, with quantum computations not yet living up to their full potential, the other important advantage of the SSE framework is that it allows efficient implementation schemes on classical computing architectures, avoiding the necessity to implement matrix exponentiation at each timestep of propagation and relying on efficient linear algebra schemes. These schemes are based on finite-difference integration, such as the Euler–Maruyama method [199, 200], the extension to SDE of the Euler finite difference methods,

$$\psi_{n+1} = \psi_n - \left(\frac{i}{\hbar}H + \frac{\gamma^2}{2\hbar}B^\dagger B\right)\psi_n \Delta t + \frac{\gamma}{\sqrt{\hbar}}B\psi_t \Delta W_n. \tag{III.53}$$

Other integration schemes are the Milstein method, which adds a correction to the strong order of convergence [201], $\mathcal{O}(\Delta t)$ instead of $\mathcal{O}(\sqrt{\Delta t})$ but maintaining the weak order of convergence, and Runge-Kutta methods, less used in the stochastic setting as their complexity rapidly increases with the order of the method [202–206].

We should point out that quantum computing implementation of the dynamics obtained in the SSE method is still possible, but with some caveats. The implementation through stochastic unitaries, discussed in detail in Chapter VI, is possible as long as the system can be described as a stochastic Hamiltonian, and therefore recast in its Stratonovich equivalent. Otherwise, different schemes must be used and relevant examples can be found in refs. [207–211].

III.5 Random Ordinary Differential Equations

In the sections above, we used two definitions of stochastic differentials, Itō and Stratonovich, to introduce the effect of noise on the quantum dynamics. On the other hand, the fluctuation in the Hamiltonian in eq. (III.1) can also be a stochastic *process*, namely a continuous function that solves its own SDE. In this case, Z_t in eq. (III.1) is a well-defined continuous function and not a distribution, therefore eq. (III.7) can be treated as an ordinary differential equation (ODE) with random and fluctuating coefficients (RODE), without the need to resort to the stochastic differential equation frameworks.

This is equivalent to setting to zero the stochastic differential terms in eqs. (III.25) and (III.30) and letting random fluctuations appear in the operator A, which now becomes random and time-dependent. In this way, we obtain precisely a Schrödinger equation with the stochastic Hamiltonian in eq. (III.7). The evolution of the system wavefunction is then well defined, continuous, and at least one time differentiable. This special case allows for the use of random processes in the effective Hamiltonian, such as the Ornstein-Uhlenbeck process (OU) [212, 213], and not their noisy increments [147, 214]. The OU process is a Gaussian stochastic process with zero mean characterized by a two-time correlation function decaying exponentially, discussed in further details in section IV.1.1. This process has been used to study memory effects in excitation transport in chromophore aggregates [214–216], and to describe random modulation of the spin Hamiltonian in magnetic resonant experiment [187]. We return to this latter application in the illustrative example below.

Since the problem of the dynamics is well posed, the numerical implementation inherits the advantages of both methods discussed above: it can be discretized in time and integrated *via* finite-difference schemes to be optimized in classical computers. It also admits the unitary propagator, as long as the constraints of the stochastic Hamiltonian hold, which allows quantum computing implementation *via* unitary gates.

Example III.3 | Spin-$\frac{1}{2}$ molecular tumbling

Continuing with the use of a two-level system and prototypical examples, let us consider the description of spin relaxation channels, relevant in magnetic resonance experiments such as NMR (nuclear magnetic resonance) and EPR (electron paramagnetic resonance). Take a single $\frac{1}{2}$-spin system in a static magnetic field Φ_0 along the z-axis direction. This system, in the absence of molecular motions, is described by the Hamiltonian

$$H_0 = \frac{\omega_0}{2}\sigma_z \tag{III.54}$$

where $\omega_0 \propto \Phi_0$ is the Larmor frequency of the system. In liquid solutions, the molecule undergoes translational and rotational diffusion. These motions

imply random modulations of the spin Hamiltonian that can be modeled by a real stochastic process. To account for a finite correlation time, the Ornstein-Uhlenbeck model mentioned above is often used [217–219], which we denote here as X_t. The final effective Hamiltonian takes then the form

$$H_t^{\text{eff}} = \frac{\omega_0}{2}\sigma_z + \mathbf{X}_t \cdot \boldsymbol{\sigma} \tag{III.55}$$

where $\boldsymbol{\sigma} = (\sigma_x, \sigma_y, \sigma_z)$ is a vector of Pauli matrices for the three axis and $\mathbf{X}_t = (X_t^{(x)}, X_t^{(y)}, X_t^{(z)})$ is a vector of OU processes representing the fluctuation of the local field experienced by the spin due to the rotational diffusion. The system evolution is solved as an RODE, propagated with finite-difference numerical methods, either by linearization with Euler method, Runge-Kutta methods, or, with the analytical exponential, eq. (III.22), by time-discretization in either classical or quantum computers. The solution for the average spin populations is shown in Figure III.6, for parameters $\omega_0 = 1$, $\gamma = 0.75$, $\theta = 1$, and $\hbar = 1$.

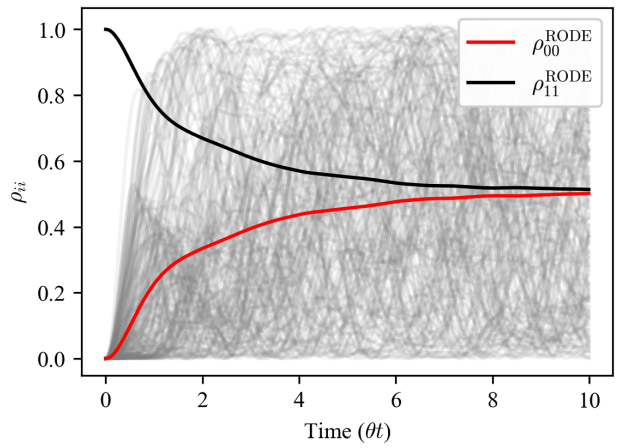

Figure III.6: Relaxation of the population of a $\frac{1}{2}$-spin populations along the z-axis, obtained by averaging over 10^3 trajectories computed in the RODE stochastic Hamiltonian approach (an ensemble of 10^2 trajectories is shown in gray transparency lines). The average for the two populations is shown in solid red and black lines.

III.6 Stochastic Hamiltonian in Liouville Equations

The previous sections rely on and exploit the use of stochastic state vectors. This allows, on the one hand, to use non-Hermitian operators in the case of Itō SDE formalism and obtain any QME in Lindblad form, and on the other hand, using Stratonovich interpretation, to obtain unitary evolutions of pure states which can be implemented on digital quantum computing architectures. The common feature, they exploit the favourable scaling $\mathcal{O}(d^2 N)$ of the wavefunction-based methods rather than $\mathcal{O}(d^4)$ with the associated density matrix, where $\dim \mathcal{H}_S = d$ and N is the number of trajectories needed to converge to the correct average.

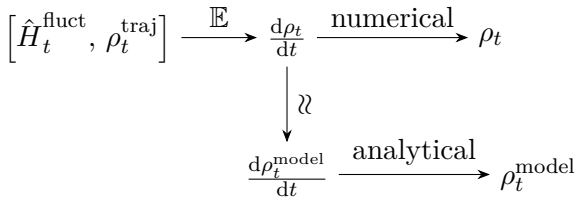

Figure III.7: A schematic map of the stochastic Liouville equation (SLE) framework, where averaging the commutator dynamics yields the exact evolution of the density matrix (upper branch), which can be solved numerically, while approximate models provide analytical solutions (lower branch).

In a further framework, one can directly work with the system density matrix and insert stochastic fluctuations into its dynamics. This can be done for various purposes, allowing for both different descriptions and different numerical implementations on either classical computers, at the cost of the worse scaling $\mathcal{O}(d^4N)$, or quantum computers, at the cost of dilating the simulation Hilbert space [220–222] and the decomposition into Kraus OSR maps [149, 207–210, 223].

The relevance of this framework becomes apparent in the following respects. In a first instance, to conclude the methods that falls under the stochastic Hamiltonian class. Additionally, the results obtained from this derivation will be used as a starting point in Chapter IV to further comment and understand the results presented for time-correlated environment, which will link different stochastic approaches to the Redfield master equation.

Several works have explored the SLE approach, producing interesting results [224–227]. However, the derivations are often presented concisely, with some assumptions and intermediate steps left implicit for the reader. This can lead to differing results, due to tacit approximations. In what follows, we aim to complement these contributions by providing a detailed derivation of different master equations, starting from the Liouville–von Neumann form with a stochastic component, and by clarifying the role of assumptions and approximations.

First, we obtain non-Markovian forms of the master equations and then, through different approximations, we obtain the Redfield master equation. Finally, we show how further approximations lead to Lindblad forms. A graphical outline of our presentation of the SLE approach, highlighting its main directions, is shown in fig. III.7.

For the stochastic Hamiltonian of eq. (III.1), we can write the stochastic Liouville equation (SLE) as

$$\frac{\mathrm{d}}{\mathrm{d}t}\rho_t^{\text{trj}} = -i[H_t^{\text{eff}}, \rho_t^{\text{trj}}] = -i[H, \rho_t^{\text{trj}}] - i[Z_t R, \rho_t^{\text{trj}}], \tag{III.56}$$

of which we can take the average to obtain the mean dynamics given by

$$\frac{\mathrm{d}}{\mathrm{d}t}\rho_t = -i[H, \rho_t] - i[R, \mathbb{E}(Z_t \rho_t^{\text{trj}})] \tag{III.57}$$

where, thanks to Z_t being a real-valued one-dimensional process and R a deterministic

operator, we can bring the average on the product $Z_t\rho_t^{\mathrm{trj}}$ inside the commutator. Since this term depends on the explicit average of the trajectory-wise product over the entire sample space, eq. (III.9), $\mathbb{E}(Z_t\rho_t^{\mathrm{trj}})$ is an open term that must be treated carefully. Due to its presence, eq. (III.57) is not a closed-form master equation in terms of ρ_t only, but explicitly depends on ρ_t^{trj} and Z_t.

As the stochastic density matrix is a functional $\rho^{\mathrm{trj}}[Z_t]$ of the random variable Z_t, under the important assumption that Z_t is Gaussian, we can apply Novikov's theorem [228, 229] which, for the quantities above, gives

$$\mathbb{E}(Z_t\rho_t^{\mathrm{trj}}) = \mathbb{E}(Z_t)\mathbb{E}(\rho_t^{\mathrm{trj}}) + \int_{t_0}^{t} \mathbb{E}(Z_tZ_s)\mathbb{E}\left(\frac{\delta\rho_t^{\mathrm{trj}}[Z]}{\delta Z_s}\right) \mathrm{d}s \tag{III.58}$$

where, for zero-mean processes, the first term on the r.h.s. vanishes and the first term in the integral is the covariance of the process, $C_Z(t,s) = \mathbb{E}(Z_tZ_s)$. It now remains to compute the functional derivative in the integrand. First, we write the formal solution of eq. (III.56) as

$$\rho_t^{\mathrm{trj}} = \rho_{t_0}^{\mathrm{trj}} - i\int_{t_0}^{t} [H + Z_rR, \rho_r^{\mathrm{trj}}]\,\mathrm{d}r \tag{III.59}$$

and then we take the functional derivative to obtain

$$\frac{\delta\rho_t^{\mathrm{trj}}[Z]}{\delta Z_s} = -i\int_{t_0}^{t} \left(\left[H + Z_rR, \frac{\delta\rho_r^{\mathrm{trj}}[Z]}{\delta Z_s}\Theta(r-s)\right] + \delta(s-r)\left[R, \rho_r^{\mathrm{trj}}\right] \right) \mathrm{d}r, \tag{III.60}$$

where $\delta(s-r)$ is the Dirac delta function and $\Theta(r-s)$ is the Heaviside function for the shifted time. Due to the definition

$$\Theta(r-s) = \begin{cases} 0 & r < s \\ 1 & r \geq s \end{cases} \tag{III.61}$$

the functional derivative of ρ_r^{trj} does not depend on its future, and we can change the inferior limit of the integral and arrive at

$$\frac{\delta\rho_t^{\mathrm{trj}}[Z]}{\delta Z_s} = -i\left[R, \rho_s^{\mathrm{trj}}\right] - i\int_{s}^{t} \left[H + Z_rR, \frac{\delta\rho_r^{\mathrm{trj}}[Z]}{\delta Z_s}\right] \mathrm{d}r. \tag{III.62}$$

It seems that we have replaced one problem with another. Yet, taking the time derivative, we can write

$$\frac{\mathrm{d}}{\mathrm{d}t}\frac{\delta\rho^{\mathrm{trj}}[Z]}{\delta Z_s} = -i\left[H + Z_tR, \frac{\delta\rho_t^{\mathrm{trj}}[Z]}{\delta Z_s}\right], \tag{III.63}$$

where we can recognize the form of a Liouville differential equation, $\dot{A} = -i[H_t^{\mathrm{eff}}, A]$, where A is the functional derivative of the trajectory density matrix. From this recasting, we thus obtain a known form of the solution, $A_t = UA_0U^\dagger$, with the unitary time-evolution operator defined by

$$U_{t,t_0} = \mathcal{T}_+ \exp\left\{-i\int_{t_0}^{t}(H + Z_rR)\,\mathrm{d}r\right\}. \tag{III.64}$$

The initial condition is obtained by evaluating eq. (III.62) at the initial time (which is s)

and corresponds to the first term in eq. (III.62), as the integral vanishes when computed at a single time. Finally, we can write

$$\frac{\delta\rho^{\mathrm{trj}}[Z]}{\delta Z_s} = U_{t,s}(-i\left[R,\rho_s^{\mathrm{trj}}\right])U_{t,s}^\dagger = -i\left[U_{t,s}RU_{t,s}^\dagger,\rho_t^{\mathrm{trj}}\right] \tag{III.65}$$

where the propagator is distributed in the commutator and acts on the density matrix, evolving it from the initial time s to the final time t. This shows that the propagation can be dealt with as a time-local evolution with respect to the trajectory density matrix, a time-convolutionless (TCL) evolution [225]. We can now take the average and combine with eqs. (III.57) and (III.58), yielding

$$\frac{\mathrm{d}}{\mathrm{d}t}\rho_t = -i[H,\rho_t] - \int_0^t C_Z(t,s)\left[R,\mathbb{E}\left(\left[U_{t,s}RU_{t,s}^\dagger,\rho_t^{\mathrm{trj}}\right]\right)\right]\mathrm{d}s \tag{III.66}$$

as the evolution equation for the mean density matrix. It is still in an open integro-differential and non-Markovian form for a generic noise or process (Z_t), and solvable only numerically through a swarm of trajectories and their average. One exception is the case of white noise, for which there are further simplifications. On the other hand, for different sources of randomness of the Hamiltonian, such as colored processes and noises, one has to rely either on the numerical implementation, or on the use of perturbative approximation schemes, the latter discussed in depth in section IV.6.6.

III.6.1 Recovery of the Lindblad form from the SLE

In the particular case of Z_t a Gaussian white noise, one can obtain a closed form master equation in a straightforward way, as the correlation function is now a delta function. In fact, the integral term greatly simplifies: substituting $C_Z(t,s) = \delta(t,s)$, the integral is evaluated at time t,

$$\frac{\mathrm{d}}{\mathrm{d}t}\rho_t = -i[H,\rho_t] - \int_0^t \delta(t,s)\left[R,\mathbb{E}\left(\left[U_{t,s}RU_{t,s}^\dagger,\rho_t^{\mathrm{trj}}\right]\right)\right]\mathrm{d}s \tag{III.67a}$$

$$= -i[H,\rho_t] - \left[R,\mathbb{E}\left(\left[\mathcal{U}_{t,t}R\mathcal{U}_{t,t}^\dagger,\rho_t^{\mathrm{trj}}\right]\right)\right] \tag{III.67b}$$

where the propagator effects vanish as $U_{t,t} = e^0$, therefore the operator R loses the randomness feature due to the propagation, and the average then acts only on the stochastic density matrix, giving the mean ρ_t, time-local and undergoing a Markovian evolution. As expected, this leads to the Lindblad form

$$\frac{\mathrm{d}}{\mathrm{d}t}\rho_t = -i[H,\rho_t] - [R,[R,\rho_t]]\,. \tag{III.68}$$

Commenting on the particular form of the dissipator obtained from this approach, using a stochastic Hamiltonian, on can note that it is not the most general Lindblad dissipator. Indeed, we obtain a double commutator, as $R = R^\dagger$. This can be recast in the

more familiar Lindblad form,

$$\begin{aligned}[R,[R,\rho_t]] &= [R,R\rho_t] - [R,\rho_t R^\dagger] \\ &= R^\dagger R\rho_t - R\rho_t R^\dagger - R\rho_t R^\dagger + \rho_t R^\dagger R \\ &= -2\left(R\rho_t R^\dagger - \frac{1}{2}\left\{R^\dagger R,\rho_t\right\}\right)\end{aligned} \tag{III.69}$$

where we exploited the identity $R = R^\dagger$ at our convenience for visualization purpose. Hence, the stochastic Hamiltonian with white noise fluctuations yields a subset of the family of Lindblad generators, characterized by symmetric dissipation.

III.6.2 Advantages of implementing density matrix dynamics

Although simple systems with only a stochastic Hamiltonian could be propagated more efficiently through wavefunction methods, the SLE methods allow for a wider range of system dynamics. They allow us to consider the effects of stochasticity on general mixed states and implement systems undergoing different non-unitary irreversible dynamics. In a general form as follows,

$$\frac{\mathrm{d}}{\mathrm{d}t}\rho_t^{\mathrm{trj}} = -i[H_t^{\mathrm{eff}},\rho_t^{\mathrm{trj}}] + \mathcal{D}[\rho_t^{\mathrm{trj}}] + \mathcal{F}[\rho_t^{\mathrm{trj}}]\,, \tag{III.70}$$

we can consider $\mathcal{D}[\tilde{\rho}_t]$ a different dissipator acting on the trajectory density matrix, in Lindblad or Redfield form, or any other, and $\mathcal{F}[\rho_t^{\mathrm{trj}}]$ to be any filtering, measurement schemes, and any other component we want to study in a particular and complex dynamics. It also allows us to perform these general dynamics on systems and then trace out part of it, allowing for three different layers of interactions: a purely non-Markovian one (the component that is traced out), irreversible dissipation and measurements on the trajectories, stochasticity on the Hamiltonian of the single realizations leading to different dissipators in the mean dynamics.

Appendices

III.A White noise properties

White noise ξ_t is an idealization of interactions with environments with correlation times much shorter than the characteristic time of the system, which can therefore be considered memoryless. It can be heuristically defined as the formal derivative of the Wiener process W_t (Brownian motion) $\xi_t = \gamma\,\mathrm{d}W_t/\,\mathrm{d}t$. This is a distribution, as W_t is not differentiable. This noise has the following properties:

(i) its mean is null, $\mathbb{E}[\xi_t] = 0$, and

(ii) it is δ-correlated in time, $\mathbb{E}[\xi_t\xi_s] = \gamma^2\delta(t-s)$,

where γ is the intensity of the noise and $\delta(t-s)$ is the Dirac delta at different times. Its properties, and those of the differential $\mathrm{d}W_t$, follow from the definition of the Wiener process W_t, a real-valued Gaussian stochastic process with independent and stationary increments, with zero mean and variance proportional to the time t. Equivalently, W_t is bestowed with the following properties:

(i) $W_0 = 0$ a.s.,

(ii) $W_t - W_s = \mathcal{N}(0, t-s)\ \forall t \geq s \geq 0$, and

(iii) $(W_t - W_s)$ is independent of $(W_s - W_r)\ \forall t \geq s \geq r \geq 0$.

We can write for its differential the following useful properties,

(i) $\mathrm{d}W_t \sim \mathcal{N}(0, \mathrm{d}t)$,

(ii) $\mathbb{E}[\mathrm{d}W_t] = 0$, and

(iii) $\mathbb{E}[\mathrm{d}{W_t}^2] = \mathrm{d}t$,

that are used throughout the whole thesis. The definition of *white* noise comes from the spectral density of the process, i.e., the Fourier transform of its autocorrelation function, which is constant, meaning that all the frequencies of the environment are contained in and contribute equally to the correlation function.

III.B Solution of the Haken-Strobl model

The Lindblad master equation representing the exact solution of the Haken-Strobl model discussed in Example III.1 is

$$\frac{\mathrm{d}}{\mathrm{d}t}\rho_t = -i[H, \rho_t] + \sum_{i=0}^{1} \Gamma_i \left(|i\rangle\langle i|\rho_t|i\rangle\langle i| - \frac{1}{2}\left\{|i\rangle\langle i|, \rho_t\right\}\right) \tag{A1}$$

where $\Gamma_i = \mathbb{E}[\delta\varepsilon_i^2(t)]$ are the dephasing rate associated with site i. We recall that the noisy components, oscillation of the sites energies, are intended as white noises $\delta\varepsilon_i(t) = \xi_i(t)$.

This serves as an exact reference for the convergence of the density matrix obtained by averaging over a finite sample space. While the Hamiltonian term of the equation drives the coherent oscillations between the sites, the effect of the dephasing term is to destroy such coherences. As a result, the off-diagonal terms of the density matrix decay exponentially

$$\frac{\mathrm{d}}{\mathrm{d}t}\rho_t^{(01)} = -i2\Omega\left(\rho_t^{(11)} - \rho_t^{(00)}\right) - \frac{\Gamma_0 + \Gamma_1}{2}\rho_t^{(01)}, \tag{A2}$$

where the superscript (ij) indicates the density matrix element, and the populations on the sites slowly equilibrate due to the effect of coherence loss, $\rho_t^{(00)}, \rho_t^{(11)} \to \rho_\infty^{(ii)}$,

$$\frac{\mathrm{d}}{\mathrm{d}t}\rho_t^{(00)} = -i\Omega\left(\rho_t^{(01)} - \rho_t^{(10)}\right) = 2\Omega\mathrm{Im}\left[\rho_t^{(01)}\right]. \tag{A3}$$

For the example reported in Figure III.4, we used the following system parameters: $\varepsilon_0 = 0$, $\varepsilon_1 = 1$, $\Omega = 2$, $\Gamma_0 = \Gamma_1 = 0.5$, and setting $\hbar = 1$.

References

[52]R. Kubo and K. Tomita, "A General Theory of Magnetic Resonance Absorption", Journal of the Physical Society of Japan **9**, 888–919 (1954) 10.1143/JPSJ.9.888

[53]R. Kubo, "Stochastic Liouville Equations", Journal of Mathematical Physics **4**, 174–183 (1963) 10.1063/1.1703941

[54]H. Haken and G. Strobl, "An exactly solvable model for coherent and incoherent exciton motion", Zeitschrift für Physik **262**, 135–148 (1973) 10.1007/BF01399723

[56]J. Preskill, "Quantum Computing in the NISQ era and beyond", Quantum **2**, 79 (2018) 10.22331/q-2018-08-06-79

[57]S. Brandhofer, S. Devitt, T. Wellens, and I. Polian, "Special session: Noisy intermediate-scale quantum (NISQ) Computers - How they work, how they fail, how to test them?", Proceedings of the IEEE VLSI Test Symposium **2021-April**, 10.1109/VTS50974.2021.9441047 (2021) 10.1109/VTS50974.2021.9441047

[58]K. Bharti, A. Cervera-Lierta, T. H. Kyaw, T. Haug, S. Alperin-Lea, A. Anand, M. Degroote, H. Heimonen, J. S. Kottmann, T. Menke, W. K. Mok, S. Sim, L. C. Kwek, and A. Aspuru-Guzik, "Noisy intermediate-scale quantum algorithms", Reviews of Modern Physics **94**, 015004 (2022) 10.1103/RevModPhys.94.015004

[59]R. J. De Keijzer, L. Y. Visser, O. Tse, and S. J. Kokkelmans, "Qubit fidelity distribution under stochastic Schrödinger equations driven by classical noise", Physical Review Research **7**, 023063 (2025) 10.1103/PHYSREVRESEARCH.7.023063

[60]A. Baratz, L. M. Cangemi, A. Hamo, S. Refaely-Abramson, and A. Levy, "Data-Driven Reconstruction and Characterization of Stochastic Dynamics via Dynamical Mode Decomposition", (2025)

[61]S. Cialdi, M. A. Rossi, C. Benedetti, B. Vacchini, D. Tamascelli, S. Olivares, and M. G. Paris, "All-optical quantum simulator of qubit noisy channels", Applied Physics Letters **110**, 81107 (2017) 10.1063/1.4977023

[62]S. Cialdi, C. Benedetti, D. Tamascelli, S. Olivares, M. G. Paris, and B. Vacchini, "Experimental investigation of the effect of classical noise on quantum non-Markovian dynamics", Physical Review A **100**, 052104 (2019) 10.1103/PhysRevA.100.052104

[65]A. Barchielli and M. Gregoratti, *Quantum Trajectories and Measurements in Continuous Time: The Diffusive Case, Lect. Notes Phys. 782* (Springer, Berlin Heidelberg, 2009), 10.1007/978-3-642-01298-3

[66]N. Gisin, "Quantum Measurements and Stochastic Processes", Physical Review Letters **52**, 1657 (1984) 10.1103/PhysRevLett.52.1657

[67]A. Barchielli and V. P. Belavkin, "Measurements continuous in time and a posteriori states in quantum mechanics", Journal of Physics A: Mathematical and General **24**, 1495 (1991) 10.1088/0305-4470/24/7/022

[70]N. Gisin and I. C. Percival, "The quantum-state diffusion model applied to open systems", Journal of Physics A: Mathematical and General **25**, 5677 (1992) 10.1088/0305-4470/25/21/023

[71]H. J. Carmichael, *An Open Systems Approach to Quantum Optics, Lect. Notes in Phys. Monogr. 18*, edited by W. Beiglböck (Springer Berlin, Heidelberg, 1993), https://doi.org/10.1007/978-3-540-47620-7

[146]P. De Checchi, F. Gallina, B. Fresch, and G. G. Giusteri, "On the Noisy Road to Open Quantum Dynamics: The Place of Stochastic Hamiltonians", Annalen der Physik **538**, e00482 (2026) 10.1002/ANDP.202500482

[147]P. De Checchi, F. Gallina, B. Fresch, and G. G. Giusteri, "Quantum trajectories and reduced dynamics in time-correlated environments", (2025), submitted.

[149]K. Kraus, *States, Effects, and Operations: Fundamental Notions of Quantum Theory*, edited by K. Kraus, A. Böhm, J. D. Dollard, and W. H. Wootters (Springer Berlin, Heidelberg, Aug. 1983), p. 40, https://doi.org/10.1007/3-540-12732-1

[179]H. Hasegawa and H. Ezawa, "Stochastic Calculus and Some Models of Irreversible Processes", Progress of Theoretical Physics Supplement **69**, 41–54 (1980) 10.1143/PTP.69.41

[180]P. Gaspard and M. Nagaoka, "Non-Markovian stochastic Schrödinger equation", The Journal of Chemical Physics **111**, 5676–5690 (1999) 10.1063/1.479868

[181]P. Szańkowski and Ł. Cywiński, "Noise representations of open system dynamics", Scientific Reports **10**, 1–19 (2020) 10.1038/S41598-020-78079-7

[182]P. Szańkowski, "Measuring trajectories of environmental noise", Physical Review A **104**, 022202 (2021) 10.1103/PhysRevA.104.022202

[183]B. Gu and I. Franco, "When can quantum decoherence be mimicked by classical noise?", The Journal of Chemical Physics **151**, 14109 (2019) 10.1063/1.5099499

[184]D. Calvani, A. Cuccoli, N. I. Gidopoulos, and P. Verrucchi, "Parametric representation of open quantum systems and cross-over from quantum to classical environment", Proceedings of the National Academy of Sciences of the United States of America **110**, 6748–6753 (2013) 10.1073/PNAS.1217776110

[185]C. Foti, T. Heinosaari, S. Maniscalco, and P. Verrucchi, "Whenever a quantum environment emerges as a classical system, it behaves like a measuring apparatus", Quantum **3**, 179 (2019) 10.22331/q-2019-08-26-179

[186]A. G. Redfield, "On the Theory of Relaxation Processes", IBM Journal of Research and Development **1**, 19–31 (1957) 10.1147/rd.11.0019

[187]R. Kubo, "A Stochastic Theory of Line Shape", in *Stochastic processes in chemical physics*, Vol. 15, edited by K. E. Shuler (Wiley, Dec. 1969), pp. 101–127, 10.1002/9780470143605.ch6

[188]R. Kubo, "The fluctuation-dissipation theorem", Reports on Progress in Physics **29**, 255 (1966) 10.1088/0034-4885/29/1/306

[189]G. Gasbarri and L. Ferialdi, "Stochastic unravelings of non-Markovian completely positive and trace-preserving maps", Physical Review A **98**, 042111 (2018) 10.1103/PhysRevA.98.042111

[190]K. Itô, "Stochastic integral", Proceedings of the Imperial Academy **20**, 519–524 (1944) 10.3792/PIA/1195572786

[191]R. L. Stratonovich, "A New Representation for Stochastic Integrals and Equations", SIAM Journal on Control **4**, 362–371 (1966) 10.1137/0304028

[192]L. Evans, *An Introduction to Stochastic Differential Equations* (American Mathematical Society, Dec. 2013), 10.1090/mbk/082

[193]K. Itô, "Stochastic calculus", in International symposium on mathematical problems in theoretical physics, edited by H. Araki (1975), pp. 218–223, 10.1007/BFb0013327

[194]W. Magnus, "On the exponential solution of differential equations for a linear operator", Communications on Pure and Applied Mathematics **7**, 649–673 (1954) 10.1002/CPA.3160070404

[195]S. Blanes, F. Casas, J. A. Oteo, and J. Ros, "The Magnus expansion and some of its applications", Physics Reports **470**, 151–238 (2009) 10.1016/J.PHYSREP.2008.11.001

[196] A. Barchielli, C. Pellegrini, and F. Petruccione, "Stochastic Schrödinger equations with coloured noise", Europhysics Letters **91**, 24001 (2010) 10.1209/0295-5075/91/24001

[197] J. Łuczka, "Non-Markovian stochastic processes: Colored noise", Chaos **15**, 10.1063/1.1860471/922643 (2005) 10.1063/1.1860471/922643

[198] G. G. Giusteri, F. Recrosi, G. Schaller, and G. L. Celardo, "Interplay of different environments in open quantum systems: Breakdown of the additive approximation", Physical Review E **96**, 10.1103/PhysRevE.96.012113 (2017) 10.1103/PhysRevE.96.012113

[199] V. Bally and D. Talay, "The Euler scheme for stochastic differential equations: error analysis with Malliavin calculus", Mathematics and Computers in Simulation **38**, 35–41 (1995) 10.1016/0378-4754(93)E0064-C

[200] V. Bally and D. Talay, "The law of the Euler scheme for stochastic differential equations: I. Convergence rate of the distribution function", Probability Theory and Related Fields **104**, 43–60 (1996) 10.1007/BF01303802/

[201] G. N. Milstein, *Numerical Integration of Stochastic Differential Equations* (Springer Netherlands, 1995), 10.1007/978-94-015-8455-5

[202] E. Platen and P. E. Kloeden, *Numerical Solution of Stochastic Differential Equations*, edited by I. Karatzas and M. Yor, Vol. 23 (Springer-Verlag, Berlin Heidelberg, 1992)

[203] C. M. Mora, "Numerical Simulation of Stochastic Evolution Equations Associated to Quantum Markov Semigroups", Mathematics of Computation **73**, 1393–1415 (2004)

[204] E. Platen and N. Bruti-Liberati, *Numerical Solution of Stochastic Differential Equations with Jumps in Finance*, edited by B. Rozovskii and G. Grimmett, Vol. 64 (Springer, Berlin, 2010)

[205] A. Rößler, "Second order Runge-Kutta methods for Itô stochastic differential equations", SIAM Journal on Numerical Analysis **47**, 1713–1738 (2009) 10.1137/060673308

[206] A. Rößler, "Runge-Kutta methods for the strong approximation of solutions of stochastic differential equations", SIAM Journal on Numerical Analysis **48**, 922–952 (2010) 10.1137/09076636X

[207] Z. Hu, R. Xia, and S. Kais, "A quantum algorithm for evolving open quantum dynamics on quantum computing devices", Scientific Reports 2020 10:1 **10**, 1–9 (2020) 10.1038/s41598-020-60321-x

[208] R. Sweke, I. Sinayskiy, D. Bernard, and F. Petruccione, "Universal simulation of Markovian open quantum systems", Physical Review A - Atomic, Molecular, and Optical Physics **91**, 062308 (2015) 10.1103/PHYSREVA.91.062308

[209] R. Sweke, M. Sanz, I. Sinayskiy, F. Petruccione, and E. Solano, "Digital quantum simulation of many-body non-Markovian dynamics", Physical Review A **94**, 022317 (2016) 10.1103/PHYSREVA.94.022317

[210] A. W. Schlimgen, K. Head-Marsden, L. A. M. Sager, P. Narang, and D. A. Mazziotti, "Quantum simulation of the Lindblad equation using a unitary decomposition of operators", Physical Review Research **4**, 023216 (2022) 10.1103/PhysRevResearch.4.023216

[211] A. Miessen, P. J. Ollitrault, F. Tacchino, and I. Tavernelli, "Quantum algorithms for quantum dynamics", Nature Computational Science 2022 3:1 **3**, 25–37 (2022) 10.1038/s43588-022-00374-2

[212] G. E. Uhlenbeck and L. S. Ornstein, "On the Theory of the Brownian Motion", Physical Review **36**, 823 (1930) 10.1103/PhysRev.36.823

[213]D. T. Gillespie, "Exact numerical simulation of the Ornstein-Uhlenbeck process and its integral", Physical Review E **54**, 2084 (1996) 10.1103/PhysRevE.54.2084

[214]F. Gallina, M. Bruschi, and B. Fresch, "From stochastic Hamiltonian to quantum simulation: exploring memory effects in exciton dynamics", New Journal of Physics **26**, 083017 (2024) 10.1088/1367-2630/AD6A7B

[215]T. Fujita, J. C. Brookes, S. K. Saikin, and A. Aspuru-Guzik, "Memory-Assisted Exciton Diffusion in the Chlorosome Light-Harvesting Antenna of Green Sulfur Bacteria", Journal of Physical Chemistry Letters **3**, 2357–2361 (2012) 10.1021/JZ3008326

[216]A. G. Dijkstra, C. Wang, J. Cao, and G. R. Fleming, "Coherent exciton dynamics in the presence of underdamped vibrations", Journal of Physical Chemistry Letters **6**, 627–632 (2015) 10.1021/JZ502701U

[217]R. Kubo and N. Hashitsume, "Brownian Motion of Spins", Progress of Theoretical Physics Supplement **46**, 210–220 (1970) 10.1143/PTPS.46.210

[218]A. Abragam, *Principles of Nuclear Magnetism (The International Series of Monographs on Physics)* (Clarendon Press, 1983), p. 614

[219]T. R. Field and A. D. Bain, "Dynamical theory of spin relaxation", Physical Review E **87**, 022110 (2013) 10.1103/PhysRevE.87.022110

[220]W. F. Stinespring, "Positive functions on *-algebras", Proceedings of the American Mathematical Society **6**, 211–216 (1955) 10.1090/S0002-9939-1955-0069403-4

[221]B. Sz.-Nagy, "Prolongement des transformations de l'espace de Hilbert qui sortent de cet espace dans Appendice au livre "Leçons d'analyse fonctionnelle"", in *Leçons d'analyse fonctionnelle* (Akadémiai Kiadó, Budapest, 1955), pp. 439–573

[222]M. Kliesch, T. Barthel, C. Gogolin, M. Kastoryano, and J. Eisert, "Dissipative Quantum Church-Turing Theorem", Physical Review Letters **107**, 120501 (2011) 10.1103/PhysRevLett.107.120501

[223]K. Kraus, "General state changes in quantum theory", Annals of Physics **64**, 311–335 (1971) 10.1016/0003-4916(71)90108-4

[224]A. A. Budini, "Non-Markovian Gaussian dissipative stochastic wave vector", Physical Review A **63**, 012106 (2000) 10.1103/PhysRevA.63.012106

[225]A. A. Budini, "Quantum systems subject to the action of classical stochastic fields", Physical Review A **64**, 052110 (2001) 10.1103/PhysRevA.64.052110

[226]A. Kiely, "Exact classical noise master equations: Applications and connections", Europhysics Letters **134**, 10001 (2021) 10.1209/0295-5075/134/10001

[227]A. Chenu, M. Beau, J. Cao, and A. Del Campo, "Quantum Simulation of Generic Many-Body Open System Dynamics Using Classical Noise", Physical Review Letters **118**, 10.1103/PhysRevLett.118.140403 (2017) 10.1103/PhysRevLett.118.140403

[228]E. A. Novikov, "Functionals and the random-force method in turbolence theory", J. Exptl. Theoret. Phys. (U.S.S.R.) **47**, 1919–1926 (1964)

[229]V. I. Klyatskin and V. I. Tatarskii, "Statistical averages in dynamical systems", Theoretical and Mathematical Physics **17**, 1143–1149 (1973) 10.1007/BF01037265

Chapter IV

Unraveling of Correlated Quantum Master Equation

The assumption of white noise, and the resulting Markovian dynamics, is often inadequate in molecular sciences and emerging quantum technologies, where environments exhibit finite correlation times, structured spectral densities, and nontrivial back-action effects. Motivated by the recent ability to experimentally engineer and control environmental noise [62, 230], this Chapter explores the effect of different noise profiles on the dynamics of a two-level system. In particular, we consider a direct generalization of the white noise stochastic Schrödinger equation, in which memory effects are introduced in the SSE dynamics by an explicit colored noise, using the differential of an exponentially correlated Ornstein–Uhlenbeck (OU) process [196], replacing white-noise increments. By considering the OU differential, we define an effective correlated noise, whose properties analyzed and used to construct a colored-noise SSE unraveling of its associated open-form quantum master equation.

The average dynamics generated by the colored SSE is analyzed through a direct comparison with the analog dynamics generated by the standard white noise SSE and a stochastic Hamiltonian defined through the related OU process. Using colored noise and processes as stochastic potentials leads to master equations that are open-form and not of Lindblad type, yet are positive definite by construction due to the averaging over pure-state trajectories. This paves the way for using SSE as more than an efficient numerical strategy for known QMEs, but also as a framework for formulating non-trivial effective descriptions in regimes where a closed master equation may be difficult — or impossible — to derive explicitly. As a consequence of the interaction with different environments, we observe how, in a particular setting of correlated noise source and operator, different dissipation

timescales can be obtained, even reaching coherent robust steady states, according to the symmetry of the system.

Recently, the same formal setting has been elaborated with a more application-oriented focus in Ref. [59] where the origin of the colored noise is identified with the random fluctuations of qubit driving fields. Together with subsequent works [231, 232], these studies further underline the significance and practical relevance of the theoretical framework (and results) presented, highlighting the suitability of this investigation approach to address unconventional noise sources.

To gain insight into the peculiar features of colored-noise-induced dynamics, we introduce an approximate closure for the open correlation terms appearing in the ensemble-averaged QME. This is a microscopically-inspired model for the correlation contributions, based on the perturbative treatment of the system–environment interaction commonly done in the Redfield theory, as discussed in Chapter II. With this construction, we build a transparent cause–effect intuition connecting the noise statistics to the non-Markovian dynamics of the open quantum system. We further investigate the approximations employed and their effects connecting to the results obtained in the previous Chapter, comparing the structure and properties of the open correlation terms arising from different modeling strategies, with particular emphasis on cross-correlations and temporal nonlocality.

This Chapter builds upon results originally developed by the author in Ref. [147], and extends the analysis introduced in the previous Chapter, providing additional developments beyond those presented in Ref. [146].

IV.1 Stochastic modeling of the environment

Aiming to characterize the environments stochastically, it is important to describe the mean, variance, and covariance of the stochastic process driving the SSE. Many examples of different phenomenological baths can be found in the literature.[18, 54, 162, 233, 234] The use of δ-correlated noise, i.e. white noise, is one of the most frequent, as it can be used to unravel Markovian QMEs in Lindblad form, as we discussed in the previous chapter. Considering instead a colored noise is one straightforward way to introduce memory effects into the open system's dynamics, computationally more efficient than other approaches that require computing memory kernels for the complete density matrix dynamics.

IV.1.1 Ornstein-Uhlenbeck process

One possible generalization from white noise to correlated (colored) processes is the use of the Ornstein-Uhlenbeck (OU) process. It is often used in the stochastic Hamiltonian approach to describe finite-memory effects induced by an overdamped environment whose relaxation time is comparable to the characteristic timescale of the system [187, 214–216, 235], a practical example of its application proposed in the previous chapter in Example III.3. The OU process is the random real-valued process $(X_t)_{t\geq 0}$ that satisfies the following SDE:

$$\mathrm{d}X_t = -\theta X_t \,\mathrm{d}t + \gamma \,\mathrm{d}W_t \qquad\qquad \theta, \gamma > 0 \tag{IV.1}$$

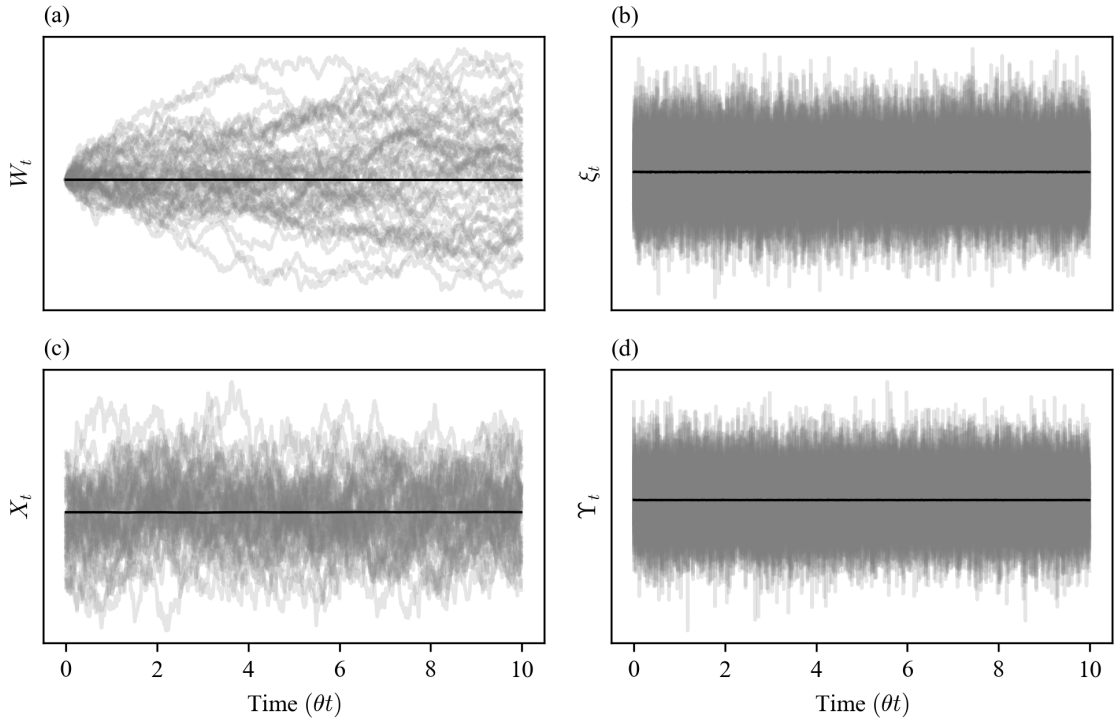

Figure IV.1: A swarm of 50 different stochastic trajectories (grey lines in transparency) and the average (black solid line) for the two stochastic processes in the left panels, Wiener W_t (a) and Ornstein-Uhlenbeck X_t (c), and their two underlying noises on the right, white noise ξ_t (b) and Ornstein-Uhlenbeck correlated noise Υ_t (d). In panels (a,b) θ is set to 1.

where θ is the inverse of the correlation time of the process, γ is the amplitude of the random fluctuation and W_t is a Wiener process. The explicit solution for the OU process is

$$X_t = X_0 e^{-\theta t} + \gamma \int_0^t e^{-\theta|t-s|}\, \mathrm{d}W_s \tag{IV.2}$$

Then, $(X_t)_{t\geq 0}$ is a Gaussian-Markov process, endowed with the following statistical properties:

$$\mathbb{E}(X_t) = X_0 e^{-\theta t} \xrightarrow{t\to\infty} 0 \tag{IV.3}$$

$$\mathrm{var}(X_t) = \frac{\gamma^2}{2\theta}\left(1 - e^{-2\theta t}\right) \xrightarrow{t\to\infty} \frac{\gamma^2}{2\theta} \tag{IV.4}$$

and, introducing $\Delta t = t - s$ for notation convenience,

$$\mathrm{cov}(X_t, X_{s=t-\Delta t}) = \frac{\gamma^2}{2\theta}\left(e^{-\theta|\Delta t|} - e^{-\theta(2t+\Delta t)}\right) \xrightarrow{t\to\infty} \frac{\gamma^2}{2\theta} e^{-\theta|\Delta t|} \tag{IV.5}$$

where the $t \to \infty$ while Δt is kept constant in the limit represents the stationary process, i.e., when the environment is at its equilibrium. Therefore, under this hypothesis for the environment, it is natural to define the initial value X_0 as a random variable itself, in particular a Gaussian with zero mean and the same variance as the stationary process.

This process is characterized by a two-time correlation function decaying exponentially,

eq. (IV.5), related to a Lorentzian spectral density, see Figure IV.2, in the form

$$J_{\mathrm{OU}}(\omega) = \int_{-\infty}^{+\infty} C_{\mathrm{OU}}(t, t_0) e^{i\omega t}\, \mathrm{d}t = \frac{\gamma^2}{\omega^2 + \theta^2}\,. \tag{IV.6}$$

IV.1.2 Ornstein-Uhlenbeck noise

The OU process as described above can be used in the stochastic Hamiltonian approach, in the RODE implementation, see section III.5. However, we note that its SDE, eq. (IV.1), can also be used as stochastic potential to drive our SSE, from the general form in eq. (III.30). In this way, $\mathrm{d}X_t$ is noise-inducing term, and we have to deal with a new noise, which is the derivative of the OU process, in analogy with what was done previously for the white noise and the Wiener process, see Appendix III.A.

We can give a firm formal definition of this noise as the time derivative of (X_t), in the distribution sense, dividing by $\mathrm{d}t$ and expressing the integral form of (X_t):

$$\Upsilon_t = \dot{X}_t = -\theta X_0 e^{-\theta t} - \theta\gamma \int_0^t e^{-\theta(t-s)}\, \mathrm{d}W_s + \gamma\xi_t\,. \tag{IV.7}$$

The mean of (Υ_t) is again zero, as the stochastic terms average to zero, and we consider the noise to be constructed over the stationary OU process. We have

$$\mathbb{E}[\Upsilon_t] = -\theta e^{-\theta t}\mathbb{E}[X_0] = 0 \qquad \text{for } X_0 \sim \mathcal{N}(0, \chi),\ t \to \infty. \tag{IV.8}$$

To evaluate the covariance of the OU noise we have to test the two-time average against two test functions, $\phi, \psi \in \mathcal{C}_C^\infty$. We first write the covariance in terms of derivatives of (X_t),

$$\mathrm{cov}(\Upsilon_t, \Upsilon_s) = \mathbb{E}[\Upsilon_t, \Upsilon_s] = \mathbb{E}[\dot{X}_t, \dot{X}_s], \tag{IV.9}$$

and now we test it in the double-integral, which can be recast by integration by parts twice into:

$$\iint_{-\infty}^{+\infty} \mathbb{E}[\dot{X}_t, \dot{X}_s]\phi_t\psi_s\, \mathrm{d}t\, \mathrm{d}s = \iint_{-\infty}^{+\infty} \mathbb{E}[X_t\, X_s]\dot{\phi}_t\dot{\psi}_s\, \mathrm{d}t\, \mathrm{d}s \tag{IV.10}$$

We have obtained a known quantity, the covariance of the Orstein-Uhlenbeck process, and by integrating one last time by parts,

$$\iint_{-\infty}^{+\infty} \mathrm{cov}(X_t, X_s)\dot{\phi}_t\dot{\psi}_s\, \mathrm{d}t\, \mathrm{d}s = \iint_{-\infty}^{+\infty} \frac{\mathrm{d}}{\mathrm{d}t}\left(\frac{\mathrm{d}}{\mathrm{d}s}\Big(\mathrm{cov}(X_t, X_s)\Big)\right)\phi_t\psi_s\, \mathrm{d}t\, \mathrm{d}s \tag{IV.11}$$

we find a way to obtain the covariance of the new noise. Then, we start by computing the double derivative,

$$\mathrm{cov}(\Upsilon_t, \Upsilon_s) = \frac{\mathrm{d}}{\mathrm{d}t}\left(\frac{\mathrm{d}}{\mathrm{d}s}\left(\frac{\gamma^2}{2\theta}\left(e^{-\theta|t-s|} - e^{-\theta(t+s)}\right)\right)\right) \tag{IV.12}$$

$$= \frac{\gamma^2}{2\theta}\frac{\mathrm{d}}{\mathrm{d}t}\left(\theta e^{-\theta|t-s|}\mathrm{sign}(t-s) + \theta e^{-\theta(t+s)}\right) \tag{IV.13}$$

$$= \frac{\gamma^2}{2\theta}\left(-\theta^2 e^{-\theta|t-s|}\mathrm{sign}^2(t-s) + \theta e^{-\theta|t-s|}\mathrm{sign}'(t-s) - \theta^2 e^{-\theta(t+s)}\right). \tag{IV.14}$$

The expression of the covariance of the noise is obtained by recalling that this is valid upon the integration, therefore we consider that the square of the sign is one, as the single point in zero brings no contribution, and the derivative of the sign function can be written as $\mathrm{sign}(x) = 2\Theta(x) - 1$, where $\Theta(x)$ is the Heaviside function. Then its derivative is not simply a Dirac's delta function, but twice that: $\mathrm{sign}'(x) = 2\delta_0(x)$. Finally, we obtained the covariance of the OU-noise, which reads

$$\mathrm{cov}(\Upsilon_t, \Upsilon_s) = -\frac{\gamma^2\theta}{2} e^{-\theta|t-s|} + \gamma^2\delta(t-s). \tag{IV.15}$$

It is interesting to note that the correlation function includes both the characteristic δ-function of the white noise and the exponential decay of the OU process. Therefore, the spectral density J_Υ consists of a constant background suppressed by a negative Lorentzian dip centered at zero frequency, namely

$$J_\Upsilon(\omega) = \int_{-\infty}^{+\infty} \mathrm{cov}(\Upsilon_t) e^{i\omega t}\,\mathrm{d}t = -\frac{\theta\gamma^2}{2}\frac{2\theta}{\omega^2+\theta^2} + \gamma^2 = \frac{\gamma^2\omega^2}{\omega^2+\theta^2} \tag{IV.16}$$

converging asymptotically to 1 at infinity and collapsing to 0 at low frequencies, Figure IV.2. This particular form of the spectral density has consequences on the system dynamics, as we will discuss in the next sections, both analytically and with numerical implementations.

To conclude, in Box IV.1 the statistical properties of the processes and noises considered are summarized, and their spectral density is depicted graphically. We recall that, for real-valued (classical) stochastic processes, spectral function and spectral density coincide.

Box IV.1 | Noises and processes features

	Mean $\mathbb{E}[\bullet]$	Variance $\mathbb{E}[\bullet_t^2]$	Covariance $\mathbb{E}[\bullet_t \bullet_s]$
W_t	0	t	$s \wedge t$
ξ_t	0	$\gamma^2\delta_0$	$\gamma^2\delta_0(t-s)$
X_t	0	$\frac{\gamma^2}{2\theta}$	$\frac{\gamma^2}{2\theta}e^{-\theta\lvert t-s\rvert}$
Υ_t	0	$-\frac{\gamma^2\theta}{2} + \gamma^2\delta_0$	$\gamma^2\delta_0(t-s) - \frac{\gamma^2\theta}{2}\left(e^{-\theta\lvert t-s\rvert} + e^{-\theta(t+s)}\right)$

Table 1: Comparison of the properties of the four stochastic processes and noises (distributions) used to model the environment effects. The properties of the Wiener process are included for sake of completeness. The mean of the processes is set to zero as they can all be rescaled to satisfy this condition, and the variance and covariance are considered at infinite time $t \to \infty$ and $(t-s) \leq \infty$, i.e., for the stationary process.

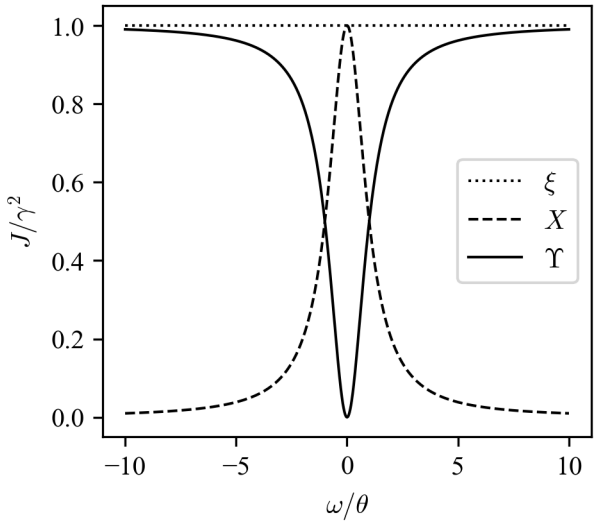

Figure IV.2: Spectral densities of white noise (ξ, dotted line), OU process (X, dashed line) and Υ_{OU}-noise (Υ, solid line). Pay attention to the different physical dimensions associated to each J/γ^2: $[J_\xi] = 1$, $[J_X] = t^2$, and $[J_\Upsilon] = 1$, see IV.A.

IV.1.3 Pauli, projection, commuting and noncommuting noises

The last ingredient to describe the system-environment interaction in the general SSE approach is the definition of the *noise* operator B, meaning that operator that defines the action of the noise on the system. In the subframe of stochastic Hamiltonians, we showed that it needs to be an anti-Hermitian operator $B = iR$, narrowing to the possible choices of the Hermitian operator R. As we will do for all the results presented, unless stated differently, we will, from now on, refer to two-level systems, being the minimal model relevant both in quantum information processing (qubit) and in modeling internal relaxation and energy transfer in molecular systems [236, 237].

We distinguish between two macro families of operators according to their commuting properties with respect to the system Hamiltonian, and further between three classes of noise operators [59], and they will be used to further describe the noise in the SSE.

Projection noises are characterized by projection noise operators, so

$$R^\dagger R = R, \quad R = |a\rangle\langle a| \tag{IV.17}$$

and they are commonly used to describe energy fluctuations on the chosen basis; see, for instance, Example III.1 modeling a Haken-Strobl system [54], as well as recent works using this type of noise to describe disordered molecular networks [214, 238]. Indeed, these operators are the ones used for the first proofs of environment-assisted quantum transport (ENAQT) [29, 30, 239, 240]. Describing energy fluctuations, they can also be used to describe frequency random variation in control fields [59, 232].[1] In this particular case, the projection noise is also a *commuting noise*.

[1] As the qubit Hamiltonian before any control or gate applied is usually described by $H_{\text{q}} = \Delta\sigma_z$, where Δ is a tunable energy difference between the two qubit levels, then $[H, R] = 0$.

Another class can be referred to as *Pauli noise*, as characterized by the use of Pauli operators to apply the noise, so

$$R^\dagger R = \mathbb{1}, \quad R = \sigma_j \tag{IV.18}$$

where σ_j is a Pauli matrix. These, too, can be either commuting or non-commuting with the Hamiltonian. *Commuting Pauli noises* satisfies the relation $[H, \sigma_j] = 0$.

When the system Hamiltonian and the noise operator are defined by different Pauli matrices, such as the case of a generic Hamiltonian, the noise is a *non-commmuting Pauli noise*,

$$[H, R] = 2i\epsilon_{jkl}\sigma_l, \qquad R^\dagger R = \mathbb{1}, \quad R = \sigma_j,\, \sigma_k \in H. \tag{IV.19}$$

In this case, it is worth noting that the effect of a $R = \sigma_z$ is similar to that of a projection noise. Indeed, for a qubit system, one can write the projection noises operator as $|0\rangle\langle 0| = (\mathbb{1}+\sigma_z)/2$ and $|1\rangle\langle 1| = (\mathbb{1}-\sigma_z)/2$. Moreover, we can imagine using only the σ_z operator as the application of a half-intensity noise on one site (one projector noise) and its opposite on the other. These result in two effective channels that are perfectly anti-correlated on the two energy levels, the fundamental difference being the application of a single σ_z Pauli noise versus two channels via two projection noises, yet with negligible effects on the dynamics of the two-level system investigated in the following.

Since the effects of projection noise are well-known and have been intensively studied, and are somehow a restrictive choice, we will focus on the use of Pauli noises, both commuting and non-commuting. We then further differentiate between *diagonal noise*, i.e., the noise applied on the diagonal of the Hamiltonian in the chosen representation, representing physical fluctuation of the "sites" energies, and can be applied either by a Pauli σ_z or a projection noise, and *coupling noise*, a Pauli noise acting on the off-diagonal elements of the Hamiltonian.

IV.2 Correlated QME from Ornstein-Uhlenbeck-driven SSE

In section III.4.1 we showed how we can recover any Lindblad QME using white noise as stochastic drive in a SSE. To introduce memory effects in the dynamics, we can use a different noise source. Starting from the general non-normalized SSE, eq. (III.30), we consider the system

$$\begin{cases} \mathrm{d}\psi_t = A\psi\,\mathrm{d}t + B\psi\,\mathrm{d}X \\ \mathrm{d}X_t = -\theta X_t\,\mathrm{d}t + \gamma\,\mathrm{d}W_t \end{cases} \tag{IV.20}$$

where we can substitute the Ornstein-Uhlenbeck SDE, eq. (IV.1), as the noise source of the system dynamics. Then, the non-normalized SSE is

$$\mathrm{d}\psi_t = (A - \theta X_t B)\psi_t\,\mathrm{d}t + \gamma B\psi\,\mathrm{d}W_t \tag{IV.21}$$

Then, in the normalization, eq. (III.32), the martingale condition eq. (III.31) is satisfied when

$$\langle\psi|\left[A^\dagger + A - \theta X_t(B^\dagger + B) + \gamma^2 B^\dagger B\right]|\psi\rangle dt = 0. \tag{IV.22}$$

Compared to the white noise case, to keep operators A and B deterministic and time-independent, we need to impose further constraints on the B operator, which must be an anti-Hermitian operator of the form $B = -iR/\sqrt{\hbar}$ with $R^\dagger = R$, see Appendix IV.C for more detail. To avoid this constraint, one would have to change the description of the dynamics using non-linear versions of the SSE [196], shifting at the same time the attention to a different response of the system [65]. Maintaining our focus on stochastic Hamiltonian dynamics, this choice does not introduce new constraints.

Then, substituting the noise operator in eq. (IV.22), we obtain the same correction term in A obtained in the white noise case, eq. (III.41), since the sum of anti-Hermitian operators cancels out. The linear normalized OU-driven SSE is then

$$\mathrm{d}\psi_t = \left(-\frac{i}{\hbar}H - \frac{1}{2\hbar}\gamma^2 R^\dagger R\right)\psi_t\,\mathrm{d}t + \frac{i}{\sqrt{\hbar}}\theta X_t R\psi_t\,\mathrm{d}t - \frac{i}{\sqrt{\hbar}}\gamma R\psi_t\,\mathrm{d}W_t, \tag{IV.23}$$

In this, we clearly see the addition of a term proportional to the colored noise process X_t. Taking the derivative of the outer product of the wavefunction, we first obtain the quantum stochastic master equation (QSME) associated with a single trajectory as

$$\mathrm{d}(\rho_t^{\mathrm{trj}}) = -\frac{i}{\hbar}[H,\rho_t^{\mathrm{trj}}]\,\mathrm{d}t + \frac{i}{\sqrt{\hbar}}[\theta X_t R,\rho_t^{\mathrm{trj}}]\,\mathrm{d}t - \frac{\gamma^2}{2\hbar}[R,[R,\rho_t^{\mathrm{trj}}]]\,\mathrm{d}t - \frac{i}{\sqrt{\hbar}}\gamma[R,\rho_t^{\mathrm{trj}}]\,\mathrm{d}W_t. \tag{IV.24}$$

By averaging over the trajectories, the mean density matrix dynamics is governed by

$$\frac{\mathrm{d}}{\mathrm{d}t}\rho_t = -\frac{i}{\hbar}[H,\rho_t] + \frac{\gamma^2}{\hbar}\left(R\rho_t R^\dagger - \frac{1}{2}\{R^\dagger R,\rho_t\}\right) + \frac{i\theta}{\sqrt{\hbar}}\left[R,\mathbb{E}\left(X_t\rho_t^{\mathrm{trj}}\right)\right]. \tag{IV.25}$$

The dynamic evolution presents itself with three distinct terms. The first one is the Hamiltonian dynamics of the system. The second one, proportional to γ^2, is a Lindblad dissipator. The last term, proportional to θ, features the correlation $\mathbb{E}(X_t\rho_t^{\mathrm{trj}})$ between the system evolution and the process associated to the colored noise modeling the environment.

Due to this cross-correlation between the single realization of the OU process and each trajectory, eq. (IV.25) is not in a closed form in terms of the mean density matrix ρ_t, let alone a Lindblad form, and we have to rely on stochastic unraveling for its numerical solution. This term affects the long-time dynamics in a way that is not immediately evident or easily predictable, owing to the open-form nature of the equation. In section IV.6, we derive an approximate closure model that helps in understanding the role of the correlation term. A striking example of the importance of the correlation term in eq. (IV.25) can be seen by considering its stationary state. Because the operators R are constrained to be Hermitian when introducing colored noise (see Appendix IV.C), by considering only the Lindblad dissipator, we would expect to reach a distribution with equally populated eigenstates. We will show in the following that this prediction is not always true when the open cross-correlation term is present.

IV.2.1 Element-wise EOM from the correlated QME

To appreciate the immediate impact of replacing white noise with a colored source in the SSE, let us look at the simplest case of a two-dimensional Hilbert space spanned by the basis vectors $\{|0\rangle, |1\rangle\}$. We consider two resonant states and set to zero the deterministic part of the interaction Hamiltonian. We choose $R = \sigma_x$ to obtain a correlated version of the Pauli master equation with symmetric decay rates. The resulting QME reads

$$\frac{\mathrm{d}}{\mathrm{d}t}\rho_t = \frac{\gamma}{\hbar}\left(\sigma_x\rho_t\sigma_x - \rho_t\right) + \frac{i\theta}{\sqrt{\hbar}}\left[\sigma_x, \mathbb{E}\left(X_t\rho_t^{\mathrm{trj}}\right)\right], \tag{IV.26}$$

where $\gamma = \sigma^2$ would be the relaxation rate of the channel in the absence of memory effects.

The variables of the system are the four elements of the density matrix. By normalization, the populations are such that $\rho_{00} + \rho_{11} = 1$ and by hermiticity the coherences satisfy $\rho_{01} = \rho_{10}^*$. So we can describe the system just by computing the time derivatives of two variables, ρ_{00} and ρ_{10}. The equation of motion (EOM) for one population is

$$\dot{\rho}_{00} = \frac{\gamma}{\hbar}(1 - 2\rho_{00}) - \frac{2\theta}{\sqrt{\hbar}}\mathbb{E}\left[X_t\mathrm{Im}(\rho_{10}^{\mathrm{trj}})\right] \tag{IV.27}$$

and the coherence term is

$$\dot{\rho}_{10} = -\frac{i2\gamma}{\hbar}\mathrm{Im}(\rho_{10}) + \frac{i2\theta}{\sqrt{\hbar}}\mathbb{E}\left[X_t\rho_{00}^{\mathrm{trj}}\right] - i\theta\mathbb{E}(X_t) \tag{IV.28}$$

where we know the mean of the OU process, $\mathbb{E}(X_t) = X_0 e^{-\theta|t-t_0|}$, conditioned on the initial value X_{t_0}.

In this simple case, we see that the effect of the cross-correlation term is to mix *trajectory-wise* the equations of motion of population and coherence terms. Populations are affected by the correlation of the single trajectory coherences with the OU process. This is an effective correlation of the system coherences with the environment, correlation that is usually neglected in the microscopic derivation of quantum master equations, when assuming the factorized form of the total density matrix in terms of system and bath density matrices at all times (the decoupling imposed by the Born approximation). The last term in eq. (IV.26) is also responsible for the possible deviation of the asymptotic value of populations from equipartition and for non-vanishing steady-state coherences.

IV.3 Stochastic Hamiltonian with Ornstein-Uhlenbeck fluctuations

Within the framework of effective stochastic Hamiltonian [146], the Ornstein-Uhlenbeck process $(X_t)_{t\geq 0}$ is often used as a random potential (not its noisy increments), implementing it in a RODE, see section III.5. As mentioned in section IV.1, this describes the interaction with an environment of overdamped oscillators, a setting that is known to give induce non-Markovian signatures and can exhibit such effects depending on the parameters [214].

Then, with the effective Hamiltonian

$$H_{\text{eff}} = H + \sqrt{\hbar} R \theta X_t, \tag{IV.29}$$

where the parameter θ is necessary to keep consistent units, see Appendix IV.A and consider Box IV.1, the dynamics of the system becomes

$$\mathrm{d}\psi_t = -\frac{i}{\hbar}\left(H + \theta\sqrt{\hbar} R X_t\right)\psi_t \,\mathrm{d}t. \tag{IV.30}$$

The average Liouville equation associated with this dynamics reads

$$\frac{\mathrm{d}}{\mathrm{d}t}\rho_t = -\frac{i}{\hbar}[H, \rho_t] - \frac{i\theta}{\sqrt{\hbar}}\left[R, \mathbb{E}\left(X_t \rho_t^{\text{trj}}\right)\right]. \tag{IV.31}$$

Here, we do not find a Lindblad-form dissipator term. The only term in addition to the closed-system Liouvillian is the correlation term we observed in eq. (IV.25), albeit with opposite sign.

We can adopt a similar approach using any other random continuous function as the fluctuation. A straightforward example, in the same fashion of using OU process X_t and its noise Υ_t, would be the use of the Wiener process W_t associated with the white noise ξ_t. This leads again to a non-Lindblad dynamics,

$$\frac{\mathrm{d}}{\mathrm{d}t}\rho_t = -\frac{i}{\hbar}[H, \rho_t] - \frac{i\gamma}{\sqrt{\hbar}}\left[R, \mathbb{E}\left(W_t \rho_t^{\text{trj}}\right)\right]. \tag{IV.32}$$

Proposing again the example dynamics investigated in section IV.2.1, the EOM of the populations reads, for a generic stochastic process fluctuation Z_t,

$$\dot{\rho}_{00} = -\alpha\mathbb{E}\left[Z_t \mathrm{Im}(\rho_{10}^{\text{trj}})\right], \tag{IV.33}$$

the factor α accounting for the different coefficients obtained according to the specific process. The dissipation on the population now depends only on the cross-correlation of the process and the coherence of the trajectory-wise propagation.

IV.4 Nature of the dissipator components

We can now identify a correspondence between components of the correlation function and terms of the dissipator in the map of the mean dynamics. The average of the SSE with white noise potential, purely δ-correlated, leads to Lindblad dissipators, eq. (III.44). The correction term arising from the normalization through the martingale property accounts for the anticommutator term of the Lindblad dissipator $\{R^\dagger R, \rho_t\}$. This is the term that accounts for the irreversible coherence loss and dissipation in the open dynamics. On the other hand, the term proportional to $\mathrm{d}W_t$, the noise component, leads to the $(R\rho_t R^\dagger)$ term in the Lindblad dissipator, accounting for the coherent part of the dissipation. This

originates from the additional term in Itō differentials product rule, eq. (III.17).

$$\begin{aligned} d\psi &= \boxed{-iH\psi\,\mathrm{d}t} + \boxed{\gamma R\psi\,\mathrm{d}W_t} - \boxed{\tfrac{1}{2}\gamma^2 R^\dagger R\psi\,\mathrm{d}t} \\ \frac{d\rho}{dt} &= \boxed{-i[H,\rho]} + \boxed{\gamma^2 R\rho R^\dagger} - \boxed{\tfrac{1}{2}\gamma^2\{R^\dagger R,\rho\}} \end{aligned}$$

The X_{OU} process is exponentially correlated, eq. (IV.5), and the dissipator is a single term that explicitly depends on the correlation with the environment, eq. (IV.31). Since there are no explicit terms proportional to $\mathrm{d}W_t$, there is no additional term, and not being an SDE to be normalized but a purely stochastic Hamiltonian dynamics with a continuous potential, no renormalization term is required either. Then the only term of the dissipator is the cross-correlation term.

The QME obtained as the average of the SSE driven by Υ_{OU} colored noise, the correlation of which has both components, eq. (IV.15), presents both the Lindblad dissipator and a correction accounting for the environment memory, eq. (IV.25). The nature of each term originates from the same considerations above, and can be related to the different terms in the correlation functions.

$$\begin{aligned} d\psi &= \boxed{-iH\psi\,\mathrm{d}t} + \boxed{\gamma R\psi\,\mathrm{d}W_t} - \boxed{\tfrac{1}{2}\gamma^2 R^\dagger R\psi\,\mathrm{d}t} + \boxed{i\theta X_t R\psi_t\,\mathrm{d}t} \\ \frac{d\rho}{dt} &= \boxed{-i[H,\rho]} + \boxed{\gamma^2 R\rho R^\dagger} - \boxed{\tfrac{1}{2}\gamma^2\{R^\dagger R,\rho\}} + \boxed{i\theta[R,\mathbb{E}(X_t\rho_t^{\mathrm{trj}})]} \end{aligned}$$

IV.5 Numerical results

In this section, we analyze the numerical results with a focus on the Υ_{OU} colored-noise SSE, in comparison with the evolutions driven by white noise and the OU process.

Let us consider a two-level system, as we did for the examples in Chapter III, defined by the Hamiltonian in the generic form

$$H_{\varepsilon,\Omega} = -\frac{1}{2}\varepsilon\sigma_z + \Omega\sigma_x. \tag{IV.36}$$

We refer to the eigenstates of σ_z as the observable basis, $\{|0\rangle, |1\rangle\}$ which, for example, can be thought of as the computational states of a qubit or two local sites in a transfer problem, such as exciton or charge transfer. Therefore, we will denote different systems by setting the parameters ε and Ω as follows: two states that are energy-degenerate and not interacting ($H_{0,0}$), coupled degenerate levels ($H_{0,\Omega}$), a two-level system which is not interacting through Hamiltonian dynamics ($H_{\varepsilon,0}$) or the most general case of two coupled states at different energies ($H_{\varepsilon,\Omega}$). The system Hamiltonian parameters are kept constant

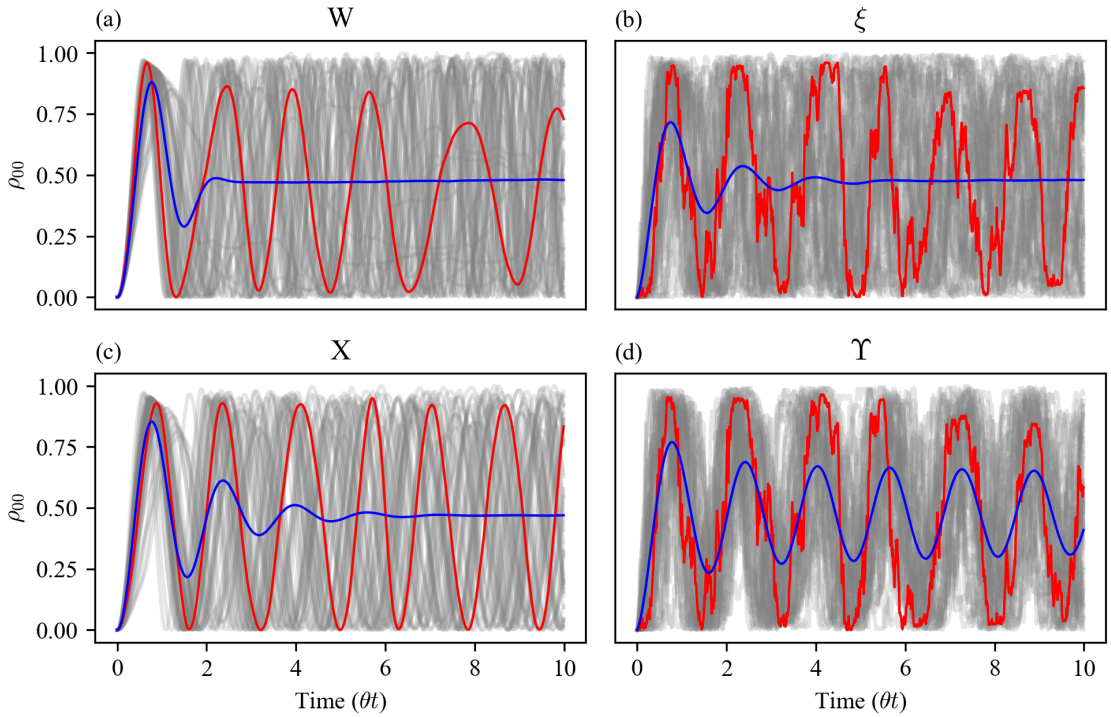

Figure IV.3: Comparison of the mean and trajectories evolution of the system under different driving stochastic processes. Swarms of 50 different stochastic trajectories (grey lines in transparency), the evolution of single trajectories (red lines) and the averaged evolution of the ρ_{00} population - the observable under investigation. The stochastic force for each unraveling: in the upper left panel (a) Wiener process fluctuations, lower left (c) OU process fluctuations, upper right white noise SSE and lower right OU noise-driven SSE. Example for the the generic Hamiltonian $H_{\varepsilon,\omega}$ system with non-commuting Pauli noise operator $R = \sigma_x$.

throughout the numerical analysis, setting $\varepsilon = \hbar\theta$ and $\Omega = 2\hbar\theta$.

The initial state of the system is set to be a pure state localized on $|1\rangle$, meaning $|\psi_0^{(n)}\rangle = |1\rangle$ for each trajectory n.

The results are obtained by averaging over $2 \cdot 10^4$ to 10^5 trajectories realization for each dynamics, computed using the Euler–Maruyama method [199], introduced in section III.4.3, with time increments such as to ensure convergence of the noise realizations ($\theta\Delta t = 10^{-5}$).

The effects of different stochastic sources will be compared, the intensity of the white noise component is set at $\gamma = 0.7\sqrt{\hbar\theta}$ unless stated differently, while the memory parameter θ is kept constant at $\theta = 1$ (the convergence to the white noise limit as $\theta \to 0$ for the Υ_{OU}-noise dynamics is reported in Appendix IV.E). The effect of changing the noise intensity, from 0.04 to 3 $\sqrt{\hbar\theta}$, can be observed in Appendix IV.D.

IV.5.1 Typicality of the trajectories and short-time evolution

We want to highlight the typicality of single-trajectory evolution in Figure IV.3. The systems whose dynamics is modeled by a stochastic Hamiltonian with a random process as the drive, namely the Wiener process W_t and the OU process X_t, eqs. (IV.31) and (IV.32),

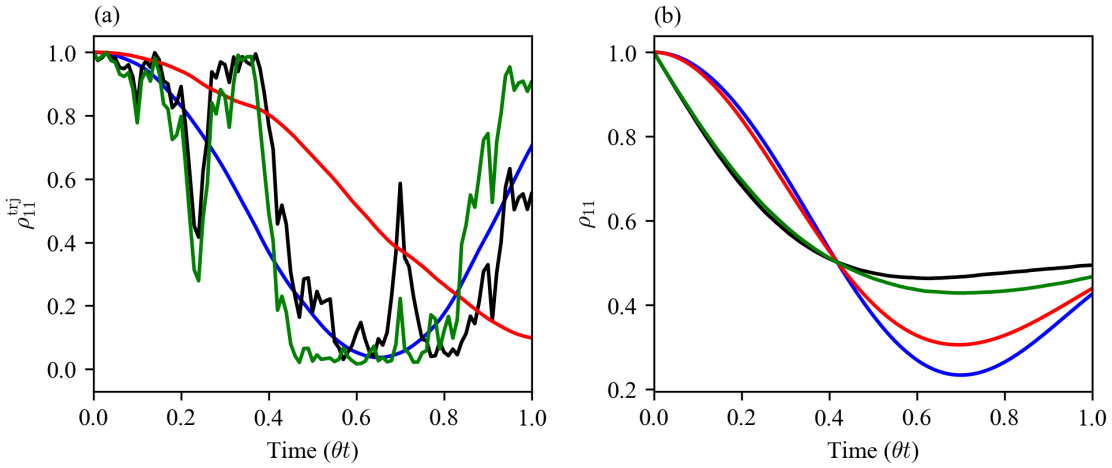

Figure IV.4: Comparison of the short-time evolution of the system under different driving stochastic processes, both at the trajectory level in panel (a) and the mean behavior in panel (b). To emphasize the difference, the plots are displayed for a stronger noise of intensity $\gamma = 0.87\sqrt{\hbar\theta}$. The dynamics are displayed with the following color code: driven by the white noise ξ_t in solid black lines, by OU noise Υ_t in solid green lines, by OU process X_t in solid red lines, and by Wiener process W_t in solid blue lines.

are smooth, continuous, and at least one-time derivable. On the other hand, the dynamics deriving from the solution of actual SDEs, i.e., constructed on stochastic noises, even if belonging to the stochastic Hamiltonian family, show a different trajectory behavior. As the noises are generalized functions, meaningful only upon integration (which again happens in the generator in the solution), the trajectories' dynamics are continuous but not nowhere differentiable. Indeed, they appear properly *noisy*.

Further, we want to comment on the differences in the short-time evolution of the systems under different driving stochastic potentials. The effect on the short-time dynamics due to Lindblad dissipators, i.e., by white noise driving, is known and discussed in section II.2.1. Then, one would expect the different environment correlation in colored processes to affect mainly the short-time dynamics of the system. Indeed, this is what happens using the OU process, Figure IV.4, in all the instances of the Hamiltonian of the system (see Figure IV.6). In contrast, the dynamics with Υ-driven dissipation start with a transient similar to that of the ξ-driven one, displayed in Figure IV.4 for a stronger noise of intensity $\gamma = 0.87$ to emphasize the difference. The noisy dynamics are characterized by the presence of a δ-correlation component, resulting in a Lindblad dissipator in the mean dynamics, and therefore they share the exponential decay issue at short times. Processes-driven realizations, on the other hand, do not suffer from this, as the dissipation depends on the dampening of the coherences, see for instance eq. (IV.33), which need to build up to begin with. While at the trajectory level the short-time behavior is less evident, there are further signatures that show the effect of driving the system with noise instead of a process. The noisy realizations are characterized by a random initial velocity, and the overall noisy behavior is an indicator of this common feature.

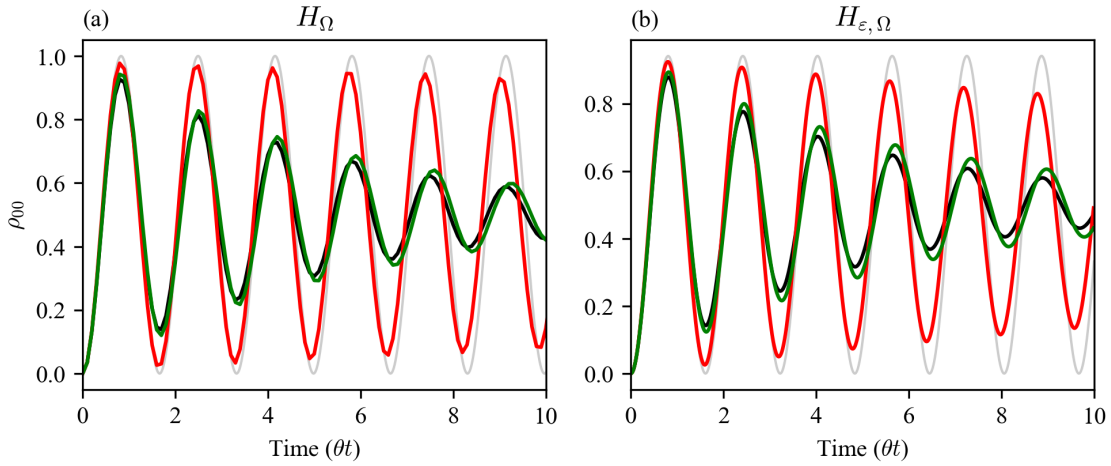

Figure IV.5: Dynamics of the system described by the Hamiltonian $H_{0,\Omega}$ in panel (a) and by the Hamiltonian $H_{\varepsilon,\Omega}$ in panel (b), with the stochastic forces applied through the Pauli σ_z operator. The dynamics are displayed with the following color code: driven by the white noise ξ_t in solid black lines, by OU noise Υ_t in solid green lines, and by OU process X_t in solid red lines. In light grey, the closed-system Schrödinger equation evolution as the reference of the coherent beating frequency of the population.

IV.5.2 Diagonal non-commuting noise

When the noise is on the diagonal of the Hamiltonian in the local state, i.e., $R = \sigma_z$, it physically represents fluctuations in the local state energies associated with the instantaneous configurations of the bath. The rationale for this model is that bath-induced coupling between different local states is small relative to the interstates coupling Ω, and the bath affects mainly the local configurations.

The average dynamics of the system affected by the different stochastic sources are shown in Figure IV.5. We chose parameters corresponding to slow relaxation so that coherent oscillations of the site population can be observed.

In this setting, the X_{OU}-driven dynamics show a slower relaxation of the beating, decaying with a single timescale. The behavior of the Υ_{OU}-driven system is similar to the white noise one, with a slightly better robustness of the coherent oscillations to the relaxation. This small effect gets more evident as the intensity of the noise increases (see Appendix IV.D). A second observation concerns the change in oscillation frequency, compared to the close system dynamics. While the ξ-driven mean dynamics does not show any frequency change, the Υ_{OU}-driven systems show a slower oscillation. In contrast, the X_{OU}-driven mean dynamics is characterized by a higher oscillation frequency, increasing with the noise intensity.

As a final comment, we observe that the initial time dynamics is characterized by a null derivative at time zero, which is expected as the physically correct behaviors of a system interacting with an environment. This happens when the noise coupling operator is purely local, as in the present case, while it is not guaranteed in other cases.

IV.5.3 Pauli coupling noise

Within the setting of the noise on the off-diagonal elements of the site-basis frame, $R = \sigma_x$, we can work with a null Hamiltonian ($H_0 = 0$). This peculiar case of commuting Pauli noise allows us to study the effect of the sole dissipators, free of the intrinsic dynamics of the system, as in the example in section IV.2.1. Using white noise as the source, the evolution with the noise applied through the Pauli σ_x unravels a Pauli Master Equation. The use of the other colored process and noise changes the dynamics. In this setting, we clearly see the peculiar effect of the OU Υ_t-noise as the driving of the dissipation channel.

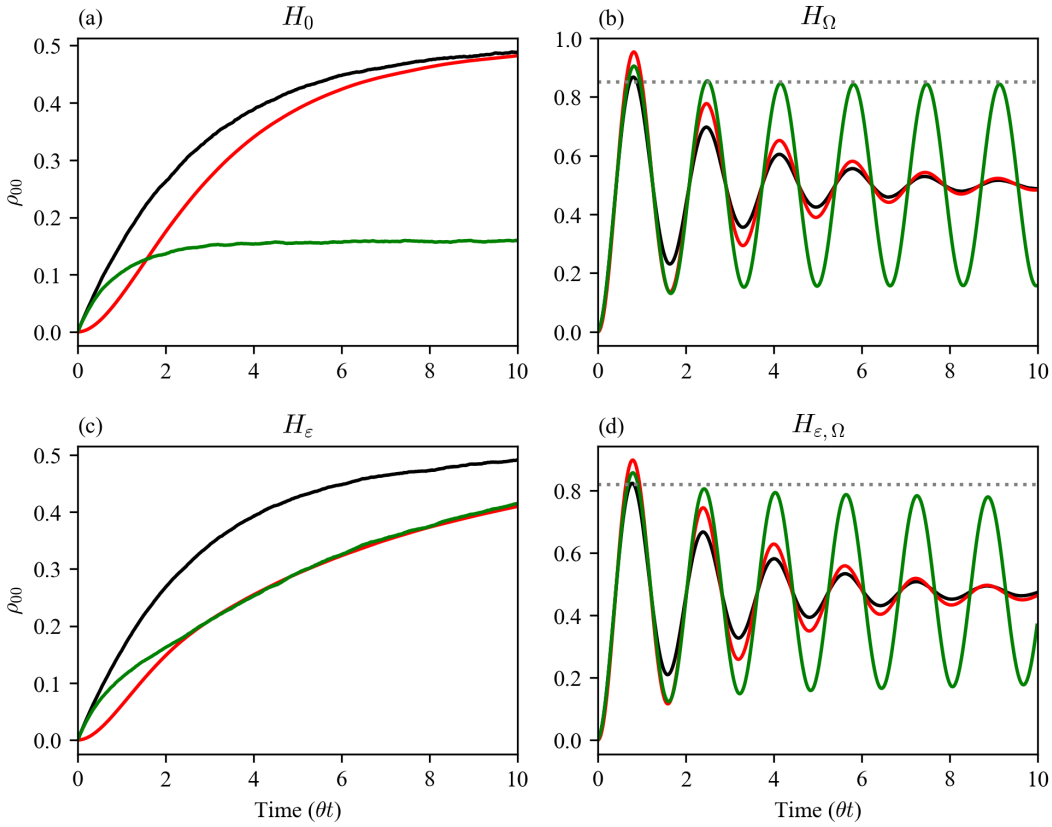

Figure IV.6: Dynamics of the system described by the different Hamiltonians, with the stochastic forces applied through the Pauli σ_x operator. The dynamics are displayed with the following color code: driven by the white noise ξ_t in solid black lines, by OU noise Υ_t in solid green lines, and by OU process X_t in solid red lines.

In Figure IV.6a, the mean dynamics described by eq. (IV.25), in particular in the form eq. (IV.26), is shown together with the mean dynamics resulting from the ξ-driven process, leading to a Lindblad dissipator, and to the OU stochastic Hamiltonian dynamics, which bears only the term of correlation with the environment, without Lindblad-like components, eq. (IV.30). The noteworthy result is that the process driven by the Υ_{OU}-noise reaches a different stationary state, while the other propagation reaches the expected equipartite distribution over the two sites. The dynamics starts by following the same short-time behavior of the white noise case, but the stationary value of the site populations depends on the intensity of the white noise component, see Appendix IV.D.

In Figure IV.6b we show a similar behavior in the resonant coupled system ($H_{0,\Omega}$),

hence still in a commuting Pauli noise setting. In this case, the long-time populations are not constant, and an oscillating steady state is reached.

One could expect the environment correlation to affect mainly the short-time dynamics of the system. Indeed, this is what happens using the OU process in all the instances of the Hamiltonian of the system. In contrast, the dynamics with Υ_{OU}-driven dissipation starts with a transient similar to that of the ξ-driven one and then settles to a different stationary state. On the other hand, the X_{OU} process-driven dynamics start with a null derivative at time zero, typical of a purely Hamiltonian dynamics, This is particularly evident in the $H_{0,0}$ system, but the same effect is present in all the dynamics using $R = \sigma_x$. The different initial time behavior of the two noise-driven dissipation can be explained by the common Lindblad dissipator in the corresponding QMEs, remarking what was previously commented in section IV.5.1. This dissipator underlines an actual SDE component and not simply a stochastic process in the Hamiltonian, and clearly induces an exponential decay even at t_0.

Up to this point, the two cases we have considered (Figure IV.6a and b) are characterized by a commuting Pauli noise, i.e., by a symmetric Hamiltonian which commutes with the coupling operator to the stochastic component, H_0 being the trivial case.

When we consider a system where the two sites are not degenerate, Figure IV.6c, or the principal directions of the Hamiltonian are changed by a coupling term, Figure IV.6d, thus breaking the symmetry of the system, the dynamics change, as the noise is now Pauli non-commuting. The common and most important difference is that all dynamics in these cases reach the equipartite distribution; however, they do so following quite different transient dynamics.

Let us first consider the simple addition of an energy asymmetry, the Hamiltonian $H_{\varepsilon,0}$, where the two sites are not coupled directly but through the interaction with the environment. For the dynamics of the observable at short time, the same considerations made above on the derivative at time zero and the similar behavior among the noise-driven and process-driven systems hold. Then, for longer times, in Figure IV.6c for the selected noise intensity, the dynamics of the Υ_{OU}-driven system becomes comparable to the X_{OU}-driven one, eventually reaching equidistribution of the populations. Depending on the intensity of the white noise component, different dynamics can be observed, see Appendix IV.D. At low intensity, the growth of the observable of the Υ_{OU}-driven system is slower than the X_{OU}-driven one, yet closing in as γ increases, see Figure A.IV.D.4. For higher noise intensity the Υ_{OU}-driven system resembles more and more the ξ-driven system at short time and X_{OU}-driven system at longer time. For $\gamma \gg 1$, the white noise component prevails and the dissipation profile becomes indistinguishable from the Lindblad evolution.

When we add the coupling into the system Hamiltonian, the coherent evolution is characterized by two different relaxation regimes, a faster decay at short times and then a slower decay (Figure IV.6d), eventually driving the system to equipartition. The correlation term seems to enhance the robustness of the coherent oscillations with respect to the noise, contrasting the Lindblad term of the dissipator. As a result, the coherent oscillations are long-lived.

IV.6 Modeling with the Redfield microscopic approach

Our intent in this section is to explicitly derive a closed model master equation for the systems under investigation, interacting with colored environments. To do so, we elaborate on the relation between the stochastic approach and the microscopic derivation of the quantum master equation in the form due to Redfield [19, 46, 164], presented in section II.3.

Let us start by summarizing the main points of the Redfield derivation to identify the underlying assumptions and approximations explicitly, and their relation with the stochastic approach used up to now. With this aim, let us consider again a two-level system with a single dissipation channel.

The starting point is the microscopic definition of the global Hamiltonian as in eq. (II.17),

$$H = H_{\mathcal{S}} \otimes \mathbb{1}_{\mathcal{B}} + \mathbb{1}_{\mathcal{S}} \otimes H_{\mathcal{B}} + H_I, \tag{IV.37}$$

where the system Hamiltonian is that described in eq. (IV.36), and the interaction Hamiltonian is $H_I = S_k \otimes B_k$.

Rotating to the interaction picture, indicated by a tilde over the objects, we focus only on the evolution due to the interaction Hamiltonian, now time-dependent. We derive the system evolution by writing the Liouville equation, integrating it, and inserting the integrated density matrix into the initial equation. Then, we trace out the bath from the resulting integro-differential equation, a recasting that preserves the exact dynamic description. Then, as we showed in section II.3.1, approximations are needed to obtain a closed and solvable equation. The initial factorization, (R1), and Born approximation, (R2), are inherently assumed in the stochastic approach; the initial condition of the system is either calibrated (a pure state) or drawn from a distribution (associated with a mixed state); nevertheless, it is uncorrelated to the state of the environment, as the stochastic potential is independent of the system. The assumption of thermalization of the bath, in the case of (Gaussian) colored noise and processes, is ensured by considering the stationary properties, i.e., drawing the value at t_0 from a (Gaussian) with variance at infinite time for the process, eq. (IV.4).[2]

Then, without the addition of any further approximation, we obtain the integrodifferential form of eq. (II.26), where we identify the correlation function of the environment, eq. (II.27). We can therefore write,

$$\frac{\mathrm{d}}{\mathrm{d}t}\tilde{\rho}_{\mathcal{S}}(t) = -\frac{1}{\hbar^2}\int_0^t \Big(C(t,t')[\tilde{S}(t), \tilde{S}(t')\tilde{\rho}_{\mathcal{S}}(t')] + C(t',t)[\tilde{\rho}_{\mathcal{S}}(t')\tilde{S}(t'), \tilde{S}(t)] \Big)\, \mathrm{d}t' \tag{IV.38}$$

where we did not have to assume the operators of the bath to be Hermitian, as both S and B are assumed to be so in the beginning, see section III.1.1 and the constraint for the colored-noise SSE to be linear, section IV.2 and Appendix IV.C.

This is clearly a non-Markovian QME, as that presented in eq. (II.28). Therefore, further approximations must be considered, in addition to those already implicit in the SSE approach.

[2] The variance of the process is the one that needs to be used also in the case of colored noise, such as the Υ_{OU} noise, as pure noises are characterized by a diverging variance, table 1.

First, let us consider explicitly the system studied above, driven by the Υ noise, recasting the equation accordingly. We can identify the operators acting on the system by setting $S = \sqrt{\hbar}R$.

We identify the correlation function of the environment with the correlation function of the stochastic noise, in particular Υ, therefore $C(t,t') = C(\Upsilon_t, \Upsilon_{t'}) = C(t-t')$, what we computed in eq. (IV.15). In the purely Redfield approach, the correlation function depends only on the time difference $(t-t')$ by virtue of the commutation properties of the bath operators and density matrix with the bath Hamiltonian. In this case, we can look at the correlation function itself to assert that it holds, at its stationarity, see eqs. (IV.5) and (IV.15). Moreover, since the stochastic process is classical, we can recognize that the additional symmetry $C(t-t') = C(t'-t)$ holds. In this setting, eq. (IV.38) can be written as:

$$\frac{\mathrm{d}}{\mathrm{d}t}\tilde{\rho}(t) = -\frac{1}{\hbar}\int_0^t C(t-t')\left([\tilde{R}(t), \tilde{R}(t')\tilde{\rho}(t')] + \text{h.c.}\right)\mathrm{d}t' \tag{IV.39}$$

In this form, we need to introduce further the first Markov approximation, (R3). We change the integration variable for simplicity with the time difference $\tau = t - t'$, as done in Chapter II. We let the equation be local in time for the system density matrix, changing its dependence to be on t and not the integration variable τ, $\rho(t-\tau) \approx \rho(t)$. This is equivalent to assuming that the system evolves slowly compared to the environment. What is obtained is the *Redfield equation with time-dependent coefficients*

$$\frac{\mathrm{d}}{\mathrm{d}t}\tilde{\rho}(t) = -\frac{1}{\hbar}\int_0^t C(\tau)\left([\tilde{R}(t), \tilde{R}(t-\tau)\tilde{\rho}(t)] + \text{h.c.}\right)\mathrm{d}\tau \tag{IV.40}$$

a time-local QME, yet with a component still depending on the dynamical history of the bath. This is sometimes described as a non-Markovian equation [50], as we are not yet enforcing the second Markovian approximation (R4). Indeed, to recover what is typically intended as the Redfield equation, the upper limit of the time integral should be extended to infinity, a full Markovian approximation that we do not invoke here.

We can now express the operator R on $\{|a\rangle, |b\rangle\}$ eigenbasis of H_S and make explicit the time dependence of the coupling operators. The action of $e^{iH_S\tau}$ in this basis is easily evaluated. For instance, we have

$$\begin{aligned} |a\rangle\langle a|\tilde{R}(t)|b\rangle\langle b| &= |a\rangle\langle a|e^{\frac{i}{\hbar}H_S t}Re^{-\frac{i}{\hbar}H_S t}|b\rangle\langle b| \\ &= e^{i(\omega_a-\omega_b)t}|a\rangle\langle a|R|b\rangle\langle b|, \end{aligned} \tag{IV.41}$$

where $\frac{E_a}{\hbar} = \omega_a$ and $\omega_{ba} = \omega_b - \omega_a = -\omega_{ab}$. This structure suggests the decomposition of the coupling operator according to the energy gaps (transition frequencies) of the system, forming the set $G = \{0, 0, \omega_{ab}, \omega_{ba}\}$, that is

$$\tilde{R}(t) = \sum_{\omega\in G} R(\omega)e^{-i\omega t} \tag{IV.42a}$$

$$= 2R(0) + e^{-i\omega_{ba}t}R(\omega_{ba}) + e^{-i\omega_{ab}t}R(\omega_{ab}), \tag{IV.42b}$$

where the tilde indicates the operators in the interaction picture, its absence the Schrödinger

picture, and the dependence of $R(\omega)$ indicates that the operator is that of the ω transition frequency of the system. With these definitions, eq. (IV.40) can be rewritten as

$$\frac{\mathrm{d}}{\mathrm{d}t}\tilde{\rho}(t) = -\frac{1}{\hbar}\sum_{\omega,\omega'}\left(\int_0^t C(\tau)e^{i\omega'\tau}\right)\mathrm{d}\tau e^{i(\omega-\omega')t}\left(\left[R^\dagger(\omega), R(\omega')\tilde{\rho}(t)\right] + \mathrm{h.c.}\right), \tag{IV.43}$$

where the integral defines a half-sided finite-time Fourier transformation. Upon explicit integration, using the analytical form for the covariance of the Υ_{OU} noise, we obtain time- and frequency-dependent coefficients

$$\Gamma(\omega', t) = \int_0^t C(\tau)e^{i\omega'\tau}\,\mathrm{d}\tau = \frac{\gamma^2}{2}\left(1 - \theta\frac{e^{(i\omega'-\theta)t}-1}{i\omega'-\theta}\right). \tag{IV.44}$$

Rotating back to the Schrödinger picture, we finally obtain

$$\frac{\mathrm{d}}{\mathrm{d}t}\rho(t) = -\frac{i}{\hbar}[H_S, \rho(t)] - \frac{1}{\hbar}\sum_{\omega,\omega'}\Gamma(\omega', t)\left(\left[R^\dagger(\omega), R(\omega')\rho(t)\right] + \mathrm{h.c.}\right). \tag{IV.45}$$

IV.6.1 Closure model for colored environments

We are now in the position of formulating an approximation of the cross-correlation term arising from the SSE unraveling. Comparing the two QMEs, from the SSE eq. (IV.25) and the Redfield eq. (IV.45), the following relation between the dissipators emerges

$$\frac{\gamma^2}{\hbar}\left(R\rho(t)R^\dagger - \frac{1}{2}\left\{R^\dagger R, \rho(t)\right\}\right) + \frac{i\theta}{\sqrt{\hbar}}[R, \mathbb{E}(X\rho^{\mathrm{trj}}(t))] \approx \tag{IV.46a}$$

$$\approx -\frac{1}{\hbar}\sum_{\omega,\omega'}\Gamma(\omega', t)\left(\left[R^\dagger(\omega), R(\omega')\rho(t)\right] + \mathrm{h.c.}\right). \tag{IV.46b}$$

By inserting the explicit form of the coefficients from eq. (IV.44), eq. (IV.46b) becomes

$$\sum_{\omega,\omega'}\frac{\gamma^2}{2\hbar}\left(1 - \theta\frac{e^{(i\omega'-\theta)t}-1}{i\omega'-\theta}\right)\left(2R(\omega)\rho(t)R(\omega')^\dagger - \{R(\omega)^\dagger R(\omega'), \rho(t)\}\right) = \tag{IV.47a}$$

$$= \frac{\gamma^2}{2\hbar}\sum_{\omega,\omega'}\left(2R(\omega)\rho(t)R(\omega')^\dagger - \{R(\omega)^\dagger R(\omega'), \rho(t)\}\right) \tag{IV.47b}$$

$$+ \frac{\gamma^2}{2\hbar}\sum_{\omega,\omega'}\theta\frac{1-e^{(i\omega'-\theta)t}}{i\omega'-\theta}\left(2R(\omega)\rho(t)R(\omega')^\dagger - \{R(\omega)^\dagger R(\omega'), \rho(t)\}\right). \tag{IV.47c}$$

The first term, eq. (IV.47b), is just the Lindblad dissipator where the jump operators are expressed in the rotated basis of Hamiltonian eigenstates. By rotating back to the original frame, such Lindbladian terms are equivalent to those emerging from the SSE, first term in eq. (IV.46a). Therefore, the approximate equivalence becomes

$$\frac{i\theta}{\sqrt{\hbar}}[R, \mathbb{E}(X\rho^{\mathrm{trj}}(t))] \approx \frac{\gamma^2}{2\hbar}\sum_{\omega,\omega'}\theta\frac{1-e^{(i\omega'-\theta)t}}{i\omega'-\theta}\left(2R(\omega)\rho(t)R(\omega')^\dagger - \{R(\omega)^\dagger R(\omega'), \rho(t)\}\right). \tag{IV.48}$$

This gives the approximate expression of the cross-correlation term as a tensorial function, based on a rotated and operator-wise weighted generator, linear in the system density matrix $\rho(t)$, effectively producing a closure model for the correlation term in eq. (IV.25). This term (with opposite sign) is the same appearing in the X_{OU}-driven QME, allowing for a closure model of eq. (IV.31) as well.

These Redfield equations allow us to understand in a more familiar format the additional correlation terms to the simple Liouvillian and Lindblad dynamics derived in the previous sections, and their unusual behavior captured by the numerical implementation shown in section IV.5.

The rationale of stationary densities prediction in the case of commuting Pauli noise, as well as the two different relaxation time scales for non-commuting noises, is presented for the prototypical example of a two-level system in the following section. Before drawing considerations from the numerical results, it is important to remark on one important difference between the two methods, as we shall recall again in section IV.6.3. The Redfield derivation returns a model for the QME obtained by the stochastic approaches, not the same QME, a closure *model*, with one immediate important difference. Since the model QME forms are not Lindblad, we cannot guarantee *a priori* the positivity of the maps. In contrast, the dynamics obtained by the average of stochastic trajectories are always positive by construction. Indeed, the Redfield model is intended as a closure model for the SSE-derived QME, within the usual considerations of the range of validity of the approximations required in the Redfield derivation. For strong couplings (i.e., large noise intensity) and for high values of the parameter θ, this model becomes less and less effective, as we move outside of the range of validity of the Redfield model.

IV.6.2 Redfield relaxation channels for the two-level system driven by Υ_{OU}-noise

The microscopic derivation of the quantum master equation provides an explicit link between the rates of different relaxation processes and the environment dynamics as described by its correlation function. Notably, the available relaxation channels are determined by the structure of the coupling, i.e., by the system operators R coupling with the bath, see eq. (IV.45).

When R commutes with the system Hamiltonian $H_{\mathcal{S}}$, there is no energy exchange between the system and the environment, and the only irreversible channel is decoherence of the energy eigenbasis. The pure decoherence model corresponds to a coupling operator R with components only for $\omega = 0$ in eq. (IV.42a). Conversely, when the coupling operator does not commute with $H_{\mathcal{S}}$, it presents components at different frequencies, triggering transitions between eigenstates of different energies with rates that are determined by the environment through $\Gamma(\omega, t)$ defined in eq. (IV.44).

We now illustrate the implication of this relaxation structure applied to the specific case of the frequency- and time-dependent transition rates associated with the Υ_{OU}-noise, for the two-level system described by the Hamiltonian form in eq. (IV.36).

Evaluating the system operators and the time-dependent rates for each frequency leads

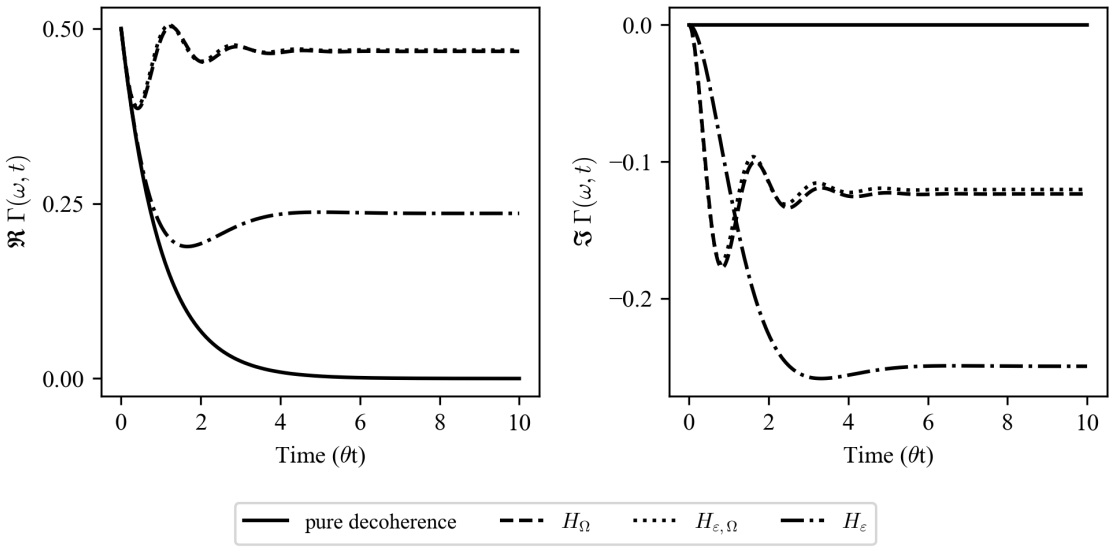

Figure IV.7: Time-dependent coefficients of the Redfield equation computed for the different Hamiltonians, computed for $\gamma = 0.45\sqrt{\hbar\theta}$ and $\theta = 1$. The real part is on panel (a) and the imaginary part on panel (b). Negative frequency coefficients are not shown as they are the complex conjugate of the positive ones. The null frequency coefficient contribution is equal for all the Hamiltonians and labeled "pure decoherence". The characteristic frequencies of the different Hamiltonians are in different line styles as depicted in the legend.

to different results about active relaxation channels and consequent stationary state, depending on the system Hamiltonian and the noise operator, Figure IV.7. Let us consider two degenerate states coupled by the Hamiltonian, $H_{0,\Omega}$, and the noise operator as the Pauli σ_x operator. This is a pure decoherence setting where the coupling to the noise commutes with the Hamiltonian of the system. The frequencies of the system obtained by diagonalizing the Hamiltonian are (Ω, Ω), but the noise coupling operator, R, does not connect different eigenstates, i.e., $R_{k,l\neq k} = 0$, nullifying the contribution of the coefficient $\Gamma(\omega \neq 0)$. On the other hand, the zero-frequency component of R is not zero. and the contribution of the coefficient $\Gamma(\omega = 0)$ is real and exponentially decaying in time, solid line in Figure IV.7. Physically, this describes a decoherence channel which is active only at early times while the decoherence rate vanishes at longer time. This correctly predicts the peculiar stationary state obtained numerically from the SSE implementation, presented in section IV.5, where we observe only partial decoherence of the initial state. The result is an asymptotic mixed state that can maintain some coherent behavior, depending on the timescale of the system and the intensity of the noise.

In the case of a non-coupled and non-degenerate system, the eigenstates of the Hamiltonian $H_{\varepsilon,0}$ correspond to the observable basis; therefore, the σ_x coupling to the noise only induces transitions between the eigenstates. Pure decoherence due to the zero-frequency term is null, whilst the components at non-zero frequency matter. These coefficients have the same value as the zero-frequency coefficient at the initial time. However, they are complex, and after a few oscillations they converge to a non-zero absolute value, lower than the initial one. Because these coefficients weigh the upward and downward transitions equally, we should expect a stationary state reflecting the equipartition of population

between the states, which is indeed what we observe numerically (see Figure IV.6c).

In the case of the generic Hamiltonian $H_{\varepsilon,\Omega}$, the σ_x noise operator has both a pure dephasing component and finite frequency components inducing transitions. Specifically, if V is the unitary transformation diagonalizing the Hamiltonian, the weight of the pure dephasing and finite frequency contributions are given by the diagonal and off-diagonal elements of the transformed coupling operator, namely

$$R \mapsto V\sigma_x V^\dagger = -\begin{pmatrix} \frac{\varepsilon+\sqrt{\varepsilon^2+4\Omega^2}}{\Omega} & \frac{\varepsilon}{\Omega} \\ \frac{\varepsilon}{\Omega} & \frac{\varepsilon+\sqrt{\varepsilon^2+4\Omega^2}}{\Omega} \end{pmatrix}. \tag{IV.49}$$

The two different main time scales for the dissipation can then be clearly seen and estimated. In the short time, the system decay is due to the effects of both the zero-frequency and the $2\omega'$ coefficients. For a longer time, the decay is due only to the coefficients at non-zero frequencies. When $\varepsilon < \Omega$, the resulting relaxation can be much slower than the oscillation frequency of the system, resulting in long-lived coherent transfer between the two sites.

On the other hand, when noise is applied on the site basis with the Pauli σ_z (the diagonal Pauli noise), the major contribution is by the non-zero frequency coefficients (the only for the degenerate coupled system), which converges to a non-zero finite value, and explains the expected infinte temperature steady state reached in the numerical propagation, see Figure IV.5.

IV.6.3 Comparison with Redfield dynamics

In this section, the numerical solution of the Redfield model dynamics is investigated, and it shows good agreement with the SSE results for the observable under study.

In the simplest case of a null Hamiltonian, only the channel at zero frequency contributes to the relaxation. We recall that the associated rate vanishes at long time as shown in Figure IV.7a. Looking at Figure IV.8a, we see that this approach correctly predicts the dynamics of the null Hamiltonian system, the absolute error is shown in Figure IV.8d and it fluctuates with an amplitude that depends on the noisiness of the SSE trajectories average. This is also true for coupled resonant systems.

When an energy difference is introduced in the system, like in the generic Hamiltonian $H_{\varepsilon,\Omega}$, the difference between the Redfield dynamics and the average obtained from the SSE accumulates at early times because of slightly detuned coherent oscillations, Figure IV.8b. At longer times, both dynamics converge to the same stationary states reaching equidistribution of populations.

The difference in the oscillation frequency is even more noticeable in the case of noise on the sites ($R = \sigma_z$), see Figure IV.8c and IV.8f. The Redfield equation shows a slight speed-up of the oscillation, while the Υ_{OU}-derived QME slows them down depending on the intensity of the noise, see also Figure IV.5.

As a final remark, we comment on the positivity of the dynamics, as pointed out in section IV.6.1. Although good agreement is observed in the comparison of the numerical results, we want to stress that the Redfield model does not ensure positivity of the dynam-

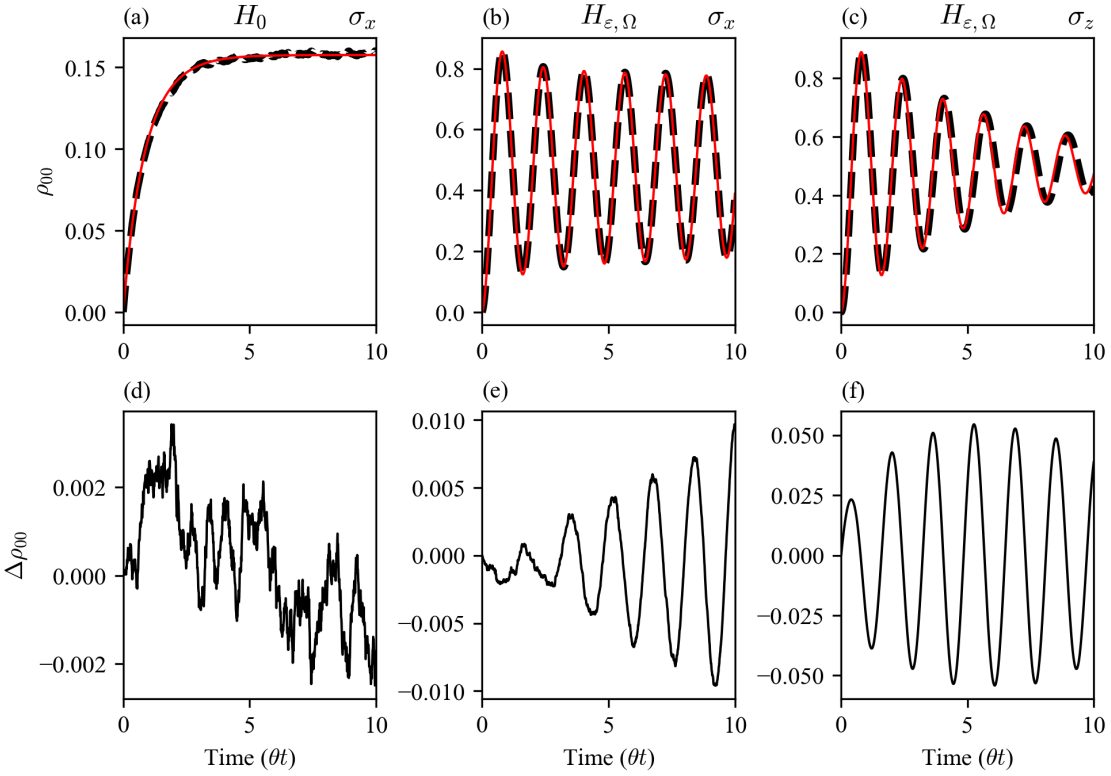

Figure IV.8: (a-c) Comparison of the ρ_{00} dynamics, for the H_0 and $H_{\varepsilon,\Omega}$ Hamiltonians. The dynamics computed by stochastic averaging are displayed as dashed bold black lines, and the Redfield model in red lines. (d-f) Absolute errors w.r.t. the SSE-obtained population. The noise is applied through σ_x in (a,d) and (b,e), and through σ_z in (c,f).

ics. For all parameters considered here (see Appendix IV.D for a wider range), including strong noise intensities γ, the numerical solution remains positive. The situation changes when the parameter θ becomes large, as the memory of the environment is well out of the regime of validity of the Redfield approach. In this case, and somewhat counterintuitively, the breakdown of positivity occurs at longer times rather than at short times, in the case of systems described by the generic Hamiltonian $H_{\varepsilon,\Omega}$. This behavior is due to oscillations of the eigenvalues of $\rho^{(\mathrm{Red})}$ around the reference value obtained from $\rho^{(\mathrm{SSE})}$, as shown in Figure IV.9. The amplitude of these oscillations increases in time and, for sufficiently large θ values, eventually leads to negative eigenvalues.

IV.6.4 Partial secular approximation and complete Markovianity

When the time scale used to propagate the dynamics is larger than the inverse of the system frequency separation, eq. (II.41), the rapid oscillating terms in eq. (IV.43) can be neglected, approximated to zero as vanishing by long-time averaging. Then, only terms with $\omega' = \omega$ survives, leading to

$$\frac{\mathrm{d}}{\mathrm{d}t}\rho(t) = -\frac{i}{\hbar}[H_S, \rho(t)] - \frac{1}{\hbar}\sum_{\omega}\Gamma(\omega, t)\left(\left[R^{\dagger}(\omega), R(\omega)\rho(t)\right] + \mathrm{h.c.}\right) \tag{IV.50}$$

which is not in Lindblad form only because the coefficients $\Gamma(\omega, t)$ are time dependent.

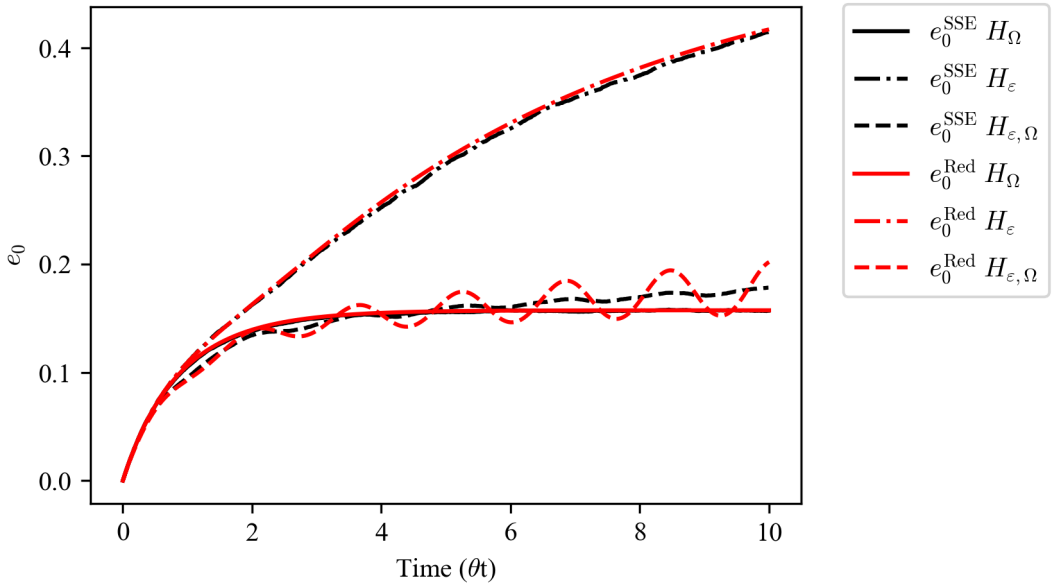

Figure IV.9: Comparison of the dynamics of the first eigenvalue $e_0(t)$ of ρ_t for the three different Hamiltonians $(H_\Omega, H_\varepsilon, H_{\varepsilon,\Omega})$, and noise operator $R = \sigma_x$.

If we were to complete the Markov approximation, extending the integration upper limit to infinite time, we would recover the Lindblad master equation. This cannot be done because of the particular Υ_{OU} colored noise correlation function, as it would wrongly lead to a white noise situation, estimating the wrong stationary state. This is due to the term asymptotically decreasing to zero, valid for each Hamiltonian, i.e., for the null frequency $\omega = 0$. The picture can be recovered partially by applying the second Markov approximation to the terms of frequency $\omega \neq 0$, so that

$$\Gamma(\omega, t) = \begin{cases} \int_0^\infty C(\tau) e^{i\omega\tau}\, \mathrm{d}\tau = \gamma_\omega & \omega \neq 0 \\ \int_0^t C(\tau)\, \mathrm{d}\tau & \omega = 0 \end{cases} \tag{IV.51}$$

IV.6.5 Real time-dependent Redfield tensor

Complete Markovianity and the recovery of a Lindblad form are not, in general, the appropriate remedies for the non-positivity of eq. (IV.45). The former does not guarantee positivity, while the latter — although ensuring complete positivity — fails to reproduce the correct master equation and the associated mean dynamics.

Instead, we investigate the use of a real Redfield tensor as a means to address the positivity issue of Redfield-approximated dynamics and, crucially, to suppress the unphysical oscillatory features observed in the eigenvalue evolution. We emphasize that the possible non-positivity of the Redfield dynamics is not any property of the underlying physical system, but rather a consequence of spurious oscillations introduced by the approximation itself, which are absent in the actual dynamics being modeled.

Among the different variants of the Redfield equation discussed in this Chapter and in Chapter II, a formulation of the Redfield tensor without imaginary components has been introduced in section II.3.4, with the caveat that additional care is needed when applied to

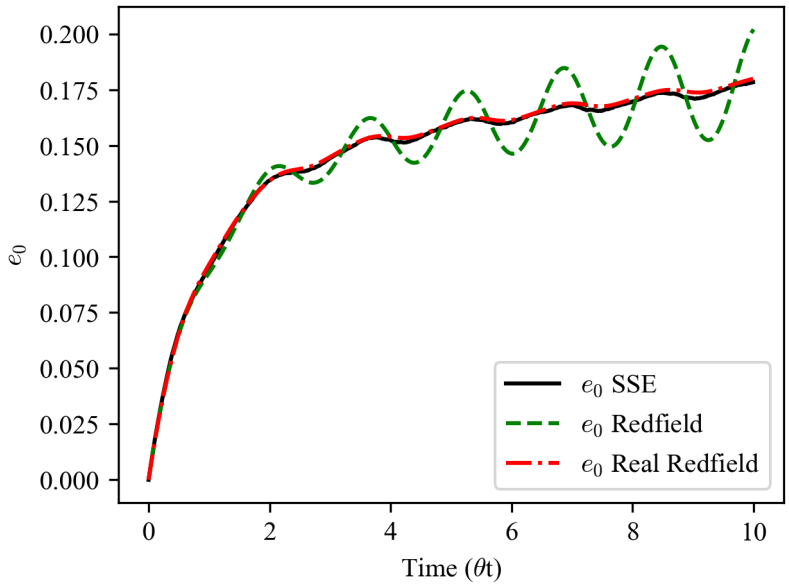

Figure IV.10: Comparison of the dynamics of the first eigenvalue $e_0(t)$ of ρ_t for the Hamiltonian $H_{\varepsilon,\Omega}$ and noise operator $R = \sigma_x$, computed from the mean open-form correlated QME obtained from the SSE approach, with the full Redfield tensor and with the real Redfield tensor dynamics.

other Redfield tensor versions. Indeed, for time-dependent Redfield tensors $\Gamma(t,\omega)$, even in the case of an environment modeled as classical stochastic potentials, the half-sided Fourier transform produces complex functions for the coefficients, see eq. (IV.44) and Figure IV.7. To gain an understanding of this phenomenon, we can rewrite the integral defining the coefficients, identifying clearly the real and imaginary components, as well as two oscillatory terms,

$$\int_0^t C(\tau)e^{i\omega\tau}\,\mathrm{d}\tau = \int_0^t C(\tau)\cos(\omega\tau)\,\mathrm{d}\tau + i\int_0^t C(\tau)\sin(\omega\tau)\,\mathrm{d}\tau \tag{IV.52a}$$

$$= \mathrm{Re}[\Gamma(t,\omega)] + i\mathrm{Im}[\Gamma(t,\omega)] \tag{IV.52b}$$

The imaginary component is clearly oscillating, and there is no direct correspondence to a Lamb shift term. Restoring the second Markovian approximation (R4) by extending the integration upper limit to infinity, one would recover real coefficients and $\Gamma(\omega) \in \mathbb{R}$, as expected from a real-valued stochastic process modeling the environment.

Here, we introduce another version of the Redfield tensor, real and time-dependent. We associate the imaginary component of the time-dependent coefficients with a *transient memory term*, accounting for *transient memory*-induced shifts.

Numerically, we observe that this is the term inducing the spurious oscillation of the eigenvalues, see Figure IV.10.

We want to stress that this procedure does not directly correspond to the removal of the dispersive component, as we cannot, in general, write the imaginary component of the dissipator as a commutator with some iH_{LS}. Indeed, the dissipator in eq. (IV.45) mixes

terms of different frequencies of the system, operators $R(\omega)$ and $R(\omega')$,

$$\sum_{\omega,\omega'} \Gamma(\omega',t)\left(\left[R^\dagger(\omega),R(\omega')\rho(t)\right]+\text{h.c.}\right)=\sum_{\omega,\omega'}\text{Re}[\Gamma(\omega',t)]\left(\left[R^\dagger(\omega),R(\omega')\rho(t)\right]+\text{h.c.}\right) +i\sum_{\omega,\omega'}\text{Im}[\Gamma(\omega',t)]\left(\left[R^\dagger(\omega),R(\omega')\rho(t)\right]+\text{h.c.}\right), \tag{IV.53}$$

and focusing only on the imaginary component, we cannot write a commutator. Only after secular approximation, imposing $\omega=\omega'$, one can write the imaginary component of each term as

$$i\text{Im}[\Gamma(\omega,t)]\left(\left[R^\dagger(\omega),R(\omega)\rho(t)\right]+\text{h.c.}\right)=i\text{Im}[\Gamma(\omega,t)]\left(\rho(t)R^\dagger(\omega)R(\omega)-R^\dagger(\omega)R(\omega)\rho(t)\right) \tag{IV.54}$$

and therefore, for all frequencies ω, reorganize into a commutator

$$-i\left[\sum_\omega \text{Im}[\Gamma(\omega,t)]R^\dagger(\omega)R(\omega),\rho(t)\right]=-i\left[H_{\text{LS}}(t),\rho(t)\right]. \tag{IV.55}$$

where we identify a time-dependent Lamb shift

$$H_{\text{LS}}(t)=\sum_\omega \text{Im}[\Gamma(\omega,t)]R^\dagger(\omega)R(\omega). \tag{IV.56}$$

IV.6.6 Use of Novikov theorem to close correlated QME

In section III.6, we introduced the use of SLE in the framework of the stochastic Hamiltonian, and the use of the Novikov theorem to address terms of the form $\mathbb{E}(Z_t\rho_t^{\text{trj}})$, where Z_t is a Gaussian variable.

Our aim in this section is twofold. Exploiting the results obtained, we show another route to the closure model of the correlated QME, leading to the same Redfield equation, and from that gaining further insights into the nature of the transient memory shifts introduced in the section above.

Let us start from the open form eq. (III.66), obtained at the end of the section, reproduced here for clarity of visualization,

$$\frac{\text{d}}{\text{d}t}\rho_t=-i[H,\rho_t]-\int_0^t C_Z(t,s)\left[R,\mathbb{E}\left(\left[U_{t,s}RU_{t,s}^\dagger,\rho_t^{\text{trj}}\right]\right)\right]\text{d}s. \tag{IV.57}$$

Without invoking complete Markovianity, falling back to Lindblad forms, we can adopt softer approximations to close the equation. Using a perturbative approach, a closed deterministic master equation can be obtained, where the propagator is simplified according to

$$\begin{aligned}U_{t,s}&=\mathcal{T}_+\exp\left\{-i\int_s^t(H+Z_rR)\,\text{d}r\right\}\\&\approx\exp\left\{-i\int_s^t H\,\text{d}r\right\}=U_{t,s}^{\text{H}},\end{aligned} \tag{IV.58}$$

where the fluctuation is considered as a small perturbation of the system Hamiltonian and approximated to zero. The resulting propagator is now a deterministic operator acting on the system. As a consequence, we can write $R_{t,s} = U^{\mathrm{H}}_{t,s} R U^{\mathrm{H}\,\dagger}_{t,s}$, which is likewise deterministic and independent of the stochastic process, and therefore unaffected by the averaging operation.

This allows us, by linearity of the average, to insert the averaging operator $\mathbb{E}[\cdot]$ in the commutator in eq. (IV.57) to act solely on the ensemble of stochastic density matrix trajectories ρ^{trj} and thereby close the equation in terms of the average trajectory, as $\mathbb{E}[\rho^{\mathrm{trj}}_t] = \rho_t$.

Evaluating the action of the approximated two-times propagator on the noise operator, one obtains a QME with *time-dependent coefficients* identical to what is obtained while applying a Redfield approach in section IV.6 and in Ref. [147]:

$$\frac{\mathrm{d}}{\mathrm{d}t}\rho_t \approx -i[H, \rho_t] - \int_0^t C_Z(t,s)\,[R, [R_{t,s}, \rho_t]]\,\mathrm{d}s. \tag{IV.59}$$

To appreciate that the form is exactly the same obtained above, one has to move to the interaction picture, noting that the operators R and $R_{t,s}$ bring different time dependence, using

$$\tilde{R}_t = e^{iHt} R e^{-iHt} \tag{IV.60a}$$

$$\tilde{R}_s = e^{iHt} R_{t,s} e^{-iHt} = e^{iHt} e^{-iH(t-s)} R e^{iH(t-s)} e^{-iHt} = e^{iHs} R e^{-iHs}. \tag{IV.60b}$$

Then, we can rewrite eq. (IV.59) as

$$\frac{\mathrm{d}}{\mathrm{d}t}\tilde{\rho}_t = -\int_0^t C_Z(t,s)\left[\tilde{R}_t, \left[\tilde{R}_s, \tilde{\rho}_t\right]\right]\mathrm{d}s, \tag{IV.61}$$

indeed the same form of eq. (IV.39). Then, assuming stationary noise, we continue with the same steps proposed in section IV.6, obtaining the usual Redfield form, clearly showing the dependence on the frequencies of the system.

The Redfield form obtained, identical to that obtained before, suffers the same issue of spurious oscillation of the eigenvalues. Contrary to the case of the microscopic derivation, where it is solved *a posteriori*, we can pinpoint where in the SLE derivation the issue arises, and compare our findings to the original correlated QME and to the previous Redfield model.

First, we remark that eq. (IV.57) is an "exact" recasting of the correlated QME derived from the SSE approach. Derived in a different framework, it relies on the same assumptions on the system-environment interactions and is modeled as a stochastic Hamiltonian. It is sufficient to substitute the Ornstein-Uhlenbeck noise Υ_t in eq. (III.57), and eq. (IV.25) is obtained.

Then, there is only one step, the perturbative approximation in eq. (IV.58), removing positivity[3] and introducing oscillations in the mean density matrix eigenvalues. The effect

[3]Recall that, as QME derived from stochastic Hamiltonians approaches are the linear average of valid pure states, the maps obtained are at CPT, see section III.1.1.

of approximating the propagator is to neglect an oscillatory term in the form of

$$U_{t,s}^{\text{stoch}} = \exp\left\{-iR\int_s^t Z_r \,\mathrm{d}r\right\}, \tag{IV.62}$$

where we need to assume that we can write $U_{t,s} = U_{t,s}^{\text{H}} U_{t,s}^{\text{stoch}}$, i.e., a first-order Suzuki-Trotter decomposition [241, 242], see step eq. (IV.63c) (and section VI.1.1).

The stochastic propagator $U_{t,s}^{\text{stoch}}$ can again be considered as a transient memory term, yet different from that obtained in eq. (IV.52a). Indeed, its removal causes the eigenvalues to oscillate, and one might then consider it as the intrinsic correction present in the open form.

To conclude, we can compare the features of the different derivations. Let us recast eq. (IV.57) in the interaction picture to compare it to the non-Markovian master equation eq. (IV.39) obtained by microscopic derivation and the correlated Master equation obtained from the SSE approach.

$$\frac{\mathrm{d}}{\mathrm{d}t}\tilde{\rho}_t = -\int_0^t C_Z(t,s)\left[\tilde{R}_t, \mathbb{E}\left(\left[U_{t,s}\tilde{R}_t U_{t,s}^\dagger, \tilde{\rho}_t^{\text{trj}}\right]\right)\right]\mathrm{d}s \tag{IV.63a}$$

$$= -\int_0^t C_Z(t,s)\left[\tilde{R}_t, \mathbb{E}\left(\left[e^{-i\int_s^t H+RZ_r\,\mathrm{d}r} e^{iHt} R e^{-iHt} e^{i\int_s^t H+RZ_r\,\mathrm{d}r}, \tilde{\rho}_t^{\text{trj}}\right]\right)\right]\mathrm{d}s \tag{IV.63b}$$

$$\approx -\int_0^t C_Z(t,s)\left[\tilde{R}_t, \mathbb{E}\left(\left[e^{-iH(t-s)} e^{-iR\int_s^t Z_r\,\mathrm{d}r} e^{iHt} R e^{-iHt} e^{iH(t-s)} e^{iR\int_s^t Z_r\,\mathrm{d}r}, \tilde{\rho}_t^{\text{trj}}\right]\right)\right]\mathrm{d}s \tag{IV.63c}$$

$$= -\int_0^t C_Z(t,s)\left[\tilde{R}_t, \mathbb{E}\left(\left[U_{t,s}^{\text{stoch}}\tilde{R}_s U_{t,s}^{\text{stoch}\dagger}, \tilde{\rho}_t^{\text{trj}}\right]\right)\right]\mathrm{d}s. \tag{IV.63d}$$

We can further substitute Z_t with the OU noise Υ_t and $C_Z(t,s)$ with its covariance, eq. (IV.15). Then, the δ-component of the covariance will give rise to the Lindblad dissipator term, in both approaches. This term is not a concern, and we can focus on the equivalences between the open term and its models.

Then, before further approximations, other than the common initial factorization and the Born approximation, the different terms are presented in the following, where we use the interaction picture frame for simplicity, and the main differences that can be observed are highlighted.

In the correlated QME from the SSE approach, we obtained

$$i\theta\left[\tilde{R}_t, \mathbb{E}\left(X_t\tilde{\rho}_t^{\text{trj}}\right)\right], \tag{IV.64}$$

and the equation is open due to the average operator, acting on the trajectory-wise product of the stochastic density matrix and the associated noise realization. Although this term seems to be time-local, we can apply Novikov's theorem, eq. (III.58), and, following the derivation as in the SLE approach, show the time dependence and non-Markovianity of this term. Indeed, the term arising from the SLE derivation is

$$\frac{\gamma^2\theta}{2}\int_0^t e^{-\theta|t-s|}\left[\tilde{R}_t, \mathbb{E}\left(\left[\mathcal{U}_{t,s}^{\text{stoch}}\tilde{R}_s\mathcal{U}_{t,s}^{\text{stoch}\dagger}, \tilde{\rho}_t^{\text{trj}}\right]\right)\right]\mathrm{d}s, \tag{IV.65}$$

where, although the trajectory density matrix $\tilde{\rho}_t^{\text{trj}}$ depends only on time t, it still cannot be moved outside of the integral. In eq. (IV.65), the stochasticity now does not depend on the process X_t, a component of the Υ_t noise, but on the stochastic propagator of the noisy component of the Hamiltonian. Then, this form shows both time non-locality and stochastic components.

On the other hand, from the Redfield microscopic approach, which is a mean-field approach, we can stop before introducing the first Markovian approximation, which would otherwise lead to the closure model presented in section IV.6.1. Then, in addition to the white noise component, we have

$$\frac{\gamma^2\theta}{2}\int_0^t e^{-\theta|t-s|}\left[\tilde{R}_t,\left[\tilde{R}_s,\tilde{\rho}_s\right]\right]\mathrm{d}s, \tag{IV.66}$$

which is an open term arising solely from the explicit time non-locality of the reduced density matrix, without explicit stochastic degrees of freedom, as these have already been averaged out in the reduction inherent to the microscopic approach.

These terms seem to have a different nature, yet they all relate to the openness of the QME, non-Markovianity of the system, and correlation of the system with the environment. A natural question arises, left for future research: can we formally relate these terms, arising from different approaches?

Appendices

IV.A A note on units consistency

In this Appendix, we remark on the units of measure of the stochastic processes and noise, the operators used in the SSE and the Redfield approach.

White noise. In the white noise case, the stochastic source $\mathrm{d}Z_t = \sigma\,\mathrm{d}W_t$, with dimension $[\mathrm{d}W_t] = \sqrt{t}$, by definition, and we recognize $[\gamma] = \sqrt{E}$, a square of energy, as it is a fluctuation of the Hamiltonian system. Then, to have dimensionless operators, we can substitute the operator B with $B = L/\sqrt{\hbar}$.

OU noise. In the SDE of the OU process, eq. (IV.1), the units of the noise are

$$[\theta] = t^{-1}, \quad [\gamma] = \sqrt{E}, \quad [\mathrm{d}W_t] = \sqrt{t}, \quad [\mathrm{d}X_t] = \sqrt{E \cdot t} \tag{A1}$$

to keep consistency. Then, as above, we need to identify $B = iR/\sqrt{\hbar}$ in the SSE associated with this noise-inducing term.

OU process. In the stochastic Hamiltonian with OU process fluctuations X_t, where $[X_t] = \sqrt{E \cdot t}$, and with the same identification of the operator $R/\sqrt{\hbar}$, we would have

$$\mathrm{d}\psi_t = -\frac{i}{\hbar} H\psi_t\,\mathrm{d}t - \frac{i}{\sqrt{\hbar}} RX_t\,\mathrm{d}t, \tag{A2}$$

where looking only at the units, is

$$[0] = \left[\frac{1}{Et}\right] \cdot [E] \cdot [t] + \left[\frac{1}{\sqrt{Et}}\right] \cdot \left[\sqrt{E \cdot t}\right] \cdot [t] = [0] + [t] \tag{A3}$$

where [0] indicates the absence of physical units, showing that we need to use a weighted process $Z_t = \theta X_t$ to have consistent units, removing the time on the r.h.s. above. This fixes the inconsistency of physical dimensions in Box IV.1.

Redfield. In the Redfield derivation, each Hamiltonian component carries the units of an energy. Then, in eq. (II.28) we need to substitute $S_\alpha = \sqrt{\hbar} R_\alpha$ to reconcile the operators with the ones used in the SSE approach.

IV.B Ornstein-Uhlenbeck updating formula

According to the Ornstein-Uhlenbeck SDE in eq. (IV.1), each X_t trajectory can be computed using the Euler-Maruyama scheme. Alternatively, an exact updating formula has been proposed by D. Gillespie in [213], namely

$$X_{t+\Delta t} = X_t e^{-\theta \Delta t} + \mathcal{X} \sqrt{\frac{\gamma^2}{2\theta}\left(1 - e^{-2\theta \Delta t}\right)} \tag{A4}$$

where $\mathcal{X} \sim \mathcal{N}(0, 1)$ is a random number drawn from a normal unitary distribution, and X_0 is the initial value, again a random value obtained for each trajectory drawing from a Gaussian distribution with the same variance as the stationary process.

IV.C Constraint due to the normalization condition

Proposition 1. *Using the stochastic differential* $\mathrm{d}X_t$ *of an Ornstein-Uhlenbeck process* $(X_t)_{t\geq 0}$*, defined in eq.* (IV.1)*, as the noise source in the SSE eq.* (III.30) *with deterministic operators* A *and* B*, the martingale property of the norm is ensured if and only if the* B *operator is an anti-Hermitian operator given by* $B = iR$*, with* $R^\dagger = R$*.*

Proof.

($\leftarrow$) If $B = iR$, we compute the term to set to zero

$$A^\dagger + A - \theta X_t(-iR + iR) + \gamma^2 R^\dagger R = 0 \tag{A5}$$

that simplifies to $A^\dagger + A + \gamma^2 R^\dagger R = 0$ and the normalization term is obtained in the same fashion as for the white noise-driven SSE, eqs. (III.38) and (III.41),

$$A = -iH - \gamma^2 \frac{1}{2} R^\dagger R \tag{A6}$$

($\rightarrow$) Given $(X_t)_{t\geq 0} \in \mathbb{R}, \mathcal{C}$ Gaussian r.v. with $\mathbb{E}[X_t] = 0$, then $\forall \omega \, \exists t = t_c : X_{\omega,t_c} = 0$. Then, $\forall \omega, \forall t = t_c$ the condition of normalization becomes again

$$A^\dagger + A + \gamma^2 B^\dagger B = 0 \tag{A7}$$

leading to the same normalization term as in eq. (III.41). Since this normalization must hold true at all times, then

$$\forall t \neq t_c, X_t \neq 0 \;\text{ then } \theta X_t(B^\dagger + B) = 0 \implies B^\dagger = -B \tag{A8}$$

□

IV.D Dynamics of the populations for different noise intensities

In this section, we present additional numerical results illustrating the system dynamics driven by white noise ξ_t, the Ornstein–Uhlenbeck process X_{OU}, and Υ_{OU} noise, with the intensity of the noise component varied in the range 0.04–1.3$\sqrt{\hbar\theta}$. The Hamiltonian parameters are kept fixed, and each figure refers to a different Hamiltonian system. In consistency with the main text, the dynamics are displayed with the following color code: driven by the white noise ξ_t in solid black lines, by OU process X_t in solid red lines, and by OU noise Υ_t in solid green lines.

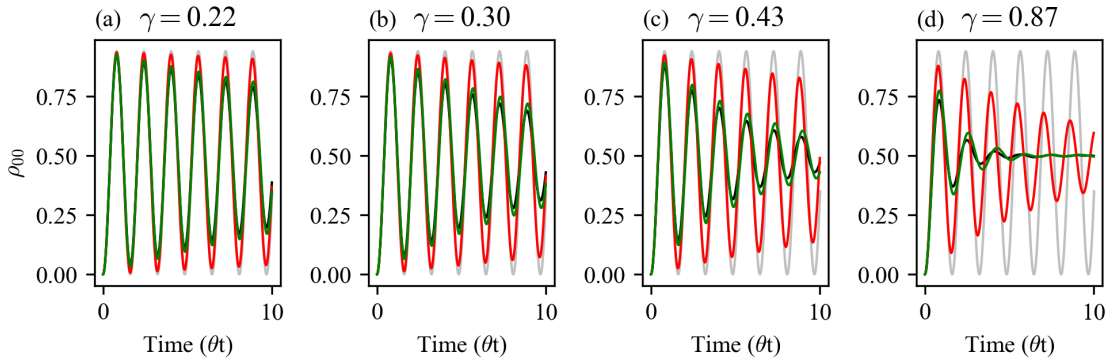

Figure A.IV.D.1: Few selected dynamics of the system described by the Hamiltonian $H_{\varepsilon,\Omega}$, with the stochastic forces applied through the Pauli σ_z operator.

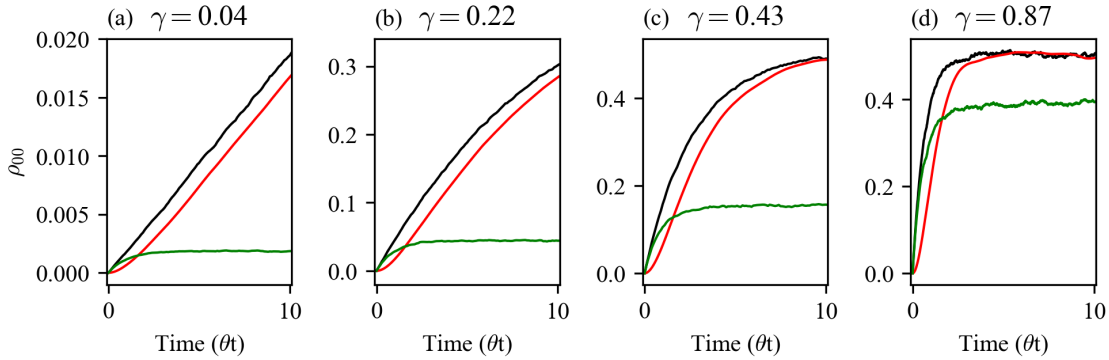

Figure A.IV.D.2: Few selected dynamics of the system described by the Hamiltonian $H_{0,0}$ with the stochastic forces applied through the Pauli σ_x operator.

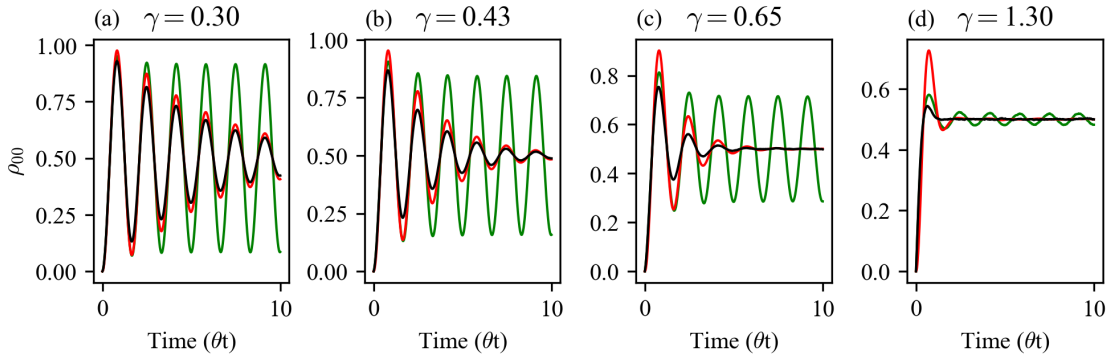

Figure A.IV.D.3: Few selected dynamics of the system described by the Hamiltonian $H_{0,\Omega}$ with the stochastic forces applied through the Pauli σ_x operator.

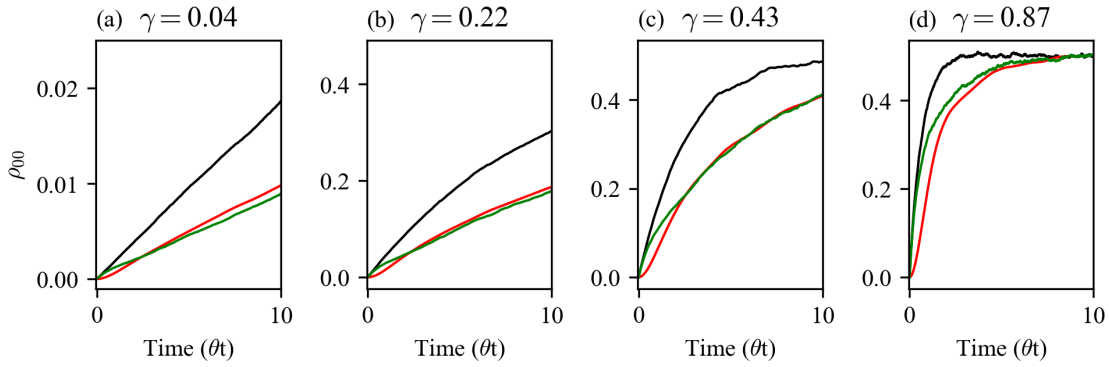

Figure A.IV.D.4: Few selected dynamics of the system described by the Hamiltonian $H_{\varepsilon,0}$ with the stochastic forces applied through the Pauli σ_x operator.

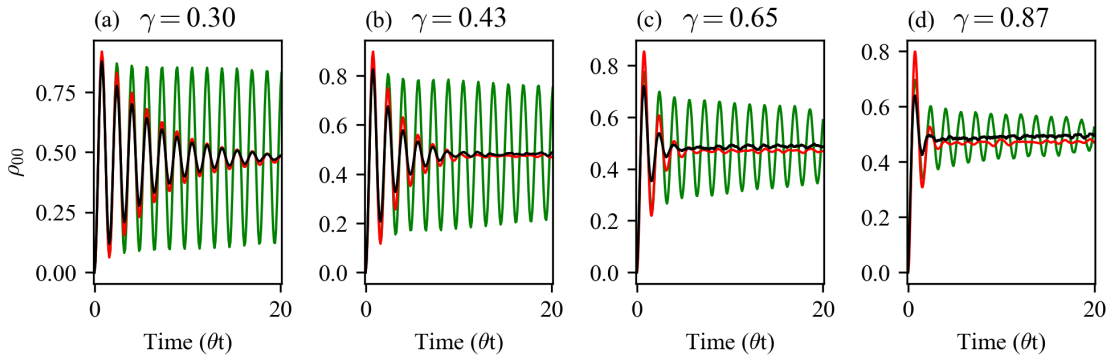

Figure A.IV.D.5: Few selected dynamics of the system described by the Hamiltonian $H_{\varepsilon,\Omega}$, with the stochastic forces applied through the Pauli σ_x operator.

IV.E Convergence to white noise dynamics

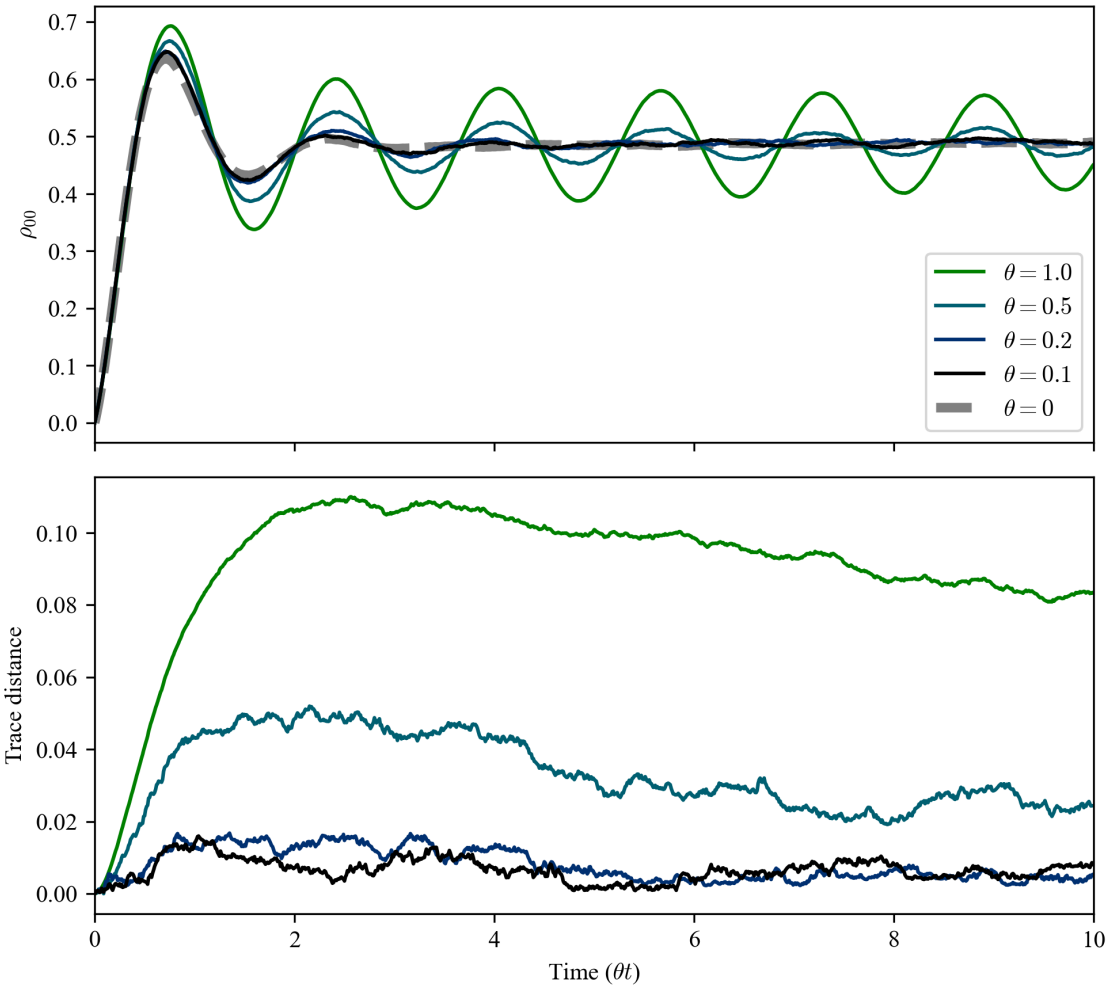

Figure A.IV.E.1: Convergence to the white-noise dynamics as the θ value decrease to zero. (a) Dynamics of the population ρ_{00} of the $H_{\varepsilon,\Omega}$ system with σ_x noise operator, obtained averaging over Υ_{OU}-driven SSE trajectories, for noise intensity $\gamma = 1.3$ and $\theta \in \{0.1, 0.2, 0.5, 1\}$ (colored solid lines) and the white noise dynamics (bold dashed gray line). (b) Trace distance of the density matrix for the dynamics driven by colored noise with different θ parameter with respect to the white-noise limit dynamics.

IV.F Comparison with Redfield dynamics for different noise intensities

Additional numerical results illustrating the comparison of the numerical solution of the Redfield with time-dependent coefficients and the ensemble-averaged dynamics of the SSE drive by the Υ_{OU}-noise, for different noise intensity, varied in the range 0.04–$1.3\sqrt{\hbar\theta}$.

In all figures of this section, the noise intensity is indicated by the color code in each legend. Solid lines represent dynamics obtained by averaging Υ_{OU}-driven SSE trajectories, whereas bold dashed grey lines denote the corresponding results from the Redfield equation with time-dependent coefficients.

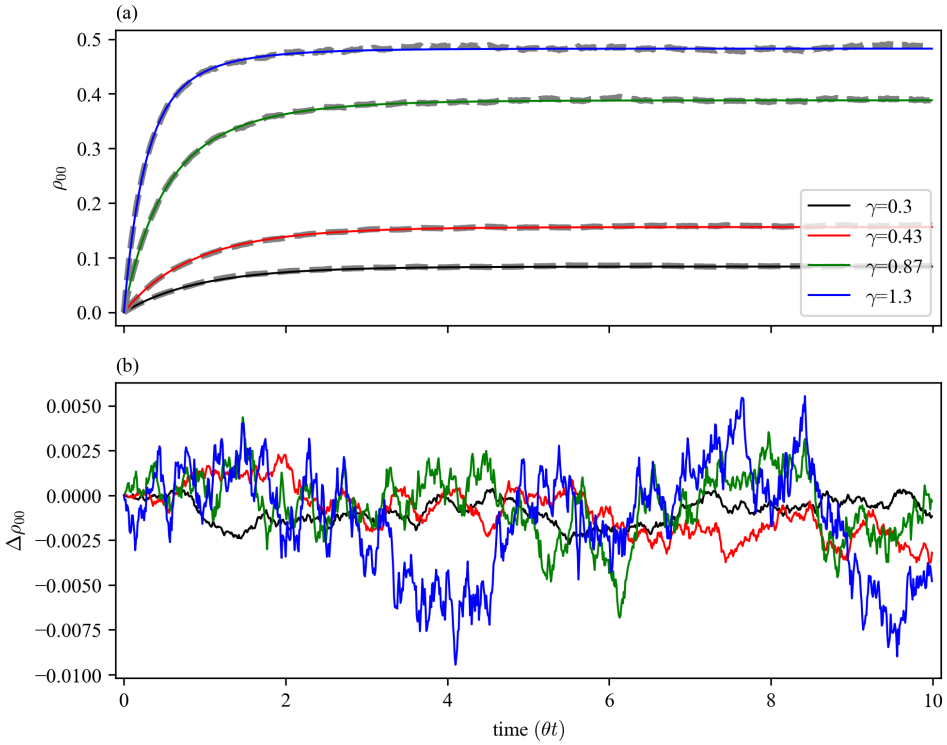

Figure A.IV.F.1: (a) Dynamics of the population ρ_{00} of the $H_{0,0}$ system with σ_x noise operator. (b) Absolute error in the population dynamics.

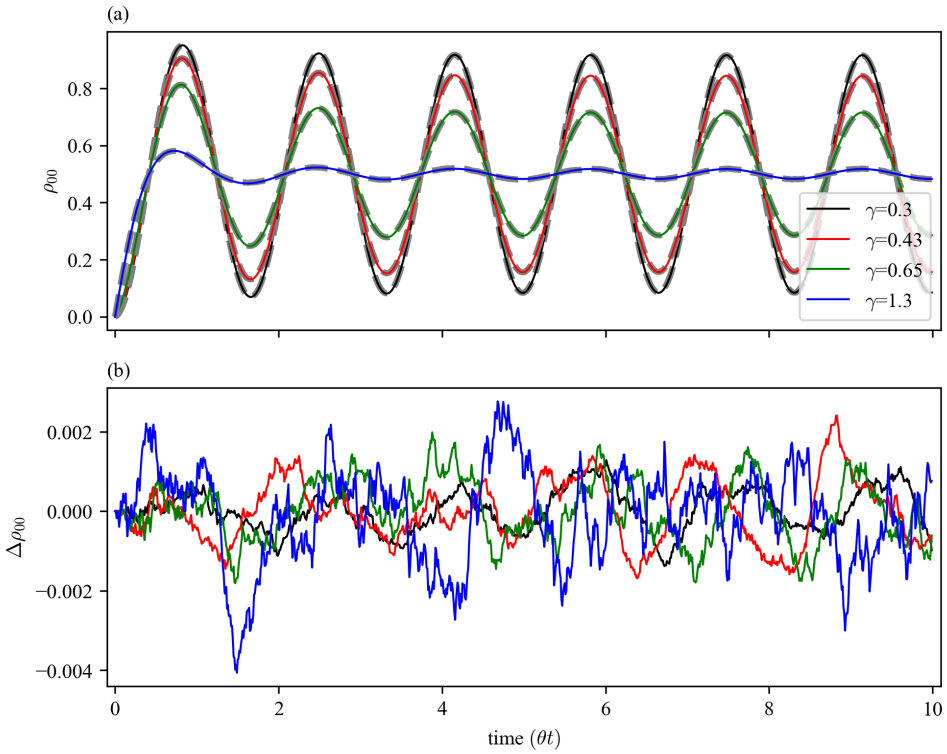

Figure A.IV.F.2: (a) Dynamics of the population ρ_{00} of the $H_{0,\Omega}$ system with σ_x noise operator. (b) Absolute error in the population dynamics.

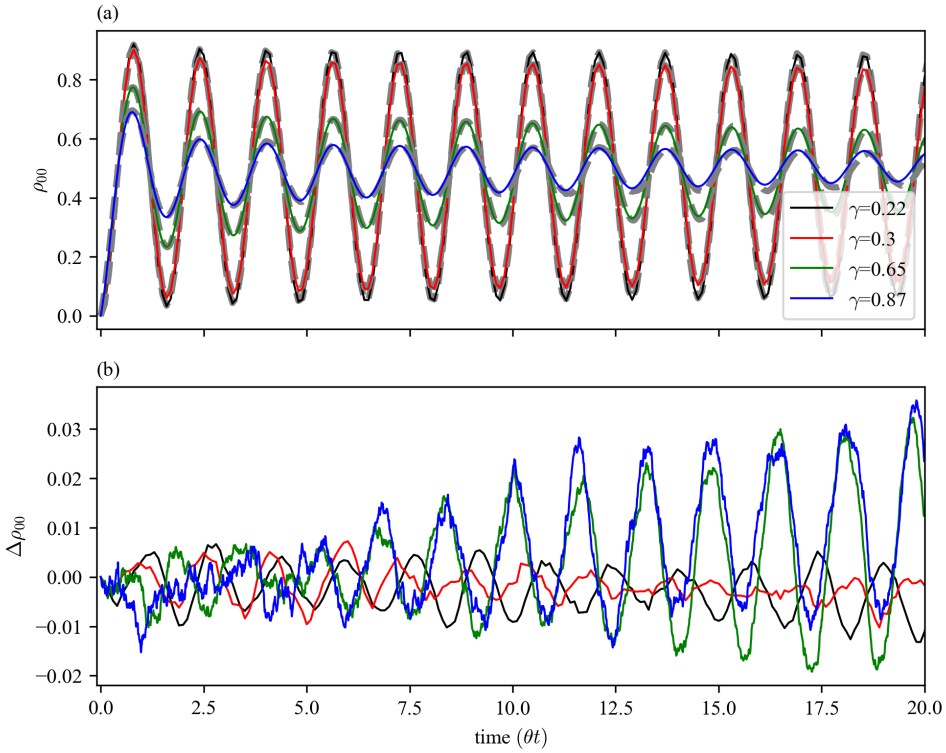

Figure A.IV.F.3: (a) Dynamics of the population ρ_{00} of the $H_{\varepsilon,\Omega}$ system with σ_x noise operator. (b) Absolute error in the population dynamics.

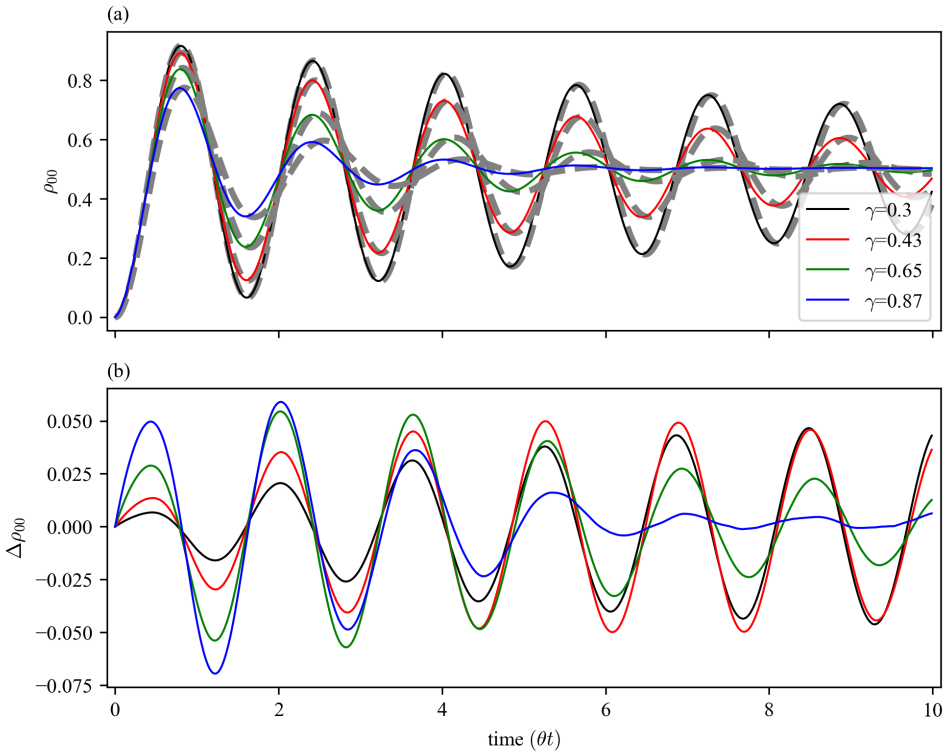

Figure A.IV.F.4: (a) Dynamics of the population ρ_{00} of the $H_{\varepsilon,\Omega}$ system with σ_z noise operator. (b) Absolute error in the population dynamics.

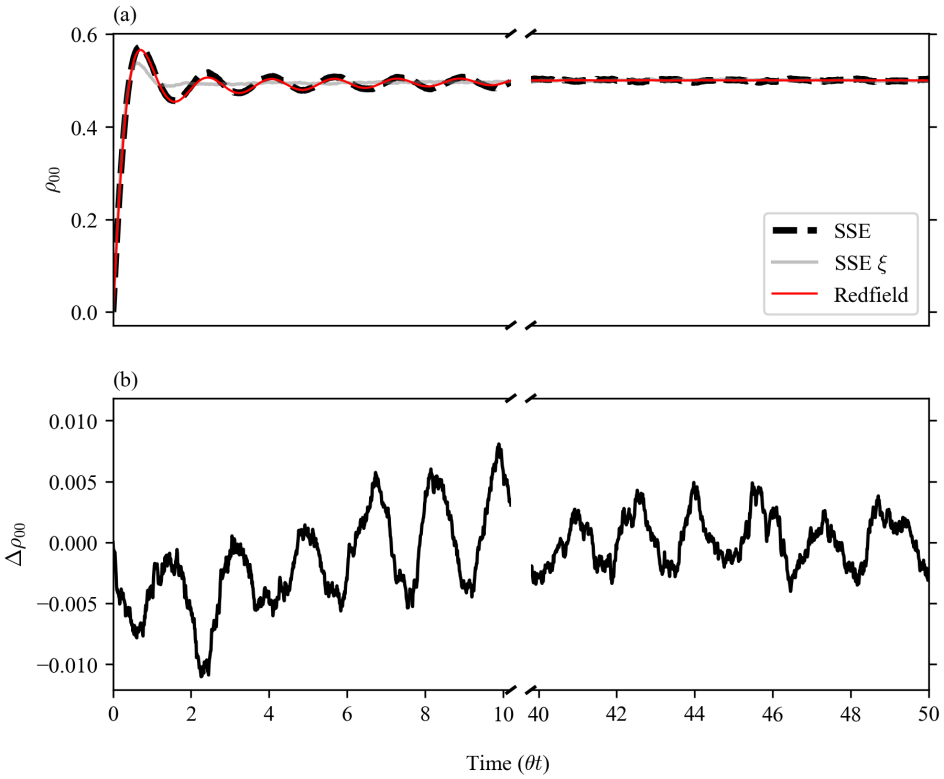

Figure A.IV.F.5: Convergence to the equipartite stationary state. (a) Dynamics of the population ρ_{00} of the $H_{\varepsilon,\Omega}$ system with σ_x noise operator, obtained averaging over Υ_{OU}-driven SSE trajectories (bold dashed line), from the Redfield with time-dependent coefficients (red line), and using white noise (light gray line), for noise intensity $\gamma = 1.3$ and $\theta = 1$. (b) Absolute error in the population dynamics.

References

[18]H.-P. Breuer and F. Petruccione, *The Theory of Open Quantum Systems*, 1st ed. (Oxford University Press, Oxford, Jan. 2002), 10.1093/acprof:oso/9780199213900.001.0001

[19]B. Vacchini, *Open Quantum Systems: Foundations and Theory* (Springer Cham, Dec. 2024), 10.1007/978-3-031-58218-9

[29]M. B. Plenio and S. F. Huelga, "Dephasing-assisted transport: quantum networks and biomolecules", New Journal of Physics **10**, 113019 (2008) 10.1088/1367-2630/10/11/113019

[30]P. Rebentrost, M. Mohseni, I. Kassal, S. Lloyd, and A. Aspuru-Guzik, "Environment-assisted quantum transport", New Journal of Physics **11**, 033003 (2009) 10.1088/1367-2630/11/3/033003

[46]A. G. Redfield, "On the Theory of Relaxation Processes", IBM Journal of Research and Development **1**, 19–31 (1957) 10.1147/rd.11.0019

[50]D. Manzano, "A short introduction to the Lindblad master equation", AIP Advances **10**, 025106 (2020) 10.1063/1.5115323

[54]H. Haken and G. Strobl, "An exactly solvable model for coherent and incoherent exciton motion", Zeitschrift für Physik **262**, 135–148 (1973) 10.1007/BF01399723

[59]R. J. De Keijzer, L. Y. Visser, O. Tse, and S. J. Kokkelmans, "Qubit fidelity distribution under stochastic Schrödinger equations driven by classical noise", Physical Review Research **7**, 023063 (2025) 10.1103/PHYSREVRESEARCH.7.023063

[62]S. Cialdi, C. Benedetti, D. Tamascelli, S. Olivares, M. G. Paris, and B. Vacchini, "Experimental investigation of the effect of classical noise on quantum non-Markovian dynamics", Physical Review A **100**, 052104 (2019) 10.1103/PhysRevA.100.052104

[65]A. Barchielli and M. Gregoratti, *Quantum Trajectories and Measurements in Continuous Time: The Diffusive Case, Lect. Notes Phys. 782* (Springer, Berlin Heidelberg, 2009), 10.1007/978-3-642-01298-3

[146]P. De Checchi, F. Gallina, B. Fresch, and G. G. Giusteri, "On the Noisy Road to Open Quantum Dynamics: The Place of Stochastic Hamiltonians", Annalen der Physik **538**, e00482 (2026) 10.1002/ANDP.202500482

[147]P. De Checchi, F. Gallina, B. Fresch, and G. G. Giusteri, "Quantum trajectories and reduced dynamics in time-correlated environments", (2025), submitted.

[162]A. O. Caldeira and A. J. Leggett, "Path integral approach to quantum Brownian motion", Physica A: Statistical Mechanics and its Applications **121**, 587–616 (1983) 10.1016/0378-4371(83)90013-4

[164]E. B. Davies, "Markovian master equations", Communications in Mathematical Physics **39**, 91–110 (1974) 10.1007/BF01608389

[187]R. Kubo, "A Stochastic Theory of Line Shape", in *Stochastic processes in chemical physics*, Vol. 15, edited by K. E. Shuler (Wiley, Dec. 1969), pp. 101–127, 10.1002/9780470143605.ch6

[196]A. Barchielli, C. Pellegrini, and F. Petruccione, "Stochastic Schrödinger equations with coloured noise", Europhysics Letters **91**, 24001 (2010) 10.1209/0295-5075/91/24001

[199]V. Bally and D. Talay, "The Euler scheme for stochastic differential equations: error analysis with Malliavin calculus", Mathematics and Computers in Simulation **38**, 35–41 (1995) 10.1016/0378-4754(93)E0064-C

[213]D. T. Gillespie, "Exact numerical simulation of the Ornstein-Uhlenbeck process and its integral", Physical Review E **54**, 2084 (1996) 10.1103/PhysRevE.54.2084

[214]F. Gallina, M. Bruschi, and B. Fresch, "From stochastic Hamiltonian to quantum simulation: exploring memory effects in exciton dynamics", New Journal of Physics **26**, 083017 (2024) 10.1088/1367-2630/AD6A7B

[215]T. Fujita, J. C. Brookes, S. K. Saikin, and A. Aspuru-Guzik, "Memory-Assisted Exciton Diffusion in the Chlorosome Light-Harvesting Antenna of Green Sulfur Bacteria", Journal of Physical Chemistry Letters **3**, 2357–2361 (2012) 10.1021/JZ3008326

[216]A. G. Dijkstra, C. Wang, J. Cao, and G. R. Fleming, "Coherent exciton dynamics in the presence of underdamped vibrations", Journal of Physical Chemistry Letters **6**, 627–632 (2015) 10.1021/JZ502701U

[230]A. Carmele, S. Parkins, and A. Knorr, "Quantum-optical realization of an Ornstein-Uhlenbeck-type process via simultaneous action of white noise and feedback", Physical Review A **102**, 033712 (2020) 10.1103/PhysRevA.102.033712

[231]R. J. De Keijzer, L. Y. Visser, O. Tse, and S. J. Kokkelmans, "Fidelity-enhanced variational quantum optimal control", Physical Review A **111**, 052625 (2025) 10.1103/PhysRevA.111.052625

[232]D. Janse van Rensburg, R. de Keijzer, R. Venderbosch, Y. van der Werf, J. d. P. Mellado, R. Lous, E. Vredenbregt, and S. Kokkelmans, "Fidelity Relations in an Array of Neutral Atom Qubits – Experimental Validation of Control Noise", (2025)

[233]C. W. Gardiner and P. Zoller, *Quantum Noise - A Handbook of Markovian and Non-Markovian Quantum Stochastic Methods with Applications to Quantum Optics*, 2nd Enlarged Edition (Springer Berlin, Heidelberg, 2000)

[234]U. Weiss, *Quantum dissipative systems, fourth edition* (World Scientific Publishing Co., Jan. 2012), pp. 1–566, 10.1142/8334

[235]A. S. Bondarenko, J. Knoester, and T. L. Jansen, "Comparison of methods to study excitation energy transfer in molecular multichromophoric systems", Chemical Physics **529**, 110478 (2020) 10.1016/j.chemphys.2019.110478

[236]J. R. Reimers, L. K. McKemmish, R. H. McKenzie, and N. S. Hush, "A unified diabatic description for electron transfer reactions, isomerization reactions, proton transfer reactions, and aromaticity", Physical Chemistry Chemical Physics **17**, 24598–24617 (2015) 10.1039/C5CP02236C

[237]D. Giavazzi, F. Di Maiolo, and A. Painelli, "The fate of molecular excited states: modeling donor–acceptor dyes", Physical Chemistry Chemical Physics **24**, 5555–5563 (2022) 10.1039/D1CP05971H

[238]F. Gallina, M. Bruschi, and B. Fresch, "Strategies to simulate dephasing-assisted quantum transport on digital quantum computers", New Journal of Physics **24**, 023039 (2022) 10.1088/1367-2630/AC512F

[239]I. Kassal and A. Aspuru-Guzik, "Environment-assisted quantum transport in ordered systems", New Journal of Physics **14**, 053041 (2012) 10.1088/1367-2630/14/5/053041

[240]E. Zerah-Harush and Y. Dubi, "Universal Origin for Environment-Assisted Quantum Transport in Exciton Transfer Networks", Journal of Physical Chemistry Letters **9**, 1689–1695 (2018) 10.1021/ACS.JPCLETT.7B03306

[241]H. F. Trotter, "On the product of semi-groups of operators", Proceedings of the American Mathematical Society **10**, 545–551 (1959) 10.1090/S0002-9939-1959-0108732-6

[242]M. Suzuki, "Generalized Trotter's formula and systematic approximants of exponential operators and inner derivations with applications to many-body problems", Communications in Mathematical Physics **51**, 183–190 (1976) 10.1007/BF01609348

Chapter V

Densification of Stochastic Trajectories

In this Chapter, we discuss different quantitative descriptors of the properties of open quantum systems. Within the framework of stochastic unravelings of open system dynamics, we show that trajectory-based methods can provide access to additional information with respect to quantum master equations, on quantities that are not directly accessible from the mean evolution alone. Indeed, while the master equations offer an effective description of the mean dynamics, they inherently reduce the information in the average step, discarding the information encoded in individual stochastic realizations.

Building on this perspective, we propose two quantitative descriptors that, to the best of our knowledge, have not been previously studied.

The first descriptor is a dynamical measure that quantifies the extent to which stochastic trajectories exhibit collective behavior during their evolution within a given unraveling. Although this concept bears intuitions of some sort of "synchronization" among stochastic trajectories, the term synchronization is commonly used to refer to a phenomenon that has been intensively studied in reference to the mean dynamics of coupled systems [174, 175, 243–247], mostly two-qubit systems. The setting considered here is fundamentally different, as we consider a single quantum system and investigate one property arising solely from the structure of its stochastic unraveling. To avoid confusion with established notions of synchronization, we refer to this quantity as a *densification measure*, emphasizing its relation to the geometrical visualization of the states of a single qubit.

From this measure, we further introduce a second descriptor, the *re-densification character* of the unraveling and of the corresponding averaged map. Rather than constituting a rigorous classification of dynamical maps, this quantity is meant to provide qualitative

insight into the relationship between stochastic trajectories, and their associated mean evolution, employing a quantitative descriptor.

Before introducing these new measures, we review some of the most well-known and used quantitative descriptors for the dynamics of open quantum systems. These will serve as a methodological foundation underlying the construction of the new measures developed, and as a basis of reference for the considerations that can be drawn from our construction.

We then construct the densification measure, the re-densification character, and illustrate its behavior for a simple single-qubit model. We conclude by proposing an extension to n-dimensional systems, valid both for n-qubit systems and d-level n-site systems.

V.1 Quantitative descriptors for quantum systems

There are many different ways to observe and describe a quantum system, its properties and dynamics. For instance, in the previous Chapters, we focused on the dynamics of the populations of the mean density matrix expressed on the σ_z basis. The dynamics of the population ρ_{00} is, up to an affine transformation, equivalent to the observable $\langle\sigma_z\rangle$.[1] Another quantity of interest we investigated to understand the dynamics of the systems, the dynamics of the density matrix eigenvalues, in particular e_0.

To obtain concise information on certain phenomena, we can define quantitative descriptors, extracting knowledge from the whole dynamics of the systems. We start from basic quantities in the theory of open quantum systems, borrowing from information and quantum information theory. One central question for information theorists regarding quantum systems is how states can be distinguished, knowledge that is fundamental to understanding how information is preserved, transferred, and lost during a process. One clear way to do it is the definition and use of metrics and distances.

We will discuss the use of the *trace distance* and of *quantum fidelity* and descriptors that we can derive from them, in relation to two questions: is an open evolution Markovian, and if not, by what degree? How close are two density matrices during an evolution, and how sharp is the distribution of the pure state processes unraveling their dynamics?

V.2 Purity of a state

We introduced the concept of purity of a state in section I.3, and thereafter it has been recalled when discussing the origin of mixed states in Chapter III. Here, we briefly recall its more formal definition, and discuss the use of the purity of a density matrix as an indicator of environment-induced decoherence of the system. The *purity* of a quantum system is defined as

$$\varrho := \mathrm{Tr}[\rho^2] \tag{V.1}$$

[1] Recall that an affine transformation is a linear rescaling with a shift, and indeed, we can write $\langle\sigma_z\rangle = \mathrm{Tr}(\rho_t\sigma_z) = \rho_{00} - \rho_{11} = 2\rho_{00} - 1$.

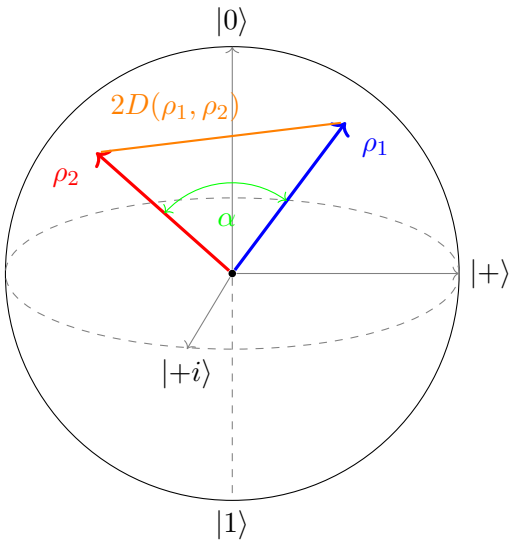

Figure V.1: Representation of two Bloch vectors associated with the two density matrices ρ_1 and ρ_2, in blue and red. Their trace distance is proportional to the Euclidean distance between the vectors, orange line, and the angle α related to the quantum fidelity of the two states, in green. The purity of the two states is indicated by the length of the Bloch vectors.

taking value in $\varrho \in [\frac{1}{n}, 1]$, where $\varrho = 1$ for pure states (i.e., that can be described by a statevector), $\varrho < 1$ for mixed states, with the lower bound $\frac{1}{n}$ for the maximally mixed state. From the geometrical point of view, it is related to the length of the Bloch vector representing the state, presented in section I.3 in eq. (I.41).

This descriptor then gives immediate information on these particular aspects of the average dynamics: starting on a localized deterministic pure state, we start with the maximum purity, which decreases due to the effects of the dissipator $\mathcal{D}$, but can still possibly increase if we transfer irreversibly to a particular state. In Figure V.2, we show the purity of the states for the dynamics presented in Examples III.1 and III.2. Both are strictly contractive dynamics, purely Markovian, but the sole purity of the states can not distinguish properties of the maps. In the first example, the Haken-Strobl, Figure V.2a, the system reaches the maximally mixed state, related to infinite temperature of the bath, and we can immediately recognize the contraction induced by the dissipator. In the second example, Figure V.2b, we investigate the spontaneous emission of an exited state to the ground state. The purity reaches a minimum when $\rho_{00} = \rho_{11}$, and then starts increasing again as we transfer populations to the lowest energy level, eventually reaching a pure state localized on $|0\rangle$.

Indeed, this descriptor is limited to the description of the average dynamics of one density matrix, depending only on its state at a precise given time, and alone bears no information on the change of ρ with respect to an initial state $\rho(0)$ or another state $\tilde{\rho}$, nor gives information on the pure state trajectories.

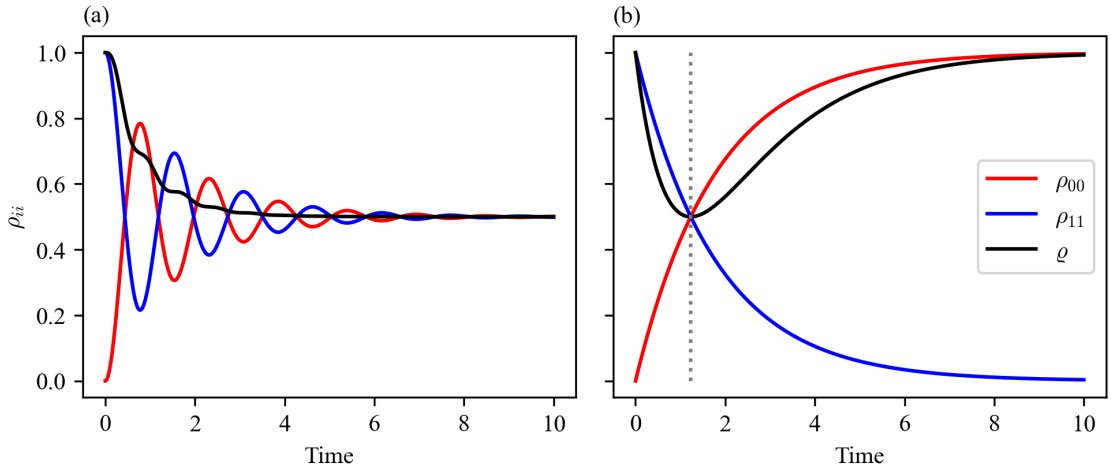

Figure V.2: Dynamics of the two-level systems of Examples II.1 and III.1, depicted by their populations ρ_{00} and ρ_{11} in red and blue solid lines, and the purity of the mean density matrix in black solid line.

V.3 Trace distance and non-Markovianity measure

We introduce here a proper metric to define the distance between different density matrices associated to the same Hilbert space. We define the trace distance as [248]

$$D(\rho_1, \rho_2) = \frac{1}{2}\|\rho_1 - \rho_2\|_1 \tag{V.2}$$

where $\|A\|_1 = \sqrt{A^\dagger A}$ is the trace norm of the matrix A, in this case the difference of the two states' density matrices. The trace distance is a proper distance, as D is positive semidefinite, bounded $D \in [0, 1]$, namely is zero if the states are identical, $D(\rho_1, \rho_2) = 0$ if and only if $\rho_1 = \rho_2$, and it is maximal if and only if the states are orthogonal, $D(\rho_1, \rho_2) = 1$ iff $\rho_1 \perp \rho_2$.

The geometric interpretation of this distance, in the framework of quantum computing, is immediate. Take two states of a qubit and represent them on a Bloch sphere; it is easy to see that the Euclidean distance of the two vectors is twice the trace distance of the two matrices, see Figure V.1.

The physical interpretation of this distance is related to the ability to distinguish states, quantifying it, and can be thought of as the probability of identifying one state by an optimal measurement. The limital cases are orthogonal and identical states. The distance is maximal for orthogonal states, and to distinguish which of the two is present, we need only one projective measure, while for completely identical states, we cannot tell which one we are observing. It can be thought of in a way as a generalization of the classical trace, L_1, or Kolmogorov distance for probability distributions. In fact, if the states commute $[\rho_1, \rho_2] = 0$, we can express ρ_1 and ρ_2 in their diagonal form in the same basis; this can be looked at as a classical distribution, and the quantum trace distance and the Kolmogorov distance are equal [248].

Many results and properties related to this distance are discussed in detail in Ref. [248].

Here, we focus on the results that are relevant for *open* quantum systems, namely the connection between trace-distance contractivity, completely positive trace-preserving (CPTP) dynamics, and quantitative notions of Markovianity.

A fundamental result, see Theorem 9.2 in [248], states that any CPTP map is a contraction with respect to the trace distance metric. In particular, given a CPTP map $\mathcal{E}_{\mathcal{L}}$, for instance those generated by a Lindbladian $\mathcal{L}$, then

$$D(\mathcal{E}_{\mathcal{L}}[\rho_1], \mathcal{E}_{\mathcal{L}}[\rho_2]) \leq D(\rho_1, \rho_2)\,. \tag{V.3}$$

Then, by the semigroup property $\mathcal{E}_{\mathcal{L}}(t+\tau) = \mathcal{E}_{\mathcal{L}}(t)\mathcal{E}_{\mathcal{L}}(\tau)$ it is straightforward to see that

$$D(\mathcal{E}_{\mathcal{L}}^{(t+\tau)}[\rho_1], \mathcal{E}_{\mathcal{L}}^{(t+\tau)}[\rho_2]) \leq D(\mathcal{E}_{\mathcal{L}}^{(t)}[\rho_1], \mathcal{E}_{\mathcal{L}}^{(t)}[\rho_2])\,, \tag{V.4}$$

showing that, for all quantum dynamical semigroups $\mathcal{E}$, the trace distance is *monotonically* decreasing in time, the two states becoming less distinguishable at each subsequent time, a progressive loss that is characteristic of Markovian open-system dynamics.

In Figure V.3, the behavior of the trace distance for the two-level system driven by the different stochastic fluctuations previously investigated in Chapter IV. The dynamics driven by white noise, leading to a Lindblad QME and therefore a CPTP map, is characterized by a strictly monotonic decrease of the trace distance, as expected by eq. (V.4). When correlated fluctuations drive the system, the results change. The trace distance for X_{OU}-driven system shows its typical null derivative at time zero, recall section IV.5.1, and then exhibits a slower decay that still leads to a null trace distance as the system reaches the maximally mixed state stationarity. On the other hand, in the presence of correlated Υ_{OU}-noise, the trace distance reaches an asymptotically non-null value, as the orthogonal realizations reach different stationary states.

V.3.1 BLP non-Markovianity measure

The inequality of eq. (V.4) gives one condition allowing us to determine, possibly, the Markovianity of a map, as it is a condition valid for CPTP maps.

This is not always true for non-Markovian processes. At certain times, the distinguishability of states undergoing a non-Markovian evolution due to a map Φ may increase, a phenomenon that can be interpreted as a backflow of information from the environment to the system. This can be appreciated by observing the trace distance as a function of time, and stated formally by defining the rate of change of the trace distance,

$$\delta_{\Phi}(t; \rho_1, \rho_2) := \frac{\mathrm{d}}{\mathrm{d}t} D\left(\rho_1(t), \rho_2(t)\right) \tag{V.5}$$

where $\rho_i(t) = \Phi_{t,t_0}\rho_i(t_0)$ is the density matrix propagated from its initial condition to the time t by the map Φ.

The time intervals where eq. (V.4) is not valid are therefore characterized by positive values of the rate $\delta_{\Phi}(t; \rho_1, \rho_2)$, and we can define a quantum process as non-Markovian if, for a pair ρ_1, ρ_2 and a time t_c such that $\delta(t_c; \rho_1, \rho_2) > 0$. From these considerations,

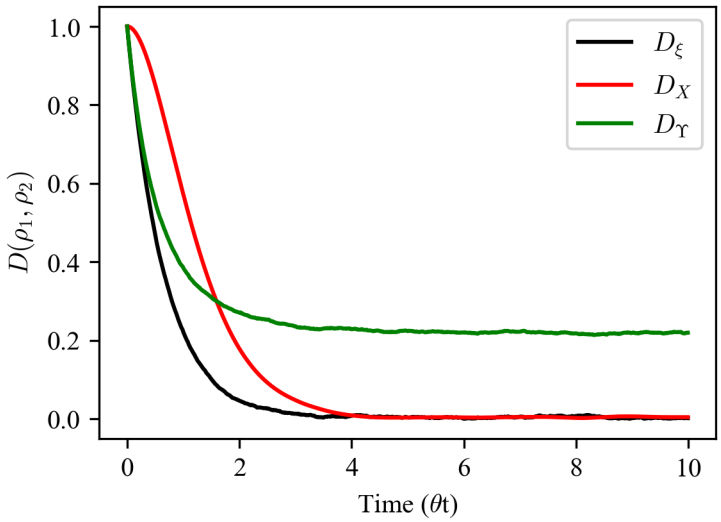

Figure V.3: Trace distance of the mean density matrices for the dynamics of a two-level system defined by Hamiltonian $H_{0,\Omega}$, driven respectively by white noise, black line, OU process, red line, and OU noise, green line. The trace distance is computed between two mean density matrices obtained by realizations of the processes starting from orthogonal initial states.

H. Breuer, E. Laine, and J. Piilo (BLP) proposed a quantitative measure of the degree of non-Markovianity [249, 250]. For a single propagator, we can write

$$\tilde{\mathcal{N}}(\Phi; \rho_1, \rho_2) = \int_{\delta>0} \delta_\Phi(t; \rho_1, \rho_2)\, \mathrm{d}t\,, \tag{V.6}$$

which ascertains whether a specific single realization under study exhibits non-Markovian features. The integral is restricted over the time intervals satisfying $\delta(t_c; \rho_1, \rho_2) > 0$, so $\tilde{\mathcal{N}}(\Phi; \rho_1, \rho_2) \geq 0$, with strictly positive values indicating non-Markovian features.

To characterize the non-Markovianity of the dynamical map Φ itself, rather than of a realization starting from a particular pair of initial states, the dependence on ρ_1 and ρ_2 must be removed. This is achieved by maximizing the quantity in eq. (V.6) over all possible pairs of initial states $\rho_1(t_0), \rho_2(t_0)$, obtaining the BLP measure of non-Markovianity,

$$\mathcal{N}(\Phi) = \max_{\rho_1(t_0), \rho_2(t_0)} \int_{\delta>0} \delta(t; \rho_1, \rho_2)\, \mathrm{d}t \geq 0\,. \tag{V.7}$$

We note that the definition of this measure of non-Markovianity requires strict positivity of the rate of change of the trace distance. Imagine a scenario as depicted in Figure V.4, the measure $\mathcal{N}$ does not distinguish between the behavior of curves in panel (a) and (b). While the first is clearly Markovian, the peculiar deviation from the expected monotony in (b) would not be noted. Indeed, this is the scenario that we observe in Figure V.3. The presence of the cross-correlation term with the environment-dependent process, eq. (IV.64), and the incomplete perturbation or Markovian approximations, resulting in the terms in eqs. (IV.65) and (IV.66), are not distinguished by this measure. Therefore, by this descriptor, all dynamics observed should be classified as Markovian.

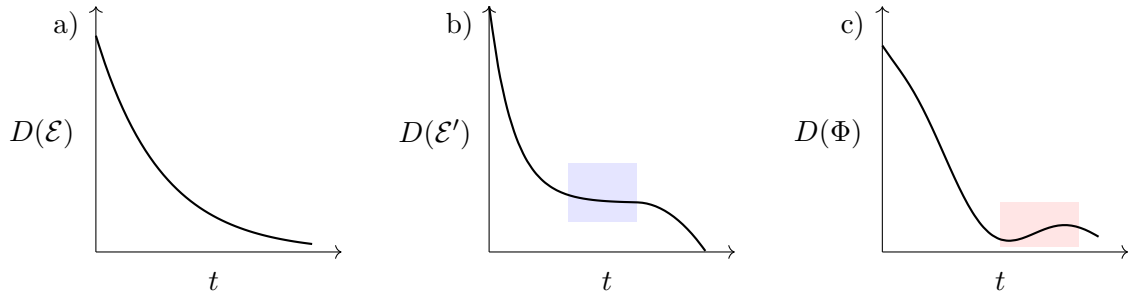

Figure V.4: Three conceptual examples of trace distance for three different maps $\mathcal{E}$, $\mathcal{E}'$ and Φ. (a) The propagation through the Markovian map $\mathcal{E}$ shows clearly the monotonic decrease of distinguishability of the states. (b) The propagation through a different map $\mathcal{E}'$ which is not in Lindblad form shows a slightly different behavior, never increasing but showing a plateau for a certain amount of time, highlighted in transparent blue. (c) The propagation through a non-Markovian map Φ shows a temporary increase in trace distance, highlighted in transparent red, showing backflow of information from the environment to the system.

We conclude remarking that the concept and definition of non-Markovianity in quantum processes can be controversial, and it is an active field of study to this day [251–254], with many different definitions and descriptors, the most famous other than the BLP measure, the RHP measure [255], based on CP-divisibility, and the LFS measure [256], based on correlation revival.

V.4 Quantum fidelity

Quantum fidelity is another descriptor used to determine if two quantum states are similar, often in the context of discussing quantum computing operations [248]. Unlike the trace distance, quantum fidelity is not a proper distance, as it does not satisfy the triangle inequality. Yet, it is a useful indicator for the properties of an evolving quantum state. The fidelity is defined, for states defined by density matrices, as

$$F(\rho_1, \rho_2) = \left[\mathrm{Tr}\left(\sqrt{\sqrt{\rho_1}\rho_2\sqrt{\rho_1}}\right)\right]^2 . \tag{V.8}$$

It is possible to simplify eq. (V.8), according to the nature of the states that we are dealing with. First, we can calculate the fidelity between a generic mixed state ρ to a pure state $|\psi\rangle$, thanks to the cyclic property of the trace, hence write

$$\begin{aligned} F(|\psi\rangle, \rho) &= \left[\mathrm{Tr}\left(\sqrt{\rho|\psi\rangle\langle\psi|}\right)\right]^2 \\ &= \langle\psi|\rho|\psi\rangle \,, \end{aligned} \tag{V.9}$$

which further simplifies for pure state dynamics

$$F(t; |\psi\rangle, |\varphi\rangle) = |\langle\psi(t)|\varphi(t)\rangle|^2 . \tag{V.10}$$

Different variants of fidelity-based descriptors can be constructed, depending on how

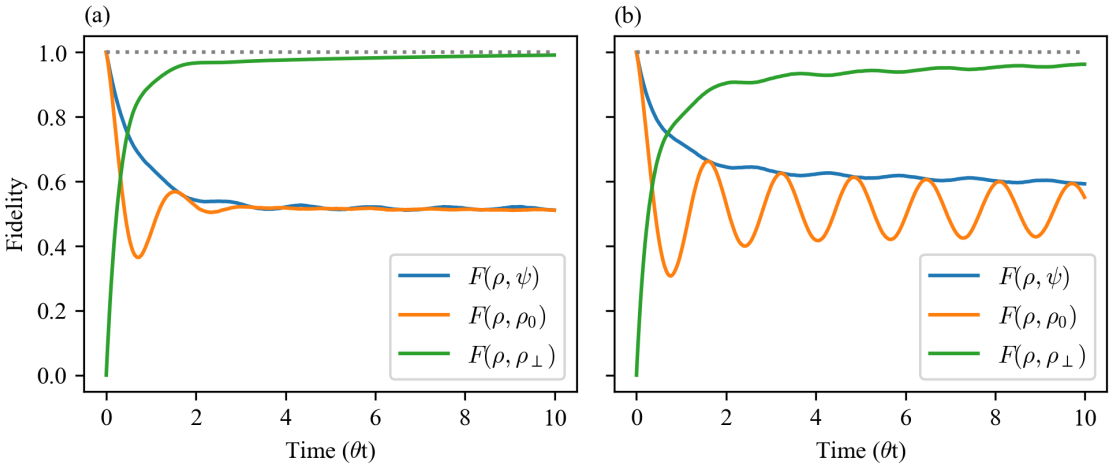

Figure V.5: Different fidelity measures of the mean density matrices for the dynamics of a two-level system defined by Hamiltonian $H_{\varepsilon,\Omega}$, driven respectively by white noise ξ_t in panel (a) and Υ_{OU} noise in panel (b). The fidelity with respect to the deterministic dynamics is depicted in blue lines, with respect to the initial state in orange. In analogy to the trace distance measure, the fidelity with respect to the dynamics starting from an orthogonal initial state is depicted in green lines.

fidelity is defined and employed. Here, we briefly point out two representative examples. In Ref. [227], A. Chenu *et al.* express the fidelity as

$$F(t) = \mathrm{Tr}\left[\rho(0)\rho(t)\right] , \tag{V.11}$$

a different quadratic version of what was stated above. Its peculiarity is that it quantifies the distance from the initial state rather than the distance from another state or an ideally behaving copy, characterizing the study of an intrinsic feature of the dynamics of the system rather than its fidelity to a desired state. It can be related to the notion of quantum speed of physical processes [227, 257, 258], relying on the distance traveled during the evolution. Another interesting example is the extensive use of quantum fidelity in the recent work of R.J. De Keijzer *et al.* [59], where the quantity of interest is the pure state fidelity, eq. (V.10), between a stochastic driven wavefunction and an ideal (deterministic) evolution of the system, i.e. in the absence of a disturbing environment.

In Figure V.5, we compare the investigation of different versions of fidelity in two limiting cases of a system described by the generic Hamiltonian $H_{\varepsilon,\Omega}$, driven with either white noise ξ_t or colored noise Υ_{OU}. The fidelity of the system with respect to a pure noiseless dynamics of the system, blue lines, behaves similarly to the trace distance measure, but returns different information. The systems start localized on the same deterministic initial state and, as the systems relax due to the effect of the dissipators, are less and less close to unperturbed evolution. The measure in eq. (V.11), proposed in Ref. [227], returns little information. As we compute the fidelity with respect to the initial state, we observe that the fidelity returns the dynamics of one population of the system, in the case of a two-level system, losing information on all other elements of the density matrix. In analogy with the analysis of the trace distance, we can compute the fidelity between two realizations

of the mean dynamics according to the same map but with orthogonal initial states. The initial fidelity is then correctly zero at t_0, and increases as the systems relax, eventually maximizing as the systems reach the mixed state distributions.

V.5 Densification of Bloch vectors

The analysis of the open dynamics has been focused so far on the mean dynamics of specific quantities, in particular the eigenstates of σ_z and the eigenstates of the mean density matrix.

Leveraging on the stochastic unraveling approach, we can access the pure state trajectory dynamics and further investigate their behavior. Here, our focus is motivated by the geometric interpretation that can be obtained from the fidelity of two quantum states. This is directly related to the cosine of the angle between the Bloch vectors representing the states ρ_1 and ρ_2, see Figure V.1. Investigating two-level systems as the case study, the visualization of the dynamics of the state on the Bloch sphere is straightforward. Moreover, we are interested in the unraveling of the states and their dynamics when governed by stochastic Hamiltonians, so the definition of fidelity for pure states, eq. (V.10), provides a natural and convenient starting point.

In Figure V.6, we plot the mean dynamics and the trajectories dynamics of a swarm of 50 trajectories of the processes in eqs. (III.42) and (IV.23) for the generic Hamiltonian $H_{\varepsilon,\Omega}$. In Figure V.6b and Figure V.6c, the stochastic trajectories of the states on the sphere are depicted by colored transparency lines, and the Bloch vectors of the associated states at time $t = 10$ as black arrows. Similar information to that discussed before in section IV.5 about the dynamics can be obtained from such plots, in particular from Figure V.6a. In addition, these plots allow us to clearly visualize the occurrence of a phenomenon reminiscent of synchronization in the Υ_{OU}-driven dynamics. Indeed, comparing Figure V.6c with Figure V.6b, we can observe an evident *densification* of the Bloch vectors, pointing to a restricted region of the sphere surface when the system is driven by the correlated Υ_{OU} noise.

V.5.1 Angular spread of trajectory vectors on the Bloch sphere

We aim to define a clear quantifier for this behavior, enabling us to describe the empirical observations obtained by observing the dynamics over time. We start by defining a correct metric based on the fidelity [248], defined by the angle between two states as

$$\alpha(\rho_1, \rho_2) = \arccos\left(F(\rho_1, \rho_2)\right) . \tag{V.12}$$

We can appreciate that α is a non-negative measure, the distance $\alpha = 0$ only if the two states are identical $\rho_1 = \rho_2$ and maximized when orthogonal,[2] and the triangular inequality is valid, see Ref. [248] for the proof. Then, the angle α is a metric on the space of the valid states.

[2]Note that the visualization in the Bloch sphere can be deceiving, since orthogonal states, such as the basis $\{|0\rangle, |1\rangle\}$, are at opposite poles of the sphere.

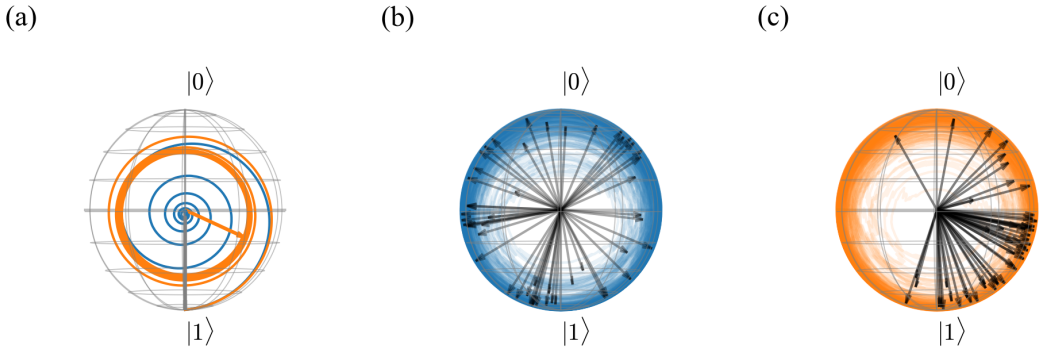

Figure V.6: Visualization of the dynamics of the $H_{\varepsilon,\Omega}$ system driven by white noise, depicted in blue, and Υ_{OU} noise, depicted in orange, on the Bloch sphere. The Bloch spheres are oriented with the x axis pointing towards the reader for better visualization of the mean dynamics and the densification phenomenon. In panel (a), the mean dynamics are depicted in solid lines, the Bloch vector associated with the density matrix at the final time $t_f = 10$ in solid matching arrows. In panels (b,c), a swarm of 50 stochastic trajectories, respectively for white and correlated noises, is depicted in color transparency lines, the Bloch vectors associated with each trajectory at the final time t_f as black arrows.

Then, we can compute the angle between all unique couples of trajectory vectors, from the fidelity computed according to eq. (V.10), as

$$\alpha_{ij}(t) = \arccos\left(F(t, |\psi_i^{\mathrm{trj}}\rangle, |\psi_j^{\mathrm{trj}}\rangle)\right). \tag{V.13}$$

By averaging over the entire set of trajectories, we obtain a descriptor for the spread of the states in the Bloch sphere. Specifically, we define the *densification measure* as

$$\bar{\alpha}(t) = 1 - \frac{2}{N(N-1)}\frac{1}{\pi}\sum_{i=1}^{N}\sum_{j>i}^{N}\alpha_{ij}(t) \tag{V.14}$$

where the normalization by π^{-1} is to bound the measure in $[0, 1]$, and we subtract the mean normalized angle measure to 1, so that increasing $\bar{\alpha}(t)$ values correspond to increasing densification phenomenon rather than the ensemble angular dispersion.

This densification measure, at present, should be regarded as a heuristic purely geometric descriptor rather than a contraction metric or classifier of dynamical dissipative maps. This measure is intended as a quantifier of observable collective features that emerge from the stochastic unravelings of open dynamics. Physically, an increase in densification indicates that the distinct stochastic realization explores, at a given time, similar regions of the state space despite their noisy nature. We remark that this behavior should not be interpreted as synchronization as per its usual meaning, but rather as the similarity in the behavior of realizations of the ensemble, showing further evidence of the effects of environmental correlations on the collective behavior.

In Figure V.7, a comparison of different descriptors for the dynamics of a two-level system described by the $H_{\varepsilon,\Omega}$ Hamiltonian and driven by the correlated Υ_{OU} noise is

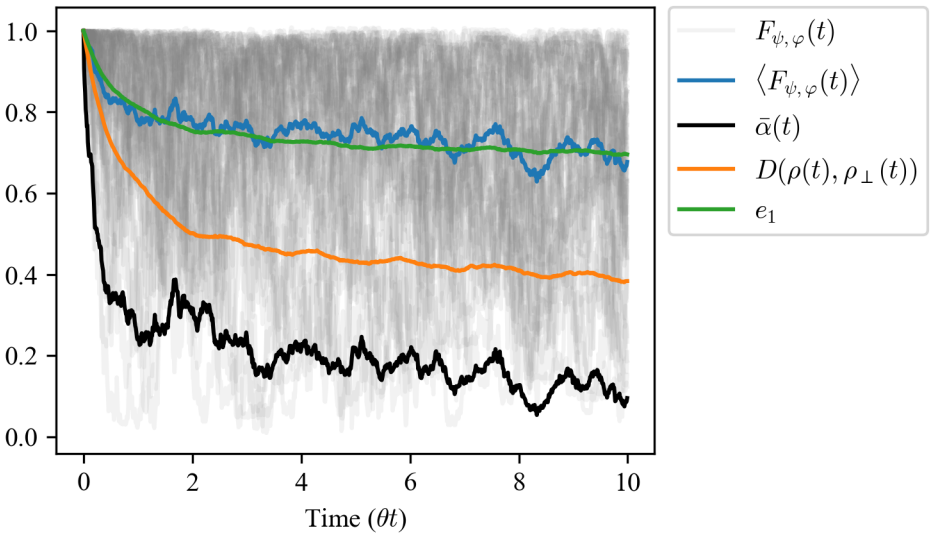

Figure V.7: Comparison of different descriptors, trajectory-based and averaged, of the open dynamics of a two-level system defined by Hamiltonian $H_{\varepsilon,\Omega}$, driven by Υ_{OU} noise. For a swarm of 50 trajectories, the individual trajectory fidelities with respect to the unperturbed coherent dynamics are depicted as gray transparency lines, their ensemble average corresponding to the fidelity of the mean density matrix in a blue solid line. The densification measure is depicted in a black solid line, the trace distance with respect to an orthogonal realization in orange, and the highest eigenvalue of the mean density matrix in green.

presented, highlighting the complementary information provided. Focusing first on the fidelity analysis, the light gray lines show the fidelity associated with individual trajectories compared to the unperturbed dynamics. This depiction has the advantage of showing only the variations arising solely from the stochastic trajectory behavior, without displaying the unnecessary information of the pure Hamiltonian dynamics. The average of the fidelity, depicted in a blue line, returns the expected behavior as in Figure V.5b, the observable fluctuation and noisy character are due to the limited dimension of the finite ensemble size (only 50 trajectories). Interestingly, it closely follows the behavior of the higher eigenvalue of the mean density matrix, depicted in a green line, returning the same information. The black curve corresponds to the densification measure $\bar{\alpha}(t)$, which quantifies the angular spread of the unraveling vectors on the Bloch sphere, and the trace distance is reported as an additional reference and comparison. Again, the visible fluctuations of the densification measure are a consequence of the finite number of trajectories.

The densification measure shows a similar behavior to the average fidelity. To some extent, this is expected, as the densification measure is constructed from the angular distance induced by the fidelity. However, the fidelity average is constructed as $\langle F(t;\psi^{\mathrm{trj}},\varphi)\rangle$, on trajectories compared to the unperturbed deterministic dynamics of $|\varphi_t\rangle$, whereas the densification measure is induced from the angle between all pairs of stochastic trajectories, eq. (V.13), without reference to a deterministic dynamics. One can also argue that a comparable monotonic decay can be observed for the trace distance. Despite the similarities, these are three different measures, differing in their numerical values, nature - only two are

correct metrics, and only two are inferred from the stochastic unraveling - and the type of information they encode and convey. The trace distance characterizes the contraction nature of the map, the fidelity quantifies the similarity to the ideal unperturbed dynamics (and, indirectly, to the spectral properties of the density matrix), and the densification probes the structure of the stochastic unraveling, providing a contour to the spread of trajectories in the fidelity space.

Taken together, these descriptors provide complementary perspectives on the open-system evolution, highlighting different dynamical features that are not accessible from any single measure alone.

V.5.2 Derived measure of re-densification

In analogy with the BLP measures of non-Markovianity, in eqs. (V.6) and (V.7), and in the same spirit of the proposal of other measures of non-Markovianity [255, 256, 259], we propose and define a measure of the *re-densification behavior* of a system. By the definition of the densification measure, eq. (V.14), we can appreciate that for a process starting localized on a specific initial state, the densification measure is a decreasing, but not necessarily monotonically decreasing, function of time. We then define the rate

$$\eta(t) = \frac{\mathrm{d}}{\mathrm{d}t}\bar{\alpha}(t) \tag{V.15}$$

which is a function of time, positive for densification of the trajectories, negative for when the angular spreading of the ensemble increases, and null when the average spread is stationary.

Then, for a given SSE, i.e., given fluctuations, operators, and initial state, its ensemble realizations and the associated QME, we define the measure of the re-densification descriptor of the process as

$$\tilde{\mathcal{S}} = \int_{\eta>0} \eta(t)\,\mathrm{d}t \tag{V.16}$$

and the re-densification character of the family of processes as

$$\mathcal{S} = \max_{\{\psi_{t_0}\},\Theta} \int_{\eta>0} \eta(t)\,\mathrm{d}t\,, \tag{V.17}$$

the maximum over the possible choices of initial states $\{\psi_{t_0}\}$ and of parameters Θ, for instance $\Theta = \{\gamma, \theta\}$ for the Υ_{OU}-driven SSE.

We conclude that, in the cases investigated throughout this dissertation, the re-densification measure does not seem to provide additional knowledge on the system non-Markovianity features, but we remark that it is obtained through different quantities than usual, and it should be considered a complementary measure. Further study is required to assess the relevance of this descriptor and its connection to other metrics, known synchronization problems, and experimentally accessible quantities.

References

[59]R. J. De Keijzer, L. Y. Visser, O. Tse, and S. J. Kokkelmans, "Qubit fidelity distribution under stochastic Schrödinger equations driven by classical noise", Physical Review Research **7**, 023063 (2025) 10.1103/PHYSREVRESEARCH.7.023063

[174]B. Bellomo, G. L. Giorgi, G. M. Palma, and R. Zambrini, "Quantum synchronization as a local signature of super- and subradiance", Physical Review A **95**, 043807 (2017) 10.1103/PHYSREVA.95.043807/

[175]F. Galve, A. Mandarino, M. G. Paris, C. Benedetti, and R. Zambrini, "Microscopic description for the emergence of collective dissipation in extended quantum systems", Scientific Reports 2017 7:1 **7**, 42050– (2017) 10.1038/srep42050

[227]A. Chenu, M. Beau, J. Cao, and A. Del Campo, "Quantum Simulation of Generic Many-Body Open System Dynamics Using Classical Noise", Physical Review Letters **118**, 10.1103/PhysRevLett.118.140403 (2017) 10.1103/PhysRevLett.118.140403

[243]G. L. Giorgi, F. Plastina, G. Francica, and R. Zambrini, "Spontaneous synchronization and quantum correlation dynamics of open spin systems", Physical Review A - Atomic, Molecular, and Optical Physics **88**, 042115 (2013) 10.1103/PHYSREVA.88.042115

[244]G. Karpat, İ. Yalçinkaya, B. Çakmak, G. L. Giorgi, and R. Zambrini, "Synchronization and non-Markovianity in open quantum systems", Physical Review A **103**, 062217 (2021) 10.1103/PHYSREVA.103.062217

[245]A. Cabot, G. Luca Giorgi, and R. Zambrini, "Synchronization and coalescence in a dissipative two-qubit system", Proceedings of the Royal Society A **477**, 10.1098/RSPA.2020.0850 (2021) 10.1098/RSPA.2020.0850

[246]F. Schmolke and E. Lutz, "Noise-Induced Quantum Synchronization", Physical Review Letters **129**, 250601 (2022) 10.1103/PhysRevLett.129.250601

[247]E. R. Bittner and B. Tyagi, "Noise-induced synchronization in coupled quantum oscillators", The Journal of Chemical Physics **162**, 104116 (2025) 10.1063/5.0246275

[248]M. A. Nielsen and I. L. Chuang, *Quantum Computation and Quantum Information (10th Anniversary Edition)* (Cambridge University Press, 2010)

[249]H. P. Breuer, E. M. Laine, and J. Piilo, "Measure for the Degree of Non-Markovian Behavior of Quantum Processes in Open Systems", Physical Review Letters **103**, 210401 (2009) 10.1103/PHYSREVLETT.103.210401

[250]E. M. Laine, J. Piilo, and H. P. Breuer, "Measure for the non-Markovianity of quantum processes", Physical Review A - Atomic, Molecular, and Optical Physics **81**, 062115 (2010) 10.1103/PHYSREVA.81.062115

[251]U. Shrikant and P. Mandayam, "Quantum non-Markovianity: Overview and recent developments", Frontiers in Quantum Science and Technology **2**, 1134583 (2023) 10.3389/FRQST.2023.1134583

[252]B. Bylicka, D. Chruściński, and S. Maniscalco, "Non-Markovianity and reservoir memory of quantum channels: a quantum information theory perspective", Scientific Reports 2014 4:1 **4**, 1–7 (2014) 10.1038/srep05720

[253]D. Chruściński and S. Maniscalco, "Degree of Non-Markovianity of Quantum Evolution", Physical Review Letters **112**, 120404 (2014) 10.1103/PhysRevLett.112.120404

[254]F. Settimo, H. P. Breuer, and B. Vacchini, "Entropic and trace-distance-based measures of non-Markovianity", Physical Review A **106**, 042212 (2022) 10.1103/PHYSREVA.106.042212

[255] Á. Rivas, S. F. Huelga, and M. B. Plenio, "Entanglement and non-Markovianity of quantum evolutions", Physical Review Letters **105**, 050403 (2010) 10.1103/PHYSREVLETT.105.050403

[256] S. Luo, S. Fu, and H. Song, "Quantifying non-Markovianity via correlations", Physical Review A **86**, 044101 (2012) 10.1103/PhysRevA.86.044101

[257] M. M. Taddei, B. M. Escher, L. Davidovich, and R. L. De Matos Filho, "Quantum Speed Limit for Physical Processes", Physical Review Letters **110**, 050402 (2013) 10.1103/PhysRevLett.110.050402

[258] A. Del Campo, I. L. Egusquiza, M. B. Plenio, and S. F. Huelga, "Quantum speed limits in open system dynamics", Physical Review Letters **110**, 050403 (2013) 10.1103/PhysRevLett.110.050403/

[259] H. P. Breuer, E. M. Laine, J. Piilo, and B. Vacchini, "Colloquium: Non-Markovian dynamics in open quantum systems", Reviews of Modern Physics **88**, 021002 (2016) 10.1103/RevModPhys.88.021002

Chapter VI

Quantum Simulation of Open-System Dynamics

In this Chapter, we aim to show how the stochastic Hamiltonian formulation, as investigated in the Stratonovich formalism in section III.3, enables the quantum simulation of open quantum dynamics in digital quantum computers (QC) through a simple but effective implementation. As a way to overcome the limitation that quantum gates are unitary operations, one can exploit averages over stochastic ensembles to implement intrinsically non-unitary dynamics of the mean density matrix, showing how the use of stochastic trajectories-based approaches to open quantum systems is gaining more and more interest for quantum simulation with digital quantum computers [99, 207, 211, 260].

In particular, we show, through an exemplifying simple quantum algorithm, how to implement both Lindblad and non-Markovian dynamics, discussing how constraints such as the hermiticity of the operators associated with the stochastic potential enable us to implement each trajectory as a unitary evolution of the system and thus be mapped into a quantum circuit. Moreover, we show how, with digital quantum computers, the parallelization of the ensemble of N trajectories is accounted for by the intrinsic need for many runs of quantum circuits [214, 238], which would be *de facto* also required by other approaches based, e.g., on the dilation of the Hilbert space [207–210]. In this regard, we show a formal convergence and error analysis in terms of the computational cost evaluated in terms of trajectory evolutions. Finally, we conclude by revising an algorithmic procedure proposed to parallelize quantum trajectories, and comment on the efficiency of this scheme and its operational limits.

VI.1 Propagation of quantum dynamics in quantum computers

The first step in the quantum simulation of a system's dynamics is the encoding of the system's Hilbert space into a quantum register, defined as the collective state of the qubits constituting the computational unit, see eq. (I.44). We refer the reader to Ref. [261] for different approaches to Hamiltonian mappings. However, the investigation of the quantum algorithm arising from the stochastic Hamiltonian is, *per se*, independent of the mapping. For the sake of completeness, we discuss the mapping of the minimal two-level model considered in the previous Chapters. Considering a two-level system, the mapping is straightforward and requires a single qubit. Indeed, the computational basis $\{|0\rangle, |1\rangle\}$ identify the two levels, and the Hamiltonian $H_{\varepsilon,\Omega}$, eq. (IV.36), encodes the closed dynamics of the system. However, even for simple extensions such as a two-site donor–acceptor model, multiple encodings are possible. In this case, we consider two sites, and each site is modeled as a two-level system, interacting by sharing and transferring excitation. Then, the same problem can be thought of as a two-site exciton single excitation manifold, in physical mapping on the site basis $\{|e_1\rangle = |01\rangle, |e_2\rangle = |10\rangle\}$, its Hamiltonian

$$H^{\text{ex}} = \sum_{i\in\{e_1,e_2\}} \varepsilon_i |i\rangle\langle i| + \sum_{i,j\in\{e_1,e_2\}, j\neq i} \Omega_{ij} |i\rangle\langle j|, \tag{VI.1}$$

that we want to express in terms of Pauli operators, and then in one-qubit gates. Furthermore, in the complete Hilbert space $\{|g\rangle = |00\rangle, |e_1\rangle = |01\rangle, |e_2\rangle = |10\rangle, |2e\rangle = |11\rangle\}$ and redefinig so the Hamiltonian in eq. (VI.1), we can access directly also the vacuum state and the double-excitation manifold. One can appreciate that these different mappings are physically equivalent for a two-level 1-excitation manifold, but lead to different circuits, with different depths and measurement efficiencies. These different mappings serve only to exemplify how we can think about simulating quantum systems, and the simplest mapping will serve hereafter as the example for the quantum algorithm.

As a last note to the mapping of the open quantum system, we remark that this is the only mapping step required in the scheme that will be presented. Other approaches, more commonly implemented [207–211], require a dilation of the Hilbert space,[1] to accommodate and map environment-modeling auxiliary qubits. In the dilated space, the contractive dynamics are embedded in unitary Hamiltonian dynamics that can be evolved in a QC, and the open dynamics recovered through the partial trace of the additional qubits. Using a stochastic Hamiltonian, we deal, by construction, with trajectories that undergo unitary propagations, ensuring that the mapping can remain the same both for a closed evolution and for an open evolution.

VI.1.1 Writing the Hamiltonian in terms of gates

Once the mapping is established, the time evolution generated by a deterministic Hamiltonian must be approximated through a sequence of elementary gates using standard

[1] Thanks to Stinespring [220] and Sz.-Nagy [221] theorems.

decomposition techniques.

The first step is to discretize the evolution in time, as anticipated in section III.3.1, a necessary step for any numerical implementation, not only for the construction of quantum algorithms. For a generic time-dependent Hamiltonian H_t, the unitary propagator describing the dynamics can be written as

$$U_t = \mathcal{T}_+ e^{-i\int_{t_0}^{t} H_s \,\mathrm{d}s}, \tag{VI.2}$$

where $\mathcal{T}_+$ represents the Dyson time-ordering operator

$$U_t = \sum_n^{\infty} U_t^{(n)}, \qquad U_t^{(n)} = (-i)^n \int_{t_0}^{t} \mathrm{d}t_1 \int_{t_0}^{t_1} dt_2 \cdots \int_{t_0}^{t_{n-1}} \mathrm{d}t_n \prod_{i=1}^{n} H(t_i). \tag{VI.3}$$

which has the problem of requiring explicit monitoring of the time-ordered expansion of nested integrals. A common alternative approach to obtain a numerically solvable form is to use instead a Magnus expansion [194, 195]. Magnus expansion provides that, for a differential equation

$$\frac{\mathrm{d}}{\mathrm{d}t} Y_t = A_t Y_t \tag{VI.4}$$

we can find a matrix function $\Omega_{t_0,t}$ such that

$$\mathcal{T}_+ e^{\int_{t_0}^{t} A_s \,\mathrm{d}s} Y_{t_0} = \exp\{\Omega(t,t_0)\} Y_{t_0} \tag{VI.5}$$

where Ω_{t,t_0} is the solution of its own differential equation [194, 195], from which one can construct the generator as the infinite series $\Omega_{t,t_0} = \sum_k^{\infty} \Omega_k(t,t_0)$, and generate the first terms of the expansion. The first two terms of the expansion are

$$\Omega_1(A)(t,t_0) = \int_{t_0}^{t} A_s \,\mathrm{d}s, \qquad \Omega_2(A)(t,t_0) = \frac{1}{2}\int_{t_0}^{t}\int_{t_0}^{s} [A_s, A_r] \,\mathrm{d}r \,\mathrm{d}s \tag{VI.6}$$

For a sufficiently small time step, considering that

$$\lim_{\tau\to 0} [A_t, A_{t+\tau}] = 0, \tag{VI.7}$$

we can truncate the expansion at the first order, highlighting the importance of choosing a small time step for convergence to the exact time-ordering solution. This way, we are effectively ignoring the time ordering requirements. Higher-order Magnus expansions can also be employed to achieve better convergence, but one can note that, to include the second term and compute it numerically, the time step τ would have to be further discretized into a finer grid, eventually forcing the use of a smaller time step $\tau' \ll \tau$. Indeed, it is usual to stop at a first-order truncation, with few works on the use of the second-order term in the case of highly oscillating systems [262–264]. Then, we consider a finite time interval $[0,T]$, discretize it into S small time steps $\tau = T/S$, and write the overall propagator as

$$U_t = \prod_{s=1}^{S} U_{s\tau,(s-1)\tau}, \tag{VI.8}$$

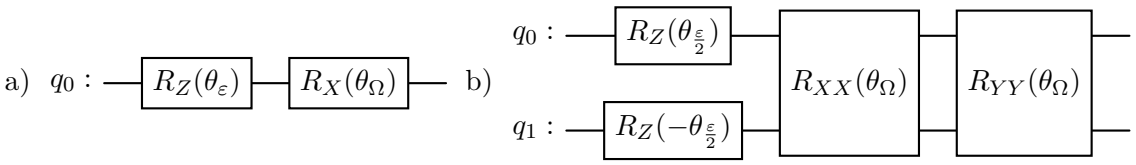

Figure VI.1: Two simple mappings of a Magnus-Suzuki-Trotter circuit block for step evolution for a system with Hamiltonian $H_{\varepsilon,\Omega}$. (a) A mapping that is both physical and logical for a qubit, or a logical mapping for a two-site exciton 1-excitation manifold. (b) Physical mapping circuit block for a two-site exciton 1-excitation manifold system.

where the propagator at each time step is

$$U_{s\tau,(s-1)\tau} = \exp\left\{-i\int_{(s-1)\tau}^{s\tau} H_r \,\mathrm{d}r\right\}. \tag{VI.9}$$

For numerical implementation in classical computers, this approximation scheme is sufficient. Translating it into the language of quantum gates, the unitary operations representing the building blocks of quantum circuits, is ensured by the unitary character of the Magnus expansion, yet requires another expansion and truncation. The generic Hamiltonian $H_{\varepsilon,\Omega}$ proposed for the two-level system is composed of two Pauli terms, which are implemented by two different gates, the rotation introduced in eq. (I.43). The energies of the levels, defined in terms of the Pauli operator σ_z, enter the system dynamics as a phase change due to the unitary rotation $U = e^{-\frac{i}{2}\varepsilon t}$, which is implemented by the gate $RZ(\theta) = e^{-\frac{i}{2}\theta\sigma_z t}$, a single-qubit rotation about the Z axis of the Bloch sphere representing the qubit. The same goes for the coupling, implemented by the $RX(\vartheta) = e^{-\frac{i}{2}\vartheta\sigma_x t}$, a single-qubit rotation about the X axis. The propagator in eq. (VI.9) must then be split in terms of gates. In general terms, the classical exponential rule $e^{A+B} = e^A e^B$ is not valid for non-commuting operators and it is instead replaced by the Baker–Campbell–Hausdorff formula [265], $e^A e^B = e^Z$ where $Z = A + B + 1/2[A,B] + 1/12([A,[A,B]] + [B,[B,A]]) + \ldots$, with increasingly nested commutator terms.

Here, for illustrative purposes, we show the famous first-order Suzuki-Trotter decomposition [241, 242], allowing us to separate the Hamiltonian components into a series of gates,

$$U_\tau = \exp\{-i\varepsilon\tau\sigma_z - i\Omega\tau\sigma_x\} \approx \left[\exp\left\{-i\frac{\varepsilon\tau}{n}\sigma_z\right\}\exp\left\{-i\frac{\Omega\tau}{n}\sigma_x\right\}\right]^n \tag{VI.10}$$

where, in general, the larger n the better the convergence. However, due to the choice of a small time step dictated by the Magnus expansion, eq. (VI.7), good results can be obtained even with a small n (e.g., $n = 1$, a single time step block-propagation in Figure VI.1).

VI.1.2 Quantum classical-noise algorithm

The construction presented serves as the backbone of the algorithm construction, by generalization to include stochastic contributions to the Hamiltonian. Here, these are treated as time-dependent classical parameters. The noise is computed *a priori* in a classical com-

puter, and the fluctuation is applied as a random rotation of the gate implementing the Hamiltonian, the random fluctuation value to either of the gates, or using a different one depending on the action of the noise operator R. The step propagator obtained by the extension of eq. (VI.10), for a white noise increment $\gamma\Delta W_\tau$ applied through the operator $R = \sigma_x$, would then be

$$U_\tau^{\mathrm{QCNA}} = \exp\{-i\varepsilon\tau\sigma_z\}\exp\{-i(\Omega\tau + \gamma\Delta W_\tau)\sigma_x\}\,. \tag{VI.11}$$

where we set $n = 1$ in the Suzuki-Trotter decomposition.

This allows us to implement each trajectory in terms of unitary evolutions, and these can be simulated in a quantum register. The non-unitary evolution typical of an open system is recovered by averaging over all different realizations of the circuit. This results in the quantum classical-noise algorithm (QCNA), an effective procedure to investigate open system dynamics through quantum simulation, presented in the following algorithm scheme, alg. 1, and graphically depicted in Figure VI.2. The choice of the following parameters is required: the total number of trajectories N, the time step τ and the total number of steps S, the time step of measurement of the circuits in terms of $m\tau$ (measure every m finite step evolution), and the total number of shot samples K performed by the quantum computer. In the following section VI.2.1, we investigate further the specific choice of the last parameter. Then, the algorithm follows this scheme, where we utilize labels [C] and [Q] to indicate whether a step is performed in a classical or quantum architecture:

Algorithm 1: QCNA

```
for n=1 to N do
    [C] Draw the initial state |ψ_0⟩ from the initial distribution
    [Q] Initialize the quantum register to the initial state (circuit A)
    for s=1 to S do
        [C] Compute the random fluctuation(s) Z(sτ)
        [Q] Apply the unitary gate U_{sτ,(s−1)τ}
        if s mod_m = 0 then
            [Q] Create a copy of the circuit A to an auxiliary circuit B
            [Q] Append measurements to circuit B and perform K measurement
              shots
            [C] Discard circuit B
        end
    end
end
```

where we recall that step 2 is optional, depending on whether we want the initial state to be in a pure deterministic state $|\Psi_0\rangle$ or a mixed state $\rho_0 = \mathbb{E}(|\psi_0^{\mathrm{trj}}\rangle\langle\psi_0^{\mathrm{trj}}|)$.

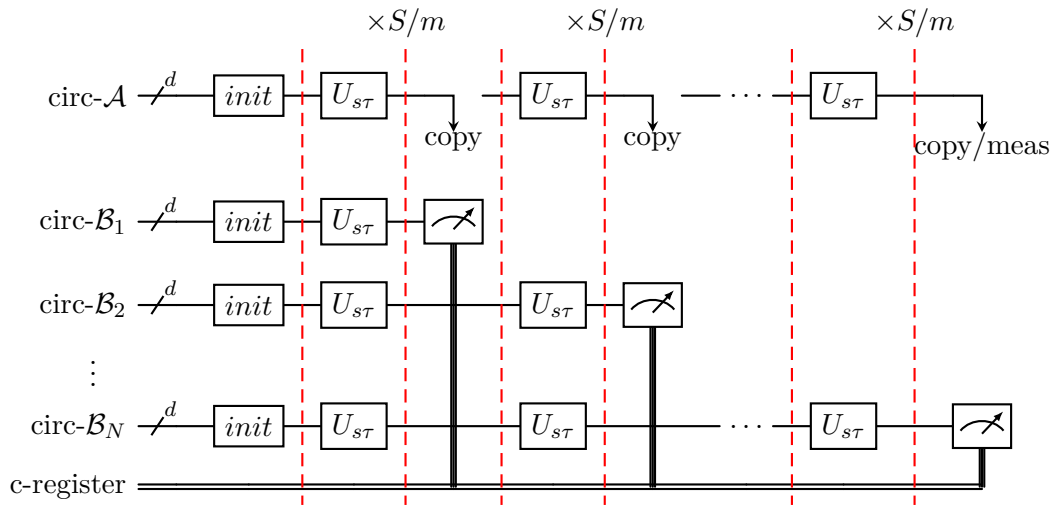

Figure VI.2: Graphical depiction of QCNA (alg. 1). The last circuit $\mathcal{B}_N$ can be avoided by performing the measure on the lead circuit $\mathcal{A}$.

It is important to note that executing copies of the lead circuit $\mathcal{A}$ and measuring on these clones is of utmost importance, as measurements collapse the quantum register, destroying coherence and changing its state. Avoiding measurements on the lead circuit guarantees the correct evolution of each trajectory. Then, step 7 is important for efficiency reasons: since we need to generate, run, and discard a new circuit for every measurement we want to perform, we sample every n steps of evolution performed. Carefully choosing the parameter m, we can avoid measuring every step, and, based on the knowledge of the deterministic system Hamiltonian, we can also measure uneven steps, allowing a finer measurement grid at the inversion points of the oscillations and a coarser grid otherwise.

This algorithm then suffers from a "classical" overhead, due to the necessity to construct different circuits for each trajectory, computing the classical noise increments, and requiring the creation of further copies of the circuits for each timestep. As a result, a total of (NSK/m) circuits are required to execute the algorithm. On the other hand, this approach avoids the introduction of auxiliary qubits to reproduce non-unitary reduced state dynamics, as commented above. Methods based on enlarged Hilbert spaces do not explicitly require the simulation of multiple trajectories; however, these are *de facto* required implicitly in all quantum-computing procedures. In section VI.2.1, we demonstrate that within the QCNA the effect of K measurements is negligible, and the convergence scaling is dominated by N. This is not true for mean state dynamics, as the value at each time must be reconstructed from an explicit ensemble of K measurements.

VI.1.3 Implementation of a subclass of the Redfield equation

Another advantage of the classical noise algorithm is that it can be adapted to any model of classical stochastic modulation of the Hamiltonian, not only white noise, but correlated processes and noise as well, allowing the investigation of different environment models. This is not the general case for mean dynamics approaches, since the equation for the

density matrix is not known *a priori*, as we have shown in Chapter IV.

In example VI.1, the results obtained with the QCNA for a X_{OU}-driven stochastic Hamiltonian dynamics are analysed. It is interesting to note that, from the results in section IV.6, in particular the closure model in section IV.6.1 and the positivity recovery in section IV.6.5, we can consider the correlated SSEs to be effective unravelings of the closure Redfield equations. This has been shown analytically for the Υ_{OU}-driven SSE, and can be derived in the same fashion for the X_{OU} process in the stochastic Hamiltonian.

Then, the QCNA approach allows us to perform quantum simulation of these particular forms of Redfield equations, implementing non-Markovian correlated open quantum dynamics.

Example VI.1 | QCNA spin-$\frac{1}{2}$ molecular tumbling

In Example III.3, a stochastic Hamiltonian dynamics driven by an OU process is proposed as a model to describe the molecular tumbling of a spin-$\frac{1}{2}$. We can map the same problem to a QCNA, where each step propagator is

$$U_\tau^{\mathrm{QCNA}} = \exp\left\{-i\frac{(\omega_0 + 2X_t)\tau}{2}\sigma_z\right\}\exp\left\{-i(\Omega\tau + X_t\tau)\sigma_x\right\}\exp\left\{-iX_t\tau\sigma_y\right\}.$$

A total of $N = 8000$ trajectories are simulated, and measured every 500 time steps. In Figure VI.3 the comparison of the QCNA and the classically computed dynamics is presented.

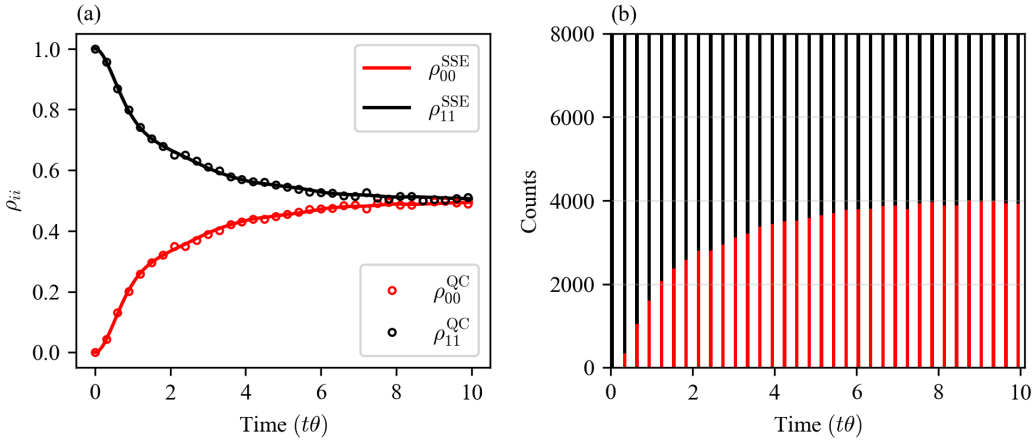

Figure VI.3: Relaxation of the population of a $\frac{1}{2}$-spin populations along the z-axis. In panel (a), the average for the two populations, obtained from the averaged RODE stochastic Hamiltonian approach, is shown in solid red and black lines, while the results of the quantum algorithm realization are depicted in empty dots, in matching color. In panel (b), for 8000 trajectories, the counts of the measures resulting in '0', black, or '1', red, as bars summing to the total of measurements.

VI.2 Trajectory measurements and error bounds

One problem arising in the discussion of the QCNA is the collapsing effect of the measurement on the trajectory evolution, and the requirement of multiple shots to retrieve the information stored in the quantum register. While classical bits can be examined to determine their state and retrieve information, leaving them intact, in there is no such possibility for quantum bits. We can only acquire information on the state by measuring it. This has the effect of collapsing the state (i.e., projecting it on a smaller subspace) and allows only for possibly partial retrieval of information, which is converted to a classical bit, one bit of information. Measuring on the computational basis implies that we can only measure *directly* observables that are diagonal in this basis, for example σ_z and the identity $\mathbb{1}$, and their compositions. So, when the qubit is measured, it returns a classical bit '0' or '1' as the measurement result, with probability $|\alpha|^2$ and $|\beta|^2$, where the qubit wavefunction is defined $|\psi\rangle = \alpha|0\rangle + \beta|1\rangle$ as in eq. (I.36), in the σ_z basis.

$$\begin{cases} |\psi\rangle \overset{k}{\mapsto} \frac{\Pi_0}{\sqrt{p_0}}|\psi\rangle \equiv |0\rangle & \text{with probability } p_0 = \langle\psi|\Pi_0^\dagger\Pi_0|\psi_k\rangle = |\alpha|^2, \quad \text{return classical bit '0'} \\ |\psi\rangle \overset{k}{\mapsto} \frac{\Pi_1}{\sqrt{p_1}}|\psi\rangle \equiv |1\rangle & \text{with probability } p_0 = \langle\psi|\Pi_1^\dagger\Pi_1|\psi_k\rangle = |\beta|^2, \quad \text{return classical bit '1'.} \end{cases} \tag{VI.12}$$

Therefore, we can formalize the act of measurement with respect to its result as a Bernoulli trial b_k with success probability $|\beta|^2$, defined in the process

$$(b)_{k=1}^{K} \sim |\beta|^2 \; : \quad \mathbb{P}(b_k = 1) = |\beta|^2. \tag{VI.13}$$

Since the measurement of a qubit returns only either '0' or '1', multiple measurements, also referred to as "shots", are required. Take the $|+\rangle = 2^{-1/2}(|0\rangle + |1\rangle)$, a single measurement on this state behaves exactly as a coin toss. From that single measurement, one would not be able to identify the state or any observable associated to it. Indeed, multiple measures are required; the results from 1024 measurements for this state are depicted in Figure VI.4.

In the following, we establish the minimal measurement requirements for the QCNA scheme and analyze the convergence speed and error bounds for different scenarios.

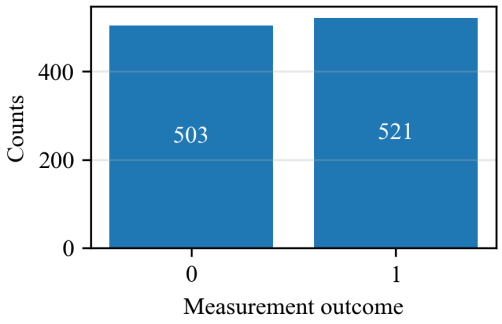

Figure VI.4: Histogram of the results of an ensemble of 1024 measurements on a $|+\rangle = 2^{-1/2}(|0\rangle + |1\rangle)$ state of a single qubit.

VI.2.1 Equivalence of measurement schemes

For dynamics obtained as the stochastic average over an ensemble of trajectories, we define the exact expectation value of an observable $P(t)$, in our case the population of the level $|1\rangle$, as the limit

$$P(t) = \lim_{\Delta t \to 0} \mathbb{E}\left[p_\omega(t = s\Delta t)\right] = \lim_{\Delta t \to 0} \lim_{N \to \infty} \frac{1}{N} \sum_{\omega=1}^{N} p_\omega(s\Delta t), \tag{VI.14}$$

where $p_\omega(t = s\Delta t)$ is the population value for the trajectory ω, which is the probability of measuring the qubit in the state $|1\rangle$, at time $s\Delta t$. We can drop the limit on the time discretization, as the results are independent of it.

In the QC implementation, the observed value of P is an average itself, the average of the outcomes of the measurement (shots) on qubits. Then, the exact expectation is obtained by the limits

$$P = \lim_{N \to \infty} \frac{1}{N} \sum_{\omega}^{N} \left(\lim_{K \to \infty} \frac{1}{K} \sum_{k}^{K} b_k\left(p_\omega\right) \right) \tag{VI.15}$$

where K is the number of measurements and $b_k(p_\omega)$ are the measurement outcomes in the form of Bernoulli trials as defined in eq. (VI.13), with probability p_ω.

Proposition 2. *In the limit of infinite trajectories, sampling a trajectory K times, eq.* (VI.15)*, is equivalent to performing a single measure per trajectory,*

$$P = \lim_{N \to \infty} \frac{1}{N} \sum_{\omega}^{N} b_\omega\left(p_\omega\right) \tag{VI.16}$$

Proof. Take the limit

$$\lim_{N \to \infty} \frac{1}{N} \sum_{\omega=1}^{N} \left(\lim_{K \to \infty} \frac{1}{K} \sum_{k}^{K} b_k\left(p_\omega\right) \right) = \lim_{N \to \infty} \frac{1}{N} \sum_{\omega=1}^{N} p_\omega = P \tag{VI.17}$$

where the measurement process $(b_k(p_\omega))_{k=1}^{K}$ is a Bernoulli process with probability

$$\begin{cases} \mathbb{P}(b_k = 1) = p_\omega \\ \mathbb{P}(b_k = 0) = 1 - p_\omega \end{cases} \quad \forall k \tag{VI.18}$$

By dominated convergence theorem, we can invert the limits order

$$\lim_{N \to \infty} \frac{1}{N} \sum_{\omega=1}^{N} \left(\lim_{K \to \infty} \frac{1}{K} \sum_{k}^{K} b_k(p_\omega) \right) = \lim_{K \to \infty} \frac{1}{K} \sum_{k}^{K} \left(\lim_{N \to \infty} \frac{1}{N} \sum_{\omega=1}^{N} b_k(p_\omega) \right) = P \tag{VI.19}$$

so, now, the first limit to compute is for an infinite number of Bernoulli trials independently not-identically distributed $(b_{\omega,k})_{\omega=1}^{N}$, also referred to as *Poisson trials* [266], converging to

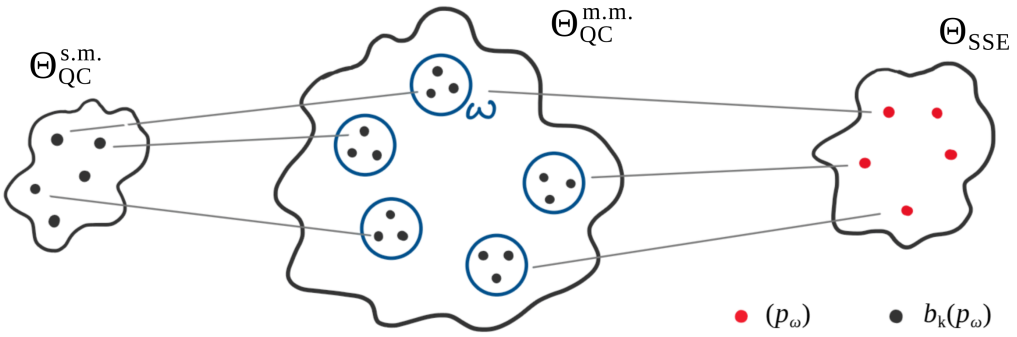

Figure VI.5: The probability spaces of the three setups for a fixed time. On the right, the space of the classical SSE implementation, each point the true probability value p_ω, their average converging to the open system probability P, i.e. $(\Theta_{\text{SSE}}, \mathbb{P}_\Theta = P)$. In the QC setting with multiple measurements per trajectory, this is obtained as the average of K measures of the Bernoulli trials $b_k(p_\omega)$, which for each trajectory form a subspace ω of i.i.d. random variable with law p_ω, then the space is $(\Theta_{\text{QC}}^{\text{m.m.}} = \bigcup(\omega, p_\omega), \mathbb{P}_{\Omega_{\text{QC}}^{\text{m.m.}}})$. Alternatively, drawing one measure for each subspace, we can construct the space for the single-shot setting, a single measure described by a Bernoulli trial $b(p_\omega)$ for each trajectory, setting the space $(\Theta_{\text{QC}}^{\text{s.m.}}, \mathbb{P}_{\Theta_{\text{QC}}^{\text{s.m.}}})$ converging in law to the same probability $\mathbb{P}_{\Theta_{\text{QC}}^{\text{s.m.}}} \to P$.

the sum of probabilities p_m, $\sum_m p_m$, and their average to the desired quantity P,

$$\lim_{N\to\infty} \frac{1}{N} \sum_{\omega=1}^{N} b_k(p_\omega) = \lim_{N\to\infty} \frac{1}{N} \sum_{\omega=1}^{N} p_\omega = P \tag{VI.20}$$

□

A graphical schematic of the probability spaces for the three situations, the classical average and the QCNA implementation for multiple and single measurements, is depicted in Figure VI.5.

VI.2.2 Single-shot convergence and error bounds

Now that we have proved that, in the infinite trajectories limit, the result obtained using a single measurement per trajectory converges to the correct expectation value, we investigate the convergence rate and error bounds associated with this procedure. We start by defining the stochastic process

$$S_n = \sum_{\omega=1}^{n} b_\omega(p_\omega) \tag{VI.21}$$

the sum of the measurements up to the n-th trajectory, and

$$P_N = \frac{1}{N} S_N = \frac{1}{N} \sum_{\omega=1}^{N} b_\omega(p_\omega) \tag{VI.22}$$

the estimator process for P, given by the average results, such that $P_N \to P$ for $N \to \infty$, and bounding the process for any N.

We want to compute the speed of convergence in probability, rate of convergence in

distribution, and in expectation, i.e., the error. Since each element of the sum is the classical outcome of the measurement of a qubit, $b_\omega(p_\omega) \in \{0, 1\}$, the average returns a probability bounded in $[0, 1]$ and we can use Hoeffding's inequality [267] to bound from above the probability of deviation from the true average,

$$\mathbb{P}\left(|P_N - P| > \epsilon\right) \leq 2\exp\left\{-\frac{2\epsilon^2 N^2}{\sum_i^N (b_i - a_i)}\right\} = 2e^{-2\epsilon^2 N} \tag{VI.23}$$

where $a_i = 0$ and $b_i = 1$ are the bounds of the random variable. This shows the convergence in probability is exponentially fast w.r.t. the total number of trajectories N.

As N increases, in the limit of large N, this process approaches that of the binomial distribution, and we can use the generalized Lindeberg–Feller central limit theorem [268], and obtain the rate of convergence in distribution of the process, $\mathcal{O}(\frac{1}{\sqrt{N}})$, and the convergence in expectation is given by the variance of the process, i.e. its standard deviation, converging in $\mathcal{O}(\frac{1}{N})$.

VI.2.3 Multiple-shots convergence and error bounds

We now want to understand how multiple measurements improve the convergence, how the bounds change, and whether the choice of performing a single shot is convenient.

As one can appreciate in Figure VI.5, there is a hierarchical structure of the full process returning P, due to the two-stage averages, the first one at the ω subspaces level, i.e., the average on the value of a single trajectory realization. We are then required to deal with both effects. The two processes are

$$B_{\omega,K} = \frac{1}{K}\sum_k^K b_k\left(p_\omega\right) \tag{VI.24}$$

the inner average on each subspace, and

$$\tilde{P}_M = \frac{1}{M}\sum_\omega^M B_{\omega,K} \tag{VI.25}$$

the outer average on the finite $K < \infty$ measurements average, recovering the estimator for the limit form in eq. (VI.15).

The convergence in probability can be computed for both processes, inner and outer, using Hoeffding's inequality as above,

$$\mathbb{P}\left(|B_{\omega,K} - p_\omega| > \epsilon\right) \leq 2e^{-2\epsilon^2 K}, \tag{VI.26}$$

and

$$\mathbb{P}\left(|\tilde{P}_M - P| > \epsilon\right) \leq 2e^{-2\epsilon^2 M}. \tag{VI.27}$$

It is clear that the internal processes converge to their own average p_ω, and that the convergence on the expectation value is dominated by the exponential decay of the outer average.

Let us set the effective number of trajectories to be performed as Q, so that for the single measurement process $N = Q$ and for the multiple measurements methods $MK = Q$. This fixes the computational cost, and we choose Q as the number of trajectories s.t. the classical convergence is ensured, eq. (VI.14). Then, substituting $M = N/K$, we show that we expect to converge faster to the true average P for the single measurement implementation,

$$\mathbb{P}\left(|P_N - P| > \epsilon\right) \leq 2e^{-2\epsilon^2 N} \leq \mathbb{P}\left(|\tilde{P}_M - P| > \epsilon\right) \leq 2e^{-2\epsilon^2 \frac{N}{K}}. \tag{VI.28}$$

as for the same fixed computational cost Q, the two-step process shows a weaker tail decay since $K > 1$ reduces the maximum number of outer averages $M = Q/K$.

This result can be appreciated by the error bounds as well, starting from a limiting (and absurd) example. As above, set Q fixed and $Q = N = MK$. If $K = 1$, we fall into the case of single measurements, converging to P by Proposition 2. On the opposite case, if $M = 1$, we are choosing a single subspace of measurements, on a single "parent" trajectory ω, and for the same computational cost $Q = K$ and with the same bounds, we converge to $p_\omega \neq P$.

Therefore, in addition to the rate of convergence in probability, it is important to consider convergence in expectation, explicitly accounting for the additional error arising from the shift of the central probability mass associated with the bias of the limiting distribution. We can write

$$\mathbb{E}(\tilde{P}_M - P) = \frac{1}{M}\mathbb{E}\left[(B_{\omega,K} - p_\omega)^2\right] + \mathbb{E}\left[(p_\omega - P)^2\right]. \tag{VI.29}$$

Then, we have the scaling to the average of MK Bernoulli trials, grouped in M groups of K trials with the same laws, scaling as discussed above $\mathcal{O}(\frac{1}{MK})$, and the shift error scaling as $\mathcal{O}(\mathrm{Var}(p_\omega)/M)$.

Therefore, one must first set Q_{class} according to the convergence threshold for the classical implementation. A single-shot simulation scheme then requires at least $N \geq Q_{\text{class}}$ to ensure convergence, while in the multiple-measurements setup, one similarly needs $M \gtrapprox Q_{\text{class}}$. Hence, for $N = M$, the average on the ω subspaces in the two-step average process translates as the presence of a *noise averaging layer*, consistent with the intended role of such averaging in QC experiments, at the expense of an increased computational cost by the factor K. This approach can be advantageous when the p_ω are clustered, i.e., when the noise is a very small perturbation, and the trajectories do not differ much from one another. In this regime, the process yields lower errors in variance, reducing the effective error at the cost of a weaker tail bounds decay and increased computational effort.

An exemplifying numerical comparison of these different approaches and their convergence to the reference classically computed dynamics is presented in Figure VI.6.

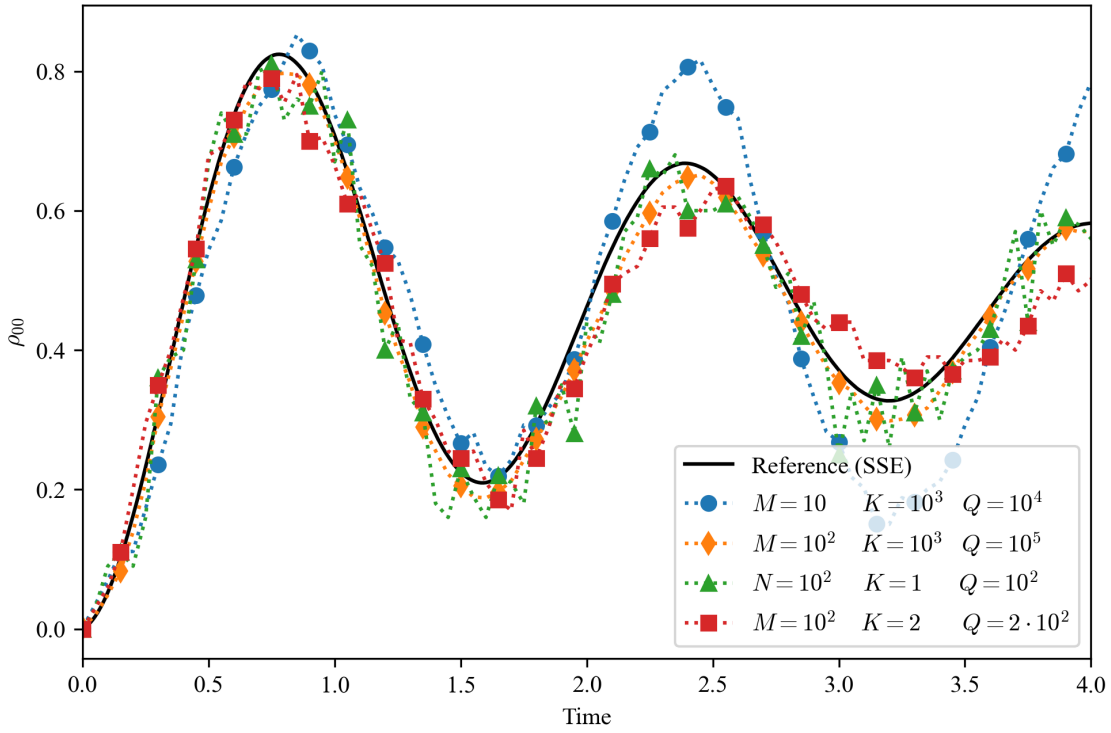

Figure VI.6: Comparison of the classical and quantum computed evolution of the dynamics of the system described by the Hamiltonian $H_{\varepsilon,\Omega}$ and driven by a white noise of intensity $\gamma = 0.43\sqrt{\hbar\theta}$. The reference SSE computed dynamics is depicted in a solid black line, and the different QCNA estimates obtained with different values of (N, M, K) and total computational cost Q are depicted in dotted lines with markers.

VI.3 Quantum forking for parallel quantum evolutions

One can note that, in the analysis above, we assumed the computational cost of trajectory implementations and of shot measurements to be the same. This is due to the no-cloning theorem (Park, Ghirardi, Wootters, Zurek, Dieks [269–272]), which ensures that, without *a priori* complete knowledge of the state to measure, we cannot duplicate (clone) it. As a consequence, each shot measurement requires us to replicate the whole trajectory, executing K identical circuits.

A possible workaround to this issue has been proposed by D.K. Park and F. Petruccione [273], from the question of whether a complex quantum state can instead be "copied", devising a strategy to circumvent the limitations imposed by the no-cloning theorem. The strategy proposed is the quantum forking (QF) procedure. In the original works of Park and Petruccione, the QF procedure is proposed for the construction of qRAM [274], and then for the parallelization of classical stochastic processes [273, 275]. Then, its use to simulate OQS dynamics has been proposed, with a different application of the QF procedure from the original work. An algorithm for single-qubit Markovian dynamics was proposed a few years later in Ref. [276], and an approach based on the QDRIFT algorithm [277], still limited to Markovian dynamics, was proposed in [278]. From this last work, the connection of the QF procedure to an efficient implementation of the QDRIFT algorithm for unitary Hamiltonian simulation in [279], in combination with the linear combinations

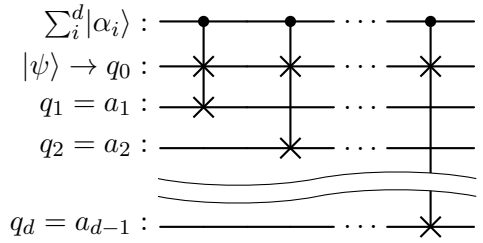

Figure VI.7: Quantum forking circuit. The target state $|\psi\rangle$, here represented in a single qubit for simplicity, is forked to a total of d independent processes (the initial state plus $d-1$ auxiliary). Each control on the qudit $\sum_i^d |\alpha_i\rangle$ acts on the α_i-th state for each internal basis state of the parent state $|\psi\rangle$.

of unitaries (LCU) method [280]. We further mention that an approach to non-Markovian classical stochastic processes has been proposed in [281], and then improved in [282, 283], on a similar basis as the QF, the *q-sample state*, yet it does not implement QF nor analyse *quantum* stochastic processes.

In this last section, we refer to the original proposal, that we revise here, describing the circuit for constructing forked states, showing how it could be used as a protocol to implement and parallelize open quantum dynamics, independently of their Markovian or non-Markovian character, referring to the QCNA proposed above. We comment on the efficiency of such implementations,

The fundamental idea of QF is to prepare a target state $|\psi\rangle$, an hypothetically complex-to-prepare initial state, and create an entangled state $|\Psi_{\mathrm{QR}}\rangle$ in a quantum computer register (QR), allowing for the state $|\psi\rangle$ to undergo d independent unitary evolutions. The procedure in the following requires the addition of auxiliary qubits and either one control qudit or multiple control qubits. Qudits are the multidimensional equivalent of qubits, so that their Hilbert space is $\mathbb{C}^d$ instead of $\mathbb{C}^2$, hence their computational basis is $\{|0\rangle, |1\rangle, \ldots, |d\rangle\}$ [261, 284–287]. For the sake of brevity, we will use the qudit scheme in the following, recalling that we have to consider the different scaling in two-qubit gates when translating to the use of solely qubits.

The QC state is prepared as a mapping of the initial target state with the QF circuit, depicted in Figure VI.7. For d total copies of the initial target state, we need to enlarge the total Hilbert space by adding at least $d-1$ auxiliary qubits, which store the copies of the state, and a d-dimensional qudit, its states defined in the following by the weighted $|\alpha_i\rangle$, which must all be equal if we want equally weighted copies, for example to obtain a fair average, or can be prepared according to the specific needs, the easiest way by preparing a mixed state. The target state is then copied using d controlled-swap (CSWAP or Fredkin [288]) gates, each controlled by the qudit i-th state [289]. Let us define the quantum register $|\Psi_{\mathrm{QR}}^{(0)}\rangle$ as

$$|\Psi_{\mathrm{QR}}^{(0)}\rangle = \left(\sum_{i=1}^{d} |\alpha_i\rangle\right) \bigotimes_{j=0}^{d-1} |\phi_j\rangle, \tag{VI.30}$$

and, state before forking, the state $|\psi\rangle$ is encoded in the qubit in position 0, therefore

$$|\Psi_{\text{QR}}^{(in)}\rangle = \left(\sum_{i=1}^{d}|\alpha_i\rangle\right) \otimes |\psi\rangle \bigotimes_{j=1}^{d-1}|\phi_j\rangle. \tag{VI.31}$$

Then, the construction of the forked state $|\Psi_{\text{QR}}^{(\text{QF})}\rangle$ on the quantum is

$$\begin{aligned}
|\Psi_{\text{QR}}^{(in)}\rangle \mapsto |\Psi_{\text{QR}}^{(\text{QF})}\rangle = \sum_{i=1}^{d}|\alpha_i\rangle|\phi_{i-1}\rangle \left(\bigotimes_{j=1}^{i-2}|\phi_j\rangle\right) |\psi\rangle \left(\bigotimes_{k=i}^{d-1}|\phi_k\rangle\right) \\
= |\alpha_1\rangle|\psi\rangle \otimes |\phi_1\rangle|\phi_2\rangle \cdots |\phi_{d-1}\rangle + \\
+ |\alpha_2\rangle|\phi_1\rangle \otimes |\psi\rangle \otimes |\phi_2\rangle \cdots |\phi_{d-1}\rangle + \\
+ |\alpha_3\rangle|\phi_2\rangle \otimes |\phi_1\rangle \otimes |\psi\rangle \otimes |\phi_3\rangle \cdots |\phi_{d-1}\rangle + \\
+ |\alpha_4\rangle|\phi_3\rangle \otimes |\phi_1\rangle|\phi_2\rangle \otimes |\psi\rangle \otimes |\phi_4\rangle \cdots |\phi_{d-1}\rangle + \\
\vdots \\
+ |\alpha_d\rangle|\phi_{d-1}\rangle \otimes |\phi_1\rangle|\phi_2\rangle \cdots |\phi_{d-2}\rangle \otimes |\psi\rangle
\end{aligned} \tag{VI.32}$$

where we can note how the CSWAP gates essentially create d "copies" of $|\psi\rangle$ in all the $d-1$ positions of the auxiliary register, their state arbitrary and therefore identified by the states $|\phi_j\rangle$, without violating the no-cloning theorem.

Applying different unitaries U_i at each addressed qubit, the final state $|\Psi_{\text{QR}}^{(fin)}\rangle$ becomes

$$\begin{aligned}
|\Psi_{\text{QR}}^{(\text{QF})}\rangle \mapsto |\Psi_{\text{QR}}^{(fin)}\rangle = \sum_{i=1}^{d}|\alpha_i\rangle U_1|\phi_{i-1}\rangle \left(\bigotimes_{j=1}^{i-2} U_{j+1}|\phi_j\rangle\right) U_i|\psi\rangle \left(\bigotimes_{k=i}^{d-1} U_{k+1}|\phi_k\rangle\right) \\
= |\alpha_1\rangle U_1|\psi\rangle \otimes U_2|\phi_1\rangle U_3|\phi_2\rangle \cdots U_d|\phi_{d-1}\rangle + \\
+ |\alpha_2\rangle U_1|\phi_1\rangle \otimes U_2|\psi\rangle \otimes U_3|\phi_2\rangle \cdots U_d|\phi_{d-1}\rangle + \\
+ |\alpha_3\rangle U_1|\phi_2\rangle \otimes U_2|\phi_1\rangle \otimes U_3|\psi\rangle \otimes U_4|\phi_3\rangle \cdots U_d|\phi_{d-1}\rangle + \\
\vdots \\
+ |\alpha_d\rangle U_1|\phi_{d-1}\rangle \otimes U_2|\phi_1\rangle U_3|\phi_2\rangle \cdots U_{d-1}|\phi_{d-2}\rangle \otimes U_d|\psi\rangle
\end{aligned} \tag{VI.33}$$

showing that, as each qubit undergoes all possible unitaries, we are evolving the state $|\psi\rangle$, encoded in every auxiliary qubit, under all d different unitaries.

VI.3.1 Expectation values and coherent averaging in quantum forking

In the work of D.K. Park *et al.* [273], a powerful yet concise method to implement general power summations on a QC was introduced, and in general, for expectation value measurements, of the form

$$\langle M\rangle = \sum_{i=1}^{d} p_i \prod_{j=1}^{q}\langle M_{ij}\rangle \tag{VI.34}$$

where p_i are non-negative real numbers s.t. $\sum_{i=1}^{d} p_i = 1$, i.e., probabilities, q is a positive integer that indicates the power of the summation, and $\langle M_{ij} \rangle$ are observables. It is then proposed for composite Lindblad mappings in [273] and used for classical stochastic processes in [275].

Since our interest is in summing the probability of measuring the state in one of the computational basis, we focus on linear summation ($q = 1$). We illustrate the procedure for the minimal example, averaging measurement with equal weights of one target state $|\psi\rangle_t$, encoded in a single qubit, using one auxiliary qubit $|\phi\rangle_a$ and requiring only one additional control qubit $|0\rangle_c$. The implementation of d independent processes on a target state, through a register prepared as in eq. (VI.33), and their linear average according to eq. (VI.34), is shown in Figure VI.8.

First, we initialize the control qubit to a superposition state *via* a Hadamard gate,

$$H|0\rangle_c = \frac{|0\rangle_c + |1\rangle_c}{\sqrt{2}}, \tag{VI.35}$$

so that the CSWAP gate returns the register state

$$|\Psi_{\mathrm{QR}}^{(\mathrm{QF})}\rangle = \frac{|0\rangle_c|\psi\rangle_t|\phi\rangle_a + |1\rangle_c|\phi\rangle_t|\psi\rangle_a}{\sqrt{2}}. \tag{VI.36}$$

where the weights of the two superpositions of the target state are equal. We can now evolve the two copies independently under different unitaries, U_1 and U_2, according to eq. (VI.33).

$$|\Psi_{\mathrm{QR}}^{(\mathrm{QF})}\rangle = \frac{|0\rangle_c U_1|\psi\rangle_t U_2|\phi\rangle_a + |1\rangle_c U_1|\phi\rangle_t U_2|\psi\rangle_a}{\sqrt{2}}. \tag{VI.37}$$

By *reversing the forking*, using a second ladder of CSWAP gates, see Figure VI.8, the circuit yields the final state

$$|\Psi_{\mathrm{QR}}^{(fin)}\rangle = \frac{|0\rangle_c U_1|\psi\rangle_t U_2|\phi\rangle_a + |1\rangle_c U_2|\psi\rangle_t U_1|\phi\rangle_a}{\sqrt{2}}, \tag{VI.38}$$

clearly showing the target state, encoded in the sole target qubit, virtually undergoing both unitary evolutions.

Measuring an observable M, the expectation value on the target qubit is

$$\begin{aligned}
\langle M \rangle &= \langle \Psi_{\mathrm{QR}}^{(fin)} | \mathbb{1}_c \otimes \hat{M} \otimes \mathbb{1}_a | \Psi_{\mathrm{QR}}^{(fin)} \rangle \\
&= \frac{1}{2} \left(\langle 0|0\rangle \langle \psi | U_1^\dagger \hat{M} U_1 | \psi \rangle \langle \phi | U_2^\dagger U_2 | \phi \rangle + \langle 1|1\rangle \langle \psi | U_2^\dagger \hat{M} U_2 | \psi \rangle \langle \phi | U_1^\dagger U_1 | \phi \rangle \right) \\
&= \frac{1}{2} (\langle M \rangle_1 + \langle M \rangle_2),
\end{aligned} \tag{VI.39}$$

the average of the two propagations. This scheme is readily implementable for d independent processes at the cost of using a d-dimensional qudit, initialized in a superposition with equal weights for each state, each acting as control of a CSWAP on a different auxiliary qubit.

Using this procedure, an interesting point is that the states $|\phi_j\rangle$ of the auxiliary qubits

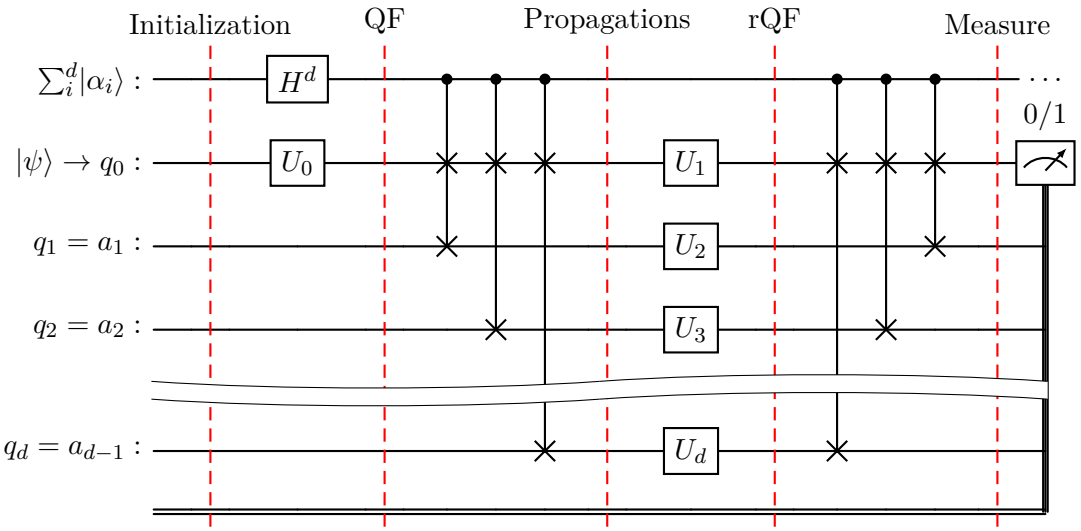

Figure VI.8: Quantum circuit implementing a quantum average, by linear summation, employing the quantum forking procedure.

can be arbitrary, even unknown; one can use any state without having to initialize the whole register to a known state. Hence, we avoid the cost of preparing the $d-1$ states, using the states that are already available - the thermal state of the qubits or leftovers from the previous run. Then, implementing multiple times the circuit becomes less expensive in terms of auxiliary costs, i.e., the time-consuming and non-negligible energetic cost of "refrigerating" the qubits to return to their $|0\rangle$ state [290–292]. On the other hand, the thermodynamic cost is moved to the initialization of the qudit, first cooling and then using a d-dimensional Hadamard gate, eqs. (VI.30) and (VI.35), and to the operations required to implement the CSWAP ladder [293]. Then, if the cost of initializing the auxiliary qubits is negligible, we can avoid the *unforking* step, and apply the measure to all addressed qubits, as long as the expectation values on the auxiliary qubits are known, see Figure VI.9. In the three-qubit example proposed above, that is by applying the operators $(\mathbb{1}_c \otimes \hat{M} \otimes \mathbb{1}_a)$ and $(\mathbb{1}_c \otimes \mathbb{1}_t \otimes \hat{M})$ to the state in eq. (VI.38). The averages obtained are

$$\langle M_1 \rangle = \frac{1}{2}\left(\langle\psi|U_1^\dagger \hat{M} U_1|\psi\rangle + \langle\phi|U_1^\dagger \hat{M} U_1|\phi\rangle\right) \tag{VI.40a}$$

$$\langle M_2 \rangle = \frac{1}{2}\left(\langle\psi|U_2^\dagger \hat{M} U_2|\psi\rangle + \langle\phi|U_2^\dagger \hat{M} U_2|\phi\rangle\right), \tag{VI.40b}$$

where we can recover the correct expectation only if we know a priori the values of $\langle\phi|U_i^\dagger \hat{M} U_i|\phi\rangle$. When dealing with stochastic trajectories of the state, this quantity might be beyond or inaccessible to our knowledge. A slightly different method can be adapted for implementing this average based on multiple measures. Instead of applying the unitaries to the different qubits, we control the application of the different unitaries depending on the state of the control qubit (qudit). Under this activation control, the final state yielded is, with the example of only one auxiliary qubit,

$$|\Phi_{\mathrm{QR}}^{(fin)}\rangle = \frac{|0\rangle_c U_1|\psi\rangle_t|\phi\rangle_a + |1\rangle_c|\phi\rangle_t U_2|\psi\rangle_a}{\sqrt{2}}, \tag{VI.41}$$

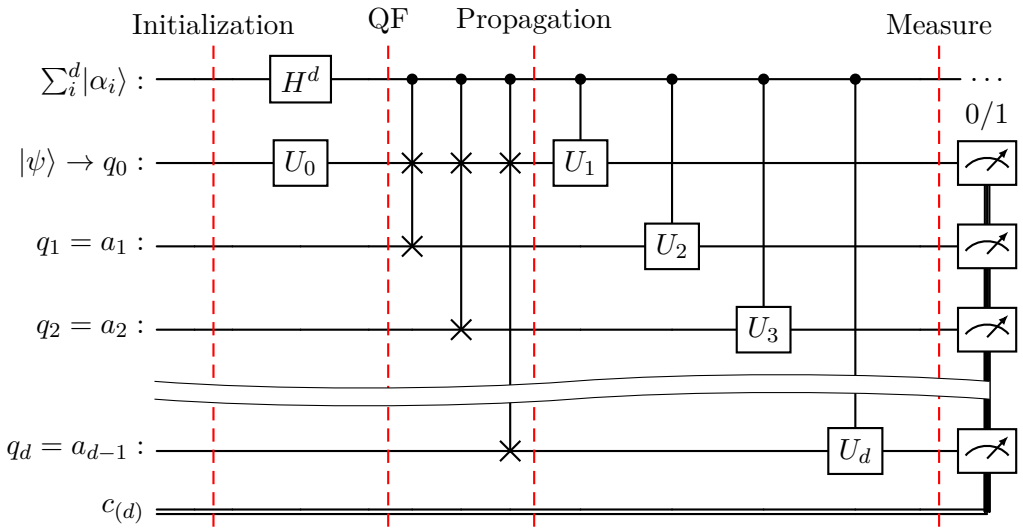

Figure VI.9: Quantum forking for the implementation of multiple trajectories, without repeating the whole circuit describing the unitary U_0, at the expense of performing multiple measurements and controlled unitaries.

so that the unitary evolutions affect only the states $|\psi\rangle$ in the different qubits. Applying simultaneous measurements to target and auxiliary qubits, we obtain the expectation of the average system weighted by the expectation on the auxiliary qubit. In the two-copies system, the measurement $(\mathbb{1}_c \otimes \hat{M} \otimes \hat{M})$ returns:

$$\begin{aligned}\langle \Phi_{\mathrm{QF}}^{(fin)} | \mathbb{1}_c \otimes \hat{M} \otimes \hat{M} | \Phi_{\mathrm{QF}}^{(fin)} \rangle &= \frac{1}{2}\Big(\langle 0|0\rangle \langle \psi | U_1^\dagger \hat{M} U_1 | \psi \rangle \langle \phi | \hat{M} | \phi \rangle + \langle 1|1\rangle \langle \phi | \hat{M} | \phi \rangle \langle \psi | U_2^\dagger \hat{M} U_2 | \psi \rangle \Big) \\ &= \frac{1}{2} \langle M_\phi \rangle \Big(\langle \psi | U_1^\dagger \hat{M} U_1 | \psi \rangle + \langle \psi | U_2^\dagger \hat{M} U_2 | \psi \rangle \Big) \\ &= \frac{1}{2} \langle M_\phi \rangle \Big(\langle M_1 \rangle + \langle M_2 \rangle \Big)\end{aligned}$$

where, since we are leaving unchanged the state of the auxiliary qubits, we can initialize their states such that $\langle \phi | \hat{M} | \phi \rangle = 1$, and we can obtain the correct average without further corrections.

VI.3.2 Sampling complexity and operational limits

The underlying idea of quantum forking is to perform averages through a full quantum procedure, exploiting quantum interference without relying on classical post-processing. The last part of this statement can be misleading at first, as the intuition is formally correct only at the level of expectation value. It should not be interpreted as implying that the average is directly accessible from a single measurement outcome. Indeed, in particular referring to unraveling schemes for open quantum dynamics, the use of QF does not translate into a reduction of the sampling complexity or measurement cost.

Quantum forking "computes" linear combinations at the Hilbert space level, a coherent averaging, yet in each experimental run, the system collapses onto only one state. In the scheme with the unforking step, eq. (VI.38) and Figure VI.8, when we perform a single

measurement on the qubit representing the target state, projecting on the computational basis, that is a single Bernoulli trial, yielding a classical bit either 0 or 1, with the averaged probability of the different trajectories as its law. Similarly, in the multiple simultaneous measurements on the register, eq. (VI.41) and Figure VI.9, we collapse on one of the d possible states of the superposition, where only one qubit contains the information about the target state ψ, effectively testing only one possible trajectory of the set implemented in the whole register. In both cases, we must recall that the measurement outcomes remain single-shot random variables, and sampling over multiple shots is still required to obtain a distribution and the correct average. Then, for a set of d trajectories implemented in a single quantum register, the circuit must be repeated and measured at least $K \geq d$ times, showing how quantum forking does not improve the sampling complexity.

The effect of QF is to reduce the number of *distinct* circuits required to encode multiple evolutions, without reducing the number of measurements required to estimate expectation. For N trajectories and a d-dimensional register, we need to write $\lceil N/d \rceil$ circuits that need to be optimized and transpiled only once, reducing the number of transpilations by an order $\mathcal{O}(d)$. This improvement comes at the cost of introducing a d-dimensional qudit, initializing it, implementing $\mathcal{O}(d)$ CSWAP gates, and dealing with a highly entangled state (maximally with respect to the control qudit).

The conclusion, in relation to the stochastic unraveling of OQS dynamics and its simulation on a quantum computer, is that quantum forking should not be regarded as a replacement or improved method for the stochastic sampling scheme proposed in the previous Section. Its requirement for the addition of hardware overhead and QC coherence time makes it not relevant for NISQ, and its applicability is limited to scenarios where circuit synthesis dominates over measurement cost. Rather, it should be regarded as an interesting concept to be investigated in future works, considering it a basis for new research and for schemes to be implemented in future, fault-tolerant, error-free architectures.

References

[99]S. Lloyd, "Universal Quantum Simulators", Science **273**, 1073–1078 (1996) 10.1126/SCIENCE.273.5278.1073

[194]W. Magnus, "On the exponential solution of differential equations for a linear operator", Communications on Pure and Applied Mathematics **7**, 649–673 (1954) 10.1002/CPA.3160070404

[195]S. Blanes, F. Casas, J. A. Oteo, and J. Ros, "The Magnus expansion and some of its applications", Physics Reports **470**, 151–238 (2009) 10.1016/J.PHYSREP.2008.11.001

[207]Z. Hu, R. Xia, and S. Kais, "A quantum algorithm for evolving open quantum dynamics on quantum computing devices", Scientific Reports 2020 10:1 **10**, 1–9 (2020) 10.1038/s41598-020-60321-x

[208]R. Sweke, I. Sinayskiy, D. Bernard, and F. Petruccione, "Universal simulation of Markovian open quantum systems", Physical Review A - Atomic, Molecular, and Optical Physics **91**, 062308 (2015) 10.1103/PHYSREVA.91.062308

[209]R. Sweke, M. Sanz, I. Sinayskiy, F. Petruccione, and E. Solano, "Digital quantum simulation of many-body non-Markovian dynamics", Physical Review A **94**, 022317 (2016) 10.1103/PHYSREVA.94.022317

[210]A. W. Schlimgen, K. Head-Marsden, L. A. M. Sager, P. Narang, and D. A. Mazziotti, "Quantum simulation of the Lindblad equation using a unitary decomposition of operators", Physical Review Research **4**, 023216 (2022) 10.1103/PhysRevResearch.4.023216

[211]A. Miessen, P. J. Ollitrault, F. Tacchino, and I. Tavernelli, "Quantum algorithms for quantum dynamics", Nature Computational Science 2022 3:1 **3**, 25–37 (2022) 10.1038/s43588-022-00374-2

[214]F. Gallina, M. Bruschi, and B. Fresch, "From stochastic Hamiltonian to quantum simulation: exploring memory effects in exciton dynamics", New Journal of Physics **26**, 083017 (2024) 10.1088/1367-2630/AD6A7B

[220]W. F. Stinespring, "Positive functions on *-algebras", Proceedings of the American Mathematical Society **6**, 211–216 (1955) 10.1090/S0002-9939-1955-0069403-4

[221]B. Sz.-Nagy, "Prolongement des transformations de l'espace de Hilbert qui sortent de cet espace dans Appendice au livre "Leçons d'analyse fonctionnelle"", in *Leçons d'analyse fonctionnelle* (Akadémiai Kiadó, Budapest, 1955), pp. 439–573

[238]F. Gallina, M. Bruschi, and B. Fresch, "Strategies to simulate dephasing-assisted quantum transport on digital quantum computers", New Journal of Physics **24**, 023039 (2022) 10.1088/1367-2630/AC512F

[241]H. F. Trotter, "On the product of semi-groups of operators", Proceedings of the American Mathematical Society **10**, 545–551 (1959) 10.1090/S0002-9939-1959-0108732-6

[242]M. Suzuki, "Generalized Trotter's formula and systematic approximants of exponential operators and inner derivations with applications to many-body problems", Communications in Mathematical Physics **51**, 183–190 (1976) 10.1007/BF01609348

[260]F. Gallina, M. Bruschi, R. Cacciari, and B. Fresch, "Simulating Non-Markovian Dynamics in Multidimensional Electronic Spectroscopy via Quantum Algorithm", Journal of Chemical Theory and Computation **20**, 10588–10601 (2024) 10.1021/ACS.JCTC.4C01204

[261]N. P. Sawaya, T. Menke, T. H. Kyaw, S. Johri, A. Aspuru-Guzik, and G. G. Guerreschi, "Resource-efficient digital quantum simulation of d-level systems for photonic, vibrational, and spin-s Hamiltonians", npj Quantum Information 2020 6:1 **6**, 1–13 (2020) 10.1038/s41534-020-0278-0

[262]K. Kormann, S. Holmgren, and H. O. Karlsson, "Accurate time propagation for the Schrödinger equation with an explicitly time-dependent Hamiltonian", Journal of Chemical Physics **128**, 184101 (2008) 10.1063/1.2916581/896230

[263]D. Fang, D. Liu, and R. Sarkar, "Time-Dependent Hamiltonian Simulation via Magnus Expansion: Algorithm and Superconvergence", Communications in Mathematical Physics **406**, 1–36 (2025) 10.1007/S00220-025-05314-5/

[264]D. An, D. Fang, and L. Lin, "Time-dependent Hamiltonian Simulation of Highly Oscillatory Dynamics and Superconvergence for Schrödinger Equation", Quantum **6**, 690 (2022) 10.22331/q-2022-04-15-690

[265]R. Gilmore, "Baker-Campbell-Hausdorff formulas", Journal of Mathematical Physics **15**, 2090–2092 (1974) 10.1063/1.1666587

[266]R. Motwani and P. Raghavan, *Randomized Algorithms* (Cambridge University Press, Cambridge, Aug. 1995), 10.1017/CBO9780511814075

[267]W. Hoeffding, "Probability Inequalities for Sums of Bounded Random Variables", Journal of the American Statistical Association **58**, 13–30 (1963) 10.1080/01621459.1963.10500830

[268]P. Billingsley, *Probability and Measure*, Wiley Series in Probability and Statistics (Wiley, 1995)

[269]J. L. Park, "The concept of transition in quantum mechanics", Foundations of Physics **1**, 23–33 (1970) 10.1007/BF00708652

[270]G. Ghirardi and G. Ghirardi, "Entanglement, Nonlocality, Superluminal Signaling and Cloning", in *Advances in quantum mechanics*, edited by P. Bracken (IntechOpen, Apr. 2013), 10.5772/56429

[271]W. K. Wootters and W. H. Zurek, "A single quantum cannot be cloned", Nature **299**, 802–803 (1982) 10.1038/299802A0

[272]D. Dieks, "Communication by EPR devices", Physics Letters A **92**, 271–272 (1982) 10.1016/0375-9601(82)90084-6

[273]D. K. Park, I. Sinayskiy, M. Fingerhuth, F. Petruccione, and J.-K. Kevin Rhee, "Parallel quantum trajectories via forking for sampling without redundancy", New Journal of Physics **21**, 083024 (2019) 10.1088/1367-2630/AB35FB

[274]D. K. Park, F. Petruccione, and J. K. K. Rhee, "Circuit-Based Quantum Random Access Memory for Classical Data", Scientific Reports 2019 9:1 **9**, 1–8 (2019) 10.1038/s41598-019-40439-3

[275]C. Blank, D. K. Park, and F. Petruccione, "Quantum-enhanced analysis of discrete stochastic processes", npj Quantum Information 2021 7:1 **7**, 1–9 (2021) 10.1038/s41534-021-00459-2

[276]I. J. David, I. Sinayskiy, and F. Petruccione, "Digital Simulation of Single Qubit Markovian Open Quantum Systems: A Tutorial", Quanta **12**, 131–163 (2023) 10.12743/QUANTA.V12I1.226

[277]E. Campbell, "Random Compiler for Fast Hamiltonian Simulation", Physical Review Letters **123**, 070503 (2019) 10.1103/PhysRevLett.123.070503

[278]I. J. David, I. Sinayskiy, and F. Petruccione, "Faster Quantum Simulation Of Markovian Open Quantum Systems Via Randomisation", (2024)

[279]I. J. David, I. Sinayskiy, and F. Petruccione, "Efficient Quantum Circuit Implementations of The qDRIFT Algorithm via Linear Combinations of Unitaries and Quantum Forking", Journal of Physics: Conference Series **2970**, 012004 (2025) 10.1088/1742-6596/2970/1/012004

[280]A. M. Childs and N. Wiebe, "Hamiltonian simulation using linear combinations of unitary operations", Quantum Information & Computation **12**, 901–924 (2012) 10.5555/2481569.2481570

[281]K. D. Wu, C. Yang, R. D. He, M. Gu, G. Y. Xiang, C. F. Li, G. C. Guo, and T. J. Elliott, "Implementing quantum dimensionality reduction for non-Markovian stochastic simulation", Nature Communications 2023 14:1 **14**, 2624– (2023) 10.1038/s41467-023-37555-0

[282]T. J. Elliott and M. Gu, "Embedding memory-efficient stochastic simulators as quantum trajectories", Physical Review A **109**, 022434 (2024) 10.1103/PhysRevA.109.022434

[283]C. Yang, M. Florido-Llinàs, M. Gu, and T. J. Elliott, "Dimension reduction in quantum sampling of stochastic processes", npj Quantum Information 2025 11:1 **11**, 34– (2025) 10.1038/s41534-025-00978-2

[284]B. E. Anderson, H. Sosa-Martinez, C. A. Riofrío, I. H. Deutsch, and P. S. Jessen, "Accurate and Robust Unitary Transformations of a High-Dimensional Quantum System", Physical Review Letters **114**, 240401 (2015) 10.1103/PhysRevLett.114.240401

[285]Y. Wang, Z. Hu, B. C. Sanders, and S. Kais, "Qudits and High-Dimensional Quantum Computing", Frontiers in Physics **8**, 589504 (2020) 10.3389/FPHY.2020.589504

[286]M. Ringbauer, M. Meth, L. Postler, R. Stricker, R. Blatt, P. Schindler, and T. Monz, "A universal qudit quantum processor with trapped ions", Nature Physics 2022 18:9 **18**, 1053–1057 (2022) 10.1038/s41567-022-01658-0

[287]M. Karácsony, L. Oroszlány, and Z. Zimboras, "Efficient qudit based scheme for photonic quantum computing", SciPost Physics Core **7**, 10.21468/SciPostPhysCore.7.2.032 (2023) 10.21468/SciPostPhysCore.7.2.032

[288]E. Fredkin and T. Toffoli, "Conservative logic", International Journal of Theoretical Physics **21**, 219–253 (1982) 10.1007/BF01857727

[289]W. Q. Liu, H. R. Wei, and L. C. Kwek, "Low-Cost Fredkin Gate with Auxiliary Space", Physical Review Applied **14**, 054057 (2020) 10.1103/PHYSREVAPPLIED.14.054057

[290]Y. H. Ma, J. F. Chen, C. P. Sun, and H. Dong, "Minimal energy cost to initialize a bit with tolerable error", Physical Review E **106**, 034112 (2022) 10.1103/PhysRevE.106.034112

[291]M. A. Johnson, M. T. Madzik, F. E. Hudson, K. M. Itoh, A. M. Jakob, D. N. Jamieson, A. Dzurak, and A. Morello, "Beating the Thermal Limit of Qubit Initialization with a Bayesian Maxwell's Demon", Physical Review X **12**, 041008 (2022) 10.1103/PhysRevX.12.041008

[292]F. Barra, "The thermodynamic cost of driving quantum systems by their boundaries", Scientific Reports 2015 5:1 **5**, 14873– (2015) 10.1038/srep14873

[293]M. Madami, G. Gubbiotti, D. J. Bedingham, and O. J. E Maroney, "The thermodynamic cost of quantum operations", New Journal of Physics **18**, 113050 (2016) 10.1088/1367-2630/18/11/113050

Chapter VII

Conclusions

Accounting for the open nature of quantum systems necessarily requires describing the environment in which they are embedded, and its effects on the system's dynamics. As quantum science advances, the practical control and application of quantum systems require a deeper understanding of the environment beyond the white-noise approximation, as well as the development of strategies to simulate their dynamics, both on classical and quantum computers. Throughout this work, we primarily employed stochastic methods to describe open quantum system dynamics, connecting them to mean density matrix dynamics, ranging from well-established forms to less common formulations. The inclusion of a non-standard time correlated noise model for the environment is central, along with its comparison with standard white noise and a standard colored process.

Part of the results presented in this work appeared in our publications, and in the context of this thesis are systematically connected and extended.

In Chapter III, we provide a unified and detailed description of different trajectory-based modeling techniques connected to the rich and flexible framework of stochastic Hamiltonians, a deliberately phenomenological approach that serves as a direct modeling tool for capturing environmental effects without reference to an explicit microscopic derivation. We traced how different formulations, such as the direct insertion of stochastic fluctuations into the systems' Hamiltonians and the stochastic Schrödinger (SSE) and Liouville (SLE) equations, can be related and systematically interpreted. The stochastic Hamiltonian formulation, in the Stratonovich formalism, allows us to write the propagator of the dynamics in analogy with the closed-system Schrödinger equation. Being a unitary operator, it yields unitary evolutions, ensuring norm preservation trajectory-wise, a result that is the foundation of the algorithm investigated in Chapter VI. On the other hand, within the Itō interpretation, we can derive the associated quantum master equations

(QME), which govern the observed mean dynamics of the open system. Furthermore, it allows us to describe beyond the stochastic Hamiltonian formulation, overcoming its limitations, by providing the example of the unraveling of all QMEs of Lindblad form. Indeed, the stochastic Hamiltonian emerges as one specific subclass of linear SSE. Within this framework, although this method does not ensure norm-preservation for each trajectory, but only on average, it allows for efficient numerical integration schemes on classical architectures. Additionally, we discussed the use of random ordinary differential equations (RODEs) as a special case where the Hamiltonian includes continuous stochastic processes, and the stochastic Liouville equation. We show how to formally move between different interpretations of the stochastic terms and the related method, and how these methods, together, offer a versatile toolkit for modeling and simulating open quantum systems.

In Chapter IV, we study a colored-noise extension of the SSE based on an Ornstein–Uhlenbeck noise drive (Υ_t), and benchmark its ensemble-averaged dynamics against the standard white-noise SSE and against a fluctuating OU random Hamiltonian. Using colored noise and processes as stochastic potentials, we obtained master equations that are open-form and not in Lindblad form, yet are positive definite by construction due to the averaging over pure-state trajectories. This paves the way for using SSE as more than an efficient numerical strategy for known QMEs, but also for writing new non-trivial QMEs and exploring situations where an explicit QME cannot even be written. We presented the normalized linear SSE driven by this noise as the unraveling of its open-form correlated QME. In addition, we showed that different terms in the dissipator of the average dynamics correspond either to a Lindblad form unraveled by white-noise SSE or to correlation terms analogous to those obtained for the average dynamics of a stochastic Hamiltonian with Ornstein–Uhlenbeck fluctuations. This way, we shed light on how different dissipative terms in a generic QME arise from the nature of the stochastic potentials in the environment models, in particular the terms that appear in their correlation functions. The analysis of the dynamics of a two-level system driven by colored SSE highlights important features. When the environment is described as a Υ_t-noise applied through the Pauli σ_x operator to the interaction between the levels, a strong effect on the coherence time is observed. When the system's Hamiltonian commutes with the noise operator, a different asymptotic density matrix is reached, and the system does not reach equipartition of populations. The steady state can be either static, for a null Hamiltonian, or an oscillating steady state for coupled levels. The coherences are therefore maintained for these symmetric systems. The introduction of an asymmetry in the system, as an energy difference between the two levels, results in reaching the equipartite distribution expected using symmetric relaxation operators. However, the coherences are long-lived, the dynamics showing two different regimes of relaxation with different time scales, i.e., a faster initial decay followed by a slower relaxation.

Through the Redfield derivation, we gained insights into the peculiarity of the dynamics obtained using Υ_{OU}-colored noise, obtaining a closure model for the correlation open term of the system with the environment in the QME corresponding to the colored SSE. Although not analytically derivable from the SSE unraveling, the presence of different

time scales is well explained by the Redfield master equation with time-dependent coefficients. The Redfield model also rationalizes the different stationary states and provides an insightful intuition on the effect of the noise in the system dynamics. The insights obtained from this formulation come at the cost of losing the complete positivity ensured by averaging over an ensemble of pure, valid states. This positivity issue in the Redfield model and the spurious oscillations observed in the dynamics of the reduced density matrix eigenvalues are addressed by investigating the construction of the relaxation tensor, introducing another version of the Redfield tensor to the wide range of Redfield approaches. Using another route, building on the stochastic approach to density matrices introduced in Chapter III, we investigated the perturbative approximation leading to the time-dependent Redfield form, gaining further insights into the nature of the correlation term in the QME and its non-Markovian feature, as well as to the removal of the oscillatory terms. Finally, though the SSE unravels a precise, but open form, master equation, we can think about the forms of Redfield QME obtained as approximate models for it—an *effective* QME for the SSE unraveling. Then, we obtain a correct unraveling of particular forms of Redfield dynamics. Unlike other approaches, which suffer from various unphysicalities, these colored-noise SSE provide a positive unraveling of time-dependent frequency-resolved Redfield equations without imaginary component.

In Chapter V, a new measure stemming from stochastic unravelings is derived–the densification measure–, which describes signatures related to non-Markovianity inferred from ensemble-average behavior. An associated character descriptor is constructed in analogy to the BLP measure of non-Markovianity. We show that stochastic unravelings, and more generally, trajectory-based methods, provide access to information that is not available at the density matrix level. From this perspective, these novel descriptors should be regarded as complementary tools for analysis and interpretation of complex dynamics when unraveled by an ensemble of trajectories.

Finally, in Chapter VI, we connected the stochastic Hamiltonian approaches discussed in Chapter III to the implementation of quantum algorithms in a simple and effective way. The resulting algorithm (QCNA) is not introduced here as a novel proposal; rather, this work complements it in several aspects. We give a formal proof of convergence to the correct expectation value in the limit of one projection measurement (a Bernoulli trial) per trajectory, yielding a Poisson (trials) process. Furthermore, we define error boundaries and convergence rates in the single-shot and multiple-shot scenarios. In this regard, an open yet concrete challenge is the definition of the optimal allocation of trajectories and measurement shots. This will require defining and setting suitable metrics and cost functions, tailored to the objectives of interest–such as the distance to the reference evolution, the smoothness of the solution, its variance, or, most importantly, avoiding the need for an explicit reference solution. Connecting further to the results in Chapter IV, we can appreciate that the constraint required for the normalization of the linear SSE for colored noise restricts the admissible dynamics to the class of stochastic Hamiltonian evolutions. Within this setting, the QCNA naturally enables the implementation of correlated open dynamics beyond the Markovian assumptions, naturally allowing for colored noises and

processes as models of environmental interactions. Moreover, since a particular Redfield form reproducing the exact open-system quantum master equation is derived, dynamics governed by this restricted class of Redfield tensors can likewise be unraveled and implemented on a quantum computer. A novel quantum computing procedure, quantum forking, is analyzed critically as a possible conceptual extension of trajectory-based methods. We show how its use, in regard to the QCNA algorithm, is limited at present by the physical constraints of available NISQ qubit architectures, as the asymptotical sampling complexity is not reduced, the only clear advantage is in the scaling of unique-circuit construction, which comes at the cost of highly entangled large quantum registers and additional entangling-gate layers. Even if this scheme might be useful only in future quantum computers, it remains appealing as an innovative strategy and as a catalyst for future developments in the quantum simulation of open-system dynamics.

In closing, this thesis emphasizes the usefulness of stochastic trajectory-based approaches as versatile and effective tools for the study of open quantum dynamics, complementing more traditional formulations rather than serving merely as technical devices. By providing a unifying framework that consistently connects phenomenological models, ensemble descriptions, microscopic derivations and reduced dynamics, we offer a coherent perspective across traditionally separated levels of description. Within this framework, we have identified dynamical regimes characterized by long-lived coherences, nontrivial stationary states-including oscillatory ones—and relaxation processes occurring on multiple time scales, with direct implications for the understanding of dissipative charge and energy transfer, as well as for noise-aware control protocols and digital quantum-simulation strategies. From this standpoint, the use of non-standard environments emerges not only as a feature to be characterized, but as a resource that can be engineered and exploited. Furthermore, we show how the study of the trajectories ensemble can provide access to gain more physical insights, encoding information that is inaccessible at the level of the reduced density matrix alone. Taken together, these elements converge toward quantum computing applications, where, on the one hand, the stochastic Hamiltonian formalism provides a useful tool for simulating open-system dynamics, and, on the other hand, could be useful for implementing noise-resistant quantum operations and controls.

Still there?

Go on, move to the next question.

"*The important thing is not to stop questioning. Curiosity has its own reason for existing.*" - A. Einstein

"*You're still here? It's over, go home. Oh, you're expecting a teaser for Deadpool 2. Well,* ***we don't have that kind of money****.*" - Deadpool